DEMONSTRATION OF INNOVATIVE APPLICATIONS
OF TECHNOLOGY FOR THE CT-121 FGD PROCESS

at

Georgia Power's

Plant Yates

Final Report

Volume 2
Operations

DOE DE-FC22-90PC89650
SCS C-90-00284

Prepared by:

Southern Company Services, Inc.
42 Inverness Parkway, Suite 340
Birmingham, Alabama 35242

January 1997

Cleared by US DOE Patent Counsel

TABLE OF CONTENTS

Page

TABLE OF CONTENTS (Continued)

Page

TABLE OF CONTENTS (Continued)

TABLE OF CONTENTS (Continued)

Page

LIST OF TABLES

LIST OF TABLES (Continued)

LIST OF TABLES (Continued)

LIST OF FIGURES

LIST OF FIGURES (Continued)

LIST OF FIGURES (Continued)

LIST OF FIGURES (Continued)

LIST OF FIGURES (Continued)

LIST OF ABBREVIATIONS

ΔP	differential pressure
AP	site ash pond (make-up water source)
Ca	calcium
$CaCO_3$	calcium carbonate (limestone)
CO_3	carbonate
CCT	Clean Coal Technology
CI	confidence interval
CT-121	Chiyoda Thoroughbred - 121 FGD process
DOE	Department of Energy
EPRI	Electric Power Research Institute
ESP	electrostatic precipitator
FFR	form filtration rate
FGD	flue gas desulfiirization
FRP	fiberglass-reinforced plastic
GP	gypsum pond (recycle process water)
GSTT	gypsum slurry transfer tank
HDPE	high density polyethylene
I.D. (Fan)	induced draft
JBR	jet bubbling reactor
JBR-D	JBR draw-off slurry
JBR-F	JBR froth zone slurry
MDL	method detection limit
Mg	magnesium
$MgCO_3$	magnesium carbonate
MRC	maximum rated capacity
Na	sodium
N/A	not applicable
NC	not calculated
O_2	oxygen

PSD	particle size distribution
PVC	polyvinyl chloride
SCS	Southern Company Services
SO_2	sulfur dioxide
TKUA	thickener unit area

LIST OF UNITS

% past #200	percent, by weight, smaller than a #200 mesh screen
acf	actual cubic feet
Btu	British thermal units
g	gram
gr	grains
in. WC	pressure in inches of water column
lb	pound
kW	kilowatt
mg	milligrams
µm	micrometers (microns)
mM	millimoles/liter
MW	megawatts
MWe	megawatts equivalent (electrical energy)
Nm^3	normal cubic meters (1 atm, 0°C)
pH	measure of alkalinity or acidity
ppm	parts per million
ppmv	parts per million by volume
ppmw	parts per million by weight
(d)scf	(dry) standard cubic feet (1 atm, 60°F)
(d)scm	(dry) standard cubic meters (1 atm, 0°C)
wt.%	percent by weight

VOLUME SUMMARY

As part of the second round (Round II) of the Clean Coal Technology (CCT) program, the Department of Energy (DOE), the Southern electric system, and the Electric Power Research Institute (EPRI) sponsored a 100 MWe demonstration of the Chiyoda Thoroughbred CT-121 wet-limestone flue gas desulfurization (FGD) system. The CCT program is a major initiative of the DOE, designed to allow coal to reach its full potential as a source of energy for the national and international marketplace. The demonstration was conducted at Georgia Power Company's Plant Yates Unit 1, located near Newnan, Georgia.

This volume of the final report discusses the results of the two-year process evaluation portion of the demonstration project. The evaluation of the CT-121 flue gas desulfiirization process at Georgia Power's Plant Yates provided insight into operation of this technology under a wide variety of process conditions. Areas of evaluation included:

- Reliability and availability of the process under a variety of ash loading and process conditions;
- SO_2 and particulate removal efficiency;
- Air toxics removal efficiency;
- Process flexibility using alternate coal and limestone sources;
- Performance of equipment and materials of construction;
- Process control systems; and
- Gypsum byproduct quality and stacking as a dewatering and disposal technique.

To accomplish the goals of the demonstration project, the process evaluation was divided into two distinct periods: a low-particulate and a high-particulate test period. Each of these test periods was further divided into a series of three test blocks: Parametric, Long-Term, and Auxiliary Test blocks.

Operating Statistics

The process performed exceptionally well during the evaluation. Availability and reliability indices were both 97% for the entire process evaluation, including test periods in which the ESP was completely deenergized and full fly ash loading was introduced to the scrubber. Much of the scrubber unavailability was related to failures in auxiliary systems that were not directly associated with the CT-121 process (e.g., ball mill failures). Reliability and availability were somewhat lower during the high-ash testing than during low-ash testing due to the effects of full ash loading on the scrubber. However, operation without a particulate collection device upstream of a CT-121 scrubber is not a likely scenario. Operating statistics showed improvement during periods of moderate-ash loading, which is a more likely CT-121 retrofit scenario.

The excellent availability of the CT-121 process is due to several factors, including the inherent reliability of the process design, the existence of installed spares for all key process instruments and critical pumps, and the forgiving nature of the process despite difficulties such as sparger tube plugging or clogged gas cooling nozzles.

SO_2 Removal Efficiency

SO_2 removal efficiency was evaluated throughout the demonstration project. SO_2 removal efficiency was generally excellent, and greater than 90% efficiency was achieved during all test periods. It was demonstrated that 95% removal efficiency can easily be maintained under all expected combinations of boiler load and coal sulfur content by selecting the appropriate process setpoints. Removal efficiency as high as 99% was reached on several occasions while operating within the normal range of the independent process variables (JBR froth zone pH, and JBR ΔP). Some decrease in SO_2 removal efficiency was observed as a result of fouling of the sparger tubes, which occurred during high-ash testing. However, target performance levels were maintained by simply adjusting the pH or JBR ΔP setpoints.

The CT-121 process was operated under a wide variety of process operating conditions and the data gathered were used to develop performance models that could be used to characterize SO_2 removal efficiency as a function of several independent process variables. Multivariable regression analyses were performed on these data and resulted in the development of several predictive performance models. A single comprehensive model (which had a goodness of fit (R^2) of 0.935) was developed for the entire range of operating conditions. Several models were also developed that covered a more limited range of operating conditions, but had R^2 values superior to that of the more comprehensive model. These types of predictive performance models serve two valuable purposes. They permit comparison of the actual SO_2 removal efficiency to that predicted by the model, which can be used to identify process problems, such as sparger tube plugging. The models can also be used to determine the operating setpoints necessary to ensure that target SO_2 removal efficiency is achieved.

Particulate Removal Efficiency

Particulate removal efficiency was evaluated at three distinct ash loading levels during the demonstration: low-particulate loading (ESP 100% energized), high-particulate loading (ESP completely deenergized), and moderate-ash loading (approximately 90% ESP efficiency). During all three particulate removal tests, particulate removal efficiency was measured above 97%, and usually in excess of 99%. Removal efficiency of particulate greater than 10 micrometers in size was typically greater than 99.9%. Typical outlet particulate loading values were around 0.01 lb/MMBtu during the low- and moderate-ash loading tests and around 0.045 lb/MMBtu during the high-ash loading tests. Quantitative analyses of the outlet catch during the moderate-ash tests indicated that approximately 20% of the outlet particulate is sulfuric acid mist and carryover from the scrubber.

Air Toxics

Two test programs measured toxic air pollutant removal efficiency during the demonstration. One program was a DOE-sponsored test and the other, which focused on inorganic toxics,

was done in conjunction with the moderate-ash particulate removal measurements. The data collected indicate that the CT-121 process was successful in removing a large fraction (generally >75%) of most inorganic toxics, however there is a high degree of uncertainty associated with many of these data, particularly in the measurement ofcobalt, mercury, manganese, and nickel.

Process Flexibility

Throughout the performance evaluation, parameters such as coal source, coal sulfur content, and limestone source were varied. The purpose of investigating these variations was to determine if the CT-121 process was a viable SO_2 and particulate removal technology at Plant Yates as well as other potential sites. By evaluating coal and from several limestone sources, it was successfully demonstrated that the CT-121 process is adaptable to many new construction or retrofit scenarios, and that excellent performance could be achieved with limestone and coal from alternate sources.

The Yates CT-121 process maintained high limestone utilization (typically greater than 97%) while achieving high SO_2 removal efficiency. Because of the unique JBR design, the CT-121 process can operate at a lower pH than conventional spray tower wet limestone FGD processes while still attaining excellent SO_2 removal efficiency. Under low-particulate conditions, it was determined that pH could be raised as high as 5.3 before any significant decrease in limestone utilization was observed. However, due to the design of the CT-121 process, little improvement in SO_2 removal efficiency is realized by raising pH above 4.5. During high-ash testing, elevated aluminum and fluoride concentrations in the scrubbing liquor resulted in inhibited limestone dissolution. To ensure greater than 97% limestone utilization was maintained when operating under elevated aluminum and fluoride concentrations, the pH range was restricted to 4.0 or lower.

Materials of Construction

The materials of construction, particularly the fiberglass reinforced plastics (FRP) used in many of the systems, were frequently inspected throughout the process evaluation period. With the exception of erosion damage in the JBR inlet, the JBR, as well as all other process equipment, piping, and vessels constructed of FRP, exhibited no signs of corrosion or erosion damage during the demonstration project. In general, the wide use of FRP for this highly abrasive, high chloride, closed-loop environment was successful. With some design modifications, such as moving the gas cooling section further upstream of the JBR, the observed inlet plenum erosion could be prevented.

Process Control

The two key process control systems, pH and JBR level control, were not initially as successful as anticipated. Of the two pH measurement devices, only the Van London probe/Rosemount transmitter arrangement worked well. The pH control circuit's transient response was improved through the use of feedforward - feedback control, and reliable redundant readings were obtained only after the pH probes were located adjacent to one another. JBR level control using three differential pressure instruments was unreliable because these instruments were prone to plugging, which resulted in erroneous readings. To resolve this problem, the existing JBR gas-side differential pressure instrument was used as a surrogate for JBR level. This system worked well, and although no redundant instrumentation was available, no problems were experienced. However, gas side differential pressure is not always proportional to JBR level, and may require adjustment to maintain a constant SO_2 removal efficiency under changing boiler load conditions

Gypsum Byproduct

One of the most unexpected findings of the demonstration project was the impact of limestone selection on gypsum dewatering characteristics. Because the first limestone evaluated resulted in smaller-than-expected gypsum particle size and poor dewatering characteristics, a bench-scale evaluation of limestone source effects on gypsum size and

dewatering was begun. While most of the limestones were very high in purity (typically > 95% $CaCO_3$), inert content and iron concentration in the limestone appeared to correlate with gypsum quality, with higher inert and iron levels resulting in poorer gypsum quality.

In general, above average gypsum byproduct quality was observed. During low-ash testing, the Dravo limestone produced gypsum that filtered and settled well, and had a mean particle size of 43 micrometers. The gypsum stack, a gravity sedimentation process chosen for dewatering and storage of the byproduct solids, worked well during the low-ash test period. The gypsum/ash disposal stack worked equally well during the high-ash test period, even with up to 40% ash in the byproduct solids.

Conclusions

The demonstration of the CT-121 scrubber technology at Plant Yates was highly successful. High SO_2, particulate, and air toxics removal efficiencies were measured under conditions of varying coal sulfur content, limestone sources, and ash loading, all while achieving 97% availability and reliability. In general, the materials of construction performed admirably although some deficiencies were noted. For each shortcoming, suitable solutions were identified and implemented when practicable, although some suggested solutions are more geared for future designs.

1.0 INTRODUCTION

The purpose of this report is to publish the results of a two year demonstration of the application of innovative design approaches to the Chiyoda CT-121 flue gas desulfurization (FGD) process at Georgia Power's Plant Yates. The operational performance testing results are contained in this volume, which is one of a five-volume final report detailing all project results. In addition to performance results, the topics covered in the final report include: construction, start-up, instrumentation and controls, materials, maintenance,economics, byproducts handling and testing, and environmental monitoring.

1.1 Project Origin

The Clean Coal Technology (CCT) Demonstration Program is being implemented in a dynamic domestic and international environment which is conducive to making major strides in efficient use of energy, securing energy supplies, and enhancing environmental quality. The CCT program, a technology development effort jointly funded by government and industry, is a major initiative of the DOE whereby coal will be able to reach its full potential as a source of energy for the national and international marketplace.

The CCT Program is consistent with and directly supportive of Department of Energy's (DOE) energy strategy and implementing legislation embodied in the Energy Policy Act of 1992. The clean coal technologies demonstrated will satisfy many of the objectives of the Coal Research, Development, Demonstration, and Commercial Application Program of the Act, namely the following:

- Ensuring a reliable electricity supply;
- Achieving emission controls at levels of proficiency greater than or equal to currently available commercial technology;
- Achieving greater efficiency in the conversion of coal to useful energy; and
- Ensuring the availability for commercial use by 2010.

1.1.1 Project Sponsors

As part of Round II of the CCT Program, DOE, the Southern electric system[1], and the Electric Power Research Institute (EPRI) sponsored a 100 MWe demonstration of the Chiyoda Thoroughbred CT-121 wet-limestone flue gas desulfurization system. The project took place at Georgia Power Company's Plant Yates Unit 1, located about 40 miles southwest of Atlanta, near Newnan, Georgia. The total project cost shared by the co-sponsors was an estimated $43 million, of which DOE provided 50%. Although the process evaluation portion of the demonstration project was completed at the end of December 1994, environmental monitoring efforts (including ground water monitoring) continued through 1996.

Southern Company Services (SCS) believes that the CT-121 process offers significant cost and technical benefits compared to other flue gas desulfurization technologies. Through effective application of fiberglass-reinforced plastics (FRP), the elimination of the prescrubber and, potentially, the electrostatic precipitator (ESP), the Plant Yates CCT project demonstrated significant cost reductions to this already cost-competitive FGD process.

1.1.2 Project Milestones

The DOE selected the Plant Yates CT-121 project for Round II of the CCT Program on September 28, 1988, and construction commenced in August of 1990. Construction was completed in October of 1992, and a three month shakedown phase began. Testing commenced in January 1993 and was completed in December 1994. Figure 1-1 contains a project timeline with significant milestones shown.

[1] The Southern electric system is comprised of Alabama Power Company, Georgia Power Company, Gulf Power Company, Mississippi Power Company, Savannah Electric and Power Company, and Southern Company Services (SCS).

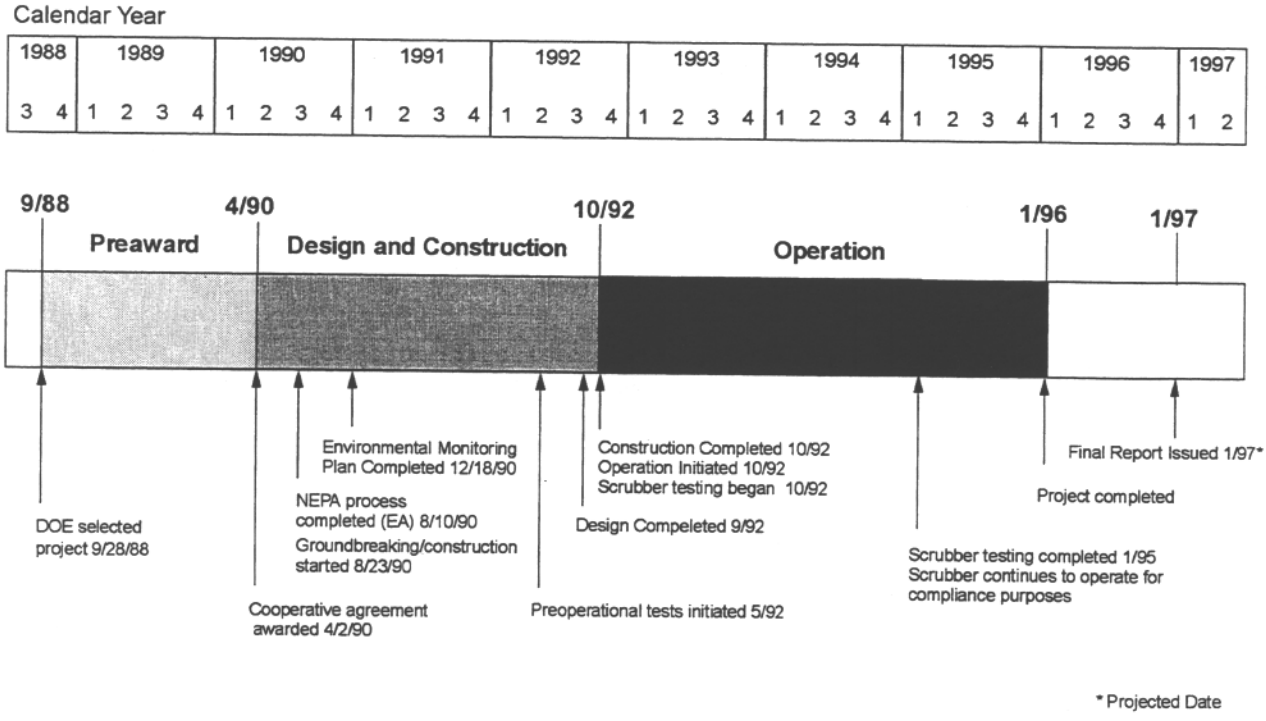

Figure 1-1. Plant Yates CT-121 Project Timeline

1.2 Host Site Description

This CCT project took place at Georgia Power Company's Plant Yates Unit 1, located about 40 miles southwest of Atlanta, near Newnan, Georgia. Plant Yates has seven operating pulverized-coal-fired generating units located in two separate buildings. Units 1-5, completed in the early 1950s, are housed in one building and have a combined nameplate capacity of 550 MWe. The furnaces for Units 2-5 are vented through a common 825-ft high stack. Units 6 and 7, built in the mid-1970s, are contained in a second building and have a combined nameplate capacity of 700 MWe. A common 800-ft stack is used to vent the furnaces of these two units. Units 6 and 7 are operated as base-load units, while Units 1-5 function as intermediate-load units. Units 1-5 incorporate once-through cooling using water from the Chattahoochee River; Units 6 and 7 use cooling towers. All units at the site use electrostatic precipitators to control particulate emissions. The collected fly ash is wet-sluiced to disposal ponds.

Unit 1, with a rated capacity of 100 MWe, was used to Supply flue gas for the demonstration program. All of the flue gas from this unitis treated by the CT-121 wet FGD process and there is no provision to bypass the scrubber. The flue gas from Unit 1 is vented through a wet chimney downstream of the CT-121 process. Figure 1-2 shows a plan view of how the CT-121 process was retrofitted to Unit 1.

1.3 Innovative Technology

The primary objective of the CT-121 CCT Demonstration at Plant Yates Unit 1 was to evaluate the effectiveness of the following innovative design approaches:

- Fiberglass-reinforced plastic (FRP) construction of the jetbubbling reactor (JBR), other key process vessels, and the wet chimney. The use of fiberglass as a construction material reduced the cost of this CT-121 system because it was less expensive than 316L stainless steel and because the prescrubber was eliminated. A prescrubber has normally been included in CT-121 process designs to minimize problems associated with chloride corrosion on 316L stainless steel. The prescrubber was eliminated because the corrosion resistance properties of fiberglass are superior to those of alloys.

- Elimination of flue gas reheat. Fluid dynamic modeling was performed to assist in wet duct and chimney design. Liquid collection devices and gas flow vanes were used in the FRP wet chimney design to ensure no rain-out would occur in the absence of flue gas reheat. The elimination of the equipment associated with reheating flue gas was another cost saving measure.

- Elimination of the need for a spare absorber. Because of the reliability advantages inherent to the JBR relative to other FOD limestone contacting devices (e.g., less likelihood of scaling), the CT-121 process operates more reliably than conventional FGD processes, eliminating the need for a spare absorber module.

- Simultaneous SO_2 and particulate collection. The CT-121 process has demonstrated the capability to achieve high particulate collection efficiencies while maintaining exceptional SO_2 removal efficiency. This capability was evaluated in three particulate collection test series conducted at various scrubber inlet particulate loading conditions.

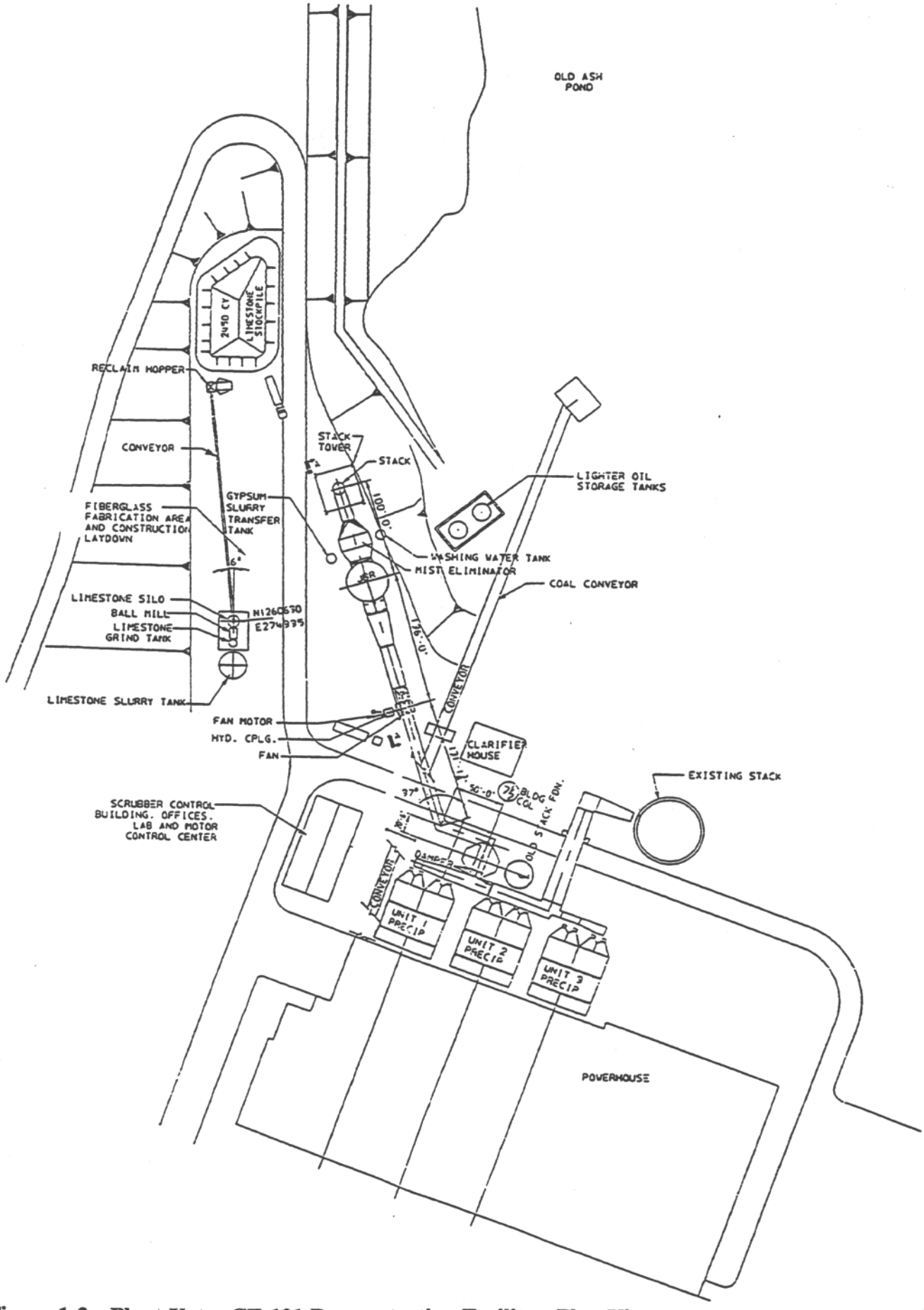

Figure 1-2. Plant Yates CT-121 Demonstration Facility - Plan View

1.4 Report Contents

This report presents results from the process evaluation portion of the demonstration. The process evaluation was divided into two test periods: a low-particulate and a high-particulate test period, each approximately one year in duration. Each test period included three similar test blocks. These test periods and test blocks are described in more detail in the Technical Approach section (Section 3) of this report volume. Section 2 contains a description of the CCT demonstration facility, Section 4 contains a detailed discussion of test results, Section 5 lists conclusions, and Section 6 details recommendations for process improvements.

Several appendices are also attached and include detailed tables of operational test data, process analytical results, coal proximate and ultimate analytical results, a process performance regression analysis summary, and detailed air toxics testing data.

2.0 FACILITY DESCRIPTION

The equipment comprising the demonstration facility can be divided into four major systems: boiler/ESP, CT-121 scrubber/wet chimney, limestone preparation circuit, and byproduct gypsum stack. Additionally, many control systems were required to maintain proper operation of the scrubber. Each of these systems is described below.

2.1 Boiler/ESP

Plant Yates has seven operating pulverized-coal-fired generating units located in two separate buildings. Unit 1, with a rated capacity of 100 MWe, was used to supply flue gas for the demonstration program. The flue gas passes through an electrostatic precipitator to remove fly ash particulate prior to entering the scrubber. All of the flue gas from this unit is treated by the CT-121 wet FGD process and there is no provision to bypass the scrubber. The flue gas from Unit 1 is vented through a wet chimney downstream of the CT-121 process.

The ESP has three fields (numbered 1 through 3), powered by a total of four electrical cabinets (A through D) as shown in Figure 2-1. Depending on the desired particulate loading to the scrubber (i.e., low-, mid-, or high-ash loading), each cabinet could be fully or partially deenergized to achieve the target loading.

2.2 CT-121 Wet FGD System

A simplified process flow diagram for the CT-121 process is presented in Figure 2-2. The CT-121 employs a unique absorber design, called a jet bubbling reactor (JBR), to combine SO_2 absorption, neutralization, sulfite oxidation, and gypsum crystallization in one reaction vessel. The process is designed to operate in a pH range (3 to 5) where the driving force for limestone dissolution is high, resulting in nearly complete reagent utilization. Oxidation of sulfite to sulfate is also promoted at the lower pH because of the increased solubility of

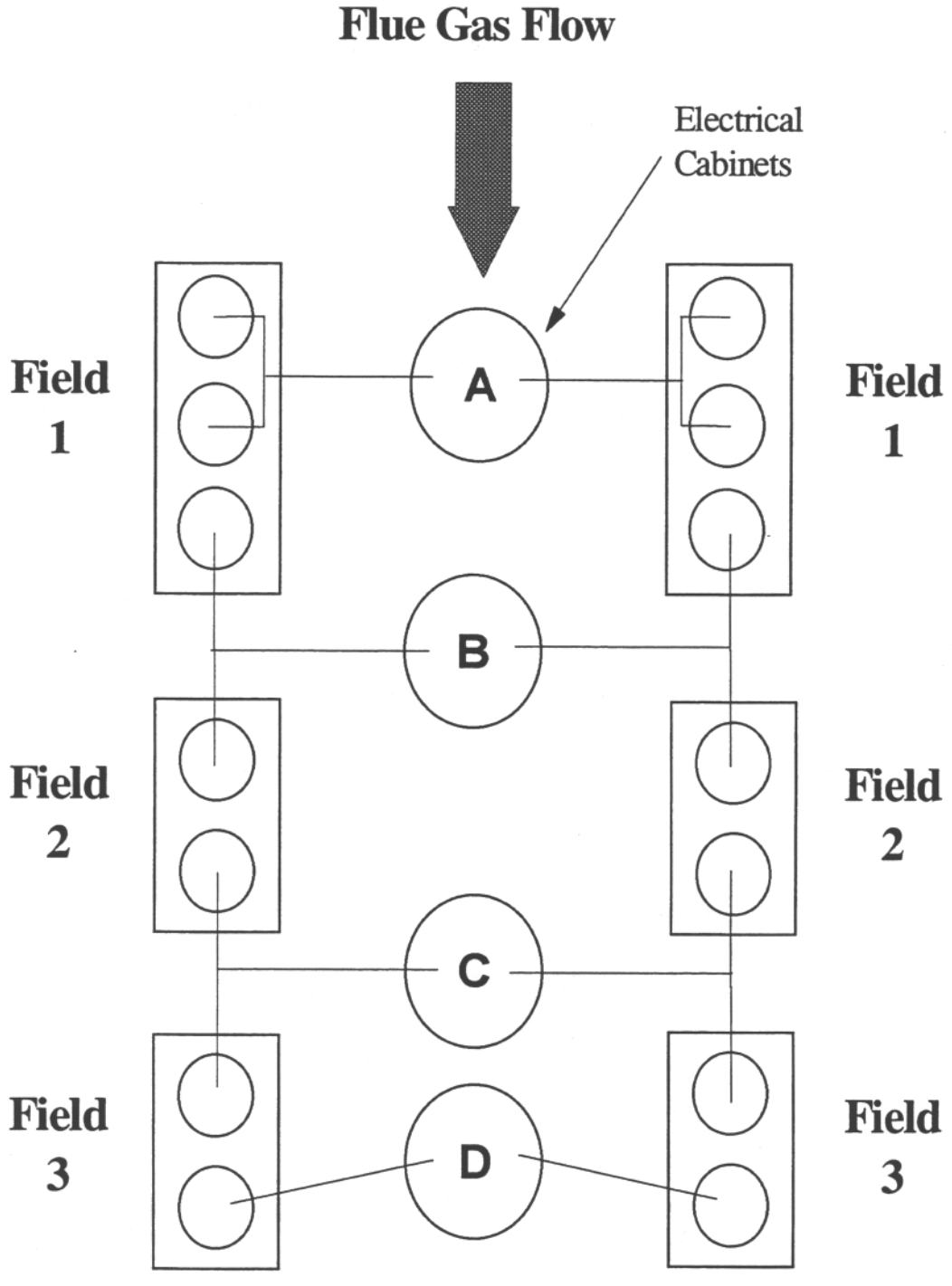

Figure 2-1. Plant Yates Unit 1 ESP Configuration

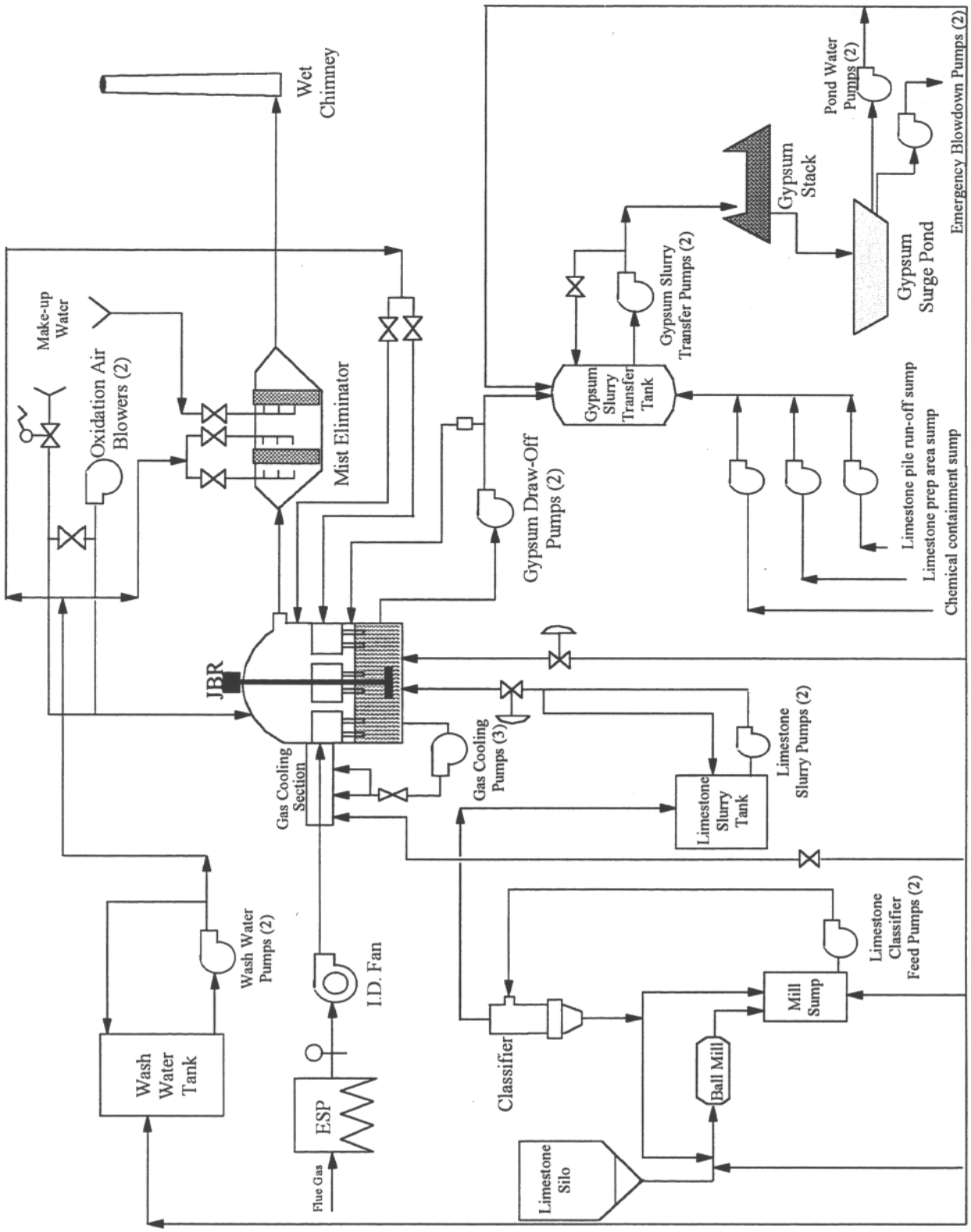

Figure 2-2. Process Flow Diagram for CT-121

naturally occurring catalysts such as iron. Because the process is designed for forced oxidation, there is sufficient surface area for gypsum crystal growth to prevent the system from becoming significantly supersaturated with respect to calcium sulfate. This significantly reduces the potential for gypsum scaling, a problem that frequently occurs in natural-oxidation FGD systems and many conventional forced oxidation systems. Since much of the crystal attrition and secondary nucleation associated with the large centrifugal pumps in conventional systems is eliminated in the CT-121 design, large, easily dewatered gypsum crystals can be produced.

2.2.1 Gas Cooling System

Flue gas from the boiler passes through the ESP and is pressurized by the Unit 1 induced draft (I.D.) and scrubber booster fan (The retrofit project replaced the two existing boiler I.D. fans with one combination I.D./booster fan). From the fan, the flue gas enters the gas cooling section, also referred to as the transition duct. Here the flue gas is cooled with gypsum recycle pond water at a liquid-to-gas ratio of 0.25 gal/1000 acf to prevent a wet-dry interface from occurring between the slurry and flue gas. The gas is then completely saturated with JBR slurry. The slurry is sprayed cocurrently into the gas at aliquid-to-gas ratio of about 10 gal/1000 acf at full boiler load using two of three installed centrifugal gas cooling pumps. The suction for the slurry gas cooling pumps is located near the bottom of the JBR. Suction screens were added late in the demonstration project to prevent the gas cooling nozzles from being plugged by foreign material entering the gas cooling pump suctions.

2.2.2 JBR

From the gas cooling section, the flue gas enters the JBR. The JBR is the central feature of the CT-121 process. A simplified cross-section of this vessel is shown in Figure 2-3. The gas enters an enclosed plenum chamber formed by an upper deck plate and a lower deck plate. Sparger tube openings in the lower deck plate force the gas into the slurry contained in the jet bubbling (froth) zone of the JBR vessel. After bubbling through the slurry, the gas flows upward through gas risers which pass through both the lower and upper deck plates.

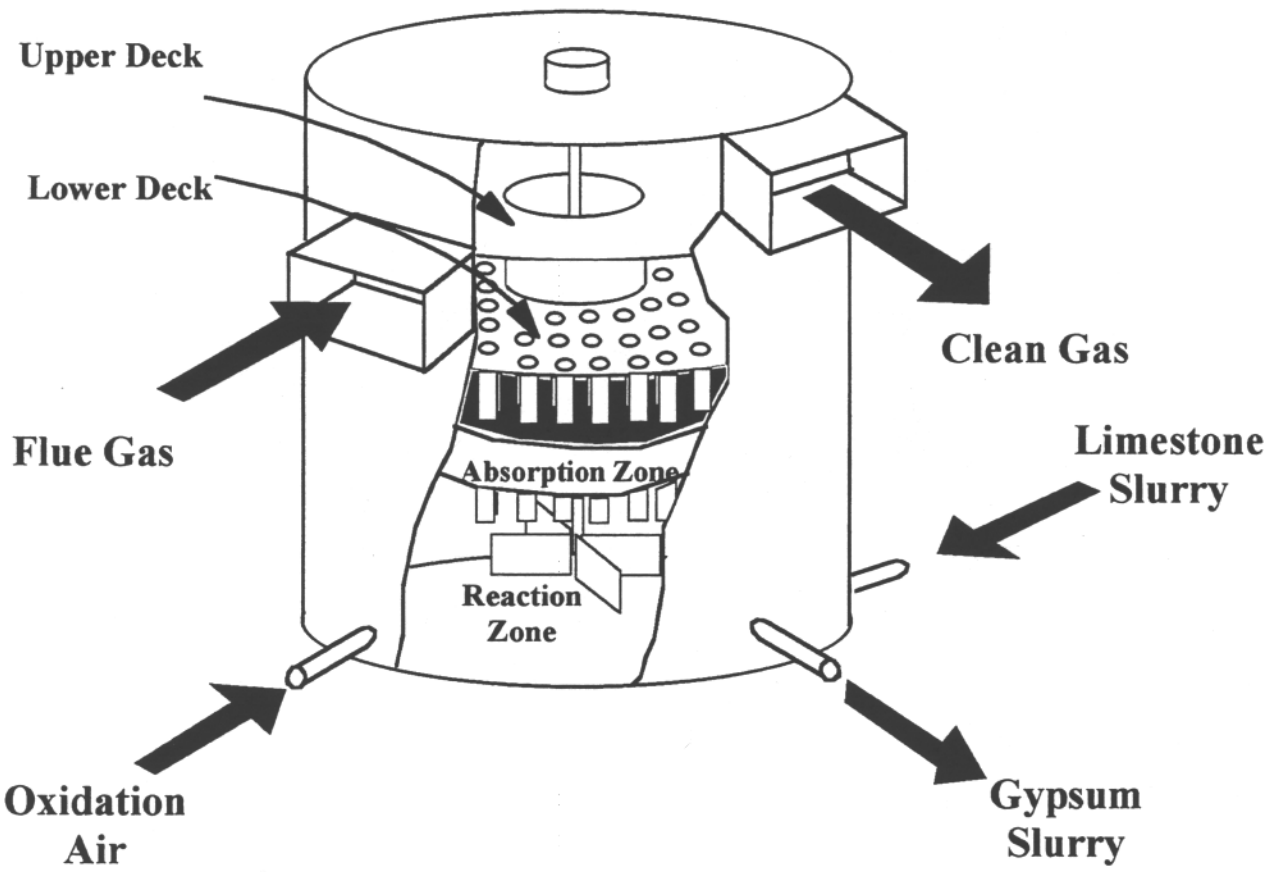

Figure 2-3. JBR Cross Section

Entrained liquor in the gas disengages in a second plenum above the upper deck plate, and the cleaned gas passes to the mist eliminator.

The slurry in the JBR can be divided into two zones: the jet bubbling or froth zone, and the reaction zone. SO_2 absorption occurs in the froth zone, while neutralization, sulfite oxidation, and crystal growth occur in both the froth and reaction zones. The froth zone is formed when the untreated gas is accelerated through hundreds of sparger tubes in the lower deck and bubbled beneath the surface of the slurry at a depth of 8 to 20 inches. The froth zone provides the gas-liquid interfacial area for SO_2 mass transfer to the slurry, as well as particulate removal. The bubbles in the froth zone are continually collapsing and reforming to generate new and fresh interfacial areas and to transport reaction products away from the froth zone to the reaction zone. The amount of interfacial area can be varied by changing the level in the JBR, and consequently, the injection depth of flue gas. The deeper the gas is injected into the slurry, the greater the interfacial area for mass transfer and the greater the SO_2 removal. In addition, at deeper sparger depths, there is an increase in the gas-phase residence time. SO_2 removal can also be increased by increasing the pH of the slurry in the froth zone, since a higher pH results in higher slurry alkalinity and more rapid neutralization of the absorbed SO_2. The pH is controlled by the amount of limestone fed to the reaction zone of the JBR. The solids concentration in the JBR is maintained by removing a slurry stream from the bottom of the reaction zone and pumping this stream to a holding tank (i.e., gypsum slurry transfer tank), where it is diluted with pond water before being pumped to the gypsum stack.

The oxygen that reacts with absorbed SO_2 to produce sulfate is provided to some extent by oxygen diffusion from the flue gas, but predominantly by air bubbled into the reaction zone of the JBR. The oxidation air lines enter the very top of the JBR vessel, penetrate the upper and lower deck plates, and introduce the air near the bottom of the JBR. Before the oxidation air enters the JBR, it is saturated with service water to prevent a wet-dry interface at the discharge of the oxidation air lines. Oxygen diffuses from the air into the slurry as the bubbles rise to the froth zone of the JBR. Excess oxidation air mixes with the flue gas and exits the JBR.

2.2.3 Mist Eliminator

From the plenum above the upper deck plate, the clean gas passes horizontally through the mist eliminator. Figure 2-4 shows a plan view of the mist eliminator section (Section labeling: 1F - first stage, front; 2R - second stage, rear, etc.). The mist eliminator is a horizontal-gas-flow, two-stage chevron design. The upstream and downstream surfaces of the first stage were washed for 1 minute every 2 and 4 hours, respectively, with gypsum pond return water (this frequency was doubled mid-way through the test block as part of the mist eliminator wash evaluation). The upstream face of the second stage was washed with make-up water for 1 minute every 24 hours. The wash liquor was returned to the reaction zone of the JBR.

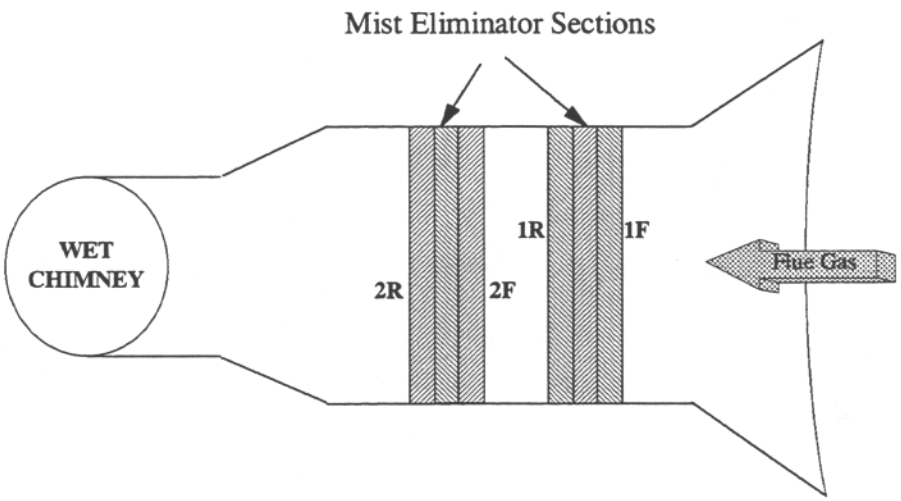

Figure 2-4. Mist Eliminator (Plan View)

2.2.4 Wet Chimney

After leaving the mist eliminator, the clean gas exits the system through a wet chimney. Since the gas enters the chimney saturated with water, any heat loss results in gas cooling and water condensation in the gas stream. To prevent carryover of the condensed water, a system

of gutters attached to the inside of the chimney collect and return the condensate to the JBR. FRP grating sections located in the elbow of the chimney provide a dead zone in the gas path, which allows the collected condensate to drain to the JBR without being re-entrained in the flue gas stream.

2.3 Limestone Preparation Circuit

The limestone preparation circuit is used to grind the limestone to a small enough particle size so that the amount of unreacted limestone needed in the JBR can be kept to a minimum.

Limestone is received in trucks and pushed into a pile with a front-end loader. From the pile, the limestone is transferred to a silo which feeds the wet ball mill system. Fresh limestone, gypsum pond water, and limestone slurry from the hydrocloneunderflow are fed to the mill. The effluent from the mill is held in a mill sump. Slurry from the mill sump is pumped to a hydroclone where the coarse and fine limestone particles are separated, with the fine limestone stream sent to the limestone slurry storage tank and the coarser material returned to either the mill inlet or recycled to the mill sump. From the slurry storage tank, the limestone is pumped to the JBR as required to maintain the froth zone pH. The baseline limestone grind for the demonstration project was 90% less than #200 mesh. Tuning of the wet ball mill was necessary to retain this grind size when the limestone source was changed for two Alternate Limestone Test periods.

2.4 Gypsum Stack

The slurry from the gypsum slurry transfertank was sent to one of two stacks designed for the purpose of dewatering and storing the gypsum byproduct solids. The gypsum stack, the smaller of the two stacks, was used during the low-particulate test period, and a larger, gypsum/fly ash stack was placed into service for the high-particulate test period. The gypsum/fly ash stack was larger since it had to dewater and store gypsum byproduct with a

high ash content compared with the relatively pure gypsum in the gypsum stack. Figure 2-5 shows an elevation view of the gypsum stacking area.

The stacking technique involves filling a high-density polyethylene- (HDPE-) lined diked area with slurry. The filled area is then partially excavated to increase the height of the containment dikes. The process of sedimentation, excavation, and raising perimeter dikes will continue on a regular basis during the active life of the stack. Process water is decanted, stored in the gypsum recycle water pond, and then returned to the process. A more complete discussion of gypsum byproduct handling, storage, and uses can be found in the Gypsum Quality Volume of this report.

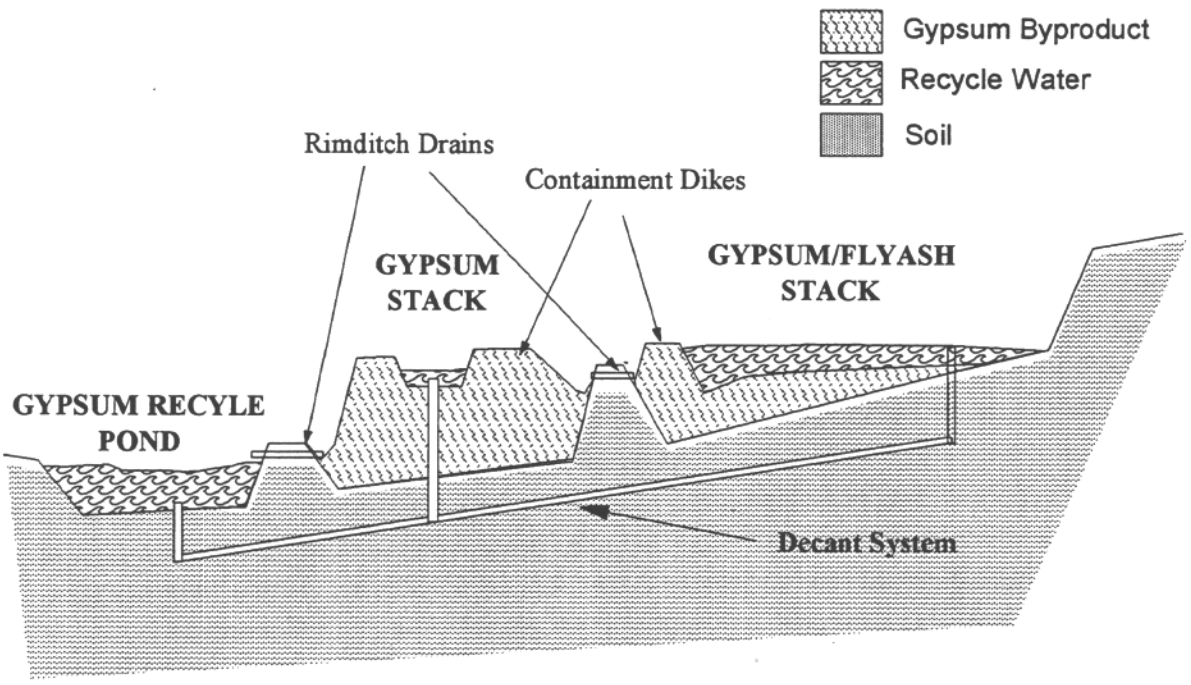

Figure 2-5. Gypsum Stacking Area - Elevation View

2.5 System Control

The three most critical control circuits *in* the process were the JBR level/ΔP control system, the JBR froth zone pH controller, and the JBR solids density controller. Each of these, as well as other key control systems, are described in detail below.

2.5.1 SO_2 Removal

During normal operation of the FGD system, the amount of SO_2 removed from the flue gas is controlled by varying the JBR ΔP (gas side differential pressure across the JBR). The ΔP is varied by changing the submergence depth of the gas sparger tubes. By increasing the ΔP across the JBR, the amount of gas-liquid surface area in the froth zone is increased. The increased surface area results in increased SO_2 removal. If the ΔP needed to reach the target SO_2 removal efficiency is outside of the established operating range, the froth zone pH set point can be varied as a secondary method of control. Increasing the froth zone pH provides more slurry alkalinity, and therefore, a greater capacity for SO_2 removal in the froth zone of the JBR. In certain cases, the pH can be increased (within a limited range) without lowering limestone utilization significantly, allowing higher SO_2 removal efficiency without the added fan power costs associated with raising the JBR ΔP.

2.5.2 JBR ΔP Control

JBR ΔP is the measure of gas side pressure drop between the inlet and outlet plenums of the JBR. The ΔP across the JBR is composed of two components, static head and dynamic head. The dynamic head results from the flow of the flue gas through the sparger tubes and gas risers. The static head is caused by bubbling the gas below the slurry surface; the greater the depth of the sparger tubes in the slurry, the greater the froth zone ΔP. The JBR deck ΔP is controlled by varying the static head (by varying the level of slurry in the JBR).

The option to directly control JBR level instead of deck ΔP was included in the design of this system; however, JBR level instrumentation did not perform as well as expected. Since level control could not be used without an accurate level indication, control of JBR deck ΔP was used exclusively for the demonstration project.

2.5.3 pH/Limestone Feed Rate Control

The pH in the froth zone of the JBR is controlled by varying the amount of limestone fed to the reaction zone. An increased limestone feed rate will increase the pH in both the reaction and froth zones. The two installed pH probes are located just below the sparger openings and provided a good representation of the pH in the froth zone of the JBR.

The limestone feed rate can be controlled in two ways: 1) feed-forward with pH trim; or 2) direct pH feedback control. At different times during testing, both means of control were used. A key factor determining the feasibility of feed-forward control was whether an adequate amount of data had been collected at similar process conditions to allow process modeling. For feed-forward control, the primary signals are the unit load and SO_2 pickup rate (a function of SO_2 removal efficiency and inlet SO_2 concentration). The amount of limestone that needs to be fed is then calculated based on a relationship between unit load, SO_2 pickup rate, and limestone feed rate. The limestone feed rate is trimmed with a feedback signal to maintain the pH set-point. The alternate method of control was to only use the pH feedback signal to control limestone feed. Feedback control merely requires a comparison of actual pH with a known pH setpoint.

2.5.4 Level Control

The levels in the JBR, gypsum slurry transfer tank (GSTT), and wash tank are maintained by adding gypsum surge pond water. The inability to use the JBR level control system was discussed in section 2.5.2, above. Because the gypsum slurry transfer pumps continuously pump approximately 1000 gpm from the GSTT to the gypsum stack to prevent settling in the

transfer line, the bleed rate from the slurry transfer tank will always be large enough to require some pond water to maintain level in the GSTT. The wash water tank was only used hourly as the mist eliminator wash, lower deck wash, and upper deck wash systems were automatically actuated. A tank level sensor signaled when the tank was low so that gypsum pond recycle water could be added to the tank.

2.5.5 JBR Solids Concentration Control

The suspended solids concentration in the JBR is controlled by discharging reaction zone slurry to the slurry transfer tank. The required feed rate to the slurry transfer tank is determined from the density of the JBR blowdown slurry. A dead-band controller is used to set the upper and lower JBR wt.% solids limits. For the majority of the demonstration project, the upper and lower JBR density limits were established at 24 wt.% and 22 wt.%, respectively. These limits were lowered to an average density of 15 wt.% while burning low-sulfur coal to maintain a consistent JBR solid phase residence time (approximately 30-35 hours) and to ensure that the JBR was operated with a negative water balance.

Water is added to maintain level in the JBR whenever slurry is drawn off for solids concentration control. Water is also added to the JBR for the purposes of deck washing, mist eliminator washing, or routine level control. To maintain a negative water balance, solids must be produced at a rate greater than or equal to the rate at which they are drawn off from the JBR. With the lower SO_2 pickup associated with the low-sulfur coal, fewer gypsum solids are produced per unit time; however, the routine addition of water is not similarly decreased. Because of this lower solids production rate, a lower equilibrium solids concentration will result and the percent solids setpoint must be lowered to maintain a negative water balance.

3.0 TECHNICAL APPROACH

The approach to the Yates CT-121 CCT project was to develop a series of test plans that would allow a complete evaluation of both the scrubber technology and the innovative design features incorporated into the Yates application of this technology.

3.1 Objectives

The primary objective of the CT-121 demonstration at Plant Yates Unit 1 was to evaluate the effectiveness of the following innovative design approaches:

- Fiberglass-reinforced plastic (FRP) construction of the jet bubbling reactor (JBR), other key process vessels, and the wet chimney;
- Elimination of the need for a prescrubber;
- Elimination of flue gas reheat;
- Elimination of the need for a spare absorber; and
- Simultaneous SO_2 and particulate collection.

To evaluate the effectiveness of these design advances, the following specific objectives of the two-year demonstration[1] program were established:

- Demonstrate long-term, reliable operation of the CT-121 FGD system;
- Evaluate particulate removal efficiency of the JBR and system operation at normal and elevated particulate loadings;
- Correlate the effects of pH and JBR gas-side pressure drop (ΔP) on system performance;
- Correlate the effect of limestone grind on system performance;
- Evaluate the impact of boiler load on system performance;
- Evaluate the effects of alternate fuels and reagents on system performance;

- Evaluate equipment and construction material reliability and performance; and
- Monitor solids properties, gypsum stack operation, and possible impacts of the gypsum stack on ground water.

3.1.1 Overall System Reliability

One of the specific objectives of the demonstration program was to evaluate the operability and reliability of the Yates CT-121 process, as constructed. The reliability of an FGD system is a function of the amount of outage time caused by equipment failures in the system. The performance indicators used to characterize and evaluate system reliability consist of Availability Index, Reliability Index, FGD Utilization Index, and Operability Index. These terms are defined as:

Availability Index	=	Hours the FGD system was available for operation divided by the hours in the period.
Reliability Index	=	Hours the FGD system was operated divided by the number of hours it was called on to operate.
FGD Utilization Index	=	Hours the FGD system was operated divided by the total hours in the period.
Operability Index	=	Hours the FGD system was operated divided by the hours of boiler operation in the period. (Due to the fact that the FGD system must always be operated when the boiler is in service, this value will always be unity).

3.1.2 Particulate Removal Evaluation

The ability to simultaneously remove SO_2 and particulate is a key advantage of the CT-121 process. To evaluate this capability, three different series of particulate measurements were performed. These measurements occurred at low-, high-, and moderate-particulate loading, and were completed concurrently with parametric testing used to characterize SO_2 removal efficiency under varied process conditions.

3.1.3 JBR ΔP, pH, and Boiler Load Effects on System Performance

JBR ΔP and pH are the principal operator-controlled variables used to control SO_2 removal efficiency in the CT-121 process. The SO_2 removal efficiency increases with increasing pH and with increasing ΔP (i.e., increasing sparger tube submergence depth). The selection of the operating setpoints for these variables in a commercial CT-121 application will depend on an economic evaluation of the trade-offs between SO_2 removal efficiency and the costs of increasing JBR ΔP and pH, while complying with the SO_2 removal efficiency determined by regulatory requirements. One of the specific objectives of the demonstration was to evaluate the response of the process to changes in JBR ΔP, pH and boiler load while varying the source of limestone and coal. The CT-121 process' response to these variables was measured under normal and elevated particulate loading conditions.

3.1.4 Limestone Grind Effects

Limestone is ground from 1" x 3/4" limestone to a size range of 90% <#200 mesh in a wet ball mill grinding circuit. Grinding the limestone is necessary to provide adequate surface area for dissolution and to maintain good limestone utilization. A trade-off exists between the cost of the energy used to grind the limestone and the raw materials cost savings resulting from the higher utilization.

Tests using an alternate limestone grind were performed to determine the impact of increased particle size on limestone utilization. These results were used in the optimization analysis to determine the most economical limestone grind for long-term operation. Determining the effect limestone particle size has on scrubber performance is an important step in optimizing scrubber operation. Grind size can impact limestone dissolution (which will affect limestone utilization), SO_2 removal efficiency, and the cost of operation. The larger the grind size at which the scrubber can operate successfully, the lower the ball mill power consumption. In cases of new installations, this information can be useful in ball mill sizing, thus potentially reducing capital costs.

3.1.5 Effects of Alternate Fuels and Reagents

For the CT- 121 process to be commercially viable, it must demonstrate flexible operation under a wide range of conditions. These conditions include varying limestone reagent sources, fuel sources, and fuel sulfur content. Coal from four different sources (with significantly different sulfur contents) and limestone from three different suppliers were used during the demonstration program to provide a wide spectrum of test conditions. Limestones from several different regions (i.e., geologically different) were evaluated to determine whether the CT-121 process had the flexibility to operate successfully in widely differing geographic regions. Likewise, scrubber performance was evaluated with the boiler burning coals with sulfur contents ranging from 1.2% to 4.3% to ascertain the flexibility of the scrubber with regard to boiler fuel selection.

3.1.6 Equipment and Materials Evaluation

The evaluation of the equipment and materials of construction is critical to the evaluation of system reliability. The scrubber system cannot operate in a reliable manner if any critical equipment fails or if there is a systemic problem with any of the materials of construction.

Equipment failures, as well as all maintenance actions, were documented during this demonstration project. Periodic inspections of the system, special material samples, and erosion resistant coatings were used in the evaluation of installed and optional materials of construction. This was especially critical during periods of elevated particulate loading, as was the case during the high-ash test period. Additionally, the susceptibility of the sparger tubes to plugging was monitored during the moderate-ash tests. During testing with the ESP completely de-energized, the fly ash exhibited a tendency to agglomerate on the inside surfaces of the sparger tubes.

3.1.7 Solids Dewatering Properties and Gypsum/Ash Stack Operation

The FGD byproduct gypsum solids are disposed of by stacking. Stacking combines the advantages of ponding and landfills -- low operating costs and equipment requirements, and

smaller space requirements and reduced environmental impact, respectively. For the high-ash test period, the previously unused "gypsum-fly ash" stack was placed into service. The gypsum-fly ash stack used for the high-ash period of testing was approximately twice the size of the stack used during the low-ash test period to accommodate the larger amount of solids produced due to ash removal in the scrubber. During both test phases, handling, stackabilty, and trafficability of the stacks were carefully monitored.

3.1.8 Air Toxics Removal Efficiency

An additional test objective was added after the test program began. This objective involved DOE-sponsored air toxics testing conducted at the Yates CT-121 scrubber. The testing was designed to evaluate the ability of the CT-121 process to remove both organic and inorganic toxic air pollutants. Additional, limited air toxics testing was added in conjunction with the last round of particulate testing to develop data on inorganic toxics removal under moderate-ash loading conditions. These tests were designed to provide a more detailed analysis of inorganic toxic species removal as a function of particle size.

3.2 Overall Test Schedule

The overall demonstration test consisted of two periods: a low-particulate test period with the ESP energized, and a high-particulate period with the ESP de-energized in a step-wise fashion. Figure 3-1 shows the final test schedule for the entire demonstration program. This plan incorporates revisions to the original test plan that were developed based on intermediate test results and plant scheduling requirements. As more was learned about the CT-121 process during testing, it was discovered that some tests were no longer necessary and others needed to be added or expanded. An example of this was the additional particulate removal testing that was conducted simultaneously with the first part of the High-Particulate Alternate Limestone Test period. This testing was added to develop more data on particulate removal under moderate-ash loadings, which was considered the most likely scenario for a future CT-121 retrofit. Also, because mist eliminator performance changed very slowly, the mist eliminator wash test plan (conducted concurrently with other testing, as shown in Figure 3-1) was expanded to allow a more lengthy evaluation period.

Figure 3-1. Final Demonstration Project Test Schedule

Another change involved altering the high-particulate test period to include testing at moderately elevated particulate loadings at the scrubber inlet. This change was in direct response to problems encountered during the High-Particulate Parametric Test block, specifically sparger tube plugging. The more moderate-ash loading was continued for the remainder of the test period, which included the Long-Term and Auxiliary Test blocks, to more realistically approximate the type of conditions expected in a retrofit to a boiler with a marginally performing particulate collection device.

3.3 Test Block Descriptions

As discussed above, the testing was divided into two periods, a low-ash test period and a high-ash test period. Each test period was further divided into three test blocks: Parametric, Long-Term, and Auxiliary Test blocks. Although the intent was to conduct each test block of the two test periods at identical conditions, so as to have a strong basis for comparison, this was not always possible due to the impacts of the high-ash loading in the second test period. Nor was duplication of test matrices always practical, since lessons learned in early testing were often applied in test plan revisions. The test plan for each test block is described in detail below.

3.3.1 Parametric Test Blocks

A full factorial parametric test matrix was planned for the Low- and High-Particulate Parametric Test blocks. A full-factorial matrix was designed to eliminate the need for a complex statistical analysis to evaluate the collected data and to provide for a comprehensive multi-variable regression model to be developed using the collected data. In addition to the full factorial matrix, the test plan also included selected tests to evaluate limestone grind.

The parametric tests characterized the performance of the process as a function of controllable process parameters. The following parameters were varied during these periods:

- Slurry pH;
- JBR ΔP; and
- Boiler load.

Table 3-1 shows the Low-Particulate Parametric Test matrix that was used.

Generally, the tests were divided into sets of three individual ΔP tests, with each individual test lasting 24 hours. An additional 24 hour line-out period was used between each test set to allow the system chemistry to reach equilibrium following a change in boiler load or pH. A similar test matrix was also intended to be used for the High-Particulate Parametric Test block. Due to unforeseen problems with inhibited limestone dissolution (a result of Al-F complexes in the slurry due to elevated ash concentrations), the pH was lowered from the original test matrix setpoints. The High-Particulate Parametric Test matrix is shown in Table 3-2.

3.3.1.1 Test Plan Deviations

There were several deviations from what was originally planned and the actual test matrix that was executed. These deviations were incorporated into the testing to learn more about the behavior of the process, as well as to respond to unexpected findings. Thus, the test plan was frequently "tuned" throughout the demonstration project.

Because the first limestone evaluated was relatively soft, it was difficult to tune the ball mill to provide a grind size larger than the baseline 90% < #200 mesh. It became obvious that no economic advantage could be gained by increasing the ball mill throughput to increase grind size and lower grinding costs. As a result, only four of the planned six coarse grind tests were performed (P1-31 to P1-34). Results from these tests showed that no measurable decrease in limestone utilization occurred with the coarser grind while within the design pH range. The limestone grind tests were subsequently removed from the High-Particulate Parametric Test matrix. The last two tests (P1-35 to P1-36) included operation with higher pH values (5.3 and 5.5) to determine the pH at which limestone utilization decreases.

TABLE 3-1
LOW-PARTICULATE PARAMETRIC TEST MATRIX

Test (P1-X) Number	Overflow pH	JBR ΔP in. WC	Boiler Load MW	Limestone Grind	Particulate Sampling
P1-1	4.5	8	100	90% <#200 Mesh	Y
P1-2	4.5	12	100		Y
P1-3	4.5	16	100		Y
P1-4	4.5	8	75		Y
P1-5	4.5	12	75		Y
P1-6	4.5	16	75		Y
P1-7	4.5	8	50		Y
P1-8	4.5	12	50		Y
P1-9	4.5	16	50		Y
P1-10	5	8	50		
P1-11	5	12	50		
P1-12	5	16	50		
P1-13	4	8	50		
P1-14	4	12	50		
P1-15	4	16	50		
P1-16	4	8	75		
P1-17	4	12	75		
P1-18	4	16	75		
P1-19	5	8	75		
P1-20	5	12	75		
P1-21	5	16	75		
P1-22	4.5	8	100		
P1-23	4.5	12	100		
P1-24	4.5	16	100		
P1-25	5	8	100		
P1-26	5	12	100		
P1-27	5	16	100		
P1-28	4	8	100		
P1-29	4	12	100		
P1-30	4	16	100		
P1-19R	5	8	75		
P1-20R	5	12	75		
P1-21R	5	16	75		
P1-31	4	12	100	70% <#200 Mesh	
P1-32	4.5	12	100		
P1-33	5	12	100		
P1-34	5.5	12	100		
P1-35	5.3	12	100	90% <#200 Mesh	
P1-36	5.5	12	100		

TABLE 3-2
HIGH-PARTICULATE PARAMETRIC TEST MATRIX

Test (P2-X) Number	pH	JBR ΔP (in. WC)	Boiler Load (MWe)	ESP Efficiency	Particulate Sampling
1	4.5	10	50	90	Y
2	4.5	16	50	90	Y
3	4.5	10	100	90	Y
4	4.5	16	100	90	Y
5	4.0	16	100	50	Y
6	3.5	10	100	0	Y
7	3.5	16	100	0	Y
8	3.5	10	50	0	Y
9	3.5	16	50	0	Y
10	3.75	13	50	0	
11	3.75	13	75	0	
12	3.75	13	100	0	
13	4.0	10	50	0	
14	4.0	13	50	0	
15	4.0	16	50	0	
16	3.5	10	50	0	
17	3.5	13	50	0	
18	3.5	16	50	0	
19	3.5	10	75	0	
20	3.5	13	75	0	
21	3.5	16	75	0	
22	4.0	10	75	0	
23	4.0	13	75	0	
24	4.0	16	75	0	
25	3.75	10	100	0	
26	3.75	13	100	0	
27	3.75	16	100	0	
28	4.0	10	100	0	
29	4.0	13	100	0	
30	4.0	16	100	0	
31	3.5	10	100	0	
32	3.5	13	100	0	
33	3.5	16	100	0	

A set of tests (P1-19 through P1-21, as shown in Table 3-1) were also repeated during the Low-Particulate Parametric Test block. This was done to capitalize on an unplanned deviation in coal sulfur content (from 2.5% S to 2.75% S). This deviation added an extra independent variable (inlet SO_2 concentration) to the statistical analysis of scrubber SO_2 removal efficiency.

The High-Ash Parametric Test matrix shown in Table 3-2 was originally planned to mirror the low-ash matrix. In fact, the first five tests used the same pH setpoints. Of course, the range of JBR ΔP values tested was altered slightly as more had been learned about the usable range of JBR ΔP during the low-ash test phase. During test P2-5, symptoms of aluminum fluoride inhibition of limestone dissolution (Al-F blinding) began to occur, requiring a decrease in the pH range tested to maintain acceptable limestone utilization. A more detailed discussion of this phenomenon is contained in Section 4 of this report.

One of the key differences between the Low- and High-Particulate Parametric Test matrices was the planned de-energization of the electrostatic precipitator (ESP). A step-wise approach was used to remove power from the ESP fields, both for safety reasons and to allow particulate loading measurements to be performed at several inlet particulate loading conditions.

3.3.2 Long-Term Test Blocks

The original strategy of the Low- and High-Particulate Long-Term Test blocks was to select an appropriate set of conditions and then operate at those conditions for an extended period of time. This is generally what occurred in both test blocks, although it was anticipated that some minor tuning of the test parameters might be necessary at the beginning of each test block.

The focus of these test blocks was to evaluate process variability and stability over an extended operating period and to determine the response of the process to transients, such as load changes and process upsets. A long-duration test, maintaining a consistent set of

operator-controlled process parameters, was determined to be the best means of accomplishing this goal. Load was allowed to vary with system electrical demand.

3.3.2.1 Low-Particulate Long-Term Test

Following completion of the Low-Particulate Parametric Test block, complete data analysis was not immediately available, so the long-term test was started with a set of process conditions, shown as test L1-1 in Table 3-3, designed to minimize limestone use during a period of supplier difficulties. The selected conditions also served to minimize SO_2 pickup and gypsum production, thus conserving space in the gypsum stack until appropriate long-term test conditions could be determined.

By the second week of testing, long-term test conditions were finalized, based on an analysis of the parametric test data and the decision to maintain the daily average SO_2 removal at 95%. These test conditions are shown as test L1-2 in Table 3-3.

Further evaluation of parametric test data led to a final revision of the test parameters, shown as test L1-3 in Table 3-3, to allow a safety margin between operating pH and the pH range (pH > 5.2) known to cause a significant drop in limestone utilization. Fortunately, parametric testing had established that SO_2 removal efficiency is not affected significantly by decreasing pH to as low as 4.5.

TABLE 3-3
LOW-PARTICULATE LONG-TERM TEST OPERATING PARAMETERS

Test I.D.	Start Date	End Date	pH	JBR DP (in. WC)	Unit Load (MWe)
L1-1	4/01/93	4/08/93	4.0	12	a
L1-2	4/15/93	4/28/93	5.0	14	a
L1-3	5/28/93	9/10/93	4.5	14	a

[a] Unit load on automatic load control, maintained in the range of 50-105 MW.

3.3.2.2 High-Particulate Long-Term Test

The primary purpose of this test block was to evaluate the ability of the Yates CT-121 process to successfully operate with elevated ash loading while in a load-following mode (i.e., operating at a load determined by system electrical demands), over an extended period of time. Another purpose was to compare the results of this operating period to those of the Low-Particulate Long-Term Test block.

Originally, the entire high-particulate test period was to be conducted with the ESP completely de-energized. After the High-Particulate Parametric Test block was completed, it was decided to conduct the remainder of the high-ash test period at a more moderate ash loading. It was decided that a lower ash loading, but one still more elevated than typically observed with the ESP fully in operation, would provide a more realistic operating scenario (i.e., one in which a CT-121 process was retrofitted to a boiler with a marginally performing particulate collection device). Based on mass-loading measurements performed at several different ESP conditions during the High-Ash Parametric Test block[2], an ESP configuration was selected that would result in approximately 90% particulate removal efficiency in the ESP.

The test plan called for the same test parameters as used in test L1-3 of the Low-Particulate Long-Term Test, shown in Table 34 as test L2-1. Because of the relatively high ash content in the slurry, elevated aluminum fluoride (Al-F) concentrations inhibited the limestone

TABLE 3-4
HIGH-PARTICULATE LONG-TERM TEST OPERATING PARAMETERS

Test I.D.	Start Date	End Date	pH	Controlling pH Probe	JBR DP (in. WC)	Unit Load (MWe)
L2-1	6/6/94	6/7/94	4.5	B	14	a
L2-2	6/7/94	8/17/94	4.0	B	14	a
L2-3	8/17/94	8/28/94	4.0	A	14	a

[a] Unit load determined by automatic load control, maintained in the range of 5010 5 MWe

dissolution at the tested JBR slurry pH of 4.5. This phenomenon is commonly referred to as "limestone blinding." As a result, the pH setpoint was lowered to 4.0, a level shown to favor more complete limestone dissolution during the high-ash parametric testing, even with the elevated concentrations of Al-F. This test condition, shown as test L2-2 in Table *3A*, was maintained for a majority of the test block.

Near the end of the test block, the control signal for the limestone reagent flow was switched from pH probe B to probe A. Since the pHs at these 2 locations had been differing by up to 0.5 pH units, the test was assigned a new reference number - L2-3. Test L2-3 was conducted until the end of the test block.

3.3.3 Auxiliary Test Blocks

The Low- and High-Particulate Auxiliary Test blocks were each comprised of the following three separate test periods, each approximately one month in duration:

- High Removal Tests;
- Alternate Coal Tests; and
- Alternate Limestone Tests.

The original test plan called for each test to be conducted at only a single set of specified conditions and with boiler load determined by automatic dispatch (based on system wide electrical demand). These plans were later revised to include limited parametric testing during each period so that data could be used to refine the existing parametric performance regression models. Test plans for each of these test periods are discussed in detail below.

3.3.3.1 High Removal Test Periods

The purpose of the High-Removal Tests was to evaluate system performance with low- and high-ash loadings under operating conditions that would yield the maximum SO_2 removal

efficiency, while maintaining safe and reliable operation of the scrubber. To accomplish this goal, the scrubber was operated at the highest practical pH and JBR ΔP setpoints. Although identical conditions for the low- and high-ash tests were planned, the presence of limestone blinding during the high-ash tests precluded operations at identical pH setpoints.

The test conditions for the Low-Particulate High Removal Tests are listed in Table 3-5. JBR slurry pH and pressure drop were held constant at levels determined to provide high SO_2 removal efficiency and reliable operation, while unit load was varied in the first three tests to provide parametric data to be integrated intothe performance model. The coal sulfur content during all four tests was approximately 2.5%.

TABLE 3-5
LOW-PARTICULATE HIGH REMOVAL REST MATRIX

Test I.D.	pH	JBR DP (in. WC)	Unit Load (MWe)
HR1-1	4.8	18	50
HR1-2	4.8	18	75
HR1-3	4.8	18	100
HR1-4	4.8	18	a

[a]As required by electric system load demand

The test conditions for the High-Particulate High Removal Test period are shown in Table 3-6. The test matrix consisted of 3 short tests, in which boiler load was again varied to quantify the effect of load under high SO_2 removal efficiency conditions. The fourth test was a longer, load-following period, in which boiler load was allowed to vary in response to the system electrical demand. Additionally, it was learned (since the Low-Particulate High Removal Test) that the JBR ΔP set point could be raised as high as 20 in. WC (as compared to 18 in. WC during the low-ash test) without jeopardizing scrubber operation.

TABLE 3-6
HIGH-PARTICULATE HIGH REMOVAL TEST MATRIX

Test I.D.	Duration (days)	Unit Load (MWe)	pH	JBR DP (in. WC)	ESP Efficiency (%)
HR2-1	2	100	4.0	20	90
HR2-2	1	75	4.0	20	90
HR2-3	2	50	4.0	20	90
HR2-4	9	a	4.0	20	90

[a] As required by electric system load demand.

Coincident with the beginning of this test series, a planned system-wide switch to low-sulfur (approximately 1.2%) coal was implemented. Additionally, the elevated ash concentrations in the slurry precluded operation at any pH above 4.0, which would risk initiating limestone blinding.

3.3.3.2 Alternate Limestone Test Periods

The purpose of the Alternate Limestone Tests was to determine the effects of limestone reagent from different sources on the operability and performance of the CT-121 process. Bench-scale test results showed that switching from the original limestone, obtained from Martin Marietta Aggregates' Leesburg, Georgia quarry, to limestone from Dravo Lime's Saginaw, Alabama quarry would yield byproduct solids that had a significantly larger gypsum particle size and better dewatering characteristics. Another limestone that performed well in bench-scale testing was from Florida Rock's Rome, Georgia quarry. The improvement in dewatering properties observed during bench-scale testing of the Dravo limestone was so significant, it was decided to switch to that limestone on a permanent basis if the full-scale Low-Particulate Alternate Limestone Test results confirmed the bench-scale results.

3.3.3.2.1 Low-Particulate Alternate Limestone Test Period

During the Low-Particulate Alternate Limestone Tests, a series of "clean" parametric tests was completed (after a scheduled outage, during which the JBR was cleaned) to determine if the JBR fouling and plugging that occurred during the long-term testing had adversely affected SO_2 removal efficiency. The "clean" parametric test data were to be compared with the "dirty" parametric test data collected at the conclusion of the High Removal Tests; however, the "dirty" parametric test data were lost due to CEM data acquisition problems. Nevertheless, the loss of data did not prevent a comparison of "clean" vs. "dirty" performance, since "dirty" performance data were available from the end of the long-term testing, and from the High Removal tests HR1-1 through HR1-4.

The test conditions for the "clean" parametric tests (tests P1B-n) and load-following tests are listed in Table 3-7. Note that these tests were conducted as part of the Alternate Limestone Test series. The duration of each parametric test varied from 9 to 30 hours, depending on the time needed to transition to each set of test conditions, the occurrence of CEM problems, and difficulties with Unit 1 operation. The load-following tests were completed over a 25-day period, with 15 days used to conduct the first test (AL1-1), and 5 days for the second test (AL1-2). Data from the "clean" parametric tests were used to supplement the performance regression model.

3.3.3.2.2 High-Particulate Alternate Limestone Test Period

The original purpose of the High-Particulate Alternate Limestone Test was to evaluate the effect of a different limestone reagent on scrubber performance and gypsum crystal morphology while at elevated particulate loadings. Several factors later altered the goal of this test period. One of those factors was the operating company's system-wide switch to low-sulfur coal (for use as Phase I compliance coal), which resulted in the opportunity to develop a parametric regression model that predicts scrubber performance at low inlet SO_2

TABLE 3-7
LOW-PARTICULATE ALTERNATE LIMESTONE TEST CONDITIONS

Test I.D.	Test Duration (hours)	Unit Load (MWe)	pH	JBR DP (in. WC)
P1B-1	17	100	4.5	10
P1B-2	26	50	4.5	16
P1B-3	11	50	4.5	10
P1B-4	21	100	4.5	16
P1B-5	10	50	5.0	16
P1B-6	23	100	5.0	16
P1B-7	16	50	5.0	10
P1B-8	11	100	5.0	10
P1B-9	30	50	4.0	16
P1B-l0	29	100	4.0	10
P1B-l1	11	100	4.0	16
P1B-12	9	50	4.0	10
ALl-1	360	System Demand	4.5	14
AL1-2	120	System Demand	4.0	10

concentrations. Another was the addition of an extra series of particulate removal and limited air toxics tests which were scheduled for the first week of this test period.

Based on these factors the test matrix shown in Table 3-8 was developed. Particulate and air toxics sampling efforts were scheduled during the first four tests of the series with the ESP partially de-energized to a target particulate removal efficiency of 90%. As it turned out, elevated particulate loading was experienced during all alternate limestone tests with the ESP fully energized because of degraded ESP performance that resulted from burning the low-sulfur coal. (The lower-sulfur coal exhibited decreased ash resistivity thus lowering the collection efficiency of the ESP).

TABLE 3-8
ORIGINAL ALTERNATE LIMESTONE COMPLIANCE COAL TEST MATRIX

Test Number	pH	JBR DP (in. WC)	Boiler Load (MWe)
AL2-1	4.0	18	100
AL2-2	4.0	10	100
AL2-3	4.0	18	50
AL2-4	4.0	10	50
AL2-5	4.5	18	100
AL2-6	4.5	10	100
AL2-7	4.5	18	50
AL2-8	4.5	10	50
AL2-9	5.0	18	100
AL2-10	5.0	10	100
AL2-11	5.0	18	50
AL2-12	5.0	10	50

During test A12-5, limestone blinding was encountered due to the elevated ash concentration in the JBR slurry. The ESP was completely energized in an attempt to decrease particulate loading and mitigate the effects of limestone blinding. However, the blinding persisted, even after the pH was lowered to 4.0. The causes and impact of this blinding are discussed in detail in Section 4.13 of this report. Due to the more tenacious nature of the blinding, the pH was eventually lowered to 3.75 to facilitate limestone dissolution. Because of the limited pH operating range available, the test plan was altered to take advantage of the flexibility of other controllable process parameters. The modified test plan is shown in Table 3-9. It was designed to permit an evaluation of the effects of JBR ΔP and boiler load on SO_2 removal efficiency. Since pH could not be raised without risking blinding, and the inlet SO_2 concentration was constrained by the low-sulfur coal, JBR ΔP and load were the only parameters that could be varied. A full factorial matrix of these test parameters was used, shown as AL2-6 through AL2-14 in Table 3-9.

TABLE 3-9
REVISED ALTERNATE LIMESTONE COMPLIANCE COAL TEST MATRIX

Test Number	pH	JBR DP (in. WC)	Boiler Load (MWe)
AL2-1	4.0	18	100
AL2-2	4.0	10	100
AL2-3	4.0	18	50
AL2-4	4.0	10	50
AL2-5	3.8	14	100
AL2-6	3.75	14	50
AL2-7	3.75	14	75
AL2-8	3.75	14	100
AL2-9	3.75	10	100
AL2-10	3.75	10	75
AL2-11	3.75	10	50
AL2-12	3.75	18	50
AL2-13	3.75	18	75
AL2-14	3.75	18	100

3.3.3.3 Alternate Coal Test Periods

The purpose of the third test series, Alternate Coal Testing, was to evaluate system performance and flexibility while using a higher sulfur coal (4.3% S, and 3.4% S for the low and high-particulate test periods, respectively) than had been previously burned (approximately 2.5% S). The calculated SO_2 absorption rate (i.e., lbs SO_2 per minute) using both of these coals exceeded the Yates CT-121 design SO_2 absorption rate. This provided a unique opportunity to evaluate the flexibility of the CT-121 system when operating outside of its design conditions. Modifications required to accommodate the higher sulfur coal included increasing the capacity of the limestone reagent slurry pumps and installing additional oxidation air blowers to ensure complete sulfite oxidation. Parametric testing wasconducted at both low- and high-ash loading conditions to further expand the range of operation for which the parametric regression model was valid.

Prior to the low-ash parametric testing, conditions were evaluated to determine the threshold oxidation air flow rate required to maintain complete sulfite oxidation in the JBR slurry.

Unfortunately, CEM difficulties prevented the collection of SO_2 removal efficiency data during this period; however, relatively accurate estimates of the $O:SO_2$ ratio could still be made from manually recorded data from control room monitors which were not affected by the CEMs calculational problems.

Operating conditions for the Low-Particulate Alternate Coal parametric tests are listed in Table 3-10. The parametric test plan was designed using standard statistical experimental design techniques, and is similar to that used during the alternate limestone "clean" parametric tests. The test data were used to create a second regression model for predicting SO_2 removal efficiency with high inlet SO_2 concentrations. Load-following operations were originally planned, but because of the limited supply of 4.3% sulfur coal, they could not be conducted during this test series. Full load operations were also not possible due to limitations on the capacity of the oxidation air blowers. This is discussed in more detail in Section 4 of this report.

The purpose of the High-Particulate Alternate Coal Test period (i.e., to evaluate system performance and flexibility) was similar to that ofthe low-ash testing, with the exception of having elevated particulate loading to the JBR. The original intention of the test was that it be conducted while burning 4.3% sulfur coal, as had been done during the low-ash test period. Unfortunately, only 3.4% sulfur coal was available, but the test did provide an opportunity to collect parametric data at a third inlet SO_2 concentration.

A parametric test series, shown in Table 3-11, was created to allow development of a more comprehensive model of the Yates CT-121 scrubber's performance over a wider range of inlet SO_2 concentrations. The test matrix was, again, limited to pH values of 4.0 to preclude aluminum fluoride blinding. During these tests, the ESP remained partially deenergized in an attempt to maintain a target ESP particulate removal efficiency of 90%.

TABLE 3-10
LOW-PARTICULATE ALTERNATE COAL TEST MATRIX
(4.3% S Coal)

Test I.D.	Unit Load (MWe)	pH	JBR ΔP (in. WC)
AC1-1	50	4.0	10
AC1-2	50	4.0	16
AC1-3	75	4.0	10
AC1-4	75	4.0	16
AC1-5	50	4.5	16
AC1-6	75	4.5	16
AC1-7	75	4.5	10
AC1-8	50	4.5	10
AC1-9	50	5.0	16
AC1-10	75	5.0	10
AC1-11	75	5.0	16
AC1-12	50	5.0	10

TABLE 3-11
HIGH-PARTICULATE ALTERNATE COAL TEST MATRIX
(3.4% S Coal)

Test Number	pH	JBR ΔP (in. WC)	Boiler Load (MWe)
AC2-1	4.0	14	100
AC2-2	4.0	14	75
AC2-3	4.0	14	50
AC2-4	4.0	10	100
AC2-5	4.0	10	75
AC2-6	4.0	10	50
AC2-7	4.0	18	100
AC2-8	4.0	18	75
AC2-9	4.0	18	50
AC2-10	4.0	14	a

[a] As required by electric system load demand

3.4 Particulate Removal Testing

The CT-121 process has the potential to remove a high percentage of fly ash entrained in a flue gas stream. This potential was evaluated at Plant Yates by performing several series of tests designed to characterize particulate (and sulfuric acid mist) removal under varying load, JBR ΔP, and inlet fly ash loading. Tests were planned that would evaluate the suitability of the CT-121 process to supplant a typical particulate control device (e.g., in a new plant application) and to control particulate emissions from a marginally performing electrostatic precipitator, as in a retrofit situation. To achieve these goals, three test series were conducted. The first two series were conducted using a 2.5% sulfur coal, and a third test series assessed system performance using a low-sulfur coal. The first test series, conducted in January 1993, provided a characterization of baseline performance under normal operating conditions. The second test series was designed to test CT-121 particulate removal performance under high-particulate loading conditions, and was completed in March 1994.

During the second test series, the ESP was also configured at some test conditions to simulate a marginally-performing ESP. The third test series, again simulating a marginally-performing ESP, was conducted in December 1994 while the unit was burning a low-sulfur coal. The desired test conditions were established by selectively detuning or deenergizing the three ESP fields or by the burning of low-sulfur coal. During each test series, a parametric test matrix was implemented to determine the effects of inlet ash-loading, unit load, and JBR ΔP on particulate emissions and particulate removal efficiency. Sulfuric acid mist removal and particle penetration as a function of size fraction were also evaluated. Sampling methodologies used during these testing events included:

- EPA Reference Method 5B[3] for determining non-sulfuric acid particulate emissions from stationary sources,
- Controlled condensation for determining sulfuric acid mist levels, and
- Cascade impactors for measuring particle size distribution.

Limited chemical characterization of collected particulate matter was alsodone during all of the testing periods. The test plan for each test series was updated from information or data gathered in the previous test series. The test conditions and detailed scope for each of the three different test periods are described in the following sections. The conditions and variables for the three test series are summarized in Table 3-12.

TABLE 3-12
SUMMARY OF PARTICULATE REMOVAL TEST CONDITIONS

Test Condition	Low-Ash Loading	High-Ash Loading	Moderate-Ash Loading
Test Date	**January 1993**	**March 1994**	**December 1994**
Coal Data:			
% Ash	11	9.5	11
% H_2O	13	12	8
% Sulfur	High	High	Low
ESP:			
On	X	x	
Off		x	
Detuned		x	x[a]
Load (MWe):			
High (100	X	x	x
Medium (75)	X		
Low (50)	X	x	x
JBR DP (in. WC):			
High (16)	X	x	x
Normal (12-14)	X		x
Low (8-10)	X	x	

[a] Although the ESP was operated normally (i.e., full energized), the low-sulfur coal caused the ESP particulate removal efficiency to drop to approximately 90%.

3.4.1 Low-Ash Particulate Removal Test

The first parametric particulate removal test was performed in January 1993 and consisted of a full factorial (3 x 3) test matrix. Triplicate samples were collected during each of nine different unit operating conditions. The ESP was operated normally (i.e., fully energized) during this test program, and the boiler was fired with the project baseline high-sulfur (2.5% S) coal. The full test matrix is presented in Table 3-13 with corresponding performance evaluation test I.D. numbers shown in parentheses.

Triplicate samples were collected at the JBR inlet and outlet to determine particulate loading and removal efficiency, sulfuric acid mist removal efficiency, and particle size distribution. In addition, selected particulate loading filters were analyzed for soluble Ca, SO_4, and SO_3. These substrates were then acid digested and analyzed for Na, K, Ca, Mg, and Fe. The substrates from one PSD sample were also water-extracted and analyzed for Ca and SO_4.

TABLE 3-13
OPERATING CONDITIONS, LOW-ASH PARTICULATE TESTING

Condition (Test I.D.)	ESP Operation	Unit Load (MWe)	JBR DP (in. WC)
1 (P1-1)	Normal	100	8
2 (P1-2)	Normal	100	12
3 (P1-3)	Normal	100	16
4 (P1-4)	Normal	75	8
5 (P1-5)	Normal	75	12
6 (P1-6)	Normal	75	16
7 (P1-7)	Normal	50	8
8 (P1-8)	Normal	50	12
9 (P1-9)	Normal	50	16

3.4.2 High-Ash Particulate Removal Test

Nine test conditions were also evaluated during the high-ash particulate removal test series. This test matrix is similar to that used during the low-ash particulate removal testing, except that load and JBR ΔP were each restricted to two conditions, and the ESP was operated at three particulate collection efficiencies (90%, 50%, and 0%). The test matrix is presented in Table 3-14. The unit was operating on project baseline high-sulfur (2.5%) coal. The ESP efficiency was controlled by only using the first field of the ESP for particulate removal. The majority of the testing was conducted with first field of the ESP either on or off. One day of testing was conducted with the first field "detuned" to increase particulate particle penetration to 50%. This test matrix provided insights into scrubber particulate removal characteristics with a marginally-performing ESP as well as how the CT-121 process might function as a combined particulate and SO_2 removal device.

TABLE 3-14
OPERATING CONDITIONS, HIGH-ASH PARTICULATE TESTING

Condition	ESP, First Field Status [a]	Unit Load (MWe)	JBR DP (in. WC)
1 (P2-1)	On	50	10
2 (P2-2)	On	50	16
3 (P2-3)	On	100	10
4 (P2-4)	On	100	16
5 (P2-5)	50% power	100	16
6 (P2-6)	Off	100	10
7 (P2-7)	Off	100	16
8 (P2-8)	Off	50	10
9 (P2-9)	Off	50	16

[a] The other two ESP fields remained completely deenergized.

Triplicate tests were again performed for particulate loading, sulfuric acid mist, and particle size distribution. An analysis of the filters and solids from the Method 5B tests was also done for soluble Ca, SO_4, and SO_3. These substrates were then acid digested and analyzed for Na, K, Ca, Mg, and Fe. The substrates from several PSD samples of the JBR outlet were also water extracted and analyzed for Ca and SO_4.

3.4.3 Moderate-Ash Particulate Removal Test

This test series characterized JBR particulate removal efficiency while burning a low-sulfur coal. The ESP was operated in a normal fashion; however, overall ESP removal efficiency dropped to approximately 90% due to reduced ash resistivity from the burning of low-sulfur coal. As a result, the ESP removal efficiency was roughly equivalent to that achieved with partially deenergized electrical fields while burning high-sulfur coals. These conditions allowed an evaluation of the particulate removal efficiency under the scenario of a marginally-performing particulate control device. The test matrix used is shown in Table 3-15.

TABLE 3-15
OPERATING CONDITIONS, MODERATE-ASH PARTICULATE TESTING

Condition	ESP [a]	Unit Load (MWe)	JBR DP (in. WC)
1 (AL2-1)	Normal	100	18
2 (AL2-2)	Normal	100	10
3 (AL2-3)	Normal	50	18
4 (AL2-4)	Normal	50	10

[a] The ESP was 100% energized, but exhibited reduced efficiency due to low-sulfur coal.

Results from the first two test series suggested that even though test methods were designed to measure non-sulfuric acid mist particulate, sulfuric acid mist was still present in the samples, especially at the JBR outlet. Therefore, the samples collected during this third test series were analyzed not only for sulfate, but also for other selected parameters so that fly ash rates could be estimated by use of a source apportionment model. Eliminating sulfuric acid

mist from samples was not deemed feasible given the low temperature and wet conditions of the JBR outlet. A complete sampling and analytical matrix for this test series is shown in Table 3-16.

TABLE 3-16
MODERATE-ASH PARTICULATE TESTING SAMPLING MATRIX

Test Condition	Number of Samples Taken			
	100 MWe High DP	**100 MWe Normal DP**	**50 MWe High DP**	**50 MWe Normal DP**
Stack				
Metals by Method 29 [a]	3	3		
Loading by Method 5B	3	3	6	6
Particle-Size Distribution by Cascade Impactor	3	2	2	2
JBR Inlet				
Metals by Method 29 [a]	3	3		
Loading by Method 5B	3	3	6	6
Particle-Size Distribution by Cascade Impactor	2	2	3	2
Process				
Mist Elim. H_2O			1	
JBR Slurry	1		1	1
Limestone			1	
Pulverized Coal	1	1	1	1

[a] Metals = Sb, As, Ba, Be, Cd, Co, Cu, ,Cr, Pb, Hg, Mo, Mn, Ni, Se, V, Al, Ca, Fe, K, Mg, Na, and Ti.

Another facet of this test series involved a comparison of sampling and analytical methods used by the U.S. EPA[4] and those provided in the Japanese Industrial Standards (JIS). This was done because all other similar particulate testing on CT-121 scrubbers was performed in Japan, and these data allowed a common basis for comparison. Samples collected by EPA Method 5B were also subjected to drying temperatures that adhere to the JIS. Table 3-17 presents an overall analytical matrix for the collected samples.

TABLE 3-17
MODERATE-ASH PARTICULATE TESTING ANALYTICAL MATRIX

Location/Type	Analysis
Multi-Metals, (EPA Method 29)	Trace: Sb, As, Ba, Be, Cd, Co, Cu, Cr, Pb, Hg, Mo, Mn, Ni, Se, S, and V. Major: Al, Ca, Fe, K, Mg, Na, and Ti.
Loading, (EPA Method 5B)	For source apportionment: Al, Ca, Fe, K, Mg, Mn, Na, S, and Ti
Process Grab Samples	
Mist Eliminator	Al, Ca, Fe, K, Mg, Mn, Na, S, Ti and Cl.
JBR Scrubber Liquor	Cl, Ca, and Mg
JBR Scrubber Solids	Metals[a]
Limestone	Al, Ca, Fe, K, Mg, Mn, Na, S, and Ti.
Pulverized Coal	Ultimate, proximate, and metals[a].

[a] Metals = Sb, As, Ba, Be, Cd, Co, Cu, Cr, Pb, Hg, Mo, Mn, Ni, Se, S, V, Al, Ca, Fe, K, Mg, Na, and Ti.

3.5 Air Toxics Testing

Air toxics testing was performed around the CT-121 process m cooperation with the DOE's program to characterize the toxic air pollutant emissions at eight coal-fired utility units. The purpose of the testing was to quantify air toxics emissions (as defined by the CAA Amendments of 1990) from the CT-121 process as well as determine the air toxics removal efficiency of the ESP and JBR. The information derived from DOE's program was furnished to the EPA for emission factor and health risk determinations. Following the DOE-sponsored air toxics program, a second and more limited inorganic air toxics characterization was conducted in conjunction with the moderate-ash particulate removal tests. The tests that were conducted during each of these air toxics test programs are described in the following sections.

3.5.1 DOE-Sponsored Testing

The test program performed by DOE was a comprehensive testing and analysis program designed to characterize the fate of inorganic and organic air toxics throughout the boiler, ESP and JBR systems. All influent and effluent streams associated with these processes were tested, along with internal process streams which were necessary to determine removal efficiencies of the various pollution control subsystems. The DOE-sponsored testing occurred in June, 1993, with the boiler operating at full load (100 MWe) on the program baseline 2.5% sulfur coal. Samples were collected from the following locations:

- Gaseous Streams—ESP inlet, JBR inlet, stack;
- Solid Streams—Raw coal, pulverized coal, pulverizer rejects, ESP hopper ash and raw limestone;
- Sluiced Streams—Bottom ash, combined ESP hopper ash, limestone and FGD scrubber solids; and
- Liquid streams—Ash pond water, gypsum pond water, ash sluice water, FGD slurry-blowdown filtrate, limestone slurry filtrate, coal pile run-off, and cooling water.

The primary targeted analytical parameters are listed by sample stream type in Table 3-18. Not all sample streams were analyzed for each parameter identified in Table 3-18. Complete program description and results are available in a separate document prepared by the DOE[5]. The information discussed in Section 4.10 of this report will focus on results from the multi-metals testing of the JBR inlet, stack, and coal feed. Results from organic analyses of the JBR inlet and outlet streams will be summarized.

TABLE 3-18
COMPREHENSIVE AIR TOXICS TESTING SAMPLING MATRIX

Analysis Type	Stream Type		
	Gaseous	Solid	Liquid
Metals	x	x	
Anions	x		
Cyanide/Ammonia	x		
Extractable Metals	x		
Metals by Size Fraction	x		
Mercury Speciation	x		
Radionuclides	x	x	
Chromium VI	x		
Particle Size Distribution	x		
Formaldehyde	x	x	x
Volatile Organics	x		x
Semivolatile Organics	x	x	x
Dioxins/Furans	x		
Ultimate/Proximate/HHV		x	

3.5.2 Limited Inorganic Air Toxics Testing

The third particulate removal test series was performed with a low-sulfur coal at moderate-ash loading. These operating conditions provided an opportunity to gain additional air toxics data while burning low-sulfur coal, so metals testing was performed on the JBR inlet and stack flue gas. Samples of the coal feed were also collected and analyzed for metals so that (limited) comparisons could be made with the results from the DOE-sponsored air toxics testing. The air toxics sampling and analytical matrix is presented in Table 3-19.

TABLE 3-19
AIR TOXICS SAMPLING AND ANALYTICAL TEST MATRIX

Sampling Location	Collection Method	100 MWe DP = 18	100 MWe DP = 10
JBR Inlet	(Draft) EPA Method 29	x	x
Stack	(Draft) EPA Method 2	x	x
Pulverized Coal Feed	Grab [b,c]	x	x

[a] Metals Sb, As, Ba, Be, Cd, Co, Cu, Cr, Pb, Hg, Mo, Mn, Ni, Se, S, V, Al, Ca, Fe, K, Mg, Na, and Ti.
[b] Ultimate, Proximate, metals
[c] Composite analysis

3.6 Mist Eliminator Wash Testing

Another facet of the test program was a performance evaluation of the mist eliminator wash system. Adequate wash rates and frequencies are critical to successfully operating the CT-121 process under elevated inlet particulate loading conditions. Based on early mist eliminator inspections, it was determined that the originally-scheduled 2-week evaluation of decreased wash frequency was insufficient for an adequate evaluation of the mist eliminator performance. The test was replaced with a program that called for varying the wash frequencies over the entire 2-year demonstration. The mist eliminator wash test matrix is shown in Table 3-20, and the associated wash frequencies are shown in Table 3-21.

TABLE 3-20
MIST ELIMINATOR WASH PERFORMANCE TEST MATRIX

Duration	Mist Eliminator Wash Frequencies	Ash Loading
5 months	Low	Low
5 months	High	Low
5 months	High	High
5 months	Low	High

TABLE 3-21
MIST ELIMINATOR WASH FREQUENCIES

Mist Eliminator Section	1F	1R	2F
High Wash Frequency	1 min. @ 2 hours	1 min. @ 4 hours	1 min. @ 24 hours
Low Wash Frequency	1 min. @ 4 hours	1 min. @ 8 hours	1 min. @ 24 hours

3.7 References

1. Sitkiewitz S.D. and O.W. Hargrove, "100-MW Demonstration of Cost Reductions to the CT- 121 FGD Process on High-Sulfur, Coal-Fired Boilers - Process Evaluation Test Plan." Radian Corporation DCN 92-261-044-01, October 28, 1992, p.4-1, 5-1 - 5-23.

2. "Particulate Sampling of Chiyoda CT-121 Jet Bubbling Reactor - Georgia Power Company Plant Yates Unit 1," Southern Research Institute Report SRI-ENV-94-497-7872.2F, July 13, 1994.

3. 40 CFR 60, Appendix A. *Test Methods.* "Method 5B: Determination of Nonsulfuric Acid Particulate Matter From Stationary Sources."

4. ibid.

5. U.S. Department of Energy, Pittsburgh Energy Technology Center. *"A Study of Toxic Emissions from a Coal-Fired Power Plant Utilizing an ESP while Demonstrating the ICCT CT-121 FGD Project."* DOE DE-AC22-93PC93253, June 1994.

4.0 RESULTS AND DISCUSSION

This section contains a detailed summary of scrubber operations and test results during the performance testing portion of the CT-121 demonstration project. Included in this summary are discussions of operating statistics, boiler operations, equipment performance, SO_2 removal efficiency, transient response, effects of alternate fuels and reagents, regression model development, particulate and air toxics removal efficiencies, variable operating costs, and analytical results.

4.1 Operating Statistics

Complete operating statistics for each test block during the entire demonstration are shown in Table 4-1. There were 19,000 potential operating hours during the CT-121 demonstration project, including the initial scrubber shakedown period. Of that time, the scrubber was operated for a total of 12,788 hours with a utilization index of 0.73, and was unavailable for operation only 654 hours resulting in an availability index of 0.97. Most of the time off-line was a result of either boiler related failures or "load-cut". Load-cut is a term used to describe a unit removed from service due to low electrical demand. Determining which units are load-cut is based on the comparative economics of operating the available units during periods of low power demand.

The low-ash test period exhibited superior operating statistics compared to those of the high-ash test period. Availability and reliability were each 0.98 during the low-ash test, while these indices were 0.95 during each the high-ash test period. The decrease in availability during the high-ash test period resulted from the increase in ash loading to the scrubber. A discussion of the operating statistics for each test block and explanations of off-line time and unavailability are detailed below. No such discussion is presented for the shakedown period that succeeded construction since this period was designed to test operation of the scrubber and the scrubber was frequently brought on- and off-line to prepare the process for the demonstration. Table 4-2 contains a summary of unavailability during the process evaluation.

TABLE 4-1
OPERATING STATISTICS SUMMARY

	Shakedown	Low-Particulate Parametric Test	Low-Particulate Long-Term Test	Low-Particulate Auxiliary Test	Low-Particulate Cumulative
Total Hours in Test Period	1914	1819	3912	4107	11749
Scrubber Available Hours	1866	1782	3750	4035	11433
Scrubber Operating Hours	1023	1689	2794	3096	8602
Scrubber Called Upon Hours	1071	1726	2840	3164	8801
Reliability[1]	0.96	0.98	0.98	0.98	0.98
Availability[2]	0.97	0.98	0.96	0.98	0.98
Utilization[3]	0.53	0.93	0.71	0.75	0.73

	High- Particulate Parametric Test	High-Particulate Long-Term Test	High-Particulate Auxiliary Test	High-Particulate Cumulative	Cumulative Project
Total Hours in Test Period	2332	2083	2836	7251	19000
Scrubber Available Hours	2151	2073	2689	6913	18346
Scrubber Operating Hours	1662	1847	1700	5209	13811
Scrubber Called Upon Hours	1795	1847	1847	5489	14290
Reliability[1]	0.93	1.00	0.92	0.95	0.97
Availability[2]	0.92	1.00	0.95	0.95	0.97
Utilization[3]	0.71	0.89	0.60	0.72	0.73

1. Reliability = Hours scrubber operated divided by the hours called upon to operate.
2. Availability = Hours scrubber available divided by the total hours in the period.
3. Utilization = Hours scrubber operated divided by the total hours in the period.

TABLE 4-2
SUMMARY OF FGD SYSTEM UNAVAILABILITY

Hours Unavailable	Description	Expected to Occur in Typical Full-Scale Installation?
37	HDPE slurry transfer pipe rupture	No
104	Scale removal in JBR	Yes, less frequent
12	Replacement of transition duct expansion joint	No
27	JBR inspection; repair broken gas cooling nozzle	Possible
19	Unblock clogged gas cooling nozzles	No
72	Wet ball mill lube-oil system failure	Not related to CT-121 process
181	Maintenance due to high-ash loading	No
10	Gas cooling header replacement	Possible
46	Gas cooling nozzle pluggage	Possible
100	Gypsum-fly ash stack leaking	Not related to CT-121 process
608	Total	

4.1.1 Low-Particulate Parametric Test Operating Statistics Discussion

There were 1829 hours in the Low-Particulate Parametric Test block. Of that time, the FGD system was called on to operate 1726 hours and was operated a total of 1689 hours. The remainder represents time that the FGD system was off-line due to boiler malfunctions or periods of low energy demand. The 37 hours of FGD system unavailability resulted from an underground rupture of a high density polyethylene (HDPE) slurry transfer pipe. It was later determined that this rupture was a result of a faulty connection and incorrect placement of the piping. The problem was quickly corrected and no other similar faults were discovered.

4.1.2 Low-Particulate Long-Term Test Operating Statistics Discussion

There were 3912 hours in the Low-Particulate, Long-Term Test block which was conducted from April through September 1993. Of that time, the unit and scrubber were on line a total of 2794 hours. The scrubber was available 3750 hours during the period, resulting in 162 hours of unavailability. Of the 162 hours, 104 hours of unavailability were due to scale removal efforts in May, a direct result of testing during which the recommended operating parameters (pH 3.0 - 5.0) were purposely exceeded. The scrubber was unavailable an additional 12 hours in June for replacement of the transition duct expansion joint, a result of improper initial installation. In July, 27 hours of unavailability resulted from an outage to inspect the JBR internals for erosion damage and to repair a broken gas cooling nozzle. The remaining 19 hours of time the scrubber was unavailable for operation occurred in August when the scrubber was taken off line to unblock some clogged gas cooling nozzles.

The scrubber was required to operate 2840 hours during the period. Most of the significant maintenance which resulted in unavailability occurred during periods when the scrubber was not required to operate, thereby resulting in a higher reliability index than the availability index, as shown in Table 4-1.

4.1.3 Low-Particulate Auxiliary Test Operating Statistics Discussion

There were 4107 hours in the Low-Particulate Auxiliary Test block time period. Of that time the scrubber was operated a total of 3096 hours. The scrubber was available for 4035 hours during this test block, resulting in 72 hours of unavailability. The 72 hours of unavailability were due solely to a failure of the wet ball mill lube-oil system. The lube-oil system failed because of limestone slurry overflow from the hydroclone underflow distribution chamber. This overflow allowed water from the slurry to enter the lube-oil system through the ball mill ring gear. This was determined to be a design flaw and should not be considered to reflect negatively on the reliability of the CT-121 process, since the ball mill system was designed and produced by another manufacturer. The ball mill failure required the system to come off-

line because of the lack of limestone reagent to neutralize the sorbed SO_2. Only one ball mill was included in this demonstration project. In most commercial applications, some redundant mill capacity would be included. There were no failures of the CT-121 scrubber island that resulted in unavailability during this test block. The 75% system utilization was a result of several boiler failures, a scheduled maintenance outage, and periods of low system load demand.

4.1.4 High-Particulate Parametric Test Operating Statistics Discussion

There were 2332 hours in the High-Particulate Parametric Test block time period. During that time the scrubber was operated a total of 1662 hours. The scrubber was available for 2,151 hours during this test block, resulting in 181 hours of unavailability. The reduced reliability (93%) and availability (92%) of the Yates CT-121 process during this test period (as shown in Table 4-1) resulted from several factors, including increased maintenance and inspection requirements associated with the high-ash loading in the flue gas entering the scrubber. The difficulties associated with operation under high-particulate loading include: the potential for aluminum fluoride-inhibited limestone dissolution, gypsum/ash plugging of the sparger tubes, and erosion damage to internal process components.

Typically, CT-121 availability exceeds 98%, so 92% availability is considered sub-standard for a CT-121 process, but it is still reasonable compared to many first-generation wet-FGD processes. Additionally, some of the time marked as unavailable was not utilized for repairs or maintenance. Instead, the time was expended waiting for parts and subcontractors to arrive. Because of low system electrical demand there was no hurry to return the unit to service during some of these periods. The week following the completion of the High-Particulate Parametric Test block was also included in the operating statistics for this period because that week was spent on maintenance required to recover from effects of the high-ash conditions of the test block.

4.1.5 High-Particulate Long-Term Test Operating Statistics Discussion

There were 2083 hours in the High-Particulate Long-Term Test block time period. Of that time the scrubber was operated a total of 1847 hours. The scrubber was available for 2073 hours during this test block, resulting in only 10 hours of unavailability. However, because the scrubber was not called on to operate during this time, no decrease in reliability resulted. The unavailability was due to a gas cooling header replacement that could not be conducted while on-line.

These operating statistics reflect excellent performance throughout the test period. The high availability and reliability indices, however, should not be interpreted to mean that operation with elevated particulate loading is without difficulties. Although the ash loading during this test period was moderate compared to that of the high-ash parametric testing (about 0.9 lb/MMBtu compared to over 5 lb/MMBtu), the highly abrasive nature of the slurry can result in faster wear of key components, such as the gas cooling system and slurry valve bodies. The elevated ash concentrations in the flue gas can also result in accelerated sparger tube fouling. While none of these events had a direct impact on the availability during this test block, the effects were cumulative and manifested themselves in required corrective maintenance at a later date. A forced outage (due to a boiler leak) near the end of the test block provided the opportunity to inspect and clean the JBR. Although the boiler problem caused the outage in this case, the scrubber would have eventually required cleaning which would have adversely affected the operating statistics.

4.1.6 High-Particulate Auxiliary Test Operating Statistics Discussion

There were 2836 hours in the High-Particulate Auxiliary Test block time period. Of that time, the scrubber was operated a total of 1700 hours with 1136 hours off-line. Of those 1136 hours, almost 600 hours were attributable to the scheduled annual boiler maintenance outage. The scrubber was available for operation 2689 hours in this test block.

Forty-six hours of scrubber unavailability were a result of gas cooling nozzle plugging which was caused when a FRP test coupon in the reaction zone shattered. The pieces of the coupon became lodged in the gas cooling nozzles, forcing the scrubber off-line to prevent excessive temperatures in the JBR inlet plenum. It should be noted that this problem is one that would not normally be associated with a commercial CT-121 installation. The test coupons were installed exclusively to gauge corrosion and erosion during the demonstration project and are not a part of the CT-121 design. The remaining (100 hours) scrubber unavailability was a result of difficulties with the gypsum-fly ash stack. Excessive weeping of process liquor through the gypsum-fly ash stack occurred when the stack's water level was raised too quickly. The scrubber and unit were brought off-line to prevent a full breach of the stack and to allow the water level to be lowered in a controlled manner. This incident is discussed in more detail in the Gypsum Quality volume of this report.

4.2 Generating Unit Operational Summary

The following section discusses boiler load and the changes in inlet SO_2 concentration throughout the demonstration project. At times during the demonstration, the boiler load was set to specific levels to accomplish specific tests. At other times, unit load was determined by system dispatch requirements. The inlet SO_2 concentration, a function of coal sulfur content, is typically expressed in units of parts per million (ppm) and is standardized to an inlet O_2 concentration of 3%.

4.2.1 Boiler Load

Boiler load for the entire performance evaluation portion of the demonstration project is shown in Figures 4-1 and 4-2 for the low-ash and high-ash test periods, respectively. 100 MWe represents 100% maximum rated capacity (MRC), although the unit can be operated under certain conditions to achieve loads as high as 108 MWe. The figures consist of plotted 4-hour averages, reduced from the collected 15-minute averages of process data.

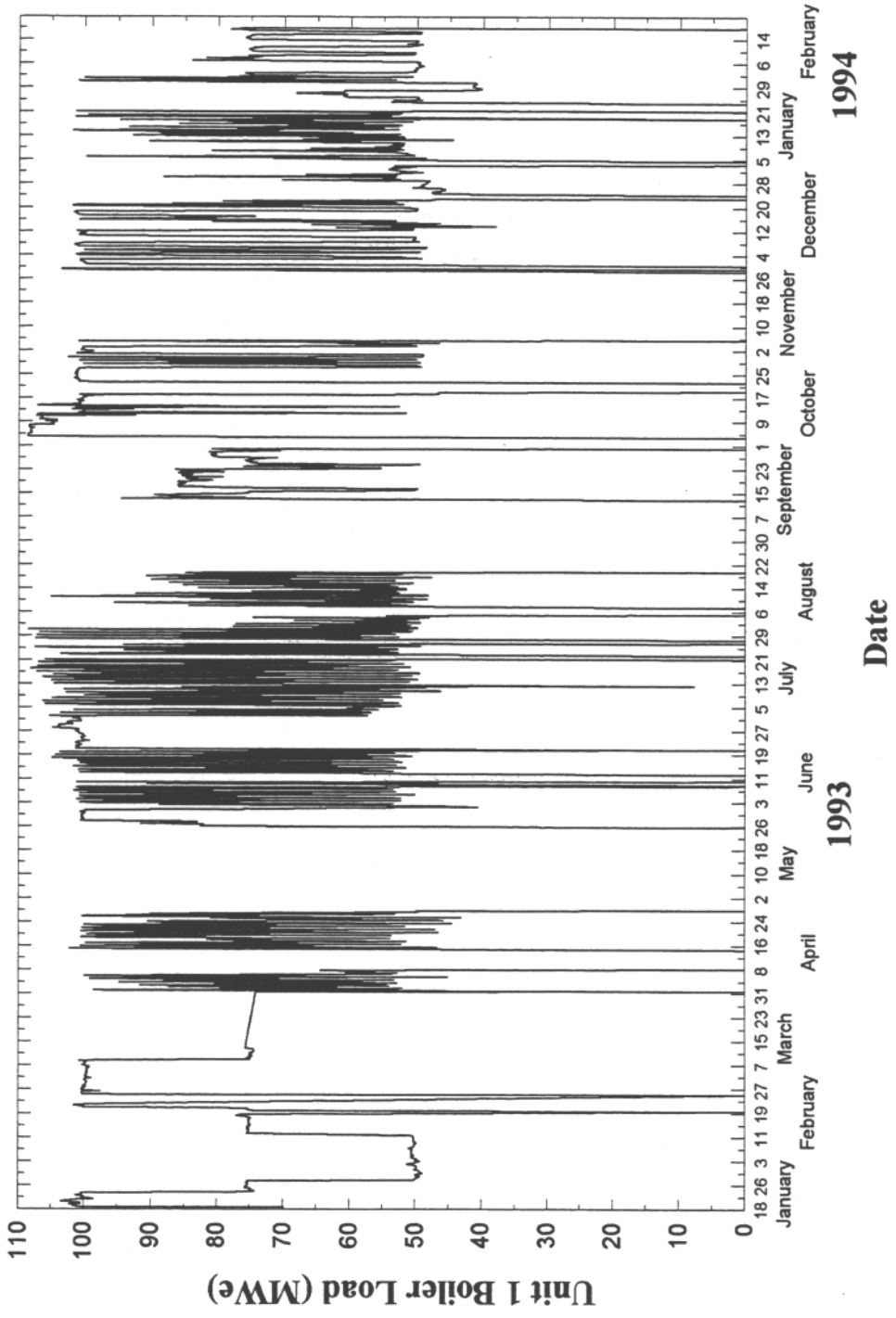

Figure 4-1. Low-Particulate Test Period Unit Load (4-hr averages)

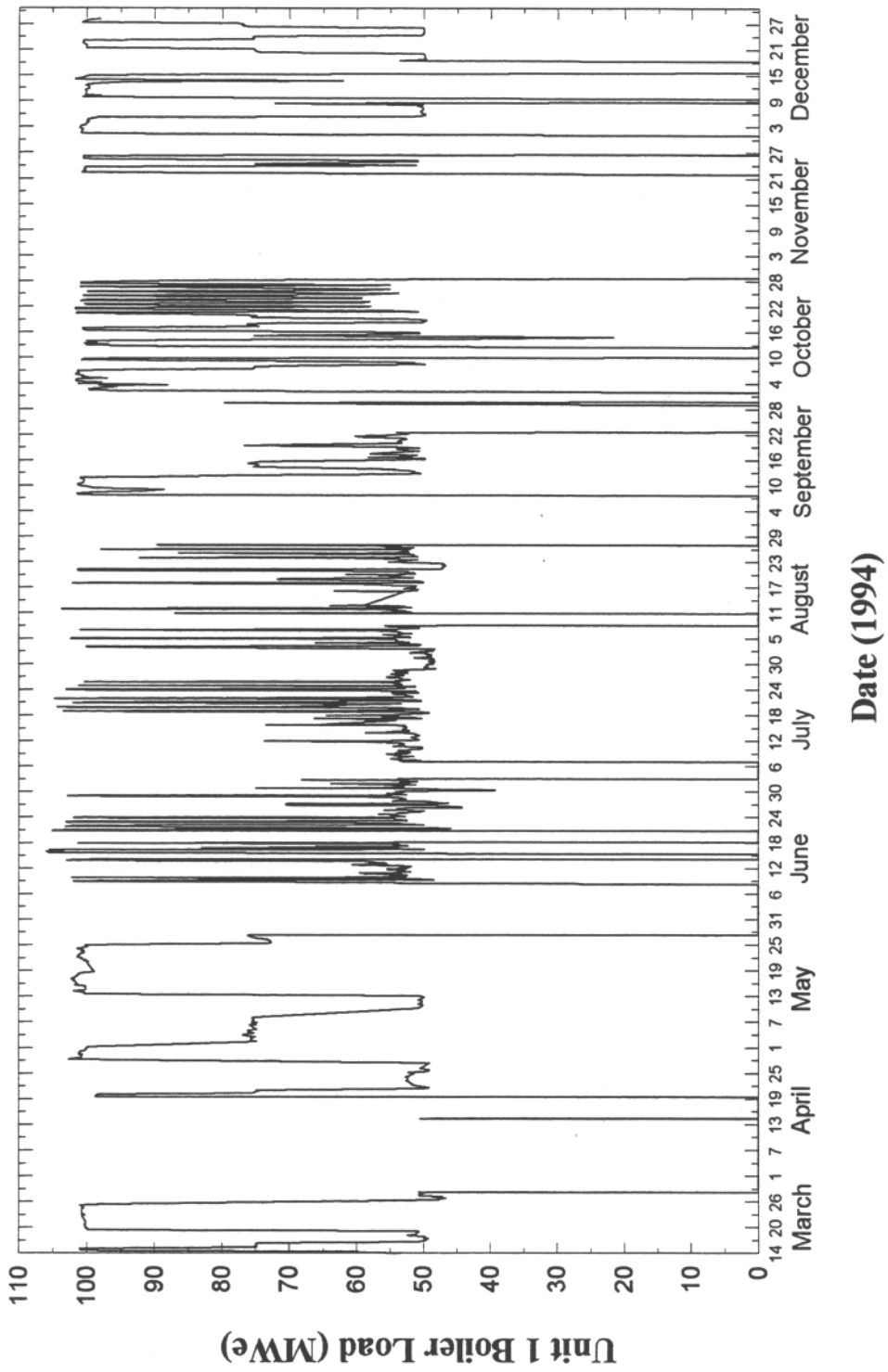

Figure 4-2. High-Particulate Test Period Unit Load (4-hr averages)

The unit was typically operated in one of two modes to accomplish the goals of the demonstration project. Load setpoints were specified while performing the parametric portions of the testing, both during the Parametric Test blocks and during selected portions of the Auxiliary Test blocks. This is the reason for the "stepped" appearance of the load data in some places on Figures 4-1 and 4-2. Load-following was used extensively during the Long-Term Test blocks, as well as during portions of the Auxiliary Test blocks. These periods are represented by the needle-like spikes seen on the plots. This is characteristic of typical load-following operations that require high loads during the peak-demand daylight hours and low loads in the low-demand evenings and nights.

Low-particulate parametric testing, which began on January 17, 1993, and ended on March 31, 1993, followed the test matrix shown in Table 3-1. The periods when the unit was off-line during the Parametric Test block were attributable to problems with the boiler I.D. fan and not attributable to the CT-121 process. One incident was related to freezing of a cooling water line that had not been heat-traced, and the other was a required outage to allow balancing of the I.D. fan. Both of these periods were of relatively short duration, as shown on Figure 4-1.

Long-term testing during the low-ash test period began on April 1, 1993 and was completed on September 10, 1993. The boiler load during this period was determined by economic dispatch, a condition where boiler load is determined by a combination of factors based on system-wide electrical demand and the cost of producing electricity, which can vary from boiler-to-boiler. The spiked appearance of the boiler load plots was a result of high electrical demand during exceptionally hot summer days, with decreased demand at night. A majority of the off-line time during this test block was the result of boiler outages and was not related to scrubber failures. The boiler-related failures included generator excitation field trips and process control electronic faults in June, and fouling of the make-up water intake on the plant ash-pond in July. These events did not have an adverse impact on the reliability and availability indices of the scrubber.

The lengthy "load-cut" outage in early May 1993 was used to clean the JBR, an effort necessary to recover from the effects of the low limestone utilization that occurred late in the Low-Ash Parametric Test block. Although scrubber fouling (including some scale build-up) existed, it did not interfere with the ability to meet scrubber SO_2 removal efficiency performance goals. The fouling eventually required cleaning, but the forgiving nature of the CT-121 process allowed this type of maintenance to be delayed until a convenient time. A brief outage was needed in August to unplug gas cooling nozzles, clogged with scale remaining from the May cleaning effort.

The Low-Particulate Auxiliary Test block took place between September 14, 1993, and February 14, 1994, and comprised three test series: High-Removal tests, Alternate Limestone tests, and Alternate Coal tests. The unit was typically operated in load-following mode, except when parametric testing was called for in the test plan (see Section 3.3.3). Load-following operations typically resulted in periods of maximum (near 100% MRC) load during the day, when demand was high, and minimum load (50% MRC) at night. Testing was suspended for several weeks in November during the scheduled annual boiler outage. The only other significant period of time off-line was during a failure of the ball mill lube oil system in October.

The High-Particulate Parametric Test block occurred between March 14, 1994, and May 28, 1994, requiring operation of Yates Unit 1 at loads of approximately 50, 75, or 100 MWe, similar to the low-ash parametric tests. No forced outages were required during this test block. The period between March 28 and April 19, 1994, was used for inspection and maintenance and is discussed in the Equipment Performance/Inspection section below.

The High-Particulate Long-Term Test block was conducted between June 6, 1994, and August 28, 1994. Load-following operation was selected to allow for process evaluation under realistic commercial operating conditions. As was done in the low-ash load-following test block, the boiler was placed on economic-dispatch. Typical summer-time load requirements are usually quite high in the southeastern U.S. Unlike the summer of 1993,

when the load on Yates Unit 1 averaged almost 75 MWe, the summer of 1994 was uncharacteristically cool and boiler load averaged only 60 MWe during this test block. Furthermore, as shown in Figure 4-2, there were very few periods of peak demand, which are useful for analyzing the scrubber's load-following, transient response capabilities.

The final test block of the demonstration, the High-Particulate Auxiliary Test block was conducted between September 7 and December 28, 1994. It comprised the same three test series as the Low-Particulate Auxiliary Test block: High Removal, Alternate Limestone, and Alternate Coal tests. From September 16 to September 23, the load demand was uncharacteristically low for this time of year, resulting in the observed, low average boiler load. Because of the desire to test the scrubber at true peak season load-following characteristics, higher load demand conditions were simulated during the load-following portion of the Alternate Coal tests. During this period, which lasted from October 20 through October 29, peak demand season load-following was simulated by increasing the load to 100 MWe during the day time and decreasing the load to 50 MWe at night. Load-following was not used during the Alternate Limestone test period (November 22 through December 28) because of the requirement for a significant amount of parametric data, which is the reason for the stepped appearance of those data in Figure 4-2.

4.2.2 Inlet SO_2 Concentration

Flue gas inlet SO_2 concentration is primarily a function of the coal sulfur content. It is one of the independent variables used in the development of performance regression models to estimate SO_2 removal efficiency. The other three variables are JBR froth zone pH, JBRΔP, and boiler load. Throughout this report, and within all figures and tables, inlet SO_2 concentration is expressed as ppm (dry basis), normalized to 3% O_2, unless otherwise indicated. Coals from several different sources, each with a different sulfur content, were used during the demonstration. The different resulting inlet SO_2 concentrations were critical to the development of the performance model, but in some cases, unplanned variations made data correlation difficult.

Plots of inlet SO_2 concentration are shown in Figure 4-3 and 4-4 for the low- and high-ash test periods, respectively. With the exception of the alternate coal tests and the planned facility-wide switch to low-sulfur coal, the inlet SO_2 concentration was fairly consistent throughout the demonstration project. This is because a separate coal pile was maintained for Yates Unit 1 to ensure consistency of the baseline coal (around 2.5% sulfur) for the duration of the demonstration project. A separate pile was also used for each of the alternate coals evaluated to avoid accidental mixing with the main coal pile.

Figure 4-3 shows some variation in inlet SO_2 concentration during the Low-Particulate Parametric Test block. The baseline 2.5% sulfur coal normally resulted in inlet SO_2 concentrations of approximately 2200 ppm. Some coal fluctuation is normal but for two brief periods, SO_2 concentration was as high as 2500 ppm. Full advantage was taken of the fluctuations, allowing inlet SO_2 to be included as an independent process variable in the regression analyses of the results.

Inlet SO_2 concentration trends during the Low-Particulate Long-Term Test period show that the coal sulfur content was relatively constant throughout the test period, allowing for a consistent basis for performance comparison. There was a slight decreasing trend in coal sulfur content during this test block, but the average coal sulfur content remained relatively constant.

The coal sulfur content during the Low-Particulate Auxiliary Test block was fairly consistent at around 2200 ppm through the end of the Alternate Limestone tests. Note that Figure 4-3 shows a drop in SO_2 concentration between the Alternate Limestone and Alternate Coal test periods (around January 15, 1994). When the coal from the Unit 1 pile was completely expended, it was necessary to operate using the Units 2-7 coal pile (lower sulfur coal) while awaiting delivery of the higher sulfur (4.3%) coal for use in the Alternate Coal test period. Once the 4.3 % sulfur coal was in place, the inlet SO_2 concentration increased to approximately 3700 ppm, and the Alternate Coal testing was begun.

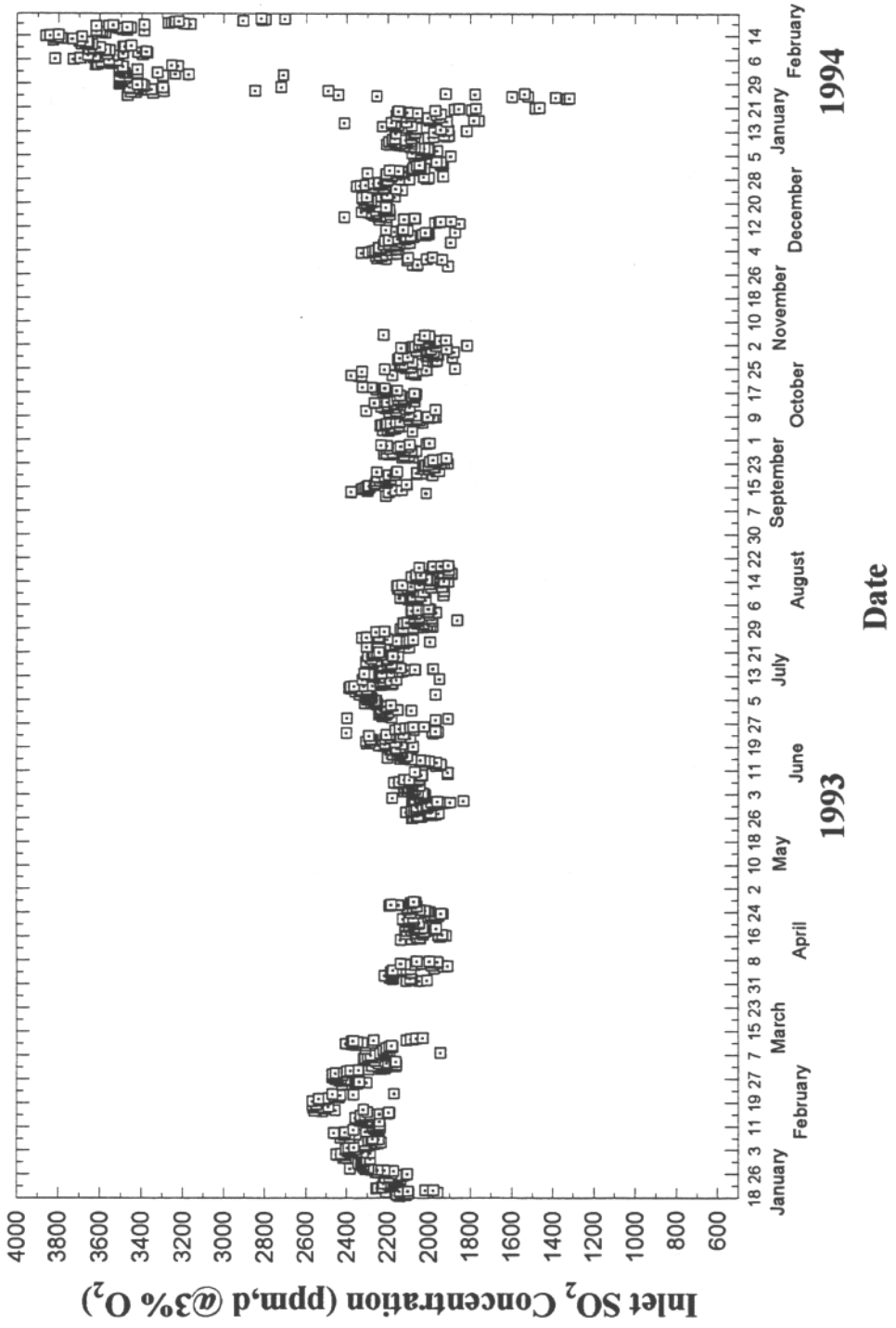

Figure 4-3. Low-Particulate Test Period Inlet SO_2 Concentration (4-hr averages)

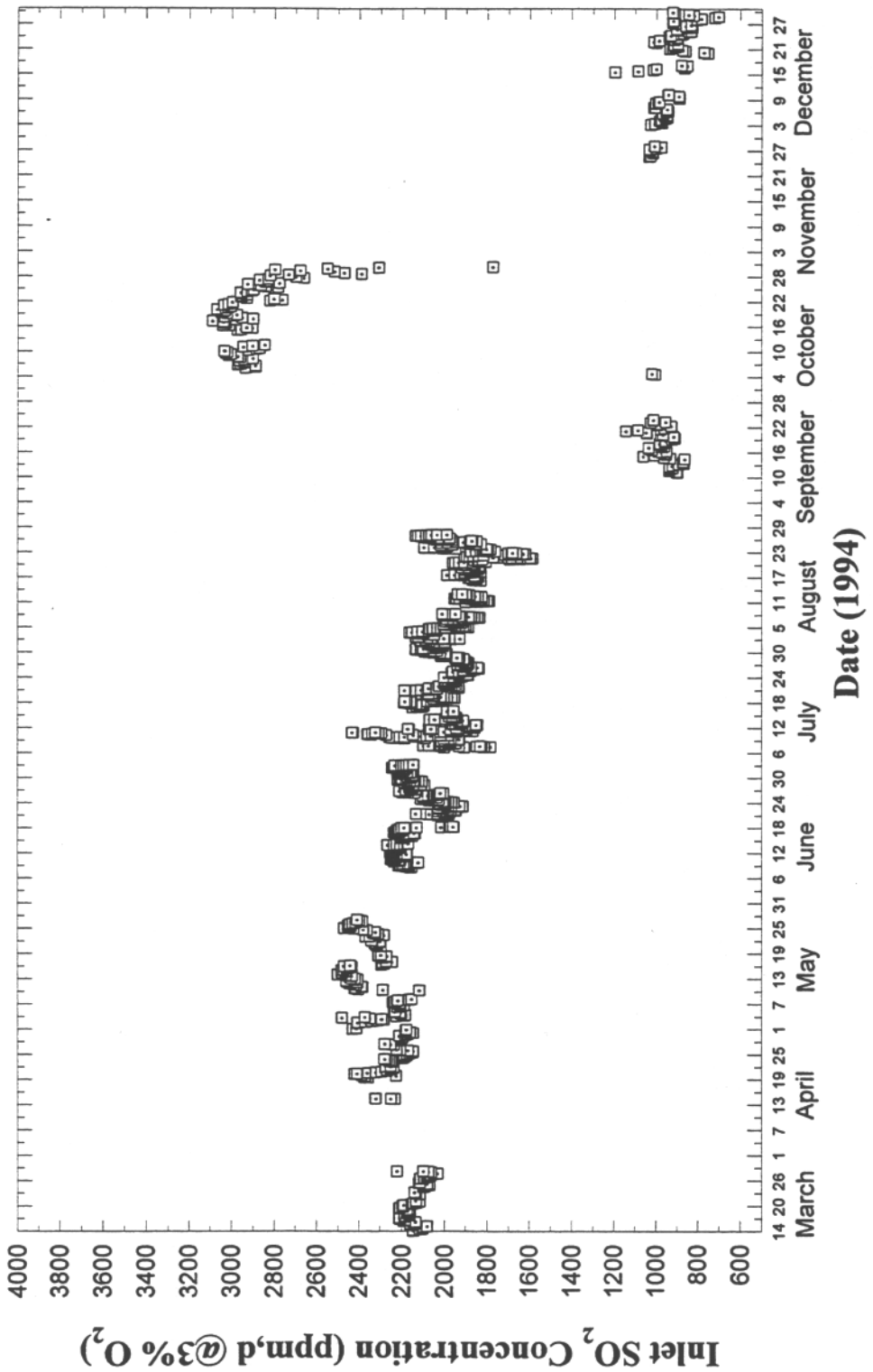

Figure 4-4. High-Particulate Test Period Inlet SO_2 Concentration (4-hr averages)

After the decommissioning of the Southern Company's central coal processing facility, the Pride Transloader, during the High-Particulate Long-Term Test block, the sulfur content of the coal burned by Unit 1 became somewhat variable during the test period as shown in Figure 4-4. During the month of July, the inlet SO_2 concentration of the flue gas entering the scrubber began to drop below the target concentration range of 2100 - 2200 ppm. This was a result of heavy rains in July. Because of these heavy rains, the Unit 1 coal pile, which contained 2.4 - 2.5% sulfur coal, became unusable. Coal from the main plant (Units 2 through 7) pile was used to supplement the coal already in the Unit 1 bunkers. Since this coal was more variable in sulfur content (a result of many different types of coal being burned over many decades), the average sulfur content of the coal burned in Unit 1 was diluted on several occasions. The average coal sulfur content burned by Unit 1 was 2.24 % in July, as determined by proximate analysis. Full coal analyses for the demonstration are located in Appendix C.

In August 1994, the remainder of the project's 2.5% sulfur coal had been used, and the Plant Yates coal pile began receiving 1.2% sulfur coal. This coal was purchased by the plant so that other units at Yates could comply with Phase I requirements of Title IV of the 1990 Clean Air Act Amendments (CAAA). The existence of several different coals on the coal pile resulted in the inlet SO_2 concentration varying between 1500 ppm and 2500 ppm throughout the month. While the inlet SO_2 concentration affects SO_2 removal efficiency, the efficiency results were normalized to a common SO_2 concentration by using the Yates performance regression model's SO_2 concentration terms. The performance model has been shown to be valid for inlet SO_2 concentration values as low as 1500 ppm. Once inlet SO_2 levels fall below 1500 ppm, the model can no longer accurately normalize SO_2 removal efficiency values. This normalization of data is discussed in more detail later in this report.

Unit 1 began burning a low-sulfur bituminous coal (approximately 1.2% S) at the beginning of the High-Ash Auxiliary Test block. This unplanned (i.e., it was not in the original test plan) switch to low-sulfur coal in Unit 1 was a result of the entire plant's shift to this coal source for Phase I compliance[2] and the decommissioning of the Southern Company's central

[2] Phase I of the Clean Air Act Amendments (CAAA) of 1990, with an effective date of January 1, 1995.

coal distribution facility, from which the high-sulfur coal had been shipped throughout the demonstration project. The burning of low-sulfur coal was interrupted in October for the Alternate Coal Test block. During this period a high-sulfur coal (approximately 3.4% sulfur) was burned to allow the evaluation of a different coal and to further develop the parametric regression model. Once the high-sulfur coal tests were completed, the scheduled annual boiler maintenance outage began and lasted through most of November, 1994. Upon completion of the outage, operation using the low-sulfur coal resumed for the Alternate Limestone tests.

4.3 Equipment Performance/Inspection Results

An evaluation of the reliability and operability of the equipment and materials of construction was an important part of the CT-121 demonstration. There were two major factors which differentiate this scrubber from other CT-121 systems evaluated in this country m the past, or operated anywhere else in the world. The first difference was the extensive use of fiberglass reinforced plastics (FRP) throughout the design. FRP was used almost exclusively in the construction of the JBR, wet chimney, scrubber inlet and outlet transition ducts, several auxiliary tanks, and several slurry piping systems. The resistance of these materials to the erosive and corrosive forces at work in the scrubber was a key focus of this evaluation. The second difference was the operation of the process in a closed-loop manner, without the use of a prescrubber. The resulting chloride (Cl^-) concentrations in the scrubber were exceptionally high and had the potential to cause corrosion of many of the materials of construction. The discussion of equipment performance in this section is limited to observations made during process inspections and to discussions of equipment failures that had a significant impact on process operations. An extensive and detailed discussion on all facets of materials and maintenance can be found in the Materials and Maintenance volume of this report.

Several difficulties persisted throughout the demonstration project. This section is organized into a discussion of these underlying material issues, followed by a test block-by-test block discussion of equipment failures and process inspections.

4.3.1 Equipment Difficulties

There were several ongoing, but intermittent maintenance issues that persisted throughout the demonstration. These issues included erosion of the FRP in the inlet transition duct and JBR inlet plenum, plugging in the gas cooling nozzles, gypsum build-up on the JBR lower deck, failures of slurry gate valves, deterioration of rubber lined piping, pH measurement difficulties, and erratic JBR level control.

4.3.1.1 Slurry Erosion

A set of forty gas cooling nozzles distributes over 4000 gpm of scrubbing slurry cocurrently into the JBR inlet transition duct to humidify and cool the flue gas upstream of the inlet plenum. The high solids content (typically about 23 wt.% solids) and high velocity of the slurry and flue gas resulted in high abrasive forces on the materials of the transition duct and upstream face of the JBR inlet plenum. Although it was initially believed that the FRP could withstand this, it soon became apparent that corrective action and further preventative measures would be required.

Figures 4-5 and 4-6 show examples of the erosion just over four months into the low-ash test period. Several types of repair techniques using purported erosion-resistant materials were employed, including the one illustrated in Figure 4-7. As shown in Figure 4-8, taken of the same location only 4 months later, some materials were unsuccessful in mitigating the erosion. A material, known as Duromix™, was evaluated as the best choice for erosion resistance during a multiple material evaluation effort. This material was applied to all wear-prone surfaces during subsequent outages as shown in Figure 4-9. Although the material was effective in the prevention of erosion damage, some adherence difficulties were encountered with the material as shown in Figures 4-10 and 4-11.

Figure 4-5.
JBR Inlet Plenum Erosion Damage

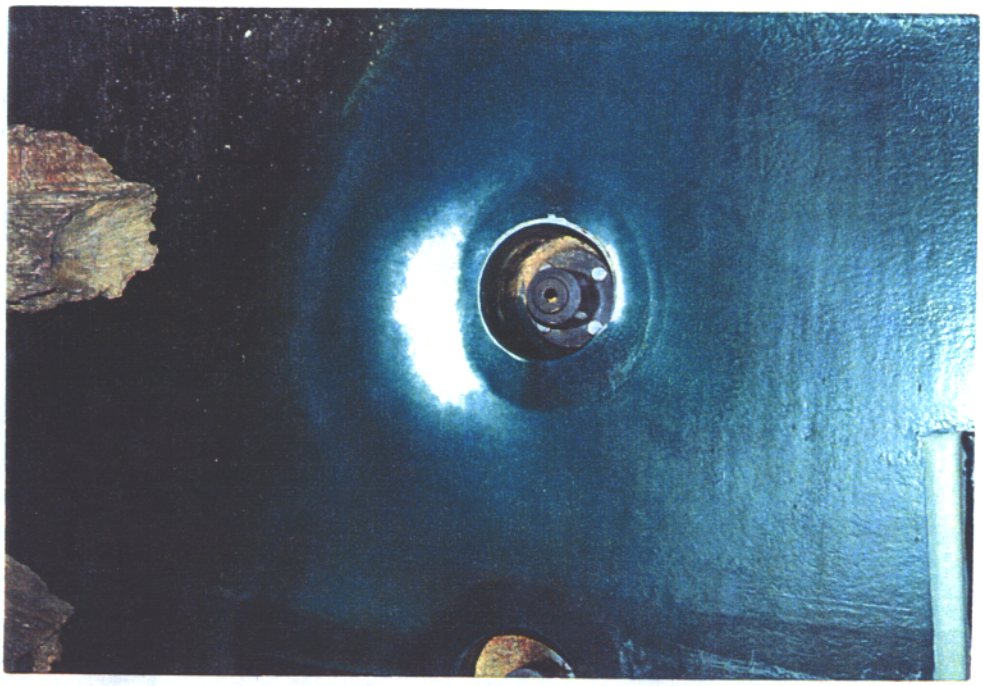

Figure 4-6. JBR Transition Duct Erosion

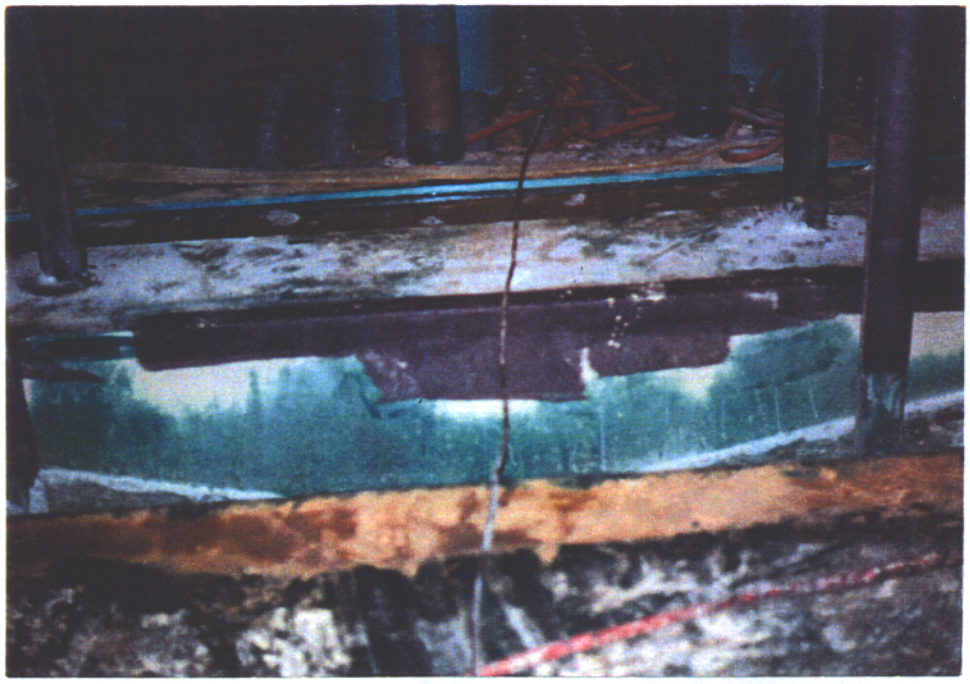

Figure 4-7. Early Patching Attempt

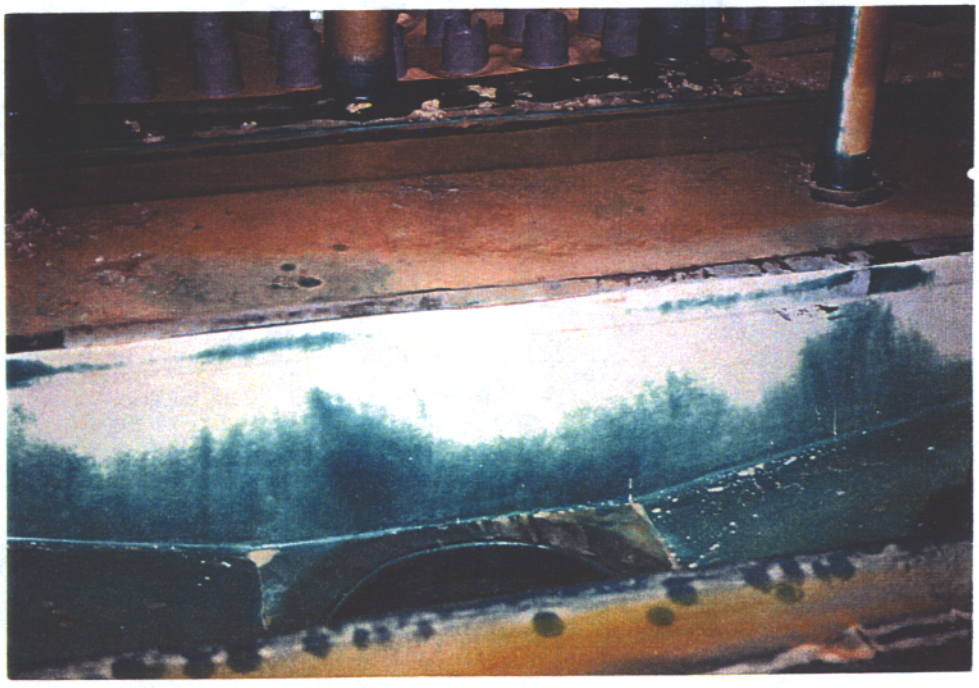

Figure 4-8. Erosion Resistant Material Effectiveness - four months later

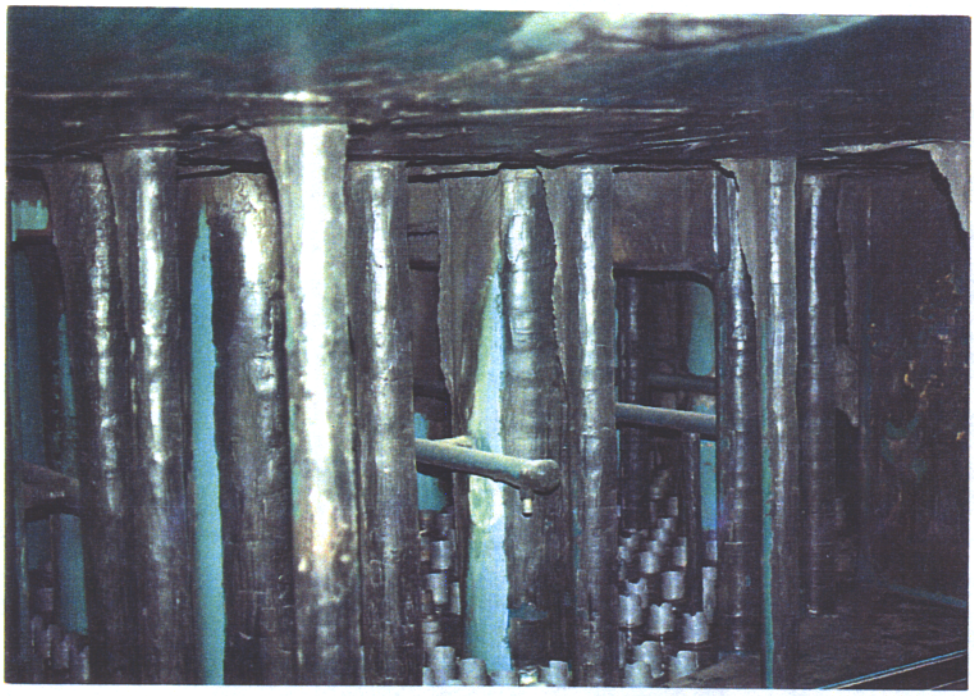

Figure 4-9. Duromix Application to the JBR Inlet Plenum

Figure 4-10. Duromix Adherence to Wall-Mounted Gas Cooling Nozzle

Figure 4-11.
Duromix Adherence
to JBR Lower Deck Support

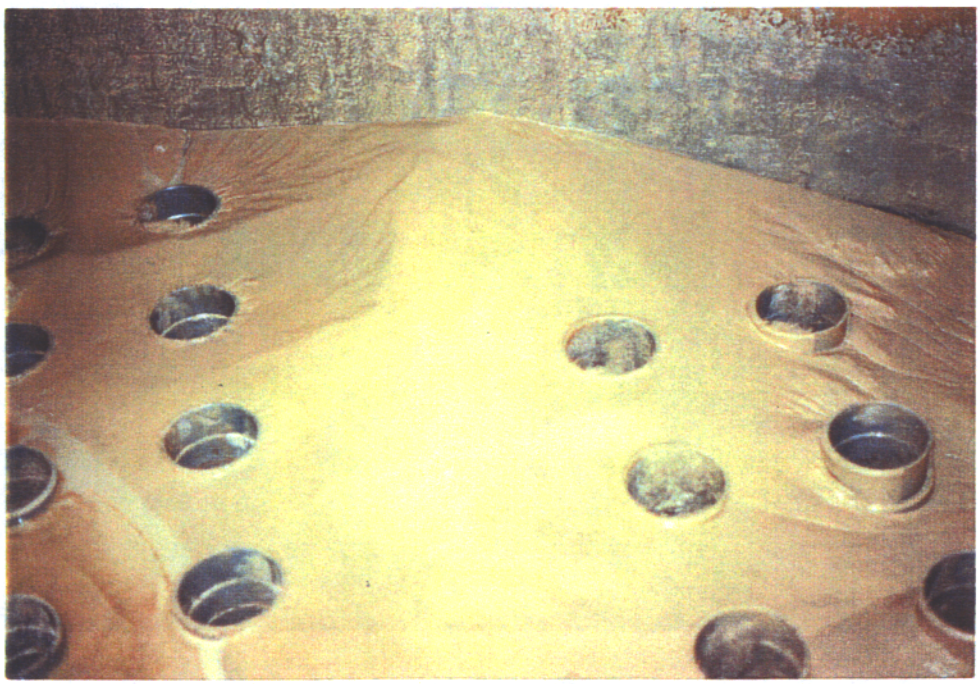

Figure 4-12. JBR Lower Deck Solids Build-up

As more advanced application procedures were developed, the adherence problems did eventually decrease, even under the highly abrasive, high-ash loading conditions of the second period of testing.

At no time did the erosion result in penetration through the outer walls of the transition duct or the JBR, but without the existing diligent inspection and repair program, it might have happened. As it was, on several occasions (including that illustrated in Figure 4-5) there was penetration through upper deck drain pipes which allowed flue gas to pass, untreated, directly from the inlet plenum to the outlet plenum. These incidents were rare and did not result in a noticeable decrease in SO_2 removal efficiency because the penetration points were relatively small.

4.3.1.2 JBR Lower Deck Solids Build-Up

The high-volume gas cooling nozzles that caused erosion of the inlet plenum material also caused deposition of a large quantity of slurry solids on the JBR lower deck. Tops of some of the sparger tubes were covered due to their proximity to the lower deck. The impact of this build-up is illustrated in Figure 4-12, taken immediately following the low-ash parametric test block.

The effect of this build-up was to close off some of the sparger tubes, rendering them useless (as shown in Figure 4-13) and resulting in small decreases in SO_2 removal efficiency. The decrease in SO_2 removal efficiency was a reflection of the method of JBR level control and is explained in more detail in Section 4.5. Periodic cleaning during outage opportunities helped prevent the build-up from becoming excessive until a more permanent solution was developed. A review of the design of the lower deck wash system showed that there was nearly adequate wash coverage, but too few deck drains. The solids were being suspended by the wash, but re-settling before they could reach the nearest drains. During the Low-Particulate Auxiliary Test block (in November 1993), the number of deck drains was increased from 14 to 51 by converting some of the sparger tubes to drains as shown in Figure 4-14.

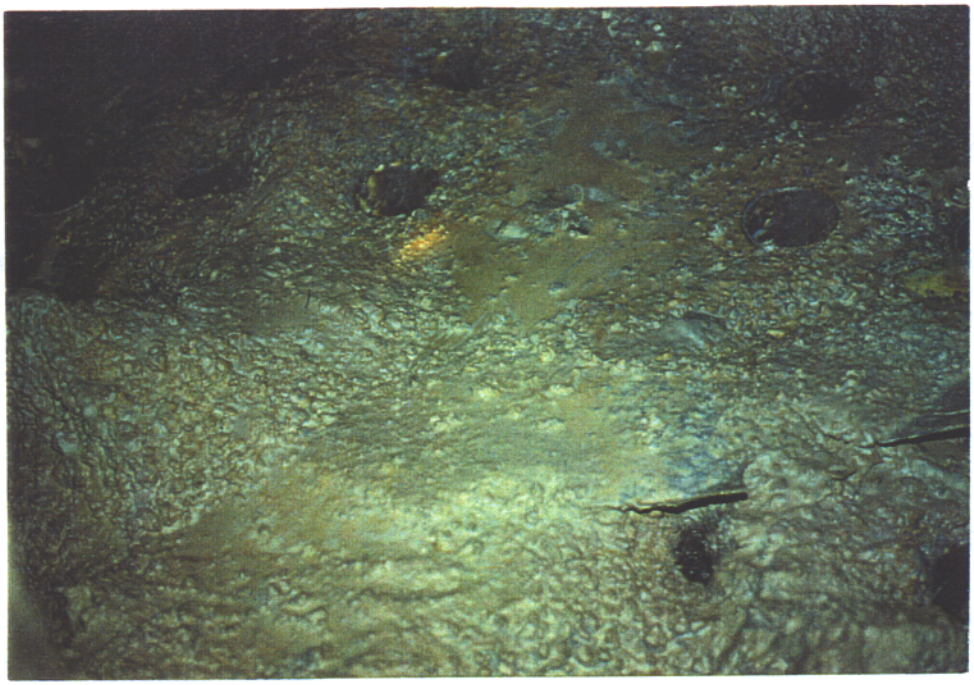

Figure 4-13. Fouled Sparger Tubes

Figure 4-14. Newly Installed Deck Drain

A redesign of the deck washing system was also performed to ensure overlapping spray coverage. These modifications resulted in considerable progress in solving this problem.

During the High-Particulate Parametric Test block, there were concerns about the impact of full ash loading on plugging in the JBR inlet plenum. An inspection was performed after the first nine parametric tests to determine the level of plugging in the sparger tubes. As illustrated in Figure 4-15, the deck remained relatively clear of solids, a result ofthe improved wash system, but some buildup was seen on the insides of the sparger tubes. The previous (i.e., during low-ash testing, before the deck wash modifications) mechanism for plugging was that the deck solids accumulated to a high-enough level to bridge across the tops of the sparger tubes. During the High-Particulate Parametric Test block, the fly ash in the flue gas stream stuck to the inside of the tubes. Because most of the deck wash nozzles do not spray directly into the sparger tubes, and the tubes protrude 3 inches above the deck, the ash solids could not be washed from the tubes. By the end of the high-ash parametric test block, the sparger tubes had become 40-50% plugged, as shown in Figure 4-16, necessitating their cleaning.

When testing resumed under more moderate-ash loading conditions (ash loading was less than 20% of that during high-ash loading), the rate of plugging decreased commensurately, but still, occasional cleaning was required throughout the end of the demonstration project. One possible solution which time and budget constraints did not permit testing, would be to make the sparger tubes flush with the lower deck to allow the deck wash water to rinse them clean. This was not considered in the initial design because this was the first CT-121 system using this gas cooling system design and these problems were not anticipated. This solution would have the same effect as turning all of the sparger tubes into deck drains, and would likely further improve the efficiency of thedeck wash system.

Figure 4-15. Sparger Tube Plugging after First 9 High-Ash Parametric Tests

Figure 4-16. Sparger Tube Plugging Following High-Ash Parametric Test Block

4.3.1.3 Slurry Gate Valves

Several different types of knife-gate valves were evaluated during the demonstration. Because of the high Cl^- concentrations in the slurry, the valve liner durability was of critical concern. On several occasions valve binding problems were traced to liner failures. Once slurry penetrated the valve liners, the 316 stainless steel valve bodies were quickly corroded by the slurry, resulting in binding and leaking of the valves. These difficulties are discussed in more detail in the Materials and Maintenance volume of this report, but the importance of selecting the best and most durable valves to ensure high availability and reliability of the scrubber is plainly evident.

4.3.1.4 Rubber-Lined Piping

Rubber-lined piping was used in several areas, including process liquor return headers, limestone slurry piping, and gas cooling slurry distribution piping. Several of these critical areas suffered failures jeopardizing the scrubber's availability. In general, it was found that rubber-lined piping was ill-suited for use in high solids concentration slurry environments. In particular, the high Cl^- concentration of closed loop processes, such as the Yates CT-121 process, essentially guarantees failure of the outer pipe body if the rubber liner is penetrated. This happened in several areas including the gypsum draw-off pump return line, the process liquor return line to the gypsum slurry transfer tank (GSTT), and in the gas cooling system distribution header.

Several substitute materials were found that were superior to rubber-lined piping. For process water return, high-density polyethylene (HDPE) was found to exhibit outstanding corrosion and erosion resistivity. The gypsum draw-off return line was replaced with a flexible steel-reinforced corrugated-rubber line which proved very successful. The rubber-lined gas cooling distribution header was replaced with a cast-basalt lined telescopic header. The cast-basalt has superior erosion and corrosion resistance and, if properly fabricated and installed, could last the lifetime of an FGD system. However, the material is approximately twice as expensive as a similarly fabricated rubber-lined header.

4.3.1.5 pH Measurement

Throughout the demonstration project several difficulties persisted with the measurement of froth zone pH. Two pH probes, each placed approximately 9 inches below the bottom of the sparger tubes and 90° radially apart from one another near the JBR wall, were used for redundant pH measurement. Initially two different probe and instrument manufacturers were used. TBI-Bailey was used for the probe and instrument on one, and the other utilized a Van London probe and a Rosemount instrument. The use of the TBI-Bailey setup was almost immediately discontinued because of the difficulty encountered in field calibrating the instrument. Another Van London-Rosemount setup supplanted the TBI-Bailey probe and instrument.

One difficulty encountered was the relatively short life span of the Van London probe. The probes would typically last 3-5 months but experienced a dampened response after 2-3 months of use. This dampened response was not always readily apparent because calibrations were typically performed at steady-state conditions. This problem was overcome by implementing an aggressive program which required bi-weekly probe reference junction cleaning and bimonthly probe changeout.

Another problem was an apparent radial stratification of pH in the froth zone. One probe would typically read 0.1 - 0.4 units higher than the other. Calibrations seemed to confirm that this phenomenon was actually occurring and was not due to instrument error. Because of the difficulty encountered in identifying a clear solution to this problem, care was taken to control pH from the same probe throughout the demonstration. This practice maintained a consistent basis of comparison for all tests conducted. One proposed solution to this problem was to locate the probes further below the froth zone to increase the stability of the as-read pH. At the end of the demonstration, it was decided to relocate the probes immediately adjacent to one another. This effectively resolved the problem while maintaining redundant pH control.

4.3.1.6 JBR Level Control

The initial design of the JBR level control system utilized three differential pressure-type level instruments, each located 120° radially apart from one another. An electronic control system was to select the median value for JBR level control. It was discovered during shake-down that differential pressure cells were ill-suited for use in this type of high-solids slurry system. The cells were prone to plugging and the oscillatory nature of the JBR's slurry level made control difficult, if not impossible.

To overcome this difficulty, the JBR gas-side differential pressure instrument was used as a surrogate parameter for JBR level control. JBR ΔP is comprised of static head and dynamic head. It is assumed that dynamic head remains constant (with constant load) since the system flow resistance coefficient is fixed by the system design. The static head is varied by raising or lowering the JBR slurry level. Unfortunately, scrubber plugging did cause the system flow resistance coefficient to increase over time between cleanings and resulted in lower SO_2 removal efficiencies at constant JBR ΔP values.

4.4 Performance Regression Model Development

An iterative approach was used to develop statistical models that could be used to predict the SO_2 removal efficiency of the Yates CT-121 scrubber. As data were developed during each test block, those results were coupled with earlier results to provide as large a source of data as possible, from which a model could be developed. Since the data were spread over variety of test conditions, the goodness of fit (R^2) of the parametric performance model decreased somewhat. So, in some cases, models were developed that represented performance over a discrete test period with limited variations in process parameters, and with a much higher R^2.

A predictive performance model can serve several purposes. These include:

- Aiding in the development of feed-forward algorithms for pH control, or for "smart" control systems used to automatically alter process control parameters to maintain a preselected SO_2 removal efficiency;

- Providing a tool so that actual performance can be compared to predicted performance to aid in identifying process equipment malfunctions and process upsets;

- Allowing normalization of data (e.g., normalizing SO_2 removal efficiency data to a common inlet SO_2 concentration) so that scientific conclusions can be more easily reached regarding the effectiveness of this type of scrubber technology; and

- Supplanting continuous emission monitor (CEM) data when necessary (i.e., as a predictive emission monitoring (PEM) system) to eliminate the need for redundant CEM systems or data substitution routines.

4.4.1 Model Building Techniques

In general, SO_2 removal efficiency was modeled as a function of four independent process variables: pH, JBR ΔP, inlet SO_2 concentration, and boiler load. All independent variables were considered in developing each model, although in some cases not all were varied in an individual tests series. The backbone of the models were the data collected during the low- and high-ash parametric tests. This model was supplemented with data from a limited parametric test series executed during the Auxiliary Test blocks. A multivariable regression analysis was performed using classical model-building techniques to develop these models. Appendix E offers significant detail on the model building techniques and philosophies employed.

4.4.2 Regression Models

Four distinct models were developed during the demonstration project to predict SO_2 removal efficiency, the latter two being products of the High-Particulate Auxiliary Test block:

1. A model based on the data collected during the Parametric Test blocks (both high- and low-ash). This model had limited variation in inlet SO_2 concentration (1800 - 2500 ppm at 3% O_2) but benefited from a full-factorial

matrix of test points. This produced a dependable model with an acceptable coefficient of determination (R^2=0.95), or "goodness of fit."

2. A more comprehensive model was developed using the data from both the parametric testing and the data from the Low- and High-Particulate Alternate Coal (4.3% and 3.4% sulfur, respectively) tests. While this model had a slightly lower goodness of fit (R^2 = 0.939), it was more comprehensive with respect to the range of inlet SO_2 concentration (1800 - 3500 ppm) included in the regression. Because of operational constraints, no data were gathered at boiler loads above 75 MWe at the highest inlet SO_2 concentration (3500 ppm).

3. A model based on burning 1.2% sulfur coal during the final Alternate Limestone test period in late 1994. Because of limitations imposed on pH (a result of the Al-F blinding discussed earlier), the SO_2 removal efficiency in this model is only a function of boiler load and JBR ΔP, since the pH was maintained constant. As a result, this third model is much simpler and has a higher R^2 (0.98).

4. A fourth model was developed that utilizes all of the performance data collected throughout the demonstration project. While this model has the lowest R^2 (0.935) of all, it is the most comprehensive with respect to the range of operating conditions covered by the model.

The third model is expected to be of the most benefit to Georgia Power during continued commercial operations because it was developed under the same conditions expected for future operation of the Yates CT-121 process: 1.2% sulfur coal, JBR slurry pH limited to a ceiling of 3.8, and limestone from a nearby Rome, Georgia quarry. The form of each model, any limitations on the use of the model, and the goodness of fit for each are presented in Table 4-3, below. The coefficients for each model are presented in Table 4-4.

These models are used throughout this report to normalize SO_2 removal efficiency data to a common inlet SO_2 concentration. This can be accomplished by calculating the difference in the model terms that contain the inlet SO_2 variable at the actual inlet SO_2 and the surrogate (normalized) SO_2 value (e.g., 1000 ppm). This difference is then applied to the actual SO_2 removal efficiency (in terms of NTU) and the resulting normalized SO_2 removal efficiency is calculated.

A comparison of measured and predicted SO_2 removal efficiency data for the High-Particulate Auxiliary Test block is shown in Figure 4-17. Model #3 was used for the High-Removal and Alternate Limestone Test periods, and the more comprehensive model #4 was

TABLE 4-3
PREDICTIVE PERFORMANCE REGRESSION MODELS - YATES CT-121

Model Number	Equation Form (Number of Transfer Units or "NTU")[a]	Applicable Data Range	R^2
1	$A+B*Load+C*SO_2+D*Load*SO_2+E*\Delta P+F*pH+G*pH^2+H*\Delta P*pH$	pH: 4.0-5.0 ΔP: 8-18 SO_2: 1800-2500 Load:50-100	0.95
2	$A+B*Load+C*SO_2+D*Load*SO_2+E*\Delta P+F*pH+G*pH^2+H*\Delta P*pH$	pH: 4.0-5.0 ΔP: 8-18 SO_2: 1800-3500 Load:50-100	0.939
3	$A+B*Load+C*\Delta P+D*\Delta P^2+E*Load*\Delta P$	pH: 3.75 ΔP: 10-18 SO_2: ~1000 Load:50-100	0.98
4	$A+B*Load+C*SO_2+D*Load*SO_2+E*\Delta P+F*pH+G*pH^2+H*\Delta P*pH$	pH: 3.75-5.0 ΔP: 8-18 SO_2: 1000-3500 Load:50-100	0.935

[a] SO_2 Removal Efficiency(%) = $100\%*(1-e^{-NTU})$

where:

Load = boiler load (MWe);
SO_2 = Inlet SO_2 concentration (at 3% O_2);
ΔP = JBR pressure drop (in. WC); and
pH = JBR froth zone pH

TABLE 4-4
REGRESSION MODEL COEFFICIENTS

Model No.	A	B	C	D	E	F	G	H
1	-14.15	0.071	0.00193	-3.75e-5	-0.38	5.55	-0.711	0.1376
2	-5.10	7.5e-3	-2.41e-5	-8.96e-6	-0.318	3.323	-0.449	0.123
3	1.266	-0.0242	0.358	-0.0117	1.25e-3	-	-	-
4	3.556	6.87e-3	-9.21e-5	-8.82e-6	-0.409	-0.1483	-0.0949	0.1406

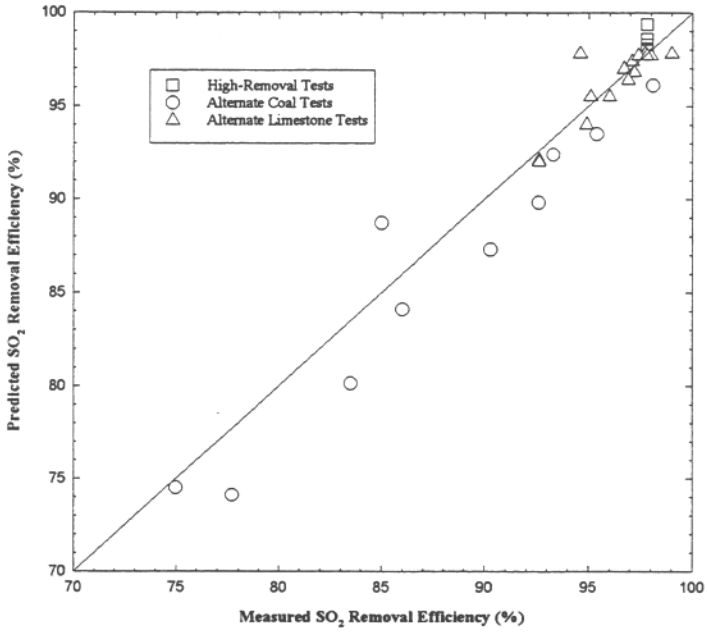

Figure 4-17. High-Particulate Auxiliary Test Block - Predicted vs. Actual Performance

used to determine predicted performance for the Alternate Coal Test period. There was good data correlation between predicted and actual performance for the Alternate Limestone and High-Removal Tests, as evidenced by the measured data's correlation with the predicted data. The correlation for the Alternate Coal Tests is not as good, likely because of the wider range on which the model was based and the limited amount of data from 3.4% sulfur coal, which was burned during this test period.

4.5 SO_2 Removal Efficiency

The CT-121 process performed well during the majority of the demonstration project. SO_2 removal efficiency was measured at a variety of process conditions. Within each test block, slurry pH, JBR ΔP, and boiler load were varied to measure their effects on SO_2 removal efficiency. The impacts of variations in inlet SO_2 concentration and ash loading were evaluated across different test blocks. The effects of these independent process variables on SO_2 removal efficiency are discussed in subsequent sections. Detailed process data for each test block are located in Appendix A.

4.5.1 Low-Particulate Parametric Test Block

SO_2 removal is dependent on slurry pH, JBR deck ΔP, boiler load (gas flow rate), and the inlet SO_2 concentration. As expected, SO_2 removal was found to increase with increasing pH and deck ΔP, and decrease with increasing load and inlet SO_2.

Slurry pH and deck ΔP are the primary operational parameters for controlling SO_2 removal. Figures 4-18 through 4-20 show the relationship between SO_2 removal efficiency, pH, and JBR deck ΔP for each of the three boiler loads tested during this test block. The SO_2 removal efficiency data used to generate these plots have been normalized to 2200 ppm inlet SO_2 (at 3% O_2) using the regression analysis described in Section 4.4 of this report.

As shown in Figures 4-18 through 4-20, SO_2 removal is most strongly affected by deck ΔP. The increase in SO_2 removal with increasing JBR ΔP is the result of increasing the gas/liquid interfacial area as the slurry level above the sparger tubes is increased. These plots also show that SO_2 removal increases substantially as the pH is increased from 4.0 to 4.5, but that there is little improvement when the pH is further increased to 5.0. This indicates that there is little increase in slurry alkalinity between pH 4.5 and 5.0.

In Figure 4-21, SO_2 removal efficiency is seen to decrease with increasing boiler load at constant pH and JBR ΔP. Because of increased dynamic head at higher loads (i.e., higher gas flows), the JBR level will be lower for a given JBR deck ΔP. Therefore, the gas-liquid interfacial surface area at 12" deck ΔP will be lower at 100 MWe than at 50 MWe. Also, the SO_2 pickup rate must increase with increasing load to maintain removal. In other words, at 100 MWe, there is roughly twice as much SO_2 entering the JBR than at 50 MWe.

The SO_2 removal efficiency was also seen to decrease with increasing inlet SO_2. This trend is readily apparent in the regression analysis, but can also be seen in Figure 4-22 which compares tests P1-1, 2, and 3 to tests P1-22, 23, and 24. The latter three tests were run with a

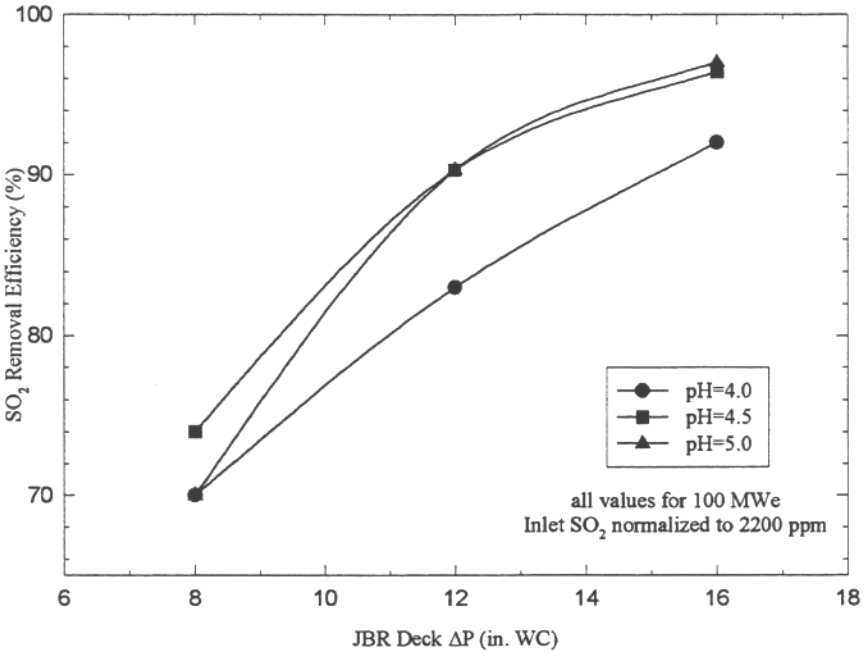

Figure 4-18. SO_2 Removal Efficiency vs JBR Deck ΔP at 100 MWe - Low-Particulate Parametric Test Block

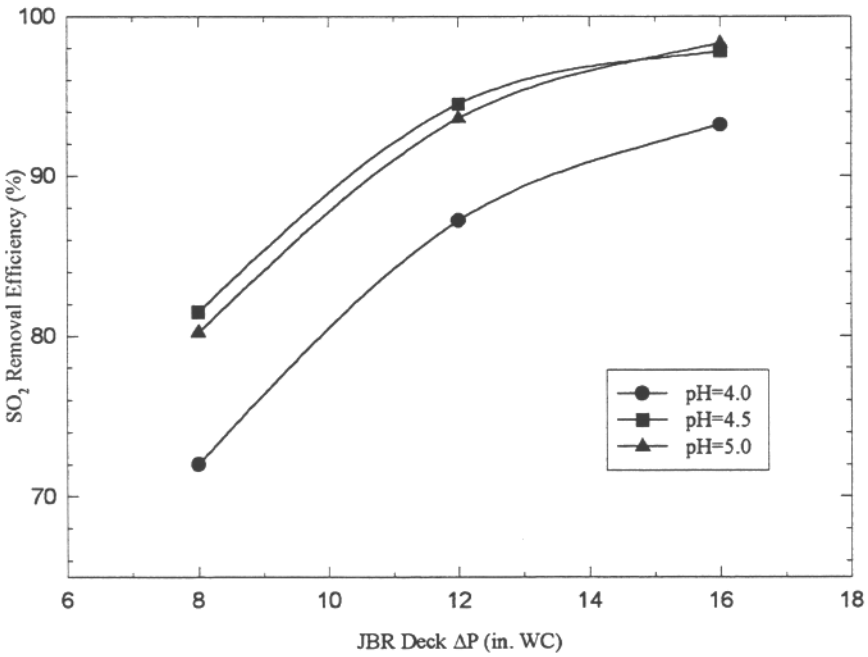

Figure 4-19. SO_2 Removal Efficiency vs JBR Deck ΔP at 75 MWe - Low-Particulate Parametric Test Block

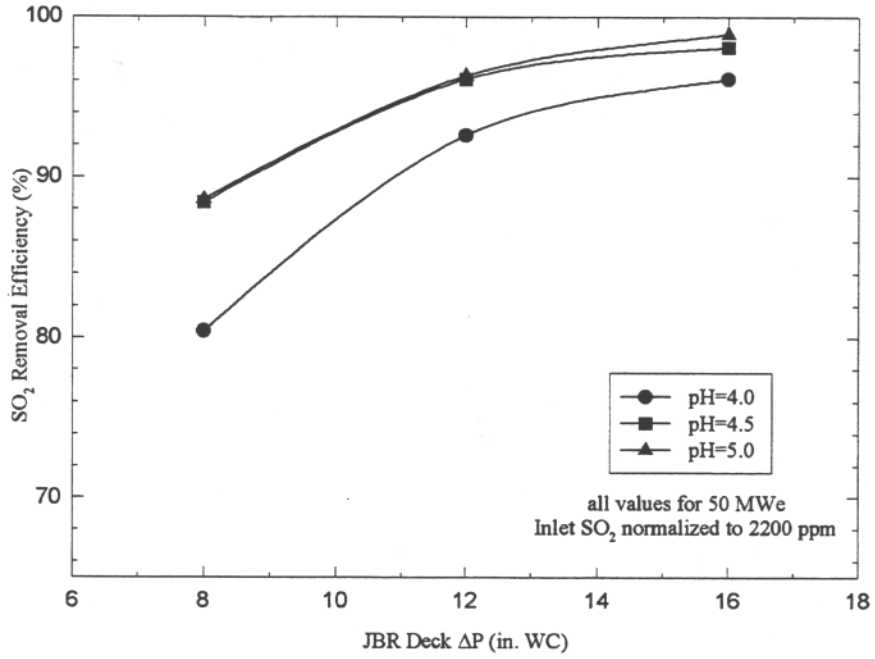

Figure 4-20. SO_2 Removal Efficiency vs JBR Deck ΔP at 50 MWe - Low-Particulate Parametric Test Block

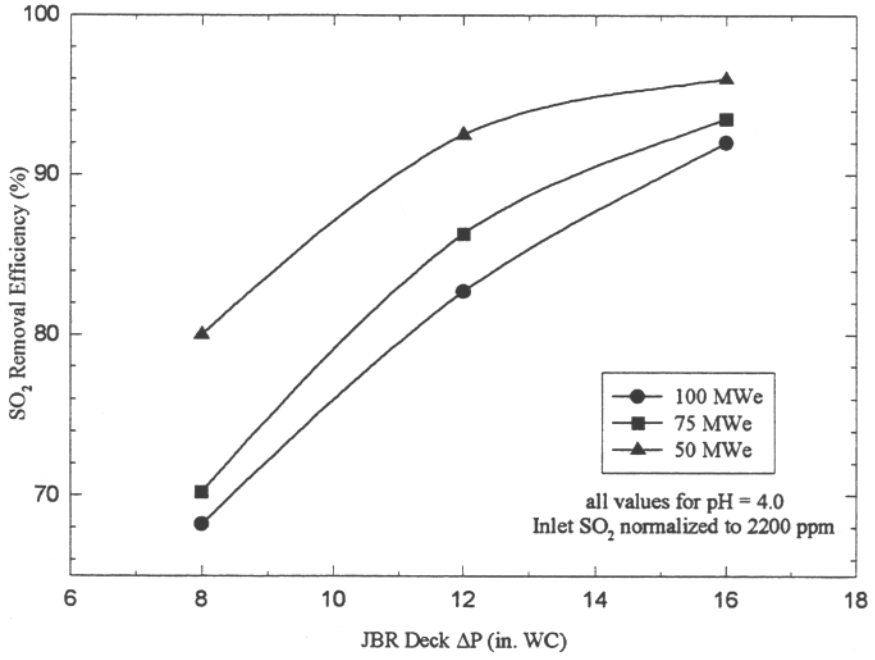

Figure 4-21. Effect of Boiler Load on SO_2 Removal Efficiency - Low-Particulate Pararmetric Test Block

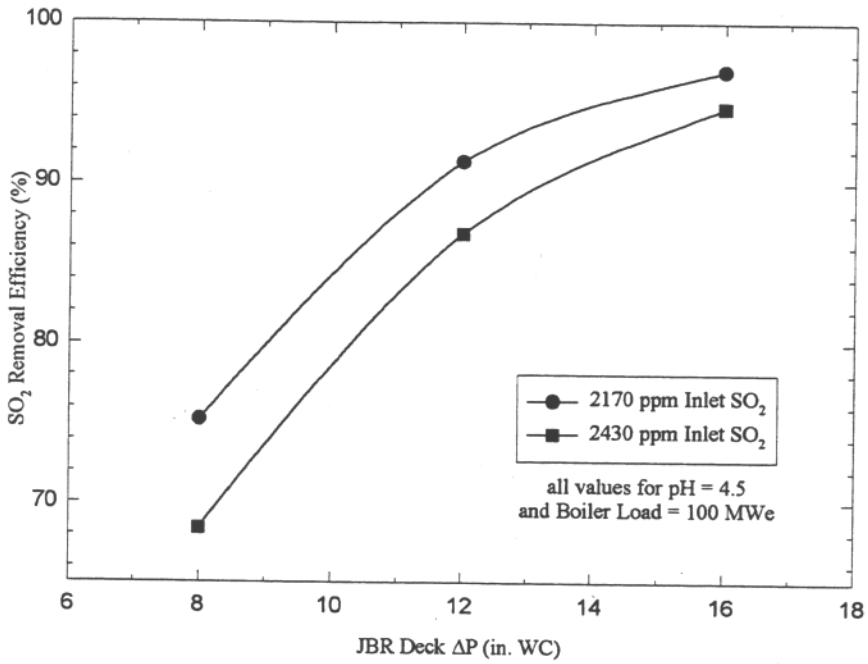

Figure 4-22. Effect of Inlet SO_2 Concentration on SO_2 Removal Efficiency - Low-Particulate Parametric Test Block

higher inlet SO_2 concentration (about 2430 ppm as compared to 2170 ppm) and had significantly lower SO_2 removal efficiency.

Six of the parametric tests were run in duplicate to determine the reproducibility of the test results. Table 4-5 presents the SO_2 removal efficiencies for these pairs. As was done in constructing Figures 4-18 through 4-21, the SO_2 removals presented here have been corrected to 2200 ppm inlet SO_2. Without this correction the differences in SO_2 removal caused by changes in inlet SO_2 would not allow the tests to be directly compared.

These results show good agreement between the duplicate tests. There were not any specific relative percent difference (RPD) goals for these duplicate tests. The acceptability of the duplicates was judged based on the SO_2 variability commonly seen with spray tower FGD systems at similar SO_2 removal levels. Tests P1-22 through P1-24 were conducted late in the

TABLE 4-5
DUPLICATE TEST RESULTS

Duplicate Pair #	Test ID	SO_2 Removal (%)	Test ID	SO_2 Removal (%)
1	P1-1	74.8	P1-22	72.5
2	P1-2	91.3	P1-23	89.0
3	P1-3	97.1	P1-24	95.8
4	P1-19	80.2	P1-19R	78.0
5	P1-20	93.6	P1-20R	93.6
6	P1-21	98.3	P1-21R	98.2

test period and these tests indicated a lower SO_2 removal efficiency than did P1-1 through P1-3, which were conducted at the beginning of the test period. The decreased performance is likely a result of the plugging of the lower deck with gypsum solids late in the test block. This problem was later resolved by modifying the lower deck wash system.

4.5.2 Low-Particulate Long-Term Test Block

In general, the SO_2 removal efficiency observed during the long-term test period was excellent, averaging around 94% as compared to the performance goal of 95%. Although it was observed early in the test period that the performance goal was not being met, the decision was made to continue with the operating conditions as they were. It was deemed more important to maintain a consistent set of operating conditions than to make adjustments to meet an arbitrarily set goal, despite the ease with which those adjustments could be made. Appendix A contains detailed process results, based on flue gas composition data, expressed in terms of 24-hour averages, for the long-term test period. All SO_2 values are presented on a dry basis, normalized to 3% O_2.

Within 2 weeks of the commencement of test L1-2, scrubber performance was jeopardized due to an upset in process conditions (Test L1-1 was a short duration test conducted at preliminary long-term test conditions. Once the long-term conditions were finalized, Test

L1-2 was used to implement those conditions). Unexpectedly, JBR inlet plenum temperatures began rising. This, coupled with a 40% decrease in the gas cooling pump operating current, indicated possible fouling of the gas cooling nozzles. While there was no danger of imminent failure of the PVC sparger tubes (150°F temperature limit), it was decided to shut the process down to investigate the temperature rise. This decision was also supported by lower-than-expected SO_2 removal, compared to the removal predicted by the parametric test regression model (discussed in more detail in Section 4.4). Upon inspection, large quantities of gypsum scale were found throughout the JBR inlet plenum in the sparger tubes, and inside some of the gas cooling nozzles. It was determined that this scale was a result of the low limestone utilization tests completed at the end of the low-ash parametric test block. Lower limestone utilization means that there is excess limestone in the recirculating slurry. This excess limestone can dissolve, react with sorbed SO_2, and cause calcium sulfate (gypsum) scaling.

Following a complete cleaning of the JBR, the unit was restarted under slightly modified long-term test conditions, shown in Table 3-3 as test L1-3. The pH level lowered slightly to 4.5 to maintain a buffer between the operating pH set-point and that pH level known to cause a severe drop in limestone utilization (i.e., about pH 5.2). Additionally, parametric testing had established that SO_2 removal efficiency is not affected significantly by decreasing the pH to 4.5.

SO_2 removal efficiency was significantly lower than predicted during test L1-1 as shown in Table 4-6. The large relative difference of 6.2% between actual and potential removals was largely due to the condition of the JBR, which was fouled significantly due to scale and solids build-up resulting from the low limestone utilization tests performed at the end of the parametric test block. SO_2 removal during test L1-2, conducted later in April, was higher than during L1-1, but still exhibited an average relative difference of 2.4%. SO_2 removal averaged 93.9 % during test L1-3 (which comprised a majority of the test period), compared to a value of 96.3% predicted by the regression model for a relative difference of 2.6%. Figure 4-23 is a graphical representation of these data.

TABLE 4-6
COMPARISON OF ACTUAL AND PREDICTED PERFORMANCE

Test I.D.	Actual SO_2 Removal %	Predicted SO_2 Removal %	Relative Difference [a]
L1-1	84.8	89.9	6.2
L1-2	94.7	97.0	2.4
L1-3	93.9	96.3	2.6

[a] Relative difference is equal to Predicted minus Actual values, divided by the Actual value, expressed as a percentage.

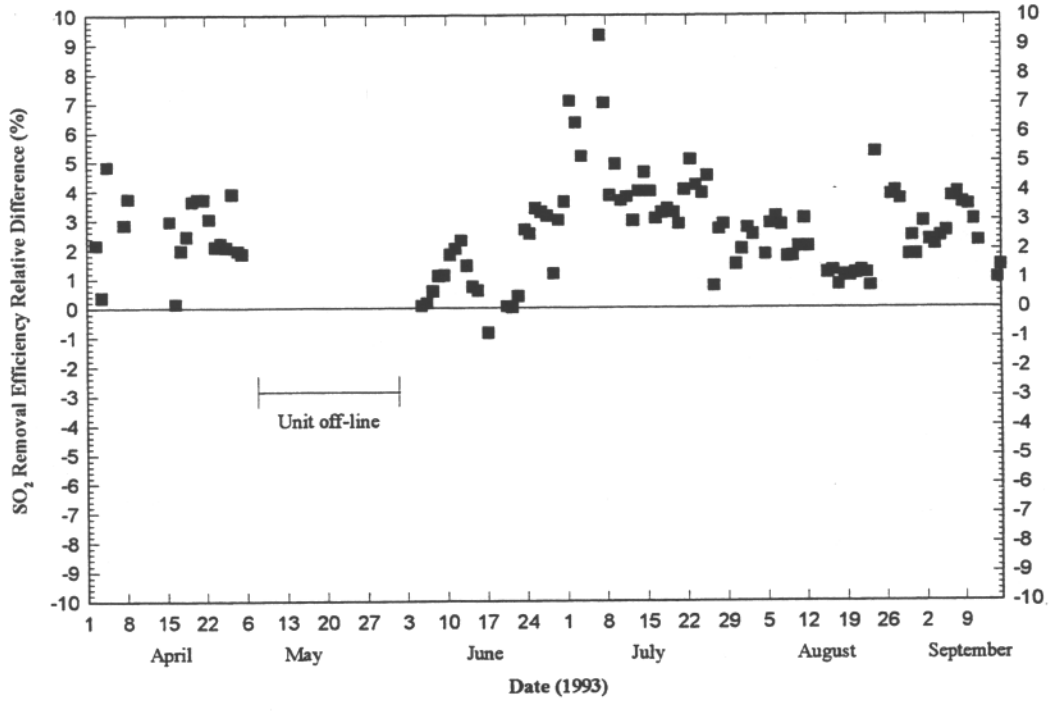

Figure 4-23. Comparison of Regression Model to Low-Particulate Long-Term SO_2 Removal Performance

The SO_2 removal was much less than predicted at the end of June, during a period of maximum load, while air toxics testing was being conducted. To allow a more thorough investigation of this trend, a limited set of parametric tests was conducted in August. The test

matrix is shown in Table 4-7. By choosing an array of JBR ΔP and pH setpoints, the effects of these parameters on performance could be evaluated and the results could be compared to the regression model predictions at various operating conditions.

TABLE 4-7
LIMITED PARAMETRIC TEST MATRIX

Test I.D.	Test Duration (hrs)	pH	JBR ΔP (in. WC)
L1-3P1-A	24	4.2	10
L1-3P1-B	24	4.8	10
L1-3P1-C	24	4.2	14

Load determined by load dispatch, based on system demand.

The results of the testing in August indicated that the relative difference was less for removal greater than 90%, as shown in Table 4-8. Compared with previously documented performance, it is clear that at lower JBR ΔPs, the relative difference was considerably greater than at higher ΔPs. One possible reason for this difference is the pulsing which occurs in the turbulent froth zone. At low JBR levels (i.e., low JBR ΔPs), this pulsing may momentarily uncover sparger tubes, allowing a portion of the flue gas to gountreated. This effect is aggravated by fouling in the JBR, which results in even less sparger tube submergence at a given JBR ΔP.

TABLE 4-8
LIMITED PARAMETRIC TEST RESULTS

Test I.D.	Actual SO_2 Removal (%)	Predicted SO_2 Removal (%)	Relative Difference (%)
L1-3P1-A	84.7	89.9	6.2
L1-3P1-B	87.5	93.2	6.5
L1-3P1-C	92.4	95.8	3.7

Changes in pH did not appear to affect the magnitude of the relative difference. For example, the relative difference was similar at pH 4.2 (Test L1-3 P1-A) compared to that at pH 4.8 (Test L1-3 P1-B).

Possible reasons for the difference between predicted and actual SO_2 removal efficiency include:

- Erosion of the JBR internals resulted in areas that provided a direct path for flue gas to bypass the froth zone and pass, untreated, directly to the outlet plenum;
- Fouling of the JBR resulted in a decreased sparger tube submergence depth, while operating at a constant JBR ΔP setpoint;
- The regression model developed (discussed in section 4.8) at the completion of the parametric test block contains an error or does not include all the parameters which can affect SO/O_2 removal; and/or
- There were errors in instrument calibration, including the CEMs, pH probes, and JBR differential pressure instruments.

Twice-daily calibration checks of the pH instruments, and calibration adjustments when there was greater than a 0.15 pH unit deviation, make pH instrument error unlikely. If errors were involved in the pH checks, it is unlikely that they would consistently result in the SO_2 removal being biased low (i.e., pH biased high since pH affects SO_2 removal). Errors in pH calibration would more likely result in random error, both low and high. This same logic also applies to the JBR deck ΔP instruments, which are checked weekly.

The CEMs are checked daily with Protocol 1 calibration gases and if they do not meet test specifications, which are twice as stringent as compliance standards, the affected data are not considered in the analysis of scrubber performance. Additionally, any errors in the CEMs calibration would also tend to be of a more random nature and would not consistently bias the removal efficiency in a negative direction. Direct calibrations were used to confirm that sampling line leaks were not the cause of the problem.

The regression model that was developed during the parametric testing was validated based on the data generated during that test period. It has since been revalidated using fundamental principles of model building and found to be statistically valid. The model has anexcellent

fit (R^2 =0.99) and exhibits no autocorrelation. It is also unlikely that the data used to develop the model were corrupted by instrumentation errors, as discussed above.

Periodic inspections of the JBR have revealed solids build-up on the lower deck, upper deck and mist eliminators. Although scale build-up is difficult to quantify, a significant amount of scale was observed in the sparger tubes during an inspection performed following completion of the test period. JBR fouling is not likely the sole cause for the performance bias but the performance degradation observed is consistent with that expected to occur with excessive solids build-up.

The remaining cause of performance degradation considered was flue gas bypass. Throughout the long-term test period, JBR inspections revealed that the erosive forces of the gas cooling spray caused holes to be worn, not only in the support materials of the transition duct, but in the upper deck drains, wash headers, and other areas of the JBR inlet plenum. Even the large gas risers have severe erosion, although none were completely worn through. The November, 1993 inspection revealed several large holes in the upper deck drain downcomers and one broken sparger tube. Based on orifice-type calculations, a single broken sparger tube could result in a 0.5 % decrease (absolute) in SO_2 removal.

The November, 1993, JBR inspection supported both fouling and flue gas bypass as contributing factors to the performance bias. Obvious paths were found for untreated flue gas to pass, and over 25% pluggage of sparger tubes was documented during this inspection.

4.5.3 Low-Particulate Auxiliary Test Block

The performance of the Yates CT-121 scrubber was evaluated during the Low-Particulate Auxiliary Test Block using both parametric and load-following testing. This test block comprised the following three test series:

- High Removal Tests;
- Alternate Limestone Tests; and
- Alternate Coal Tests.

The results of each test series are discussed separately below.

4.5.3.1 High Removal Tests

The High Removal tests demonstrated the capability of the process to achieve consistently high SO_2 removal efficiency over a wide range of boiler loads. Significant results from the testing (see Table 3-5 for test matrix) are presented inTable 4-9. The performance averaged greater than 97% SO_2 removal efficiency for the entire test period despite the widely varying load conditions. The removal efficiencies reported in Table 49 are so similar that they are not statistically different from one another.

TABLE 4-9
HIGH REMOVAL TEST PERFORMANCE

Test I.D.	Unit Load (MWe)	Actual SO_2 Removal (%)	Predicted SO_2 Removal (%)	Relative [a] Difference (%)
HRl-l	50	97.8	98.6	0.8
HRl-2	75	97.5	98.8	1.3
HRl-3	100	97.8	99.3	1.5
HRl-4	Load Following	97.0	98.7	1.8 [8]

[a] Relative Difference = l00%*(predicted Removal - Actual Removal) / Actual Removal

Note that the relative difference between the observed SO_2 removal efficiency and that predicted by the original parametric regression model indicates thatthe process consistently performed less efficiently than expected based on earlier parametric testing results. Although the predicted and actual removal efficiencies are not statistically different from each other, the consistently positive relative differences (i.e., auto correlated results) indicates that this trend may be real. The cause of this performance was discovered during the November 1993 inspection. This inspection revealed extensive fouling of the JBR lower deck and sparger

tubes, with up to 30% blockage of the total sparger tube cross-sectional area. This fouling was composed of gypsum scale and other gypsum byproduct solids. It is believed that the scaling resulted from an accidental high pH excursion (to a pH of approximately 5.5) during the long-term load-following testing conducted earlier in 1993. The low limestone utilization resulting from this high pH led to scale formation on the lower deck and sparger tubes. Because the gas cooling pumps (GCP) spray slurry on these areas, the excess limestone in the slurry reacted with the flue gas as it passed through the inlet plenum, resulting in scale formation.

The JBR and transition duct were fully cleaned following the November 1993 inspection, and follow-on testing demonstrated process performance that correlated well with the regression model. Thus, with a clean JBR, the Yates CT-121 process should be able to achieve greater than 99% SO_2 removal efficiency. This performance is discussed in Section 4.5.3.2 of this report.

It was also discovered that close attention must be paid to oxidation air stoichiometry ($O:SO_2$ ratio) during periods of exceptionally high SO_2 removal and high unit load. There is a critical ratio of $O:SO_2$ that must be maintained or exceeded using oxidation air to ensure complete oxidation - a driving force for the excellent SO_2 removal performance of the CT-121 process. For the 2.5% sulfur coal that was being used during this test, this critical $O:SO_2$ ratio was estimated to be approximately 5:1.

4.5.3.2 Alternate Limestone Tests

The Alternate Limestone testing began prior to the annual scheduled boiler outage in November 1993. Parametric testing with a "clean" (unfouled) JBR was conducted to compare the performance of the process using the Dravo limestone to the performance when using the Martin Marietta Aggregates (MMA) limestone during the Low-Particulate Parametric Test block. The testing matrix is shown in Table 3-7.

Load-following operations, conducted after the parametric tests, were used to evaluate the performance of the scrubber under typical operating conditions. The Alternate Limestone

tests were also used to validate the results of the bench-scale limestone evaluation study[1]. This study established that limestone selection could have a significant impact on gypsum crystal morphology and dewatering characteristics. The favorable impact of the limestone evaluated during the Alternate Limestone tests on gypsum dewatering is discussed in detail in the Gypsum Quality volume of this report.

Results from the "clean" parametric tests using Dravo limestone are summarized in Table 4-10. The data correlated well with the original Yates performance regression model, developed using Martin Marietta limestone, as evidenced by the low relative differences between the observed and predicted SO_2 removal efficiency. From these data, it does not appear that the change in limestone reagent had a large impact on scrubber SO_2 removal efficiency. A more complete listing of data collected during this test period can be found in Appendix A.

TABLE 4-10
ALTERNATE LIMESTONE "CLEAN" PARAMETRIC TESTS - SIGNIFICANT RESULTS

Test I.D.	Inlet SO_2[a] (ppm)	Unit Load (Mwe)	pH	JBR ΔP (in. WC)	SO_2 Removal Observed (%)	SO_2 Removal Predicted[b] (%)	Relative Difference[c] (%)
P1B-1	2210	101	4.4	10.2	82.3	82.7	0.5
P1B-2	2180	51	4.5	16.2	97.2	98.6	1.4
P1B-3	2270	52	4.5	10.2	92.7	92.8	0.1
P1B-4	2190	100	4.5	16.2	92.5	96.4	4.2
P1B-5	2220	52	5.0	16.1	98.7	98.8	0.1
P1B-6	2200	100	4.9	16.2	98.1	97.2	-0.9
P1B-7	2130	49	5.0	10.2	95.7	93.9	-1.9
P1B-9	2160	51	4.0	16.2	94.7	96.6	2.0
P1B-l0	2270	102	4.0	10.2	74.8	69.7	-6.8
P1B-11	2110	100	4.0	16.2	92.6	92.3	-0.3
P1B-12	2080	50	4.0	10.2	89.7	89.5	-0.2
P1B-13[d]	2270	80	5.1	16.2	97.2	97.9	0.7

[a] Corrected to 3% O_2
[b] Based on original Yates performance regression model.
[c] Relative Difference =100%*(Predicted Removal - Actual Removal) /Actual Removal
[d] Additional, unplanned test

4.5.3.3 Alternate Coal Tests

To evaluate the operability and performance of the Yates CT-121 process with alternate sources of fuel supplied to the Unit 1 boiler, higher sulfur coal, averaging 4.3% sulfur, was procured. This new coal's sulfur content was 172% higher than the design coal sulfur content of 2.5%. The effect of increased coal sulfur content on inlet SO_2 concentration is shown in Figures 4-3 and 4-4. Complete coal analyses for the test block are contained in Appendix C. Parametric testing of the scrubber, discussed below, was the focal point of this test series.

At 172% of its design SO_2 pickup rate (4.3% instead of 2.5% sulfur coal), the performance of the scrubber was excellent. SO_2 removal efficiency ranged from 79% to 97%, with inlet SO_2 concentrations ranging from 3380 to 3820 ppm (at 3% O_2, dry basis). Compared with data from operation at lower inlet SO_2 concentrations, key test results (reported in Table 4-11) show the effect of a large increase in inlet SO_2 concentration on removal efficiency. SO_2 removal efficiency decreased with increasing inlet SO_2 concentration, as shown in Figure 4-24. This drop in removal efficiency was a result of the increased demands on neutralization and limestone dissolution to support a higher SO_2 absorption rate.

The higher SO_2 absorption rate associated with the increase in inlet SO_2 concentration also resulted in a decrease in JBR solids residence time. This lower residence time subsequently resulted in less gypsum crystal formation time and slightly smaller particle size distribution. These results are discussed in detail in Section 4.8.2 of this report.

Since these data represent test conditions (specifically inlet SO_2) outside of the range of conditions previously tested, the original parametric regression model was not considered to be valid for evaluating the results of the alternate coal testing. An attempt was made to develop a predictive model for the high inlet SO_2 concentrations, to allow a more expanded range of process characterization and performance prediction. Due to the limited data available (a result of CEM difficulties during testing and a limited supply of higher sulfur coal), it was not possible to construct a statistically valid model for these high inlet SO_2 concentrations.

TABLE 4-11
ALTERNATE COAL PARAMETRIC TEST RESULTS

Test ID	Unit Load MWe	pH	JBR ΔP (in. WC)	Inlet SO_2 (ppm) (@3% O_2)	SO_2 Removal (%)
AC1-1	50	4.0	10	3560	81.1
AC1-2	50	4.0	16	3700	93.3
AC1-3	75	4.0	10	3580	a
AC1-4	74	4.0	16	3390	88.7
AC1-5	46	4.5	16	3610	94.2
AC1-6	75	4.5	16	3510	92.9
AC1-7	75	4.5	10	3660	a
AC1-8	50	4.5	10	3700	81.4
AC1-9	51	5.0	16	3760	97.2
AC1-10	76	5.0	10	3820	79.0
AC1-11	75	5.0	16	3590	94.5
AC1-12	50	5.0	10	3490	86.4

[a] Unavailable due to CEM output range limitations

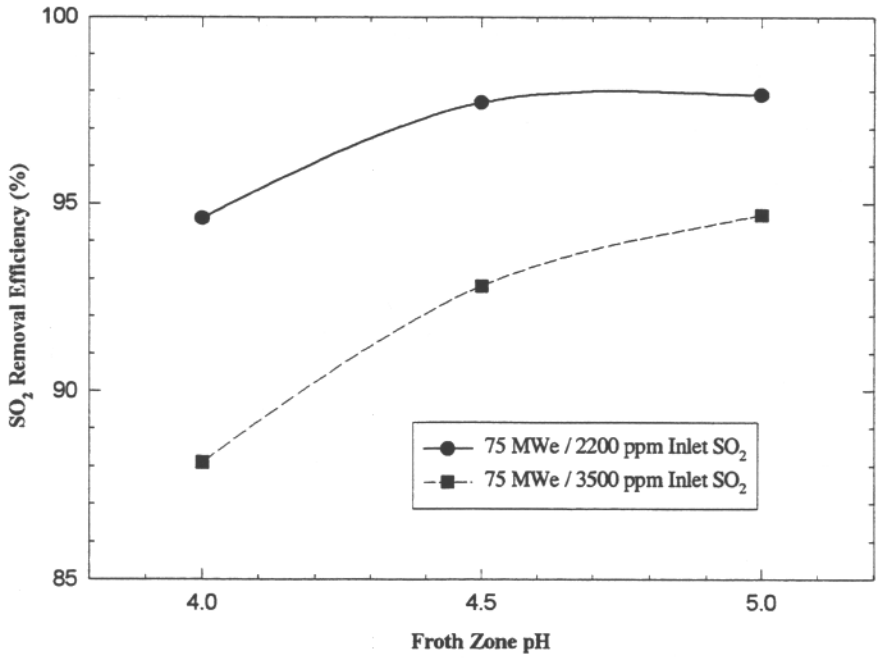

Figure 4-24. Effect of High-Sulfur Coal on SO_2 Removal Efficiency - Low-Particulate Auxiliary Test Block

4.5.4 High-Particulate Parametric Test Block

The High-Particulate Parametric Test block was essentially a repeat of the test matrix used during the Low-Particulate Parametric Test block, as shown in Table 3-2. The primary difference was that the high-particulate tests were conducted with the ESP partially or fully deenergized, depending on the individual test. The High-Particulate tests were also conducted at lower pH values than the Low-Particulate Parametric tests. This was necessitated by a decrease in limestone utilization at pH values above 4.0. This decrease in limestone utilization is believed to be an effect of a phenomenon know as aluminum fluoride blinding. Aluminum fluoride blinding is discussed in more detail in Section 4.13.3, but was believed to be a result of the elevated ash concentrations in the JBR. The lower pH setpoint was required to ensure high limestone utilization.

During the high-particulate testing, gypsum/ash plugging of the sparger tubes was problematic and created a condition that resulted in significant performance degradation over the course of the test block. Difficulty was also encountered in calibrating the process pH instruments at pH values below 4.0. The low pH and limestone loading at which the process was operated resulted in erratic pHs, as measured with both the in-situ pH instruments and a hand-held probe inserted in a slurry slip-stream. The cause of the erratic pH is not clear, but it may have been caused by operation with aluminum fluoride blinding.

As the JBR became increasingly fouled in the later High-Particulate Parametric Tests, the JBR slurry level decreased at the same JBR ΔP and unit load conditions. While an experimental JBR level indication system, consisting of capacitance-type probes, was not yet completely reliable, visual observation of the JBR froth zone sight glass did indicate that the JBR level was lower than expected, based on previous observations. This effect was observed during earlier test blocks in association with fouling of the JBR inlet plenum and sparger tubes.

This effect is most evident when comparing the results of tests P2-33 and P2-33R. Both tests were conducted at the same conditions (with the exception of inlet SO_2 concentration), but P2-33 was conducted almost 23 days into the test block, while P2-33R occurred about 46

days into the test block. Normalizing the SO_2 removal efficiency for each test to 2200 ppmv (dry basis) inlet SO_2 (at 3% 02) to account for coal sulfur content differences, the removal efficiency of test P2-33 was 78.1%, while it was only 65.6% for P2-33R. It is believed that this 17.4% relative difference in SO_2 removal is attributable to the build-up of solids inside the sparger tubes over those 23 days between tests P2-33 and P2-33R.

The lower-than-expected SO_2 removal efficiency could also be attributable to the decreased height of the froth zone - a condition believed to be a result of the high ash loading in the scrubber. This effect has also been observed in the JBR froth-zone sight glass. Whereas froth heights of 10 to 12 inches were typical at full load during the low-particulate period of testing, froth heights as low as 2 to 3 inches had been observed at similar conditions during high-ash testing. It is possible that the lower froth height could be a result of a change in slurry viscosity or surface tension due to the presence of the high ash concentration in the slurry.

4.5.5 High-Particulate Long-Term Test Block

The CT-121 process performed reasonably well during the High-Particulate Long-Term Test block. There was substantially less sparger tube plugging and performance degradation compared to the High-Particulate Parametric Test block because the ash loading was decreased to a more moderate level by partially energizing one of the ESP fields. Very few equipment failures occurred and SO_2 removal efficiency was slightly better than that predicted by the low-particulate performance regression model for the first 2 months of testing. Because of the uncharacteristically low boiler load during this historically peak-demand season, the performance data may have been biased by an abundance of low-load data. The SO_2 removal efficiency declined significantly with time at loads greater than the minimum unit load. This is a result of the JBR lower deck fouling with gypsum and fly ash solids, as well as physical changes that occurred in pH monitoring and froth zone pH control.

Although the High-Particulate Long-Term Test block was designed to repeat the testing of the Low-Particulate Long-Term Test block (with the exception of the increased ash loading), it was necessary to operate at a JBR froth zone (JBR-F) pH below that used in the earlier

long-term test block. This lower operational pH was required to avoid the occurrence of Al-F blinding, discussed in the Section 4.13.3 of this report.

On average, the SO_2 removal efficiency of the scrubber was equivalent to that predicted by the regression model developed during the low-ash parametric testing. During test L2-2, the removal efficiency averaged 93.1 %, and the efficiency predicted by the performance model was 93.3%. The average relative difference between these two values was lower than expected, largely due to the uncharacteristically low boiler load throughout the test block. This low average load was a result of unusually cool weather and large amounts of rainfall during the summer. Test block averages of key process parameters are presented in Table 4-12. A more comprehensive summary of process parameter daily averages is presented in Appendix A.

There was a large increase in the relative difference between actual and predicted SO_2 removal efficiency with increasing boiler load. At lower loads (i.e., 50-55 MWe), the actual performance was fairly close to the predicted SO_2 removal efficiency while at the highest loads (i.e., 90-105 MWe), the relative differences were typically much greater than zero (indicating performance below the predicted value). Relative differences for selected loads were plotted versus time (shown in Figure 4-25) to demonstrate the impact of moderate ash loading to the scrubber. The effects of ash loading and time since cleaning are obviously quite significant. The data for August may have been biased by changes in pH monitoring and reagent control. Control was switched from the primary probe to the secondary pH probe due to a transmitter failure. Although these probes are located at the same height in the froth zone, they are 90 degrees apart (radially) from each other. Because of the dynamics of JBR mixing, the pH measured at the two probes sometimes differs by several tenths of a pH unit.

Figure 4-25 shows that the relative differences increased (i.e., actual removal declined relative to predicted removal) as time progressed since the previous cleaning. This time dependent decrease in performance is often indicative of plugging of the sparger tubes. The slope of the degradation at low load (50-55 MWe) is not nearly as steep as that seen at high load (90-105 MWe). It is expected that the relative differences become more positive at higher load than at low load since the dynamic pressure drop is larger for higher gas flows.

TABLE 4-12
SIGNIFICANT PERFORMANCE RESULTS
HIGH-PARTICULATE LONG-TERM TEST

Process Parameter	Value	Standard Deviation
pH	4.00	0.03
JBR ΔP(in.WC)	14.1	0.1
Inlet SO_2 (ppm @ 3% O_2)	2040	120
Boiler Load (MWe)	59	9
Observed SO_2 Removal Efficiency (%)	93.1	2.8
Predicted Removal Efficiency(%) [a]	93.3	-
Relative Difference(%) [b]	0.2	-

[a] As predicted by the parametric regression model
[b] R.D. = l00%*(predicted-observed)/observed
(all values are the test average of the collected 15-minute averages)

An increase in the $\Delta P_{dynamic}$ will cause a decrease in JBR level and SO_2 removal efficiency, under conditions of constant overall JBR ΔP. Note in Figure 4-25 that the regression model under-predicted the SO_2 removal efficiency for a majority of the data collected in June. Since the parametric regression model was developed for conditions where the JBR had some fouling, it is reasonable that the scrubber out-performed the predictive model early in June when the JBR was clean.

Although high ash loading has been shown to increase the rate of solids build-up, or fouling, in the JBR, some of the fouling may also be due to causes unrelated to the ash content. One of these possible causes is the wet-dry interface located in the JBR lower deck and sparger tubes. Due to the close proximity of the gas cooling section to the JBR inlet plenum, the flue gas is not cooled completely to its adiabatic saturation temperature. At maximum load, the flue gas residence time in the gas cooling duct is less than half a second. The measured flue gas temperature in the JBR inlet plenum has been as much as 7°F higher than the saturation temperature under these conditions. This undercooling can result in a wet-dry interface in the sparger tubes, where moisture is evaporated from the slurry deposited there by the gas cooling pumps, leading to accelerated solids build-up.

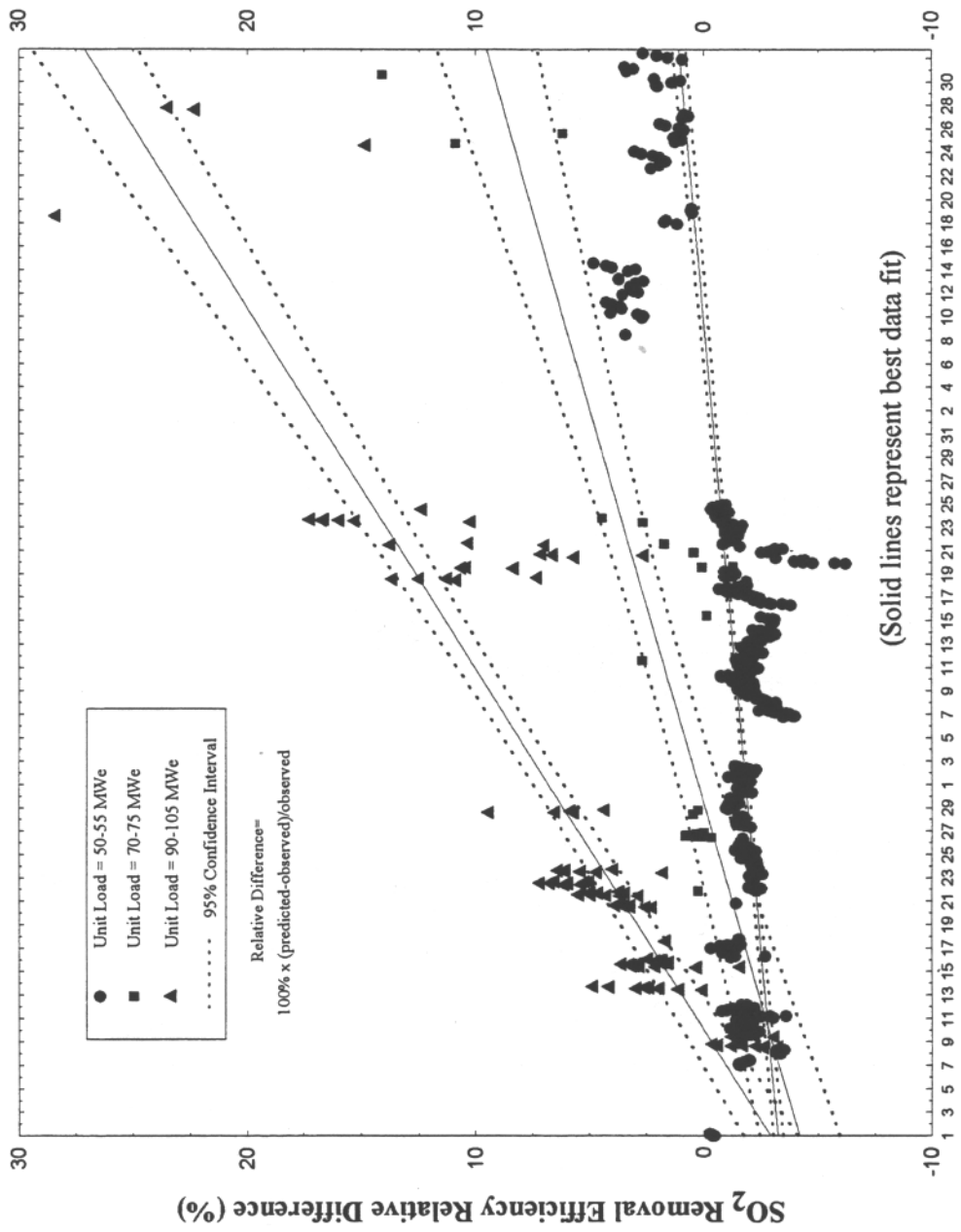

Figure 4-25. Elevated Ash Loading Effects on Scrubber Performance (Moderate-Ash Loading)

4.5.6 High-Particulate Auxiliary Test Block

The High-Particulate Auxiliary Test Block comprised three distinct test periods: High-Removal tests, Alternate Coal tests, and Alternate Limestone tests. Parametric and load-following tests were conducted as part of each test period. During each period, the impact of process parameters on SO_2 removal efficiency, as well as the impact of the changes in coal and limestone reagent sources was measured.

4.5.6.1 High Removal Tests

The CT-121 process performed well during the High-Particulate High-Removal test period. The scrubber exceeded 98% SO_2 removal efficiency under all boiler loads, during the "mini-parametric" test series (conditions shown in Table 3-6) and in load-following operation. A summary of the most significant data for the test period is shown in Table 4-13. The removal efficiency achieved during this test series was exceptional, especially considering that pH was limited to 4.0 to avoid aluminum fluoride (Al-F) blinding (which can occur under moderate ash loading and at pH values greater than 4.0). A more complete discussion of aluminum fluoride blinding is given in Section 4.13.3.

Note that the SO_2 removal efficiency did not increase measurably with decreasing load. Instead, the value was somewhat variable between 98% and 100%, regardless of boiler load. An uncertainty analysis was performed on the measurements and calculations involved in determining SO_2 removal efficiency. This uncertainty analysis took into account CEM instrument drift, errors in the calibration standards, the amount of data collected at each test point, and the standard deviation of that data. The uncertainty for each test period was approximately 2% (absolute) as shown in Table 4-13.

These test results are illustrated graphically in Figure 4-26, with the appropriate error bands for a 95% confidence interval. The SO_2 removal efficiency was normalized to a constant inlet SO_2 concentration of 1000 ppm (at 3% O_2) for use in Figure 4-26. The normalization was

TABLE 4-13
HIGH-PARTICULATE HIGH-REMOVAL TEST SIGNIFICANT PERFORMANCE RESULTS

Process Parameter	HR2-1	HR2-2	HR2-3	HR2-4
pH	4.0	4.0	4.0	4.0
JBR ΔP (in. WC)	20.1	20.1	20.1	20.1
Inlet SO_2 (ppm @3% O_2)	909	992	977	982
Boiler Load (MWe)	100.7	75.1	52.7	56.5
SO_2 Removal Efficiency (%)	98.1	99.4	98.3	98.6
Predicted SO_2 Removal (%)	97.8	97.8	97.7	97.7
Relative Error (%)[a]	0.3	1.6	0.6	0.9
Uncertainty (95% CI)	±2.0	±2.0	±2.1	±2.0

[a] Relative Error = (Actual - Predicted)/Predicted*100%
(all values are the test average of the collected 15-minute averages)

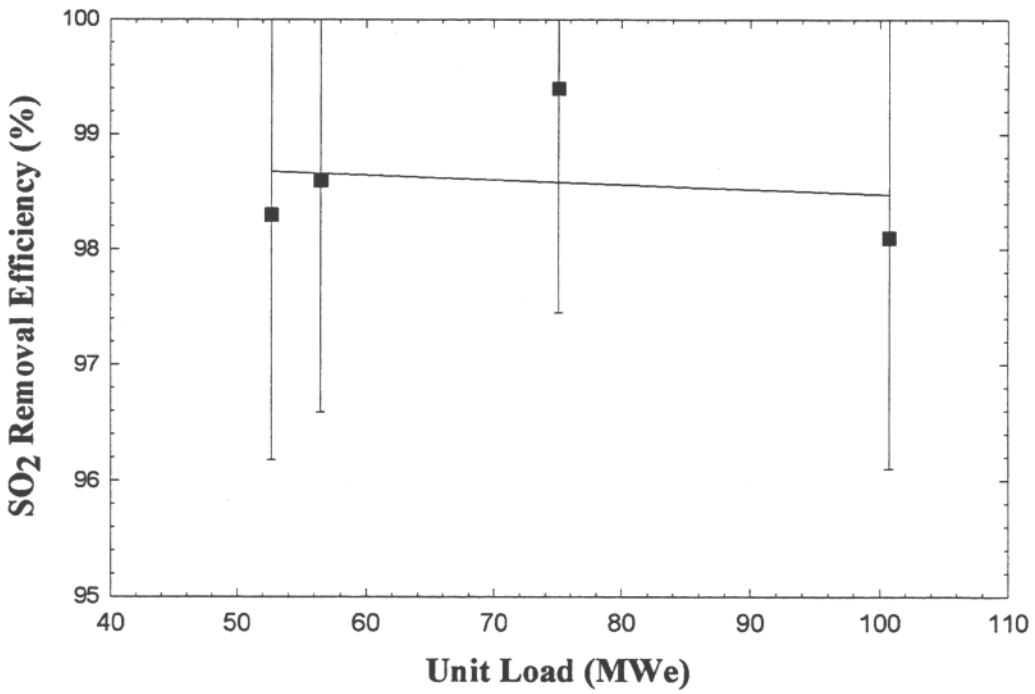

Figure 4-26. Effect of Load at High SO_2 Removal Efficiency

calculated using regression models developed from parametric results generated over a wide range of test conditions.

Because of the very high SO_2 removal efficiency measured during this test period at all conditions, the removals at one boiler load are not statistically different from those at another boiler load. The most important results were that greater than 98% SO_2 removal efficiency was achieved under all boiler loads, and moderate ash loading to the scrubber had no discernable impact on scrubber performance during this test period.

4.5.6.2 Alternate Coal Tests

High-sulfur coal was chosen as the "alternate coal" to test under moderate-ash loading conditions. This allowed a comparison with similar high-sulfur tests conducted under low-ash loading conditions. Previous high-sulfur testing was performed with 4.3% sulfur coal and the ESP completely energized, compared with a sulfur content of only 3.4% for this test series, so a direct comparison was difficult to make. These data are still useful for continued development and refinement of the high-sulfur performance regression model. This model was developed using all of the collected parametric test data, including low-, mid-, and high-sulfur coals.

Another difference between the high- and low-ash alternate coal test periods was the condition of the JBR prior to starting each test period. Although both began approximately 1 month following the previous cleaning of the JBR, the high-ash tests were performed with the JBR in a more fouled condition than the low-ash tests. As discussed earlier in this section of the report, this was a result of the boiler and the scrubber being called into service before the pressure wash contractor could complete the cleaning of the sparger tubes.

The scrubber performed exceptionally well during this period of high-ash loading. SO_2 removal efficiency was measured between 92% and 98% under all of the high JBR ΔP test conditions. During this period, the sulfur content of the fuel was 36% greater than the 2.5% coal sulfur content which was planned for the demonstration project. A summary of the most

significant test data is presented in Table 4-14. Note that AC2-10 test results are averages from the load-following portion of the test period.

The SO_2 removal efficiency results are plotted in Figure 4-27 for the different boiler loads and JBR pressure drops tested. The data for the high-ash high sulfur coal test period are denoted as filled symbols. Relevant data from the low-ash high-sulfur coal test are also presented in Figure 4-27, and are shown as hollow symbols. These data show higher SO_2 removal efficiencies, with lower SO_2 concentrations. The higher-ash operation appears to be consistent with the expected trend for SO_2 concentration.

TABLE 4-14
HIGH-ASH ALTERNATE COAL TEST PERIOD SIGNIFICANT PERFORMANCE RESULTS

Test I.D.	Load (MWe)	Inlet SO_2 (ppm @ 3% O_2)	JBR DP (in. WC)	pH	SO_2 Removal Efficiency (%)	Normalized [a] SO_2 Removal Efficiency (%)
AC2-1	101.1	2950	14.1	4.0	83.5	82.7
AC2-2	75.2	3020	14.1	4.0	90.3	90.4
AC2-3	51.1	2920	14.1	4.0	93.3	93.1
AC2-4	100.2	2920	10.1	4.0	61.5	58.7
AC2-5	75.1	3010	10.1	4.0	75.0	75.2
AC2-6	50.9	3010	10.1	4.0	86.0	86.0
AC2-7	100.5	2990	18.1	4.0	92.6	92.5
AC2-8	75.9	3040	18.1	4.0	95.4	95.5
AC2-9	49.9	3030	18.1	4.0	98.1	98.1
AC2-10[b]	78.0	2759	14.1	4.0	85.0	82.4

[a] Inlet SO_2 normalized to 3000 ppm (@3% O_2) using predictive regression model

[b] Load-following test

4.5.6.3 Alternate Limestone Tests

The SO_2 removal efficiency of the scrubber was exceptional under all process conditions during this Alternate-Limestone test period, indicating no measurable effect of limestone

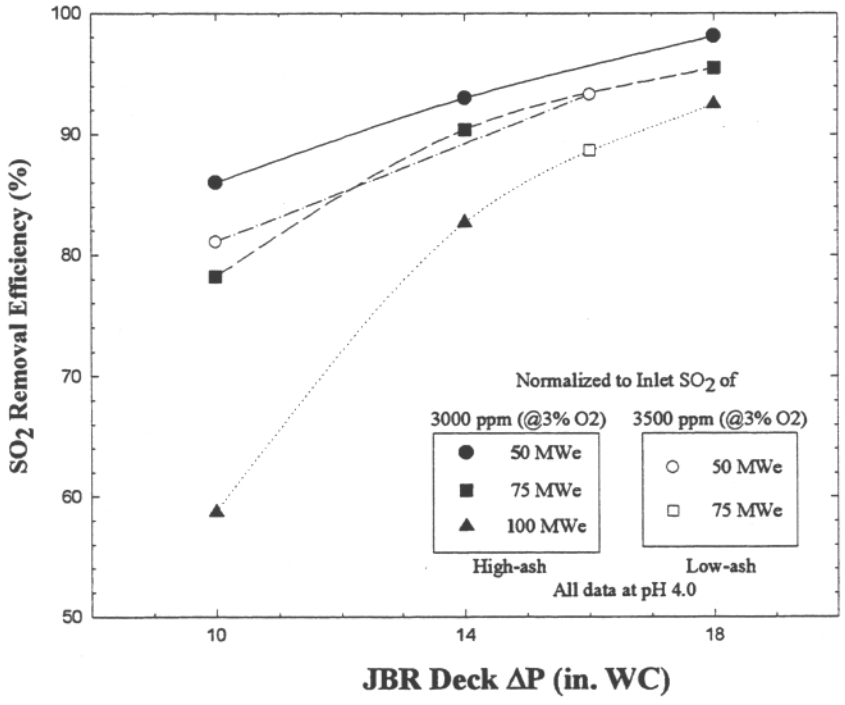

Figure 4-27. Effect of Load and JBR ΔP on SO_2 Removal Efficiency

source selection. Because the Yates CT-121 scrubber was designed for 3% sulfur coal, it was not unexpected that high removal efficiencies were easily achieved with only 1.25% sulfur "compliance" coal burned in the boiler. This removal efficiency was very good despite the low pH at which the scrubber was required to operate to ensure high limestone utilization. The low pH was adequate to ensure sufficient liquid phase alkalinity in the scrubber liquor at the low SO_2 pickup rates which allowed rapid neutralization of the sorbed SO_2. Some of the more significant performance results are listed in Table 4-15.

The test results of this period are presented graphically in Figure 4-28. The lines on the figure are plotted manually and are not the result of a mathematical curve fit. Note that only tests AL2-6 through AL2-14 were used in this plot due to the similar pH setpoints of those tests. The SO_2 removal efficiency data were normalized to a constant inlet SO_2 concentration using the predictive performance model. Note that the plots generally follow the expected

TABLE 4-15
HIGH-ASH ALTERNATE LIMESTONE TEST PERIOD SIGNIFICANT PERFORMANCE RESULTS

Test I.D.	Load (MWe)	Inlet SO_2 (ppm @3% O_2)	JBR ΔP (in. WC)	pH	SO_2 Removal Efficiency (%)
AL2-1	100.8	980	18.1	4.0	98.0
AL2-2	99.5	955	10.1	4.0	92.6
AL2-3	50.4	1000	18.1	4.0	99.0
AL2-4	50.7	905	10.1	4.0	96.0
AL2-6	50.0	920	14.1	3.75	97.1
AL2-7	75.4	960	14.1	3.75	96.7
AL2-8	100.1	920	14.1	3.75	96.9
AL2-9	100.5	900	10.1	3.75	92.6
AL2-10	75.3	880	10.1	3.75	94.9
AL2-11	50.1	840	10.1	3.75	95.1
AL2-12	50.0	920	18.1	3.75	97.6
AL2-13	76.9	750	18.1	3.75	97.4
AL2-14	100.4	875	18.1	3.75	97.8

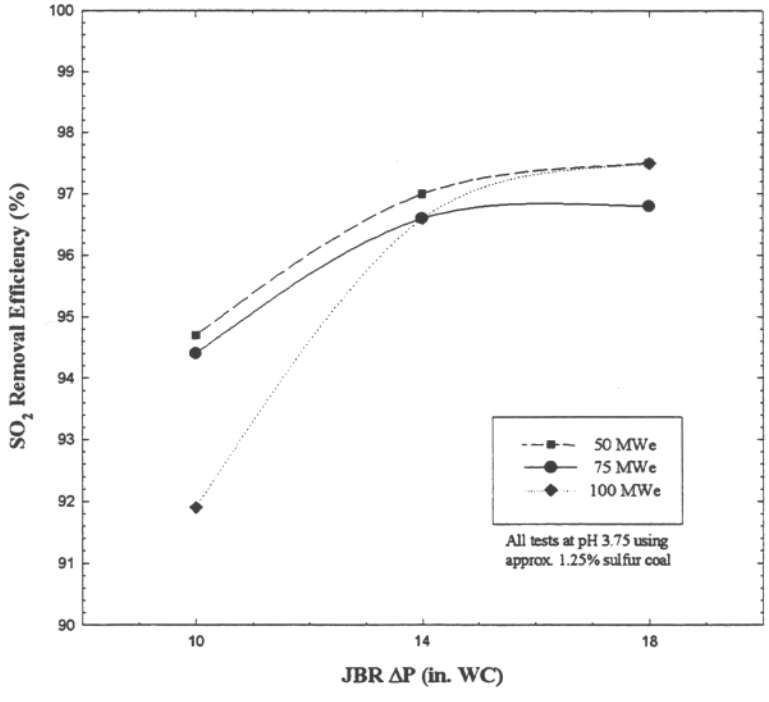

Figure 4-28. Effect of Load and JBR ΔP on SO_2 Removal Efficiency - Alternate Limestone Test

trend of increasing SO_2 removal efficiency with increasing JBR ΔP, but the effects of load on performance are somewhat uncharacteristic in that there was not a statistical difference in removal efficiency for different loads at the highest JBRΔP values. One possible reason for this trend is the uncertainty in the measurement of the SO_2 concentrations, and hence, the SO_2 removal efficiency. A statistical uncertainty analysis conducted on SO_2 removal efficiency revealed that the values had a 95% confidence interval of ±2%. Since the removal efficiency was so high, and the values so close together during this test period, the results are often not statistically different from one another.

4.6 Transient Response

The response of the CT-121 process to transients such as load changes and process upsets was specifically evaluated during both the Low- and High-Ash Long-Term Test blocks. Key parameters that affect SO_2 removal efficiency, such as pH and JBR ΔP, were monitored during these transients to allow more precise tuning of these process parameters as well as to monitor the robustness of the process.

4.6.1 Low-Ash Transient Response

One of the most important aspects of the Low-Particulate Long-Term Test block was an evaluation of the response of the CT-121 process at Plant Yates to transients, such as load changes, start-ups, and process upsets. The system responded quickly and smoothly to these transients. Some tuning of the control logic was performed during the test period to permit smoother load changes and better dampening of critical process parameters, specifically pH and JBR ΔP. Since the majority of the test period took place over the peak-demand summer months, the loading was typically characterized by full power (approximately 100 MWe) operation during daytime hours with minimum unit loading (approximately 50 MWe) at night.

Figure 4-29 shows a plot of 15-minute averages of the process response to a pH transient and a load change on April 21, 1993. The pH transient was induced by a blockage in the limestone reagent delivery piping. Once the piping was cleared at 00:30, it took until 08:30

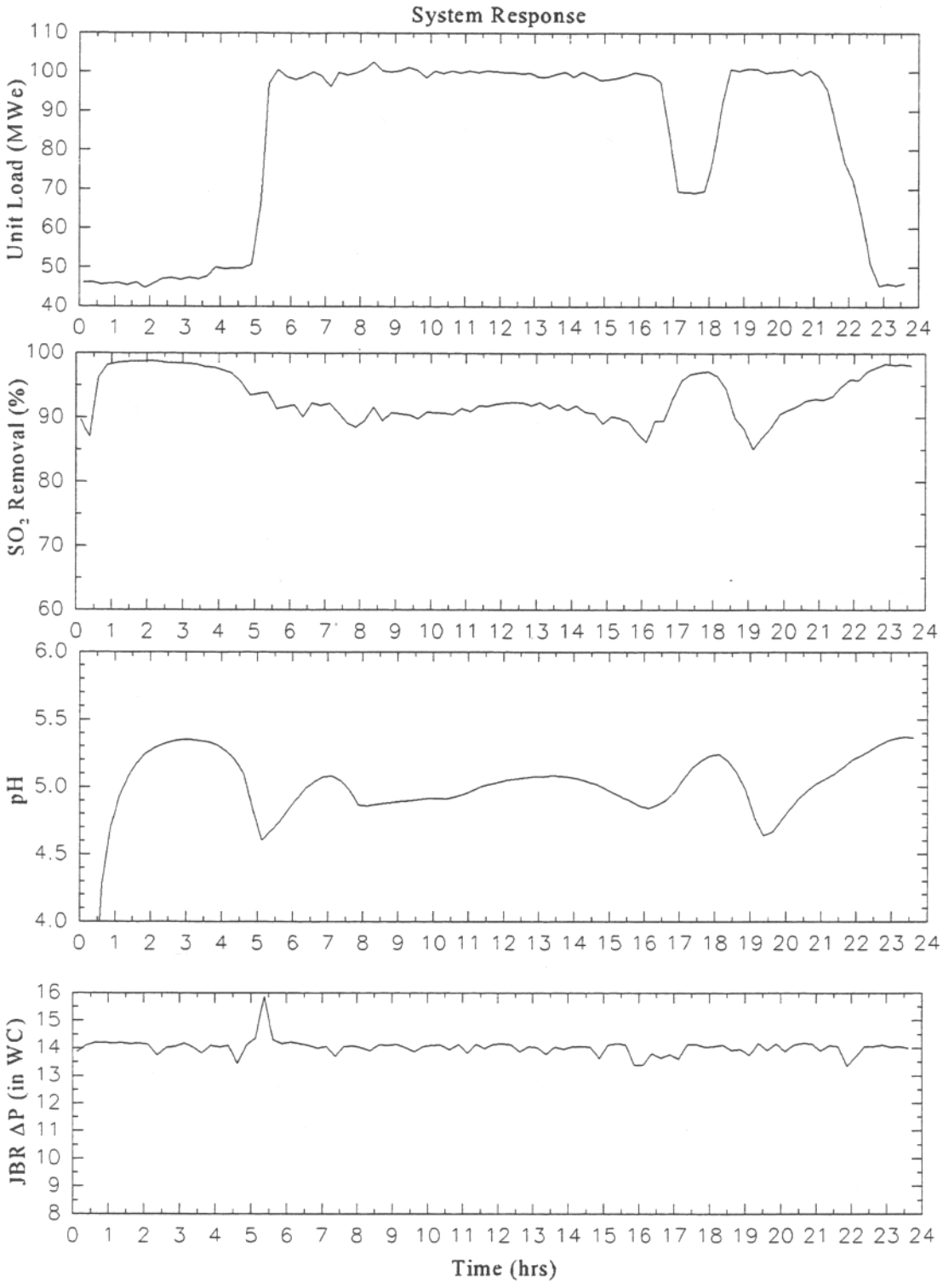

Figure 4-29. System Transient Response 4/21/93

before pH stabilized at its set point of 5.0. Of course, the transient was exacerbated by a 50 to 100 MWe load change during the recovery. At 16:30 the same day, the pH response was, once again, underdamped during a change in load. During this time, the pH was controlled by a PID-type controller, operating only on a feedback signal. Also note that at 05:30, the JBR ΔP took about a half hour to stabilize following the sudden increase in dynamic head, produced by the increase in load and flue gas flow. It was believed that a small decrease in the time constant would produce an improvement in both the pH and ΔP controller responses.

Figure 4-30 shows the effects of adjustments to the PID controller on the pH response to a change in load. Also included in this figure is the response of process parameters to the unit being brought on-line during a start-up. The controller was still being operated only in feedback mode during these transients, which took place on July 23, 1993. Note that the pH and JBR ΔP leveled out within 90 minutes of the unit coming on line at 00:30. During load changes, later in the day, the pH response was much better damped than in previous transients. While the pH was slightly perturbed by the load change, the amplitude of these effects was mitigated significantly by the tuning adjustments.

Feedforward control, used in conjunction with the existing feedback control, was added to the pH controller in early August 1993. A simple linear relationship between limestone use and unit load, under average conditions, was derived from previously collected process data. This relationship was used to ensure a more timely response to load changes, thus mitigating the lag effects on pH due to the time-dependent nature of the controller's response. Once the limestone flow rate was raised or lowered, as needed, the feedback portion of the control circuit would then trim the flow to keep pH at the desired setpoint. The multiple load changes shown in Figure 4-31 provided an excellent opportunity to evaluate the impact of the control system improvements. The behavior of the pH was well controlled with the feedforward-feedback controller, providing a well-damped response to even the most rigorous load changes.

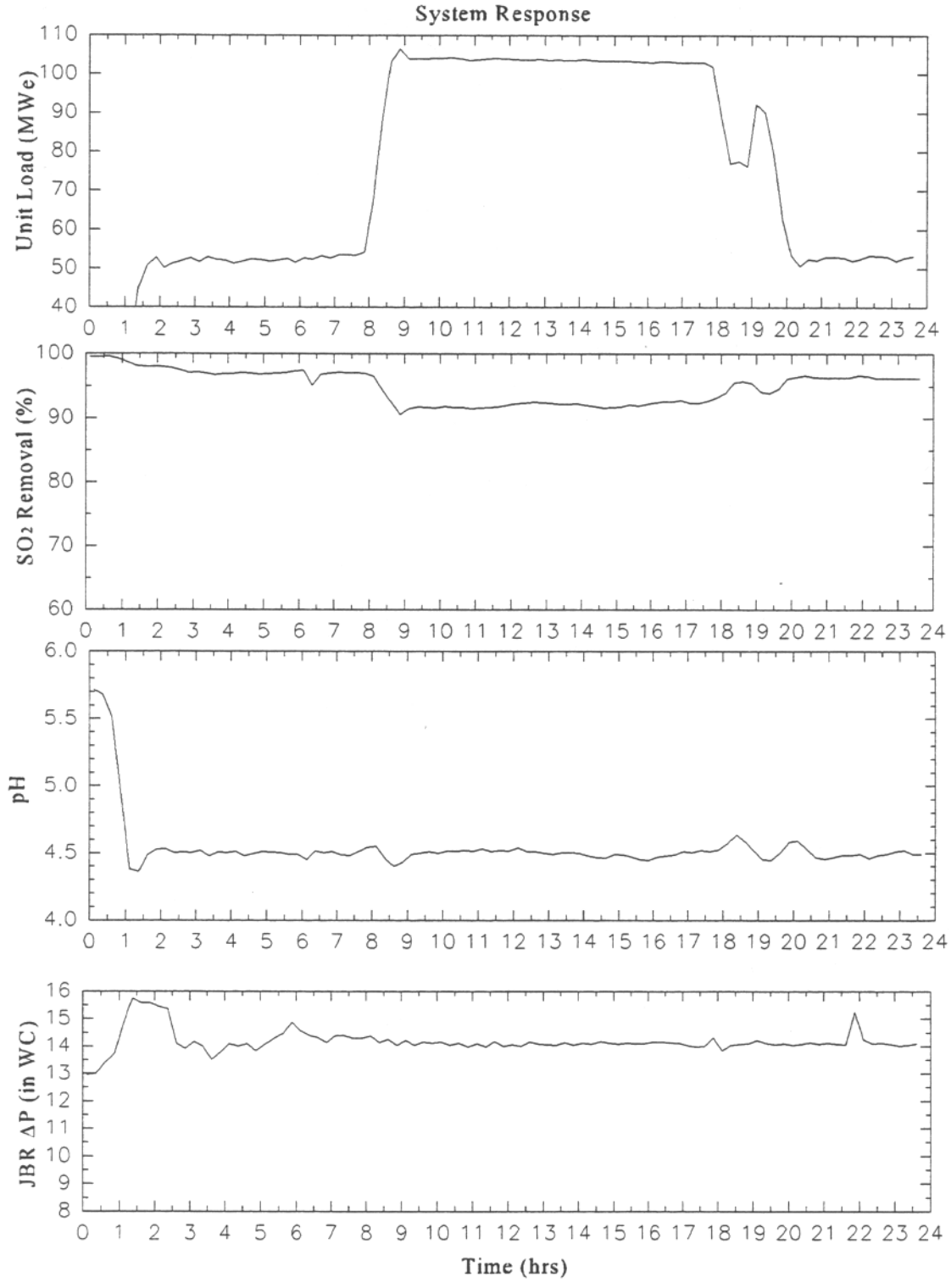

Figure 4-30. System Transient Response 7/23/93

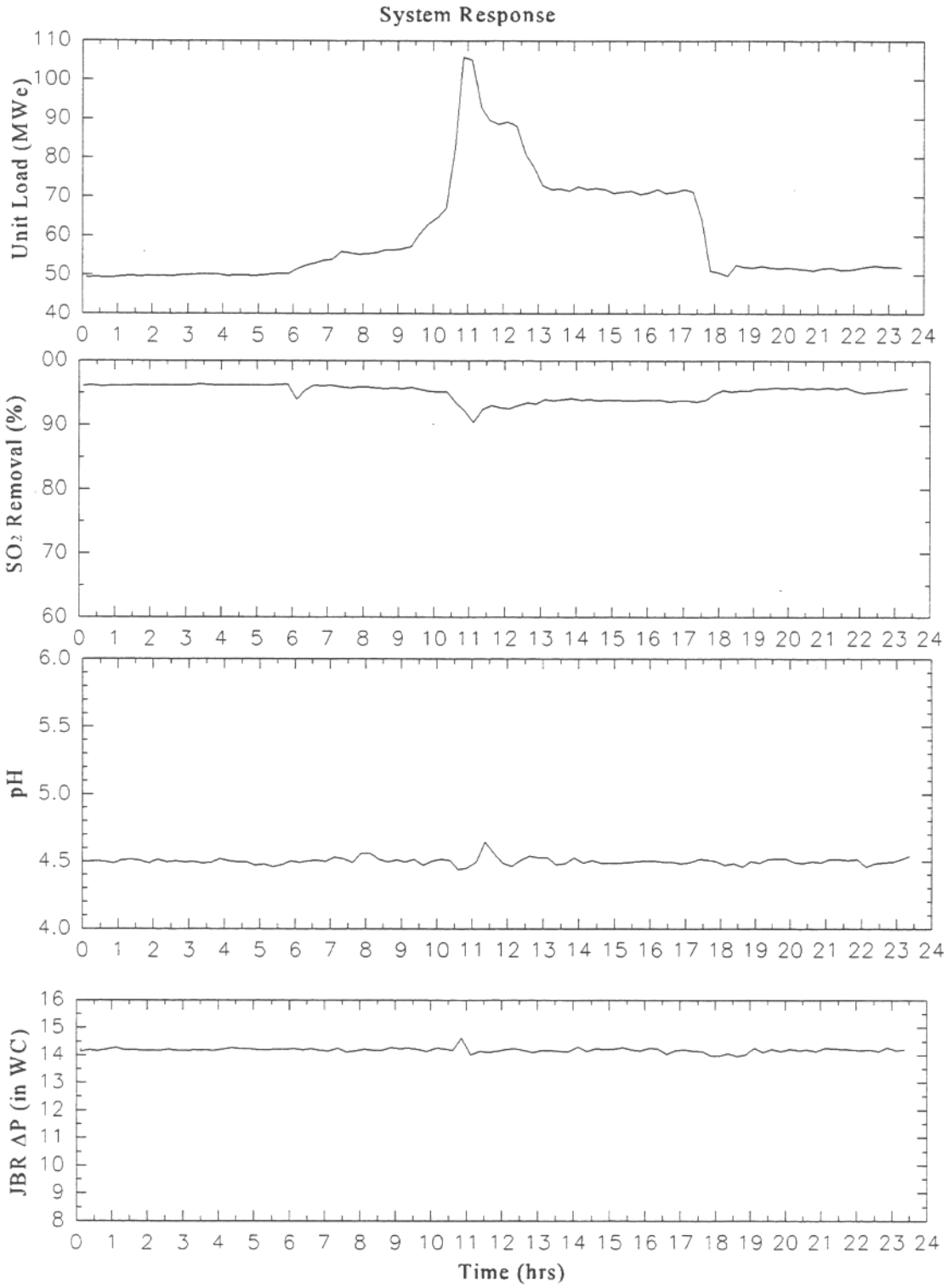

Figure 4-31. System Transient Response 8/28/93

In conclusion, the most successful control scheme utilized both feedforward and feedback, combined. However, in the absence of predictive data on SO_2 removal efficiency, feedback alone may be sufficient in some commercial applications.

4.6.2 High-Ash Transient Response

The process response to large load changes and process upsets was evaluated during the high-ash test period. Of primary concern was the response of the pH and JBR ΔP controllers to these types of transients. To maintain consistent process performance, it is desirable to maintain steady, well-damped control of these two key process variables. The JBR ΔP controller exhibited excellent control in a variety of process transient and load-change situations. Some minor tuning changes were made to this feedback-type controller to enable it to maintain the setpoint (14 in. WC for this test block) within 0.2 in. WC under almost all conditions.

The pH controller, which can be operated in feedback or a combination feedforward-feedback mode, was operated in feedback mode for the duration of the test block. Feedforward-feedback control was not possible during this test period because the limestone reagent densitometer (a necessary component for this type of control scheme) was sporadically malfunctioning during the entire test block. During several large load transients, the pH signal could not be dampened quickly using only feedback control. Typically, the pH would deviate by no more than 0.3 pH units during the largest load changes in this test block. This effect was mitigated by limiting the rate of load change to less than 3 MWe/min. A load change limit such as this is a valuable tool (but undesirable, from a boiler flexibility standpoint) for maintaining pH control, particularly in a new installation that has not developed a predictive performance model. It is recommended, however, that a combined feedforward/feedback control scheme be used when adequate data exists to do so.

The process response to load changes was also evaluated during the load-following portion of the high-ash, high-sulfur coal test period. The response of the pH controller and JBR ΔP

(level) controller was of primary interest. The PID-type controller, which controls JBR ΔP, performed well, typically not allowing more than a 0.5 in WC change, even during the most radical load changes. The JBR ΔP was usually restored to its setpoint within 15-30 minutes of the transient. As expected, this performance was similar to that observed during previous testing.

The pH controller was operated in feedback mode only during the high ash, high-sulfur tests. Although feed forward operation was available, it was not considered because of intermittent failures of the limestone slurry densitometer and because there was not an accurate mathematical model of process performance at the process conditions tested. The pH controller responded well to large load decreases since the higher sulfur content of the coal resulted in high SO_2 pickup rates. The excess limestone associated with the sudden decrease in boiler load while using feedback control was rapidly neutralized due to the high SO_2 pickup rate. A large increase in boiler load did result in some lag pH response, but generally less than 0.4 pH units. This was a result of the large increase in limestone demand associated with the higher boiler loads and high sulfur coal, and the system's response time to the resulting pH changes. Based on these results and previous experience, a feedforward-feedback control scheme is suggested for future operations.

4.7 Effects of Alternate Fuels

One of the key purposes of this demonstration project was to evaluate the effect of alternate fuels (i.e., coals with varying compositions and sulfur contents) on scrubber performance. The scrubber was designed for the burning of 2.5% (nominal) sulfur coal, and a maximum coal sulfur content of 3.0%. Significant testing was done with the demonstration project baseline coal (2.5% sulfur), and limited testing was done at coal sulfur contents of 1.2%, 3.0%, 3.4%, and 4.3%.

Figure 4-32 illustrates the effects of the varying sulfur contents on scrubber performance. Note that 90% SO_2 removal efficiency is achievable at all inlet SO_2 concentration values,

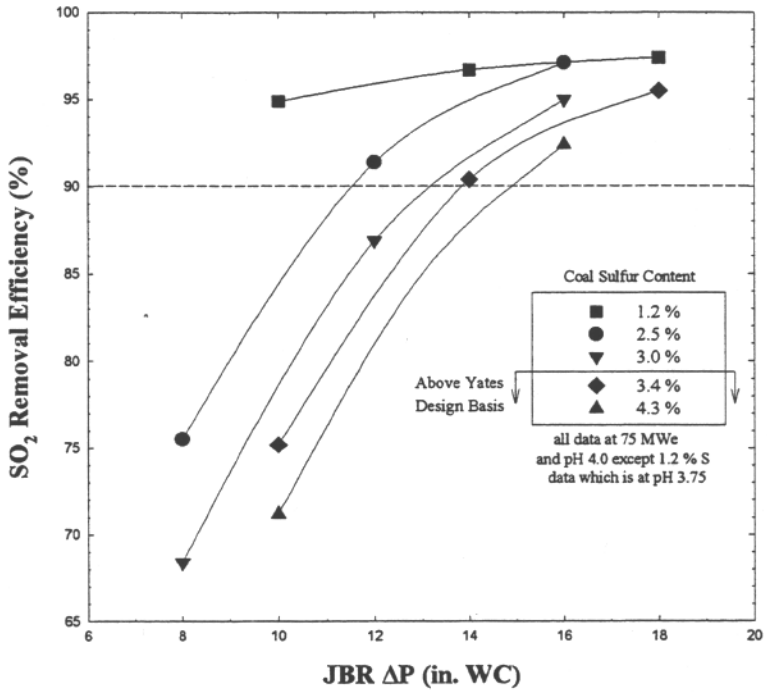

Figure 4-32. Coal Sulfur Content Effects on SO_2 Removal Efficiency

even at 3500 ppm (from the 4.3% sulfur coal test), which was 43 % above the process design coal sulfur content. This serves to illustrate the remarkable flexibility of the CT-121 process.

Although the varying coal sulfur content resulted in a varying solid phase residence time in the JBR, the gypsum crystal size and dewatering characteristics remained good regardless of coal composition. As discussed in the Process Economics volume of this report, the cost to remove SO_2 increases as coal sulfur content decreases. This is because many of the costs associated with operating the scrubber, such as fan and pump power costs, are independent of the inlet SO_2 concentration (at a constant JBR ΔP). Therefore, higher inlet SO_2 concentrations often result in decreased SO_2 removal costs on a dollars per ton of SO_2 basis. Although the SO_2 removal efficiency was over 95% for all JBR ΔP settings tested while burning the 1.2% sulfur coal (Plant Yates' planned CAA Title IV Phase I compliance coal), difficulty was experienced in maintaining a negative JBR water balance (i.e., less water was evaporated and

discharged with the slurry than was added to the JBR). This necessitated lowering the controlled solids content of the slurry from an average of 23 wt% solids to 15 wt.% solids to ensure a negative water balance was maintained. The JBR solids residence time did not change appreciably as a result of this change due to the lower coal sulfur content. Gypsum crystal size and slurry dewatering characteristics did not change significantly as a result of this change. Solids dewatering characteristics data are presented in Appendix B of this report. This coal will likely remain as Yates' compliance coal since Units 2-7 are not equipped with FGD systems and The Southern Company has arranged to purchase low-sulfur coal at similar pricing to the high-sulfur coal.

4.8 Effects of Alternate Limestones

During the demonstration, three different limestones were evaluated at the Yates CT-121 process, and eight limestones (including the three tested at Yates) were evaluated on a bench-scale JBR[1]. Several findings regarding limestone selection were made as a result of the bench-and full-scale evaluations. The original intent of the Alternate Limestone tests was to determine the impact of different limestones on SO_2 removal efficiency, process control, and process economics. It was learned through these tests that limestone selection plays a large role in gypsum byproduct particle size distribution (PSD), crystal habit, and dewatering characteristics. These variations were observed, even among limestones with similar calcium, magnesium, and inerts composition.

The first limestone chosen was one from Martin Marietta Aggregates (MMA) Leesburg, Georgia quarry. It was chosen based on the high $CaCO_3$ concentration, and low magnesium and inerts concentration. Although the gypsum produced while using the MMA stone was typical in size for a conventional FGD system, experience with other CT-121 systems has shown that the process is capable of producing much larger and more easily dewatered gypsum crystals. Table 4-16 shows a comparison of the Plant Yates gypsum to gypsum produced at the two other CT-121 sites in the United States. At both the Scholz and Abbott research projects, much larger mean particle sizes were achieved and significantly fewer fines

TABLE 4-16
COMPARISON OF YATES AND OTHER CT-121 GYPSUM

CT-121 Plant Location	Mean Particle Size (µm)	Filtration Rate ($lb/hr/ft^2$)	TKUA[a] @ 30 wt.% ($ft^2/ton/day$)	PSD[b] 50 wt.% less than (microns)	PSD[b] 10 wt.% less than (microns)
Yates/MMA	38	200-300	0.7-0.9	36	10
Abbott	78	N/A	0.8	78	39
Scholz[2]	N/A	N/A	N/A	60[c]	35[c]

[a] TKUA - Thickener Unit Area
[b] PSD - Particle Size Distribution
[c] Values may have been biased low due to sieve being used for PSD analysis instead of a micro-trac. Wet sieve analysis has the propensity to break the long crystals observed in the Scholz gypsum SEMs. Visual interpretation of SEM shows some gypsum crystals as long as 400 µm and a significant portion larger than 100 µm.

were found in the byproduct gypsum. Both of these scrubbers use a clear liquor prescrubber instead of a gypsum slurry gas cooling system. For this reason, mechanical attrition was initially suspected as a possible cause of the small gypsum size in the Yates system. A thorough investigation was conducted to evaluate possible causes of the smaller-than-expected gypsum particle size and the higher-than-average quantity of fines. Some of the avenues of investigation included particle attrition testing, chemical analyses of the gypsum and limestone, and bench-scale testing.

4.8.1 Bench-Scale Investigation

All avenues of investigation, with the exception of bench scale testing, did not result in any significant correlation between the parameter tested and gypsum particle size. A high solid phase iron content in the MMA limestone-based gypsum, which resulted in a rusty coloration of the byproduct, was initially believed to be responsible for the atypical dewatering properties of the gypsum solids. Because of this observation, a series of bench-scale studies was designed to determine the impact of various parameters on gypsum crystal habit and dewatering characteristics.

The initial bench scale test matrix was designed to identity theroot cause of the smaller-than-expected gypsum particle size. Due to the unique rust color of the gypsum solids, iron was initially suspected as one of the causes. A material balance for iron was performed around the CT-121 process at Yates and the largest iron contributors were selected to be the points of variance in the test matrix. The test plan included tests utilizing various sources of limestone and process water, as well as varying the scrubber liquor initial ionic strength. Baseline tests were conducted using typical Yates chemistry conditions and limestone.

The testing revealed that changes in the process water and ionic strength of the scrubbing liquor had no effect on crystal size. Surprisingly, the choice of limestone did have a large effect. Two other limestones were evaluated, one producing results similar to those observed during the baseline tests, and the other yielding far superior gypsum crystals. The measure of the quality of the gypsum was largely dependent on the gypsum form filtration rate; settling rate (thickener unit area), and particle size distribution (PSD). This was the first indication that limestones with similar analytical compositions could produce gypsum with vastly different gypsum dewatering properties.

Based on these results, a second test matrix was devised. This test plan varied only one parameter - limestone source. Every limestone supplier within a 150 mile radius of the site was asked to provide a sample of limestone to be evaluated. The goal of this evaluation was to provide an empirical determination of the superior limestones, with respect to resulting gypsum crystal size and composition.

The results of this evaluation were used in the selection of the limestone for the alternate limestone test period. If successful, the same limestone may have been selected for use throughout the remainder of the demonstration project. The criteria used for evaluation included: gypsum form filtration rate, settling rate, composition, and color; and limestone composition, available size, and cost. Based on these criteria, a limestone from Dravo Lime's Saginaw, Alabama quarry was selected as a source expected to provide a significant

improvement in particle size and dewatering characteristics without compromising limestone quality or resulting in a significant cost differential.

4.8.2 Dravo Limestone Evaluation

Of particular interest during the Low-Particulate Auxiliary Test block was the effect of switching from MMA limestone to Dravo limestone on the full scale CT-121 scrubber at Yates. The bench-scale test results indicated that changing the limestone source might improve the solids dewatering properties by causing an increase in the. size of the gypsum particles. The specific mechanism of this effect was not known, but evidence suggested that it may have been linked to the inerts content, inerts composition, and/or the soluble iron in the limestone.

Gypsum byproduct composition data was used to calculate the concentration of gypsum, limestone, and inerts in the byproduct. Table 4-17 contains a summary of the solids composition results from the High Removal, Alternate Limestone, and Alternate Coal tests. A complete list of the gypsum and limestone analytical results is contained in Appendix B. Throughout the Low-Particulate Auxiliary Test block, the CT-121 system produced a high quality gypsum byproduct suitable for agricultural use or wallboard manufacture (assuming adequate washing to reduce chlorides in the retained liquor). As shown in Table 4-17, the average gypsum concentration was greater than 94.9 wt.%, and the limestone and inerts concentrations were less than 3 and 2 wt.%, respectively. The undissolved magnesium carbonate concentration (not shown) was less than 0.2 wt.% during all three test series.

TABLE 4-17
GYPSUM BYPRODUCT COMPOSITION -
LOW-PARTICULATE AUXILIARY TEST BLOCK

Test Series	Limestone Source	Gypsum (wt.%)	Limestone (wt.%)	Inerts (wt.%)	Iron (ppm)
High Removal	MMA	94.9	1.9	2.0	1860
Alternate Limestone	Dravo	96.0	2.3	0.9	580
Alternate Coal	Dravo	98.1	2.3	0.5	600

With respect to byproduct composition, the only significant effect of changing the limestone source was seen in the inerts and iron concentrations. According to Table 4-17, the inerts concentration decreased by more than 50%, and the iron concentration decreased approximately 70% after switching from MMA to Dravo limestone. Both are a result of the decrease in the inert and iron concentrations in the limestone, and both may have contributed to the improvement in the gypsum byproduct dewatering properties that was seen after switching to Dravo limestone. The dewatering improvements are discussed below.

The dewatering properties are indicators of the propensity of solids to settle and filter. The settling and filtration rates expected using full-scale dewatering equipment can be estimated using standard laboratory test procedures. Settling test results provide an estimate of the thickener unit area required to achieve a specified underflow solids concentration - 30 wt.% for the Yates settling tests. Form filtration test results provide information needed to calculate the filtration rate and filter cake solids concentration expected on a full-scale vacuum filter.

Table 4-18 lists the average dewatering properties measured during the Low-Particulate High Removal tests using MMA limestone, Alternate Limestone tests using Dravo limestone, and Alternate Coal tests using Dravo limestone. According to these results, the filtration rate during the High Removal tests was 200 lb/hr/ft^2 - typical of, or perhaps worse than, that expected of traditional forced-oxidation FGD gypsum solids. In contrast, the filtration rate following the limestone change was greater than 1300 lb/hr/ft^2 - a significant improvement. Throughout the Auxiliary Test block, the thickener unit area and filter cake solids concentration were in the range expected for typical forced-oxidation FGD solids. The required thickener unit area to achieve 30 wt.% solids decreased slightly, and the filter cake solids concentration increased slightly with the limestone change. These data also show that a 40% decrease in solid residence time during the alternate coal tests did not affect the dewatering properties.

The key to improving solids dewatering properties lies in improving the crystal size and morphology, or shape. In general, larger, regularly shaped crystals dewater better than

TABLE 4-18
GYPSUM BYPRODUCT DEWATERING PROPERTIES

Low-Ash Test Series	Limestone Source	Solids Residence Time (hrs)	Thickener Unit Area @ 30 wt.% (ft^2/ton/day)	Filtration Rate (lb/hr/ft^2)	Filter Cake (wt.%)
High Removal	MMA	43	0.91	200	85.7
Alternate Limestone	Dravo	45	0.82	1330	88.2
Alternate Coal	Dravo	26	0.83	136088.0	

smaller, irregularly-shaped crystals. Figure 4-33 shows a comparison of scanning electron micrographs (SEMs) of solids generated using MMA limestone reagent, with solids generated using Dravo limestone at similar process operating conditions. The figure clearly shows the increased particle size after switching from MMA to Dravo limestone. Some of the Dravo crystals appear to have an increased length to diameter ratio while the MMA crystals were more rounded. This result suggests that a crystal habit modifier is present in the MMA limestone that is causing the growth of smaller-than-normal particles.

Another factor that affects particle size is the solids residence time. During the High-Particulate Alternate Coal tests, the solids residence time decreased by approximately 40% compared to the residence time during the Low-Particulate Alternate Limestone tests. This effect is illustrated in Figure 4-34, which shows SEMs of solids generated during the Alternate Coal tests, compared with solids generated during the Alternate Limestone tests, both using the Dravo limestone reagent. The decrease in solids residence time during the alternate coal tests resulted in no significant change in crystal size, and little change in the crystal morphology. As shown in Table 4-19, the mean byproduct particle size was smaller, however, this may be attributable to the presence of fly ash in the byproduct due to elevated ash loading, as evidenced by the higher inert content during the Alternate Coal tests.

Gypsum solids particle size measurements, shown graphically in Figure 4-35, verified the effect of switching to Dravo limestone on the solids particle size. Particle sizes were measured using a Microtrac® laser diffraction particle size analyzer. Figure 4-35 compares

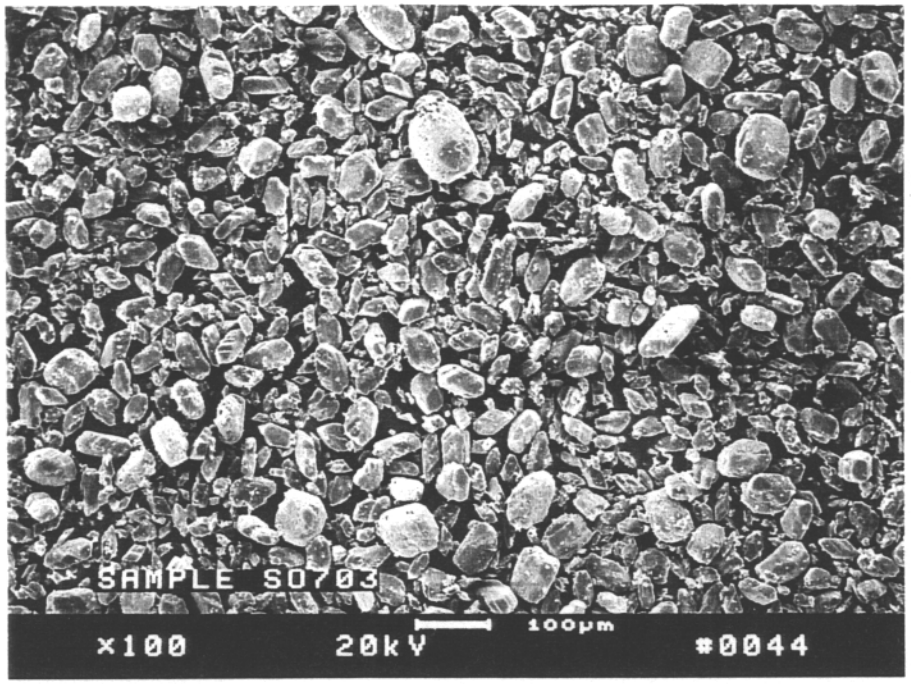

Gypsum from Operation With MMA Limestone Reagent (100X)

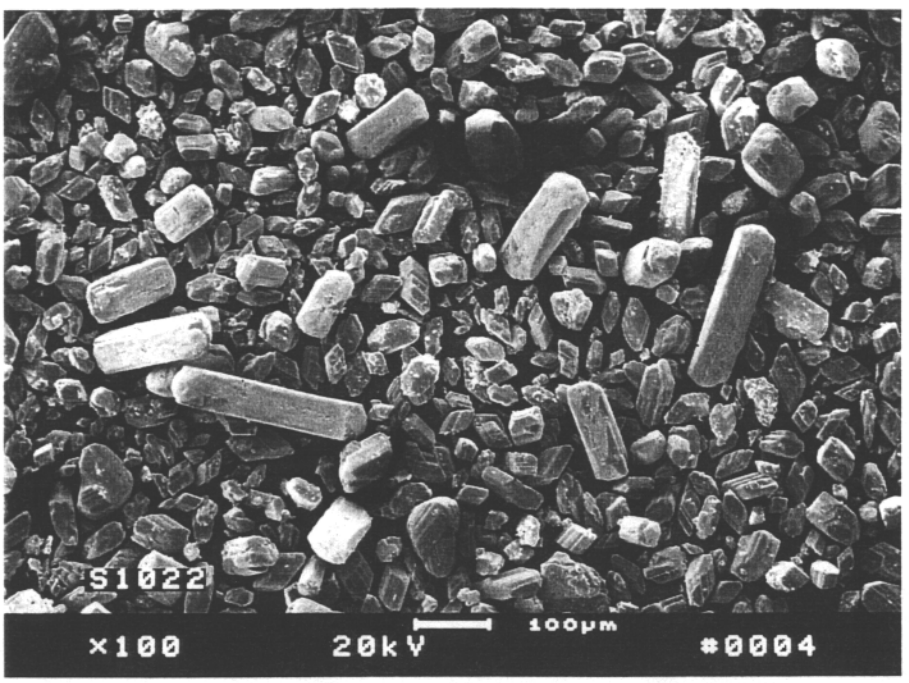

Gypsum from Operation With Dravo Limestone Reagent (100X)

Figure 4-33. Comparison of Gypsum Solids from Operation with MMA and Dravo Limestone

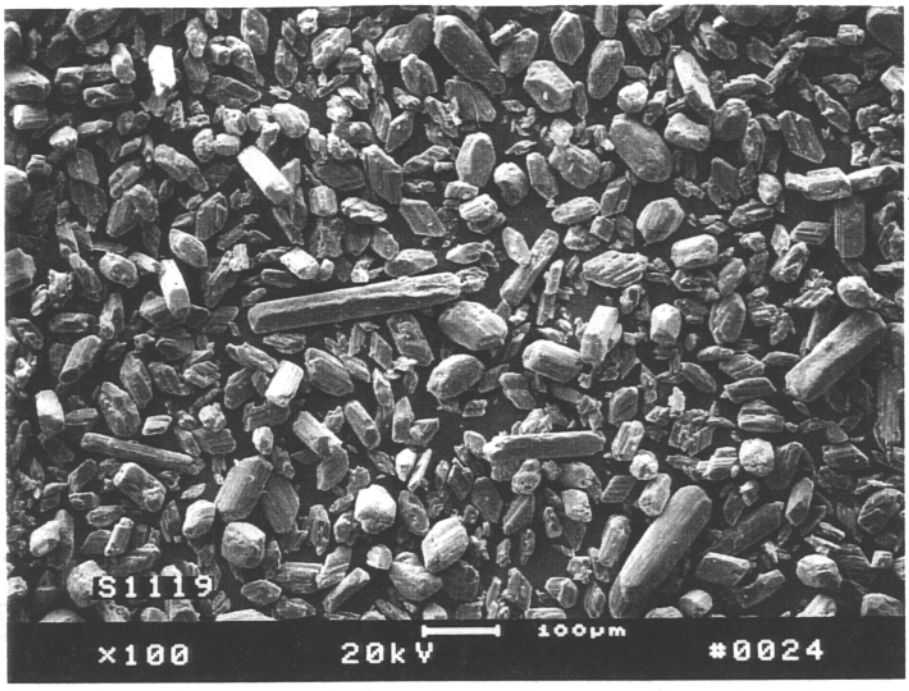

Gypsum from Alternate Limestone Test (100X)

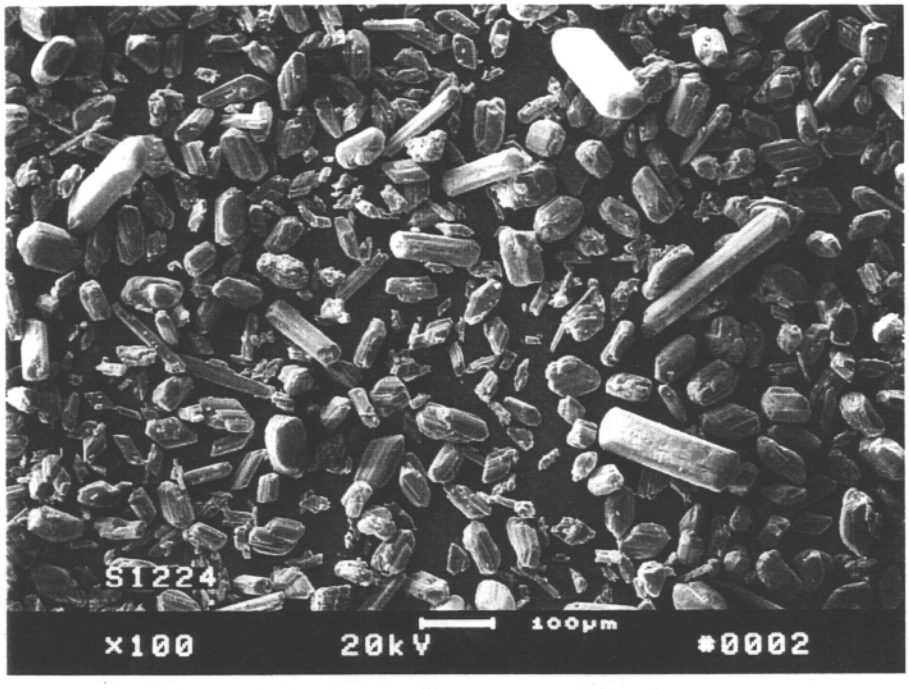

Gypsum from Alternate Coal Test (100X)

Figure 4-34. Gypsum Solids from Operation with Dravo Limestone Reagent

TABLE 4-19
COMPARISON OF GYPSUM BYPRODUCT CHARACTERISTICS DURING MODERATE ASH-LOADING WITH TWO DIFFERENT COAL SOURCES

Byproduct Characteristics (average value)	2.5 % Sulfur Coal	3.4 % Sulfur Coal
Gypsum (wt.%, dry)	97.1	90.9
$CaCO_3$ (wt.%, dry)	2.3	3.1
Inerts (wt.%, dry)	0.9	6.0[a]
Mean Particle Size (μm)	41.5	35.6
Form Filtration Rate (lb/hr/ft^2)	1330	800
Filter Cake (wt.% solids)	88.9	83.5

[a] Elevated ash loading resulted in higher inerts than in low-ash byproduct solids

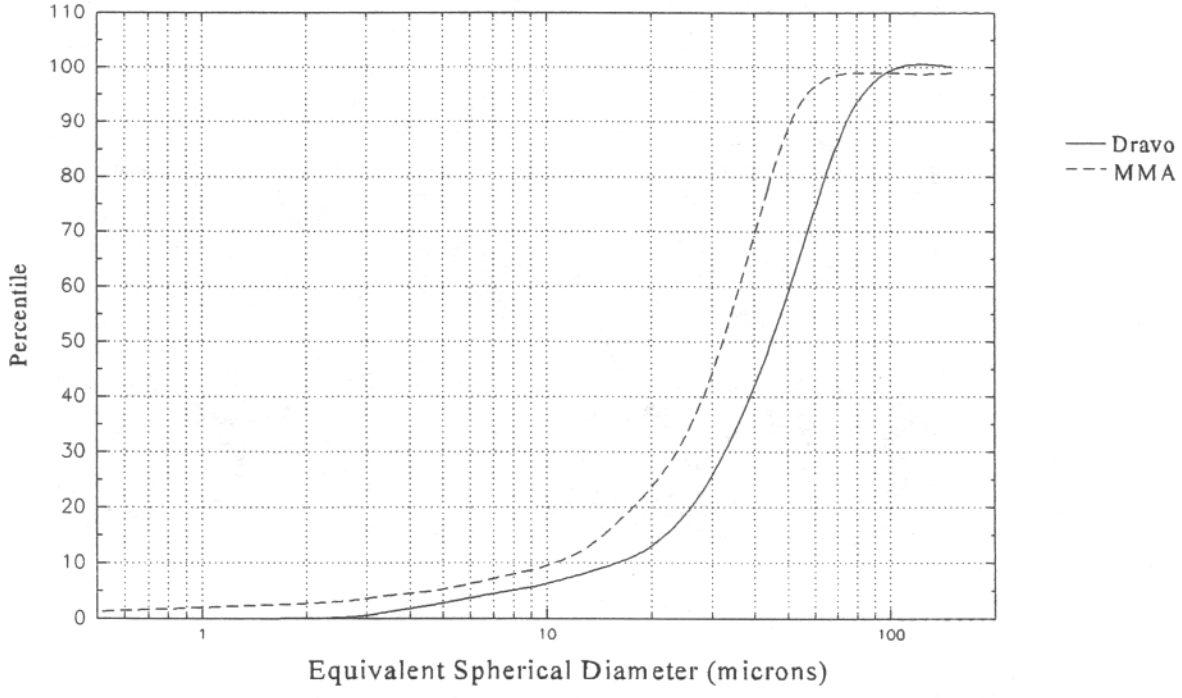

Figure 4-35. PSD Comparison of Gypsum Produced with MMA and Dravo Limestones

particle sizes from the Long-Term tests using MMA limestone with that of Alternate Limestone tests using Dravo limestone. As expected based on the SEMs, the particle size distribution was larger during the Alternate Limestone (Dravo) tests.

4.8.3 Florida Rock Limestone Evaluation

During the High-Particulate Auxiliary Test block, as part of the Alternate Limestone test, it was decided to evaluate another limestone. The primary factor in choosing a limestone from Florida Rock's Rome, Georgia quarry was cost; however, consideration was given to performance (i.e., crystal size and dewatering properties) from the bench-scale evaluation. The Florida Rock limestone performed well in that evaluation, although several other limestones may have resulted in superior dewatering characteristics. Since limestone cost makes up a significant portion of the variable cost to remove each ton of SO_2, the 30% decrease in cost of the Florida Rock stone could result in substantial overall cost savings.

The gypsum produced while using the Dravo Lime limestone had an average mean particle size of 38 µm during the High-Particulate High-Removal Tests. A scanning electron micrograph (SEM) of this byproduct is shown in Figure 4-36. The full scale test of the Florida Rock limestone supported the bench-scale results. The average particle size, about 35.6 µm, was larger than that of the first limestone used (from Martin Marietta Aggregate's Leesburg, Georgia quarry - which also performed poorly in the bench-scale evaluation and had a mean particle size of only 32 µm), but still smaller than that of the Dravo Lime limestone.

A comparison of the Dravo results during high-ash testing was required for a valid comparison since the Florida Rock stone was tested under conditions of elevated ash loading. The gypsum from operation with the Dravo Lime limestone had an average particle size of 43 µm during the low-ash test phase, but decreased to as low as 24 µm under heavy ash loading conditions, and was about 38 µm under moderate ash loading conditions, similar to those of the High-Particulate Alternate Limestone Test using Florida Rock limestone. A SEM of the gypsum byproduct from this test is shown in Figure 4-37. A summary of

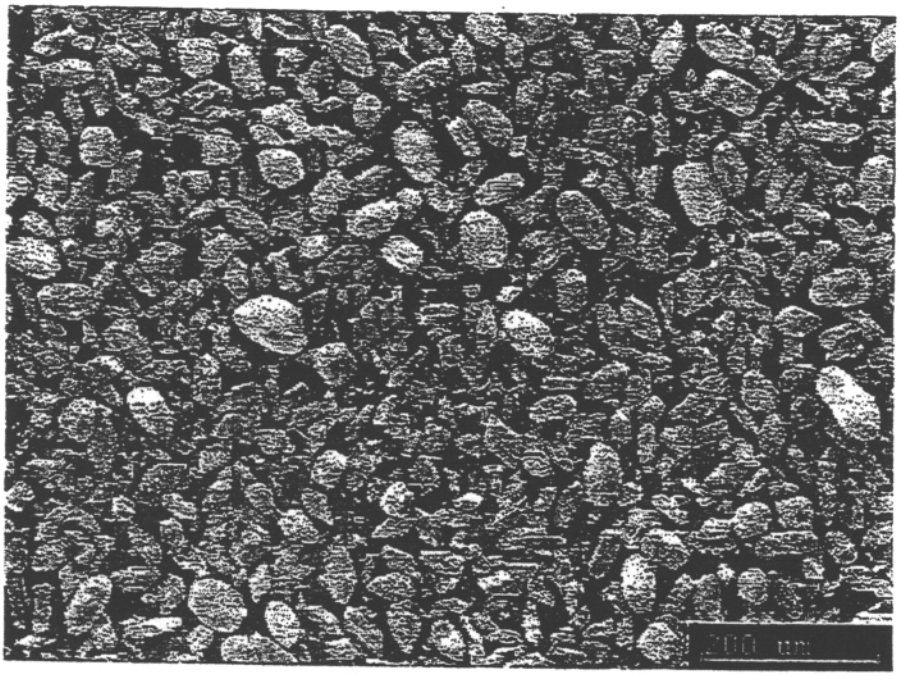

Figure 4-36. Elevated-Particulate Dravo Gypsum Byproduct SEM (100X)

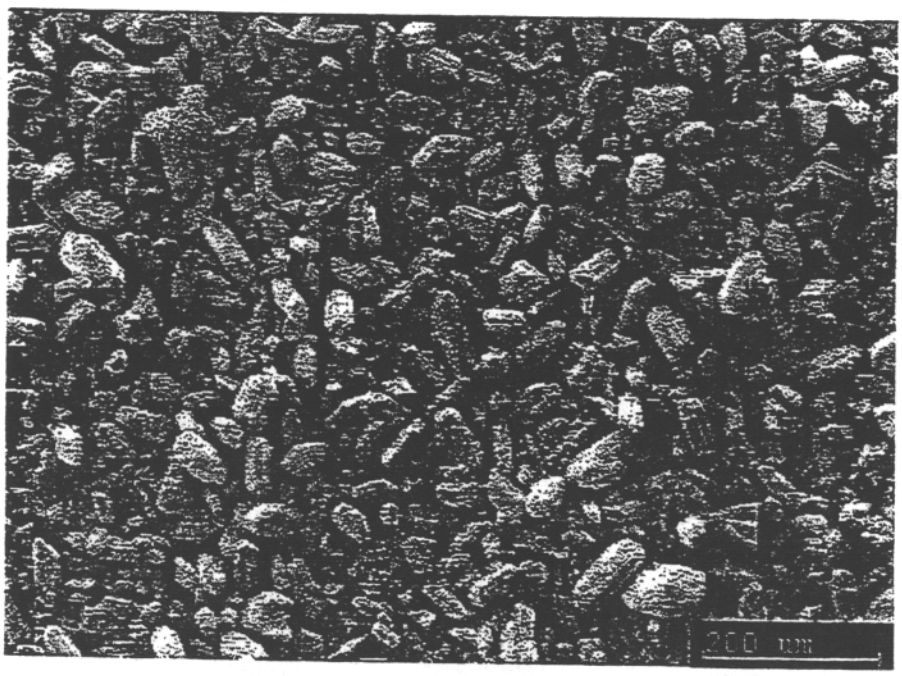

Figure 4-37. Elevated-Particulate Florida Rock Gypsum Byproduct SEM (100X)

byproduct solids characteristics is shown in Table 4-20. Complete byproduct and limestone analyses are provided in Appendix B. The results shown in Table 4-20 tend to vary because of inconsistent ESP outlet particulate loading. Although the ESP was maintained at a consistent state of energization within each of the test periods, there is still some fluctuation in performance. It is those fluctuations that resulted in the wide range of data in Table 4-20. It is likely that the ash content of the byproduct was as much responsible for the fluctuations in byproduct particle size and dewatering properties as any other factor. The most significant performance indicator, observed gypsum byproduct stackability, showed that the gypsum byproduct properties were adequate for this type of dewatering and disposal technology. Direct comparisons of PSD of the gypsum byproduct using the MMA and Florida Rock stones could not be made due to significant differences in ash loading between these tests (i.e., the MMA stone was not evaluated at elevated ash loading, nor was the Florida Rock stone evaluated at low-ash conditions).

TABLE 4-20
COMPARISON OF GYPSUM BYPRODUCT CHARACTERISTICS UNDER MODERATE ASH-LOADING WITH TWO DIFFERENT LIMESTONE SOURCES

Byproduct Characteristics	Dravo Limestone	Florida Rock Limestone
Gypsum (wt.%, dry)	82.9-94.6	80.7-94.4
$CaCO_3$(wt.%,dry)	0.4-2.6	1.0-13.8a
Inerts (wt.%, dry)	2.3-18.0	2.6-14.2
Mean Particle Size (μm)	36.2-39.8	33.5-37.8
Form Filtration Rate (lb/hr/ft^2)	110-200	65-1180
Filter Cake (wt.% solids)	77.3	61.1-64.9

[a] Includes an instance of severe Aluminum fluoride blinding

4.9 Particulate Removal Efficiency

This section contains the results of the particulate removal testing conducted under three ash-loading conditions (i.e., low-, high-, and moderate-ash loading at the JBR inlet). During each test, a parametric test matrix was implemented to evaluate the effects of ash-loading, unit load, and JBR ΔP (controlled by adjusting sparger tube submergence depth) on particulate emissions, sulfuric acid mist, and removal efficiency by particle size. The conditions and variables for the three test periods were summarized in Table 3-12 (in Section 3.4 of this report), and discussed in detail in the following sections.

4.9.1 Low-Ash Particulate Removal Test

The first parametric tests were conducted with the plant operating under three load conditions and three sparger depths (nine test conditions), and with the ESP operating normally (i.e., all fields fully energized). The particulate loading at both the JBR inlet and outlet (stack) was determined using EPA Method 5B[4], developed for the determination of nonsulfuric acid mist particulate matter. Even though a sampling method was used for "nonsulfuric acid mist," an analysis of the filter substrates following sample collection indicated the presence of considerable quantities of sulfate. This was particularly the case for samples collected at the stack, where one would expect a sulfate/calcium mass ratio of about 2.4 due to the presence of scrubber liquor carryover. The analytical results showed ratios for the stack ranging from 6 to 12. It is reasonable to assume this is due to condensed sulfuric acid mist, since maintaining the sampling conditions required for Method 5B (320°F) in the probe liner and filter holder may be impossible, given the low temperature (approximately 115°F) and saturated nature of the stack flue gas. Although the filter is heated to 320°F after sample collection, the 6-hour drying time may not have been adequate to evaporate all of the sulfuric acid mist. JBR inlet and outlet mass loadings are shown graphically for 50, 75, and 100 MWe load conditions as a function of JBR ΔP in Figures 4-38 to 4-40. The trend for decreased outlet particulate loading as the JBR ΔP increases is evident in both the 50 and 75

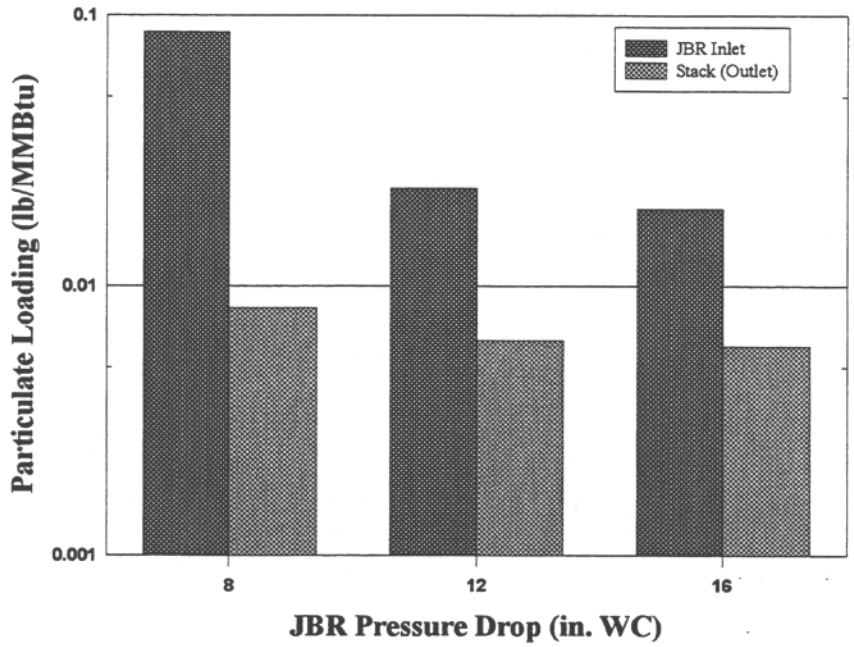

Figure 4-38. Low-Ash Particulate Loading at 50 MWe

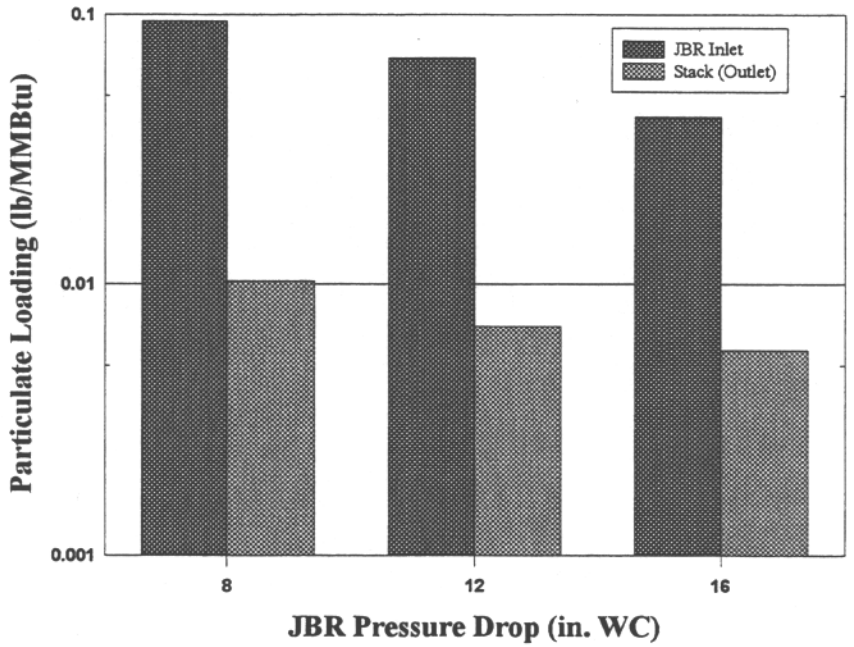

Figure 4-39. Low-Ash Particulate Loading at 75 MWe

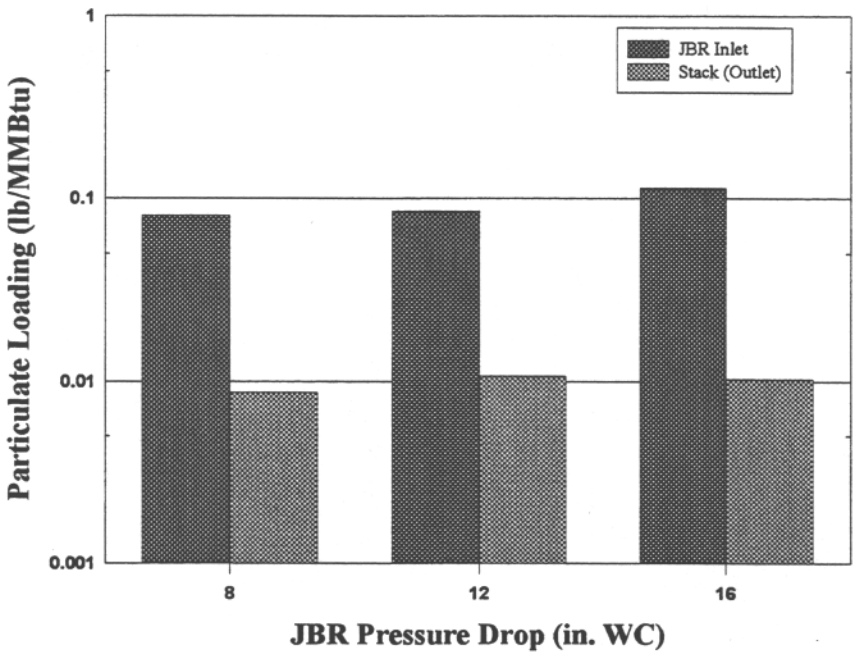

Figure 4-40. Low-Ash Particulate Loading at 100 MWe

MWe graphs, although the inlet loading is variable for these series of tests. The data also indicate decreased outlet particulate loading with decreasing inlet loading, indicating that inlet particulate is also an important variable. Stack loading appears to be fairly consistent for the 100 MWe test condition, although these tests also show the highest potential for sulfuric acid mist contamination of the particulate loading results. Regardless of the test conditions, all of the particulate loading values for the stack are well below the current NSPS limit of 0.03 lbs/MMBtu. The particulate loading values for the normal JBR ΔP (12 inches) and boiler loads are shown in Figure 4-41.

Particulate removal efficiency for the various test conditions are presented in Table 4-21 and shown graphically in Figure 4-42. This graphs shows that particulate removal across the JBR averages around 90% except under low-load (50 MWe) conditions. This is due to the low JBR inlet mass loading encountered during the 50 MWe testing. At low loads, the overall efficiency of the ESP increased due to the reduced gas velocity through the ESP, resulting in greatly reduced particulate loading to the JBR. Changes in inlet mass loading also account

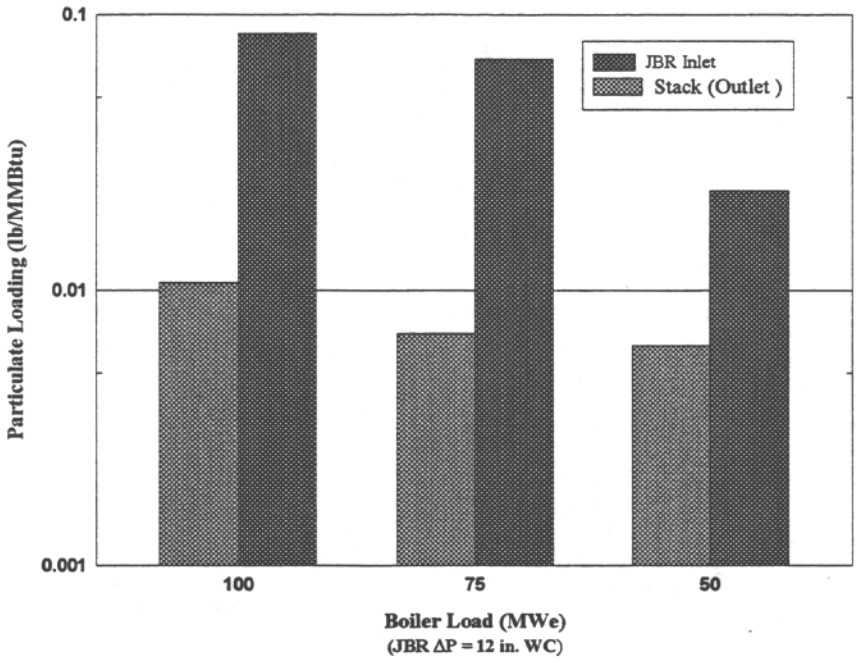

Figure 4-41. Low-Ash Particulate Loading by Unit Load

TABLE 4-21
LOW-ASH PARTICULATE REMOVAL EFFICIENCY

Test I.D.	Unit Load (MWe)	JBR ΔP (in. WC)	Average Inlet Loading (lb/MMBtu)	Average Outlet Loading (lb/MMBtu)	Particulate Removal[a] (%)	Particulate Penetration[b] (%)
P1-1	100	8	0.0807	0.0087	89.2	10.8
P1-2	100	12	0.0853	0.0107	87.5	12.5
P1-3	100	16	0.114	0.0103	91.0	9.0
P1-4	75	8	0.095	0.0103	89.2	10.8
P1-5	75	12	0.069	0.007	89.9	10.1
P1-6	75	16	0.0417	0.0057	86.3	13.7
P1-7	50	8	0.0867	0.0083	90.4	9.6
P1-8	50	12	0.023	0.0063	72.6	27.4
P1-9	50	16	0.0193	0.006	68.9	31.1

[a] % Removal = $(JBR_{in} - Stack_{out})/JBR_{in} * 100\%$
[b] % Penetration = 100% - % Removal

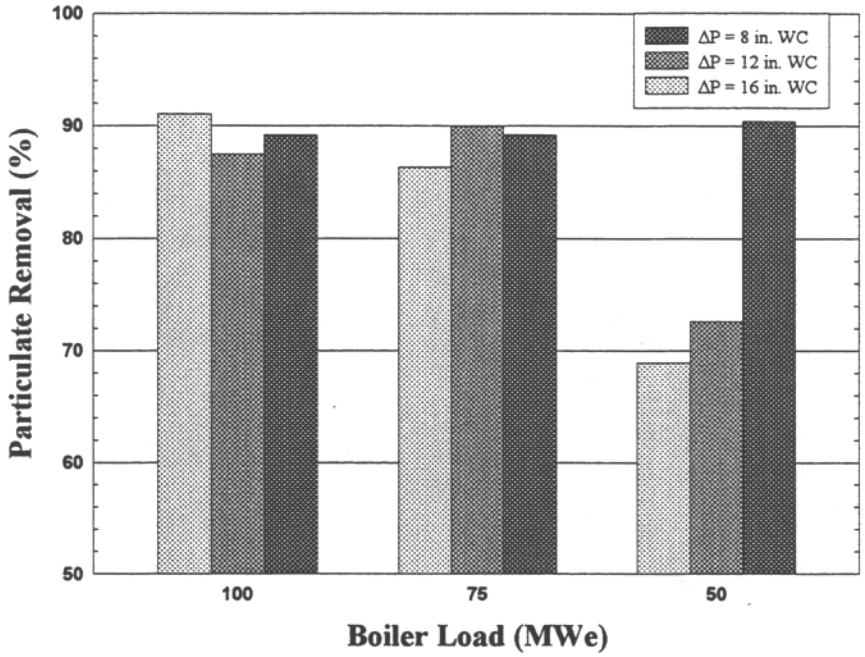

Figure 4-42. Low-Ash Particulate Removal

for the decrease in particulate removal efficiency with increasing JBR ΔP during the 50 MWe tests.

Figure 4-43 shows the outlet mass loading for all the JBR conditions by plant load. Comparing Figure 4-42 to Figure 4-43, although particulate removal efficiency is lowest at 50 MWe, the absolute mass emissions are also lowest at 50 MWe. These data may indicate that there is a lower outlet particulate threshold below which the CT-121 process at Plant Yates cannot reduce particulate emissions.

Sulfuric acid mist was also directly measured at the JBR inlet and the stack using the controlled condensation sampling technique. The results of these tests for the JBR inlet and the stack are presented in Table 4-22 and shown in Figures 4-44 through 4-46 for 50, 75, and 100 MWe, respectively. Sulfuric acid mist removal for the various test conditions is plotted

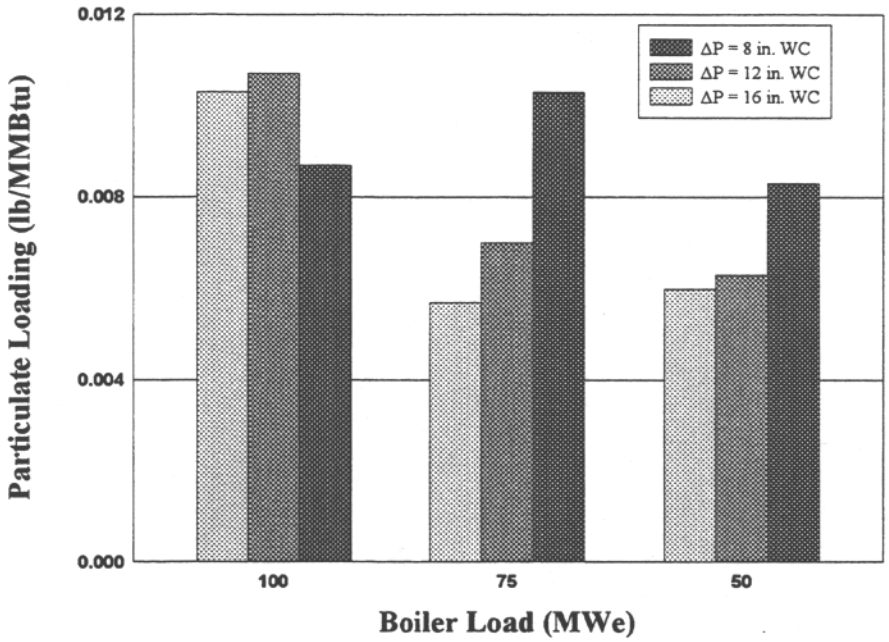

Figure 4-43. Low-Ash Outlet Particulate Loading

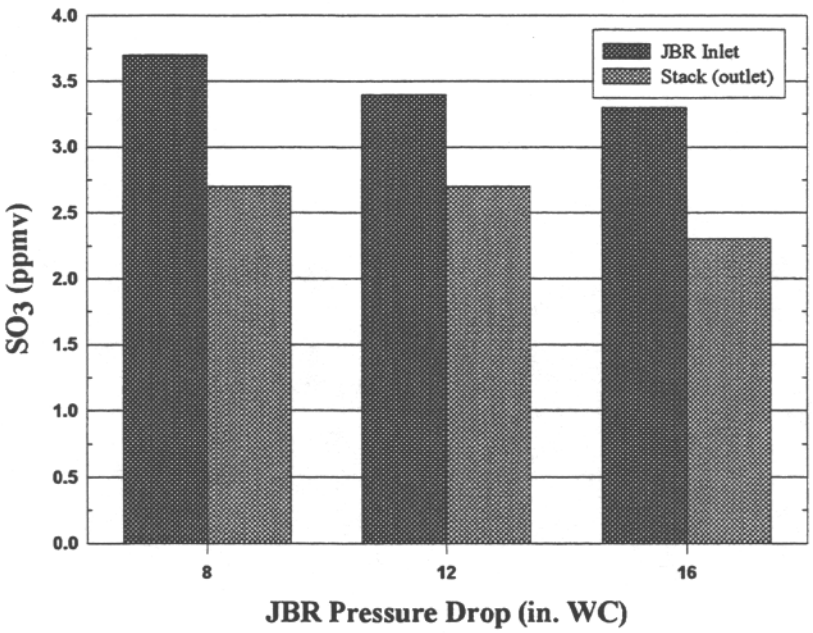

Figure 4-44. Low-Ash Sulfuric Acid Mist Loading at 100 MWe

TABLE 4-22
LOW-ASH SULFURIC ACID MIST REMOVAL EFFICIENCY

Test I.D.	Unit Load (MWe)	JBR ΔP (in. WC)	Inlet SO_3 (ppmv) a	Outlet SO_3 (ppmv) a	Removal[b] (%)
P1-1	100	8	3.7	2.7	27.0
P1-2	100	12	3.4	2.7	20.6
P1-3	100	16	3.3	2.3	30.3
P1-4	75	8	2.5	2.6	-4.0
P1-5	75	12	2.9	3.4	-17.2
P1-6	75	16	2.8	3	-7.1
P1-7	50	8	1.9	1.7	10.5
P1-8	50	12	2.3	1.5	34.8
P1-9	50	16	3.8	2.4	36.8

[a] All values corrected to 3% O_2.
[b] % Removal =$(JBR_{in} - Stack_{out})/JBR_{in} * 100\%$.

in Figure 4-47. This plot shows a 25 - 35% reduction in sulfuric acid mist across the JBR except during the 75 MWe load condition. The reasons for no apparent reduction in sulfuric acid mist under the 75 MWe load is not known, but is most likely due to errors associated with representative sample collection.

4.9.1.1 Particle Size Distribution

JBR inlet and outlet particle size distribution was measured for each of the nine operating conditions. The primary results are presented in Table 4-23. In general, the higher the plant load, the better the overall removal efficiency by particle size. This is probably due to the increase in velocity through the JBR under the higher load conditions. The increased gas velocity leads to better "jet bubbling" through the reactor which produces smaller bubbles and more intimate gas/liquid contact, increasing particle removal efficiency. Differences in JBR ΔP have a lesser impact on performance.

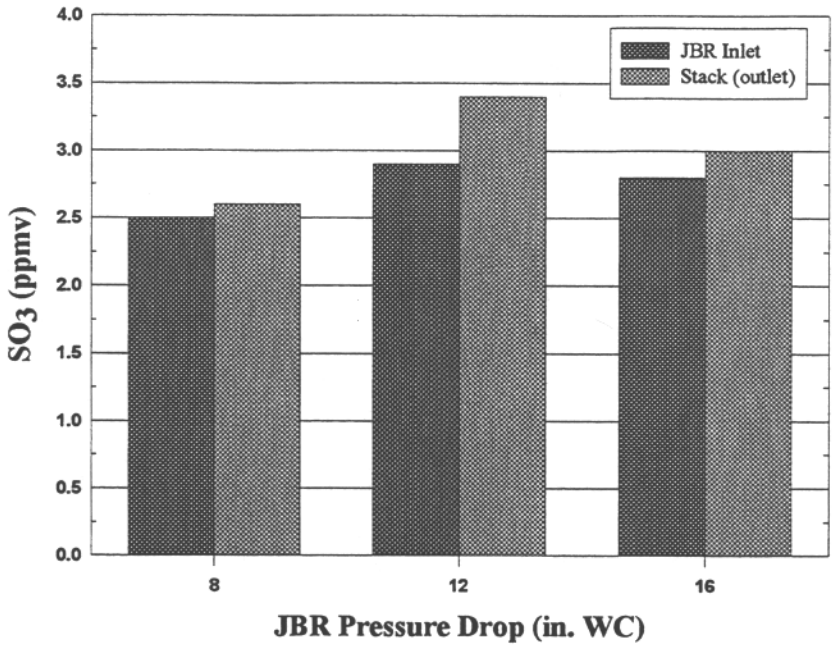

Figure 4-45. Low-Ash Sulfuric Acid Mist Loading at 75 MWe

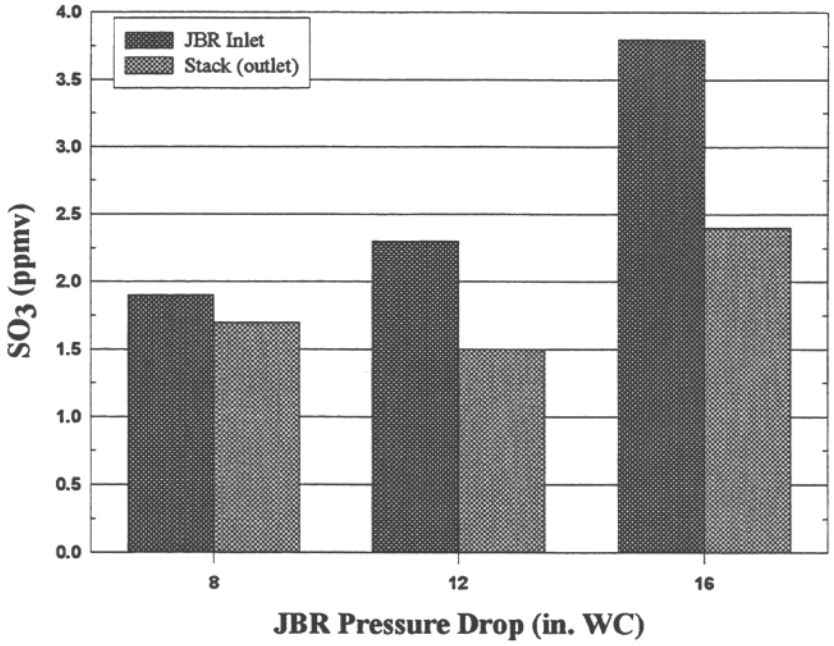

Figure 4-46. Low-Ash Sulfuric Acid Mist Loading at 50 MWe

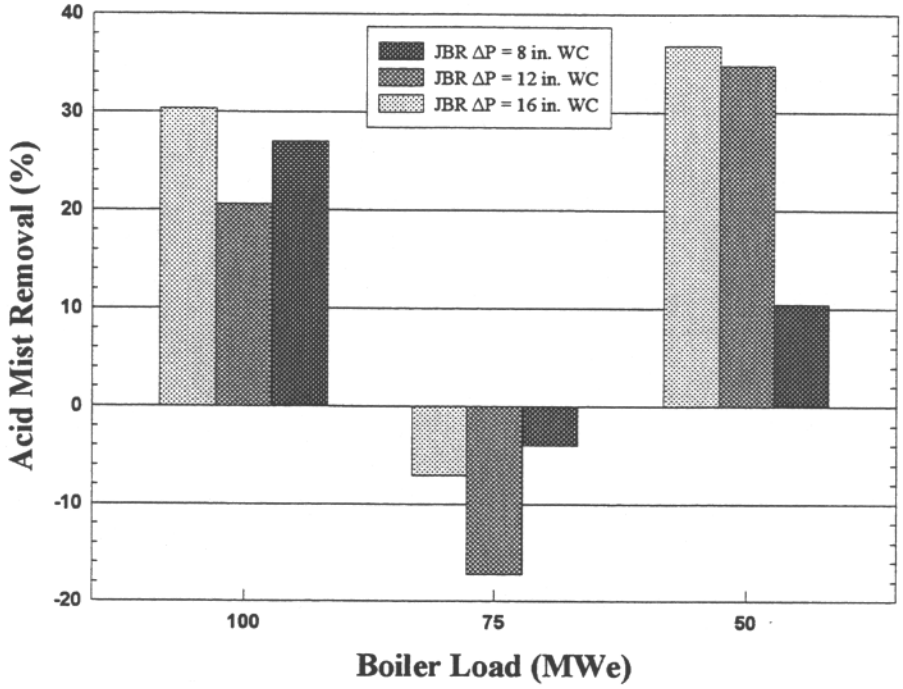

Figure 4-47. Low-Ash Sulfuric Acid Mist Removal Efficiency by Test Condition

TABLE 4-23
PARTICLE SIZE DISTRIBUTION RESULTS

Test I.D.	Load	JBR ΔP	Particle Size Showing < 90% Removal
P1-1	100	8	< 2 μm
P1-2	100	12	< 1 μm
P1-3	100	16	< 1 μm
P1-4	75	8	< 2 μm
P1-5	75	12	< 2 μm
P1-6	75	16	< 9 μm
P1-7	50	8	< 9 μm
P1-8	50	12	< 10 μm
P1-9	50	16	< 10 μm

4.9.2 High-Ash Particulate Removal Test

Particulate testing during the high-ash phase of the program was conducted at two load conditions, 50 and 100 MWe. During the 100 MWe test, the JBR was operated at gas-side pressure drops of 10 and 16 inches, and the ESP was operated using only the first field, which was either 100% energized, off, or detuned (i.e., partially energized). Testing at 50 MWe was similar except the first field ESP was either on or off. The detuned mode was not tested. The results of the particulate loading tests performed under each load conditions are shown in Table 4-24 and presented graphically in Figures 4-48 and 4-49. These results indicate that with the ESP fully deenergized, the CT-121 process was capable of up to 99% particulate removal efficiency at full load.

The data in Table 4-24 summarize the key particulate removal efficiency measurements across the scrubber. Note that the actual ESP efficiency does not decrease to zero, even with the ESP completely deenergized. This is due to gravitational "fall-out" of the larger ash particles while passing through the ESP. During the test conducted immediately after a detuning step, residual charge in the ESP may also be responsible for some additional particulate collection. JBR removal efficiency for all test conditions ranged from over 93% to greater than 99%. The tests conducted at the highest inlet particulate loading resulted in the highest particulate removal efficiency.

Removal and outlet mass loadings are shown in Figures 4-50 and 4-51 respectively. There appears to be a threshold value, below which the outlet particulate loading will not fall, as shown in Table 4-24 and Figure 4-51. In this case, there are actually two threshold values, one (around 0.013 lb/MMBtu) for the moderate inlet particulate mass loading associated with tests P2-1 through P2-5, and another higher value (around 0.049 lb/MMBtu) for the high. inlet mass loadings of tests P2-6 through P2-9. The average outlet loading value of 0.013 lb/MMBtu compares favorably with that observed during the low-ash testing previously described in section 4.9.1.

TABLE 4-24
HIGH-ASH PARTICULATE REMOVAL EFFICIENCY

Test I.D.	Target ESP Efficiency (%)	Actual ESP Efficiency (%)	Unit Load (MWe)	JBR ΔP (in. WC)	Inlet Loading (lb/MMBtu)	Outlet Loading (lb/MMBtu)	Particulate Removal (%)
P2-1	90	98.8	50	10	0.196	0.013	93.6
P2-2	90	95.6	50	16	0.168	0.011	93.5
P2-3	90	94.3	100	10	0.434	0.017	96.0
P2-4	90	93.1	100	16	0.525	0.010	98.2
P2-5	50	89.9	100	16	0.819	0.015	98.2
P2-6	0	24.3[a]	100	10	5.778	0.049	99.2
P2-7	0	30.6[a]	100	16	5.293	0.042	99.2
P2-8	0	33.9[a]	50	10	5.046	0.056	98.9
P2-9	0	35.4[a]	50	16	4.927	0.048	99.0

[a] Some particulate removal capability exists in the fully deenergized ESP due to fallout of the larger ash particles as the flue gas passes through the ESP.

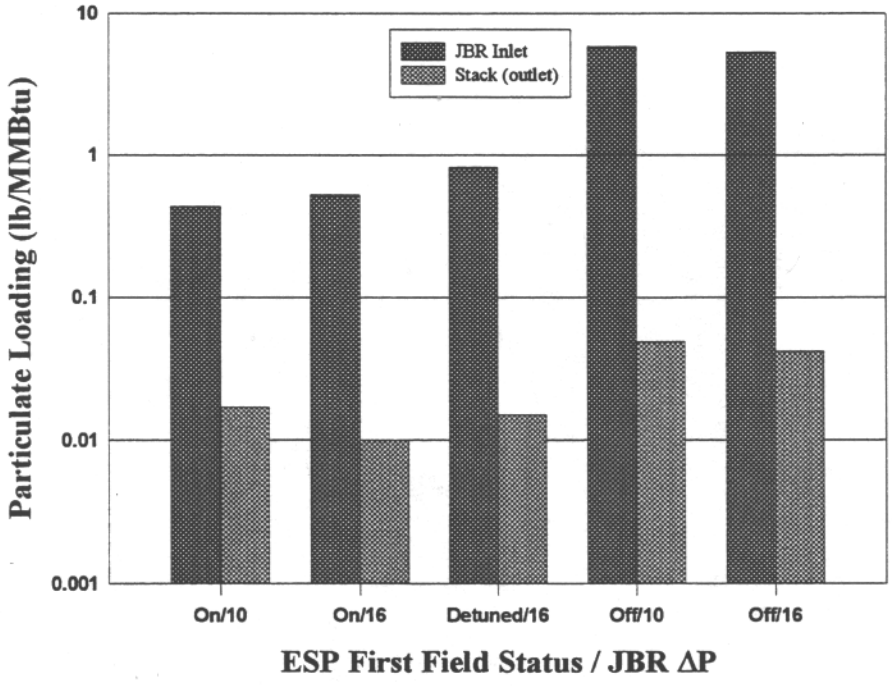

Figure 4-48. High-Ash Particulate Loading at 100 MWe

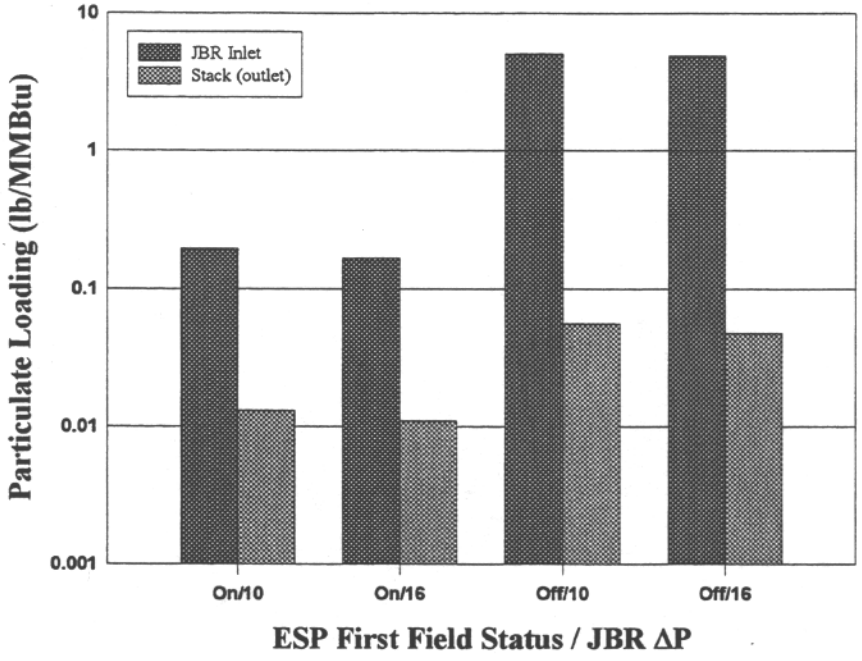

Figure 4-49. High-Ash Particulate Loading at 50 MWe

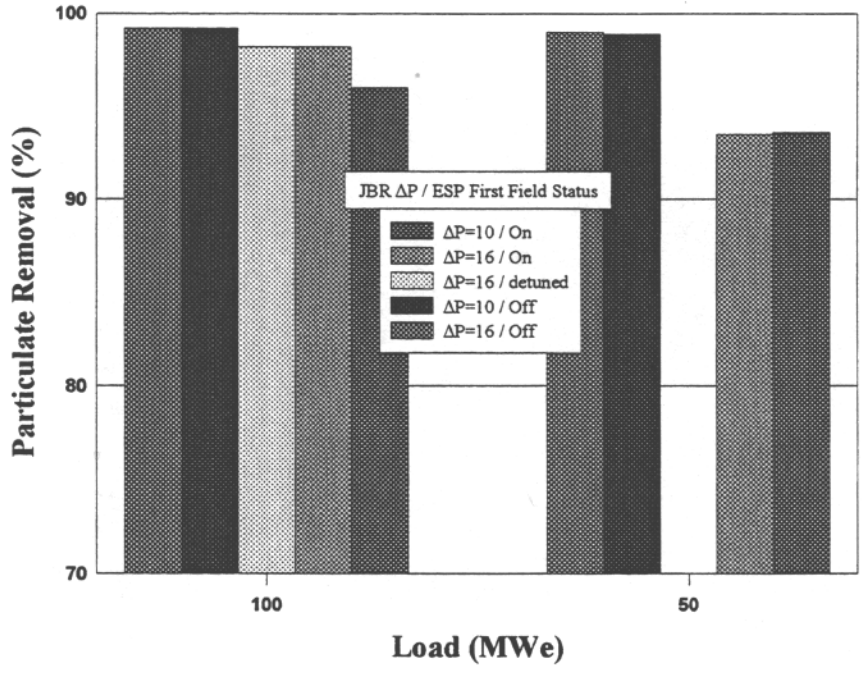

Figure 4-50. High-Ash Particulate Removal

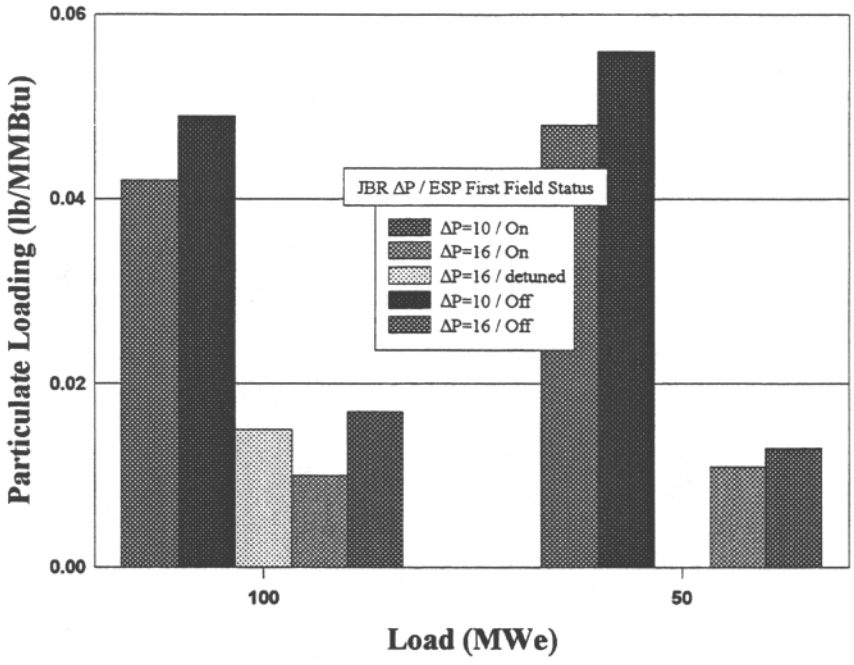

Figure 4-51. High-Ash Outlet Particulate Loading

Sulfuric acid mist was also measured during each of the test conditions described above. Results for these tests are presented in Table 4-25 and presented graphically in Figures 4-52 and 4-53. Sulfuric acid mist removal is shown in Figure 4-54.

The material on the filters and substrates from the particulate sampling was analyzed by energy dispersive x-ray analysis (EDX). During moderate-ash loading tests, the filter solids analysis indicated that 50-55% of the outlet solids were comprised of sulfate, compared to 2-4% at the inlet. Only 10-15% sulfate was measured on the outlet filters during the high-ash tests (P2-6 through P2-9). This indicates that a much larger portion of the outlet mass loading was due to ash carryover in the high-ash inlet loading tests than in those tests with low- to moderate-ash loading. A water extraction and acetone wash of the sample probes and nozzles did indicate a rise in soluble sulfate from the low- to high-particulate tests. The sulfate increased from nominally 8% to 20%.

TABLE 4-25
SULFURIC ACID MIST REMOVAL EFFICIENCY RESULTS

Test ID	Unit Load (Mwe)	JBR ΔP (in. WC)	First Field ESP	Inlet SO_3 (ppmv)[a]	Outlet SO_3 (ppmv)[a]	Removal (%)[b]
P2-1	50	10	On	1.63	2.72	-67%
P2-2	50	16	On	1.38	2.16	-57%
P2-3	100	10	On	1.93	2.96	-53%
P2-4	100	16	On	1.69	1.02	40%
P2-5	100	16	Detuned	1.54	1.32	14%
P2-6	100	10	Off	1.43	0.56	61%
P2-7	100	16	Off	0.88	<0.26	>70%
P2-8	50	10	Off	1.54	<0.2	>87%
P2-9	50	16	Off	1.38	0.41	70%

[a] All values corrected to 3% O_2
[b] % Removal $= (JBR_{in} - Stack_{out})/JBR_{in} * 100\%$

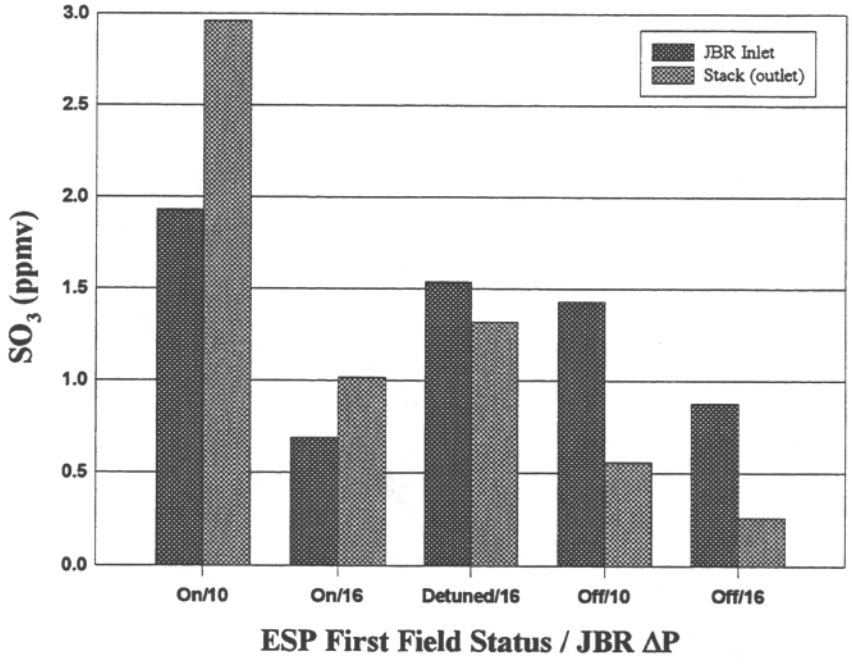

Figure 4-52. High-Ash Sulfuric Acid Mist Loading at 100 MWe

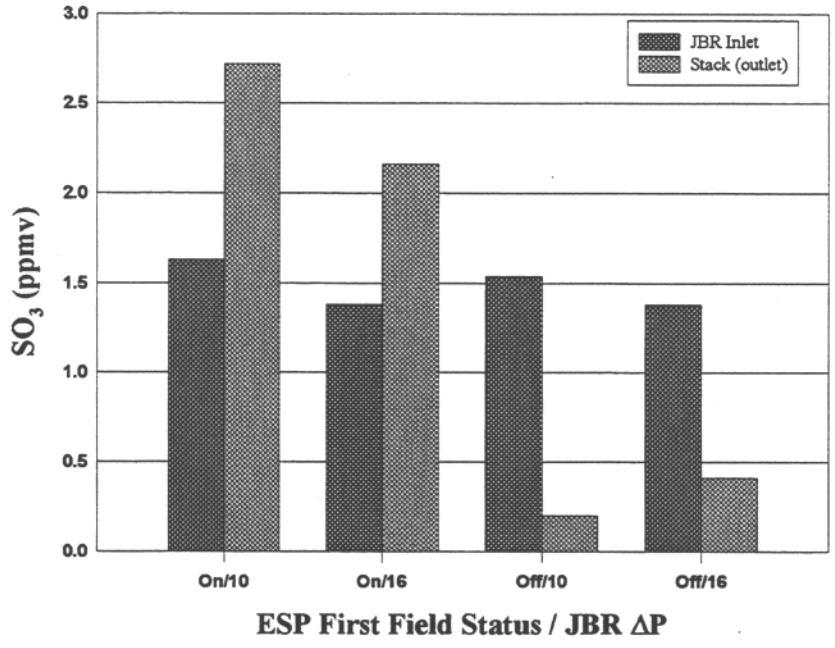

Figure 4-53. High-Ash Sulfuric Acid Mist Loading at 50 MWe

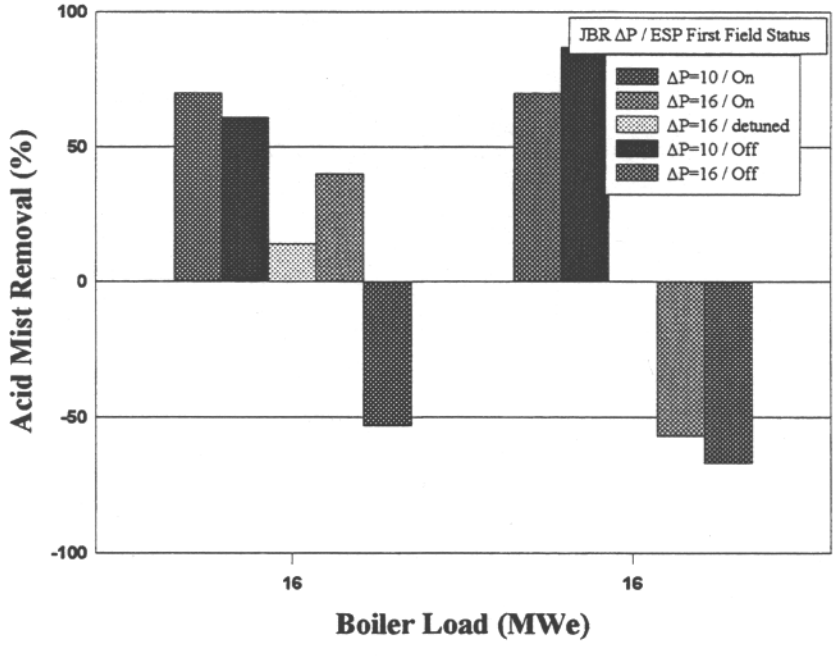

Figure 4-54. High-Ash Sulfuric Acid Mist Removal

4.9.2.1 Particle Size Distribution

Particle size was measured at the JBR inlet and stack outlet. These measurements show that the scrubber removed over 99.9% of the particles larger than 10 µm (aerodyanamic diameter) entering the scrubber. For the first two tests (P2-1 and P2-2), conducted at moderate particulate loading conditions, 99% of the particulate exiting the scrubber was less than 6 µm in diameter, as shown in Table 4-26. For the remaining tests, some of which were at moderate particulate loading and others at high particulate loading, 99% of the particulate exiting the scrubber was less than 2.5 µm in diameter.

The scrubber was more efficient at removing the larger particles. Whereas over 99.9% of the greater than 10 µm fraction was removed in all tests, the removal efficiency for the sub-micron particles only ranged from 69% to 85%. Particles in the range of 1-10 µm were removed at an efficiency of 97.3 - 99.6%. The removal of particulate matter smaller than 10 µm in this test block was slightly better than that observed during the low-particulate test period and equivalent for particles greater than 10 µm.

TABLE 4-26
SCRUBBER OUTLET PARTICLE SIZE MEASUREMENT SUMMARY

	% less than particle size (µm)		
Test I.D.	**99 wt.%<**	**90 wt.%<**	**70 wt.%<**
P2-1	4.5	*1.5*	0.1
P2-2	6.0	1.2	0.1
P2-3	*2.5*	1.2	0.2
P2-4	2.1	1.1	0.2
P2-5	2.1	1.0	0.2
P2-6	2.1	1.1	0.1
P2-7	1.9	1.1	0.2
P2-8	2.3	1.2	0.2
P2-9	2.1	1.1	0.2

4.9.3 Moderate-Ash Particulate Removal Test

Testing to simulate moderate-ash loading (i.e., a marginally performing ESP) was actually performed with the ESP operating under normal conditions (i.e., fully energized). Low-sulfur coal was burned during this test period and resulted in a lower ash resistivity and a subsequent decrease in ESP collection efficiency. Therefore, the low-sulfur coal effectively "detuned" the ESP with no required decrease in operating voltage. Testing was performed under four process operating conditions, shown in Table 4-27.

TABLE 4-27
MODERATE-ASH PARTICULATE REMOVAL EFFICIENCY MEASUREMENT TEST CONDITIONS

Test I.D.	pH	JBR DP (inches WC)	Boiler Load (MWe)
AL2-1	4.0	18	100
AL2-2	4.0	10	100
AL2-3	4.0	18	50
AL2-4	4.0	10	50

Samples were collected to determine particulate loading and particle size distribution during each of the above test conditions. From the results of the previous test efforts, it was apparent that sulfuric acid mist could not be eliminated from the particulate sample, even using the EPA Method 5B for "non-sulfuric acid mist particulate.[4]" Therefore, an alternative approach known as source apportionment was used during this test effort that would allow for calculating the particulate ash fraction at the JBR outlet. This technique involved the collection of samples from the JBR inlet, outlet, and the gypsum blowdown. Following collection, the samples were analyzed for several "indicator" elements to provide insight into the source of the material (scrubber carryover, sulfuric acid mist, or fly ash) in the outlet particulate matter (collected by Method 5B). A statistical analysis (the effective variance least squares method) was used to calculate the mass resulting from each of the various fractions. The particulate loading results are presented in Table 4-28 and shown graphically in Figure 4-55.

TABLE 4-28
MODERATE-ASH PARTICULATE LOADING

Test I.D.	Unit Load (MWe)	JBR ΔP (in. WC)	Inlet Loading (lb/MMBtu)	Outlet Loading (lb/MMBtu)	Removal (%)
AL2-1	100	18	1.28	0.0278	97.8
AL2-2	100	10	1.55	0.0095	99.4
AL2-3	50	18	0.34	0.0050	98.5
AL2-4	50	10	0.37	0.0057	98.5

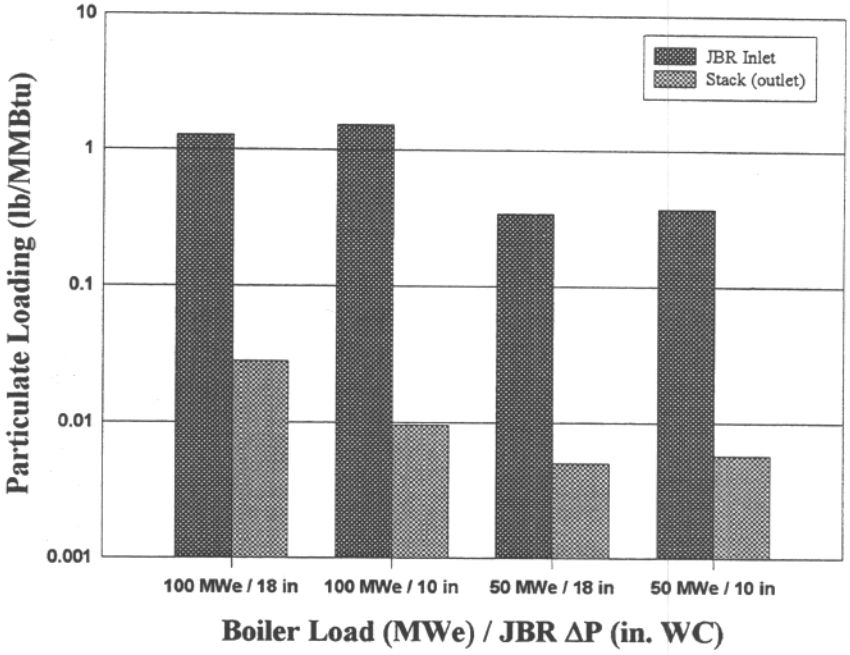

Figure 4-55. Moderate-Ash Particulate Loading Measurements

Particulate removal was quite good, averaging 98.6% removal over all test conditions. Figure 4-56 shows the stack loading measurements along with the calculated "fly-ash only" values determined by source apportionment. Since all the calculated values are less than the measured values, overall particulate removal is even higher using the calculated fly-ash penetration values, averaging an overall 99.4% removal efficiency. Removal values based

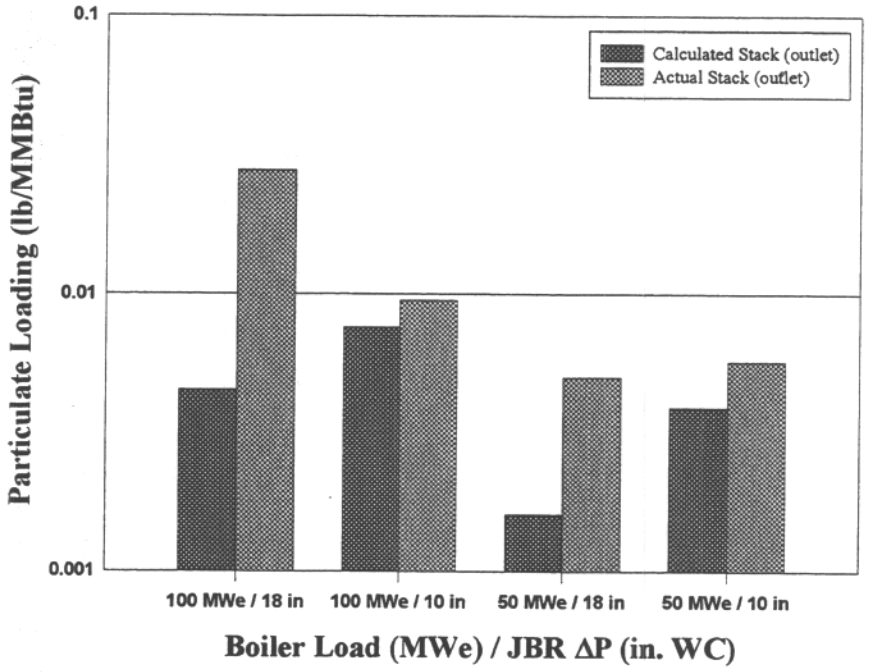

Figure 4-56. Moderate-Ash Measured vs. Predicted JBR Outlet Ash Loading

upon corrected (source apportionment derived data) for Test I.D.'s 1-4 are 99.7, 99.5, 99.5, and 98.9% respectively.

The source apportionment results are shown graphically in Figure 4-57. The ash, scrubber carryover, and acid mist fractions are shown as percentages of the total calculated emitted mass. Clearly, the samples collected during the 100 MWe, high ΔP condition are biased due to the presence of sulfuric acid mist, even though the collected samples were heated at 160°C (320°F) for several hours after collection (Method 5B).

4.9.3.1 Particle Size Distribution

Particle-size distribution was determined at the JBR inlet and at the stack at each of the four operating conditions. Figure 4-58 shows the average cumulative mass distribution by particle size for the JBR inlet under both 50 and 100 MWe boiler loads. These data show that under

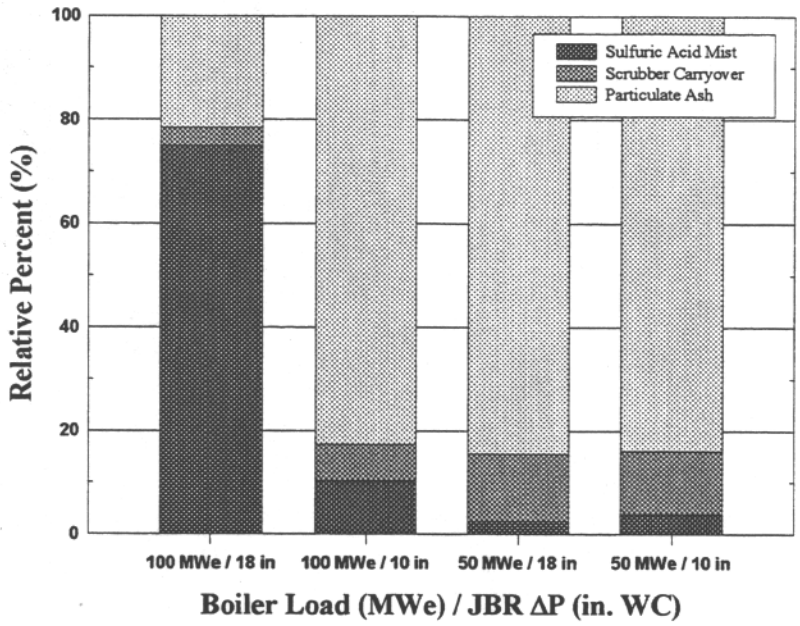

Figure 4-57. Moderate-Ash Source Apportionment Summary - Method 5B (Stack Samples)

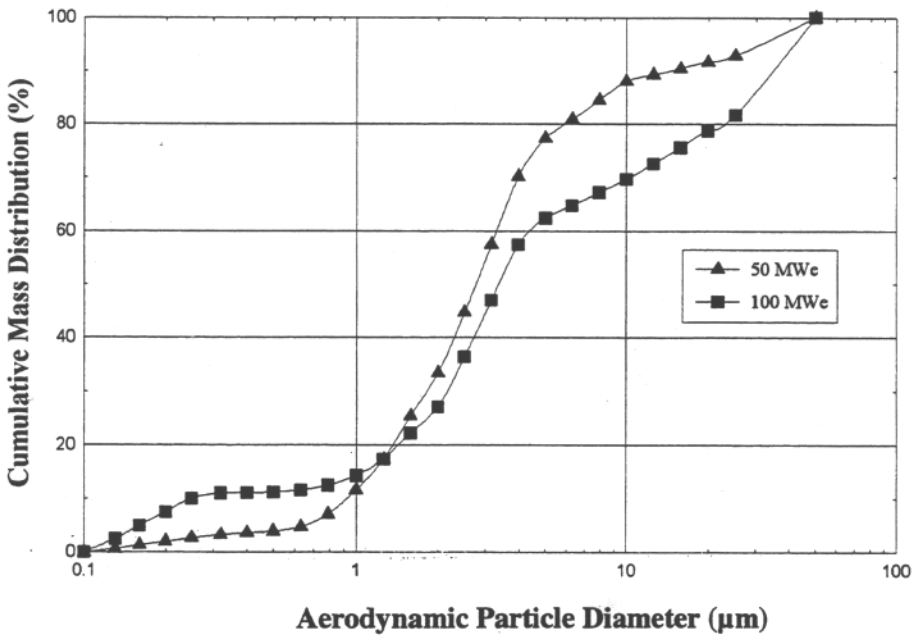

Figure 4-58. Moderate-Ash Cumulative Mass Distribution, JBR Inlet

high load (100 MWe) approximately 30% of the particulate produced *is* greater than 10 µm in diameter. This compares to only 10-12% of the particulate greater than 10 µm under 50 MWe load. As expected, the collection efficiency in the ESP was greater at lower flue gas flow rates. Under both load conditions, the predominance of particles is between 1 and 6 µm.

Figures 4-59 and 4-60 show the cumulative mass distribution at the stack for high and low boiler load and high and normal JBR ΔP. These data are very similar for all of the test conditions, showing the vast majority (80-90%) of the particulate material to be smaller than 1 µm in size.

The differential particle-size distributions are shown in Figures 4-61 and 4-62 for 100 MWe and 50 MWe respectively. The inlet mass [$dM/d(\log d_{50})$] distribution is plotted along with the stack mass distribution for both high and normal pressure drops across the JBR scrubber. While these graphs cannot be used to determine absolute particle loadings, they are useful to see the relative amounts of material in a given particle size range. They may also be used to visualize particulate removal by particle size. Each decade (factor of ten) difference between the inlet and stack values on the Y-axis represents a "9" expressed as percent removal. For instance, a one decade difference represents 90% removal. Two decades represents 99% difference and so on. Both graphs show that more than 99% of the particles greater than 2 µm are removed in the JBR. Both graphs also show a dramatic reduction in particulate removal between 0.6 and 1.0 µm. There appears to be no removal of particles in the 0.3- 0.6 µm range, but apparently removal occurs for particles below 0.3 µm. This type of behavior closely resembles the particulate removal characteristics of a venturi scrubber.

Overall removal efficiency is much better under high load conditions. This may be because there is more material entering the JBR under high load conditions and a nearly-constant outlet loading threshold; however, higher flue gas velocities could improve contacting efficiency in the JBR which could also lead to increased particle removal efficiency.

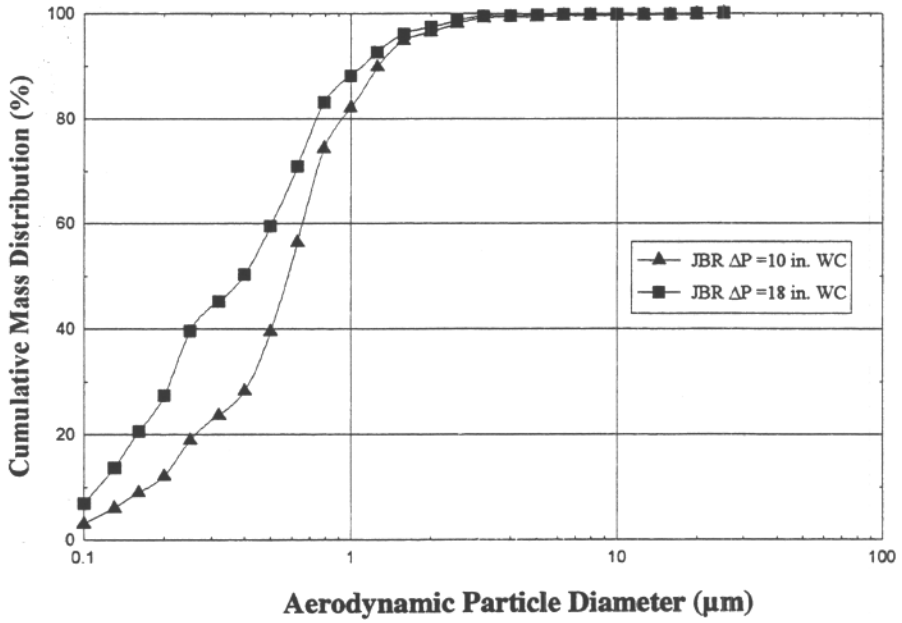

Figure 4-59. Moderate-Ash Stack (JBR Outlet) Cumulative Mass Distribution at 100 MWe

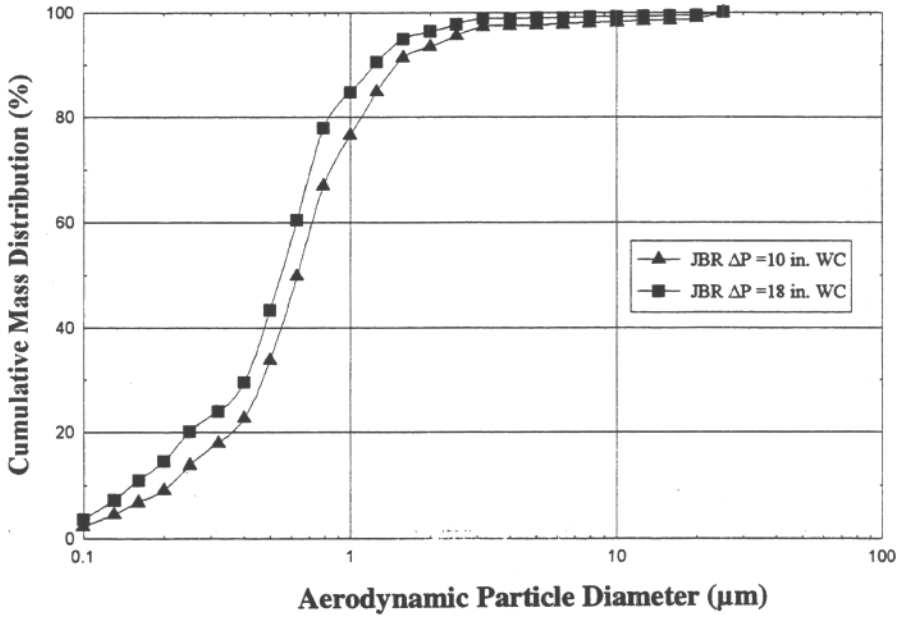

Figure 4-60. Moderate-Ash Stack (JBR Outlet) Cumulative Mass Distribution at 50 MWe

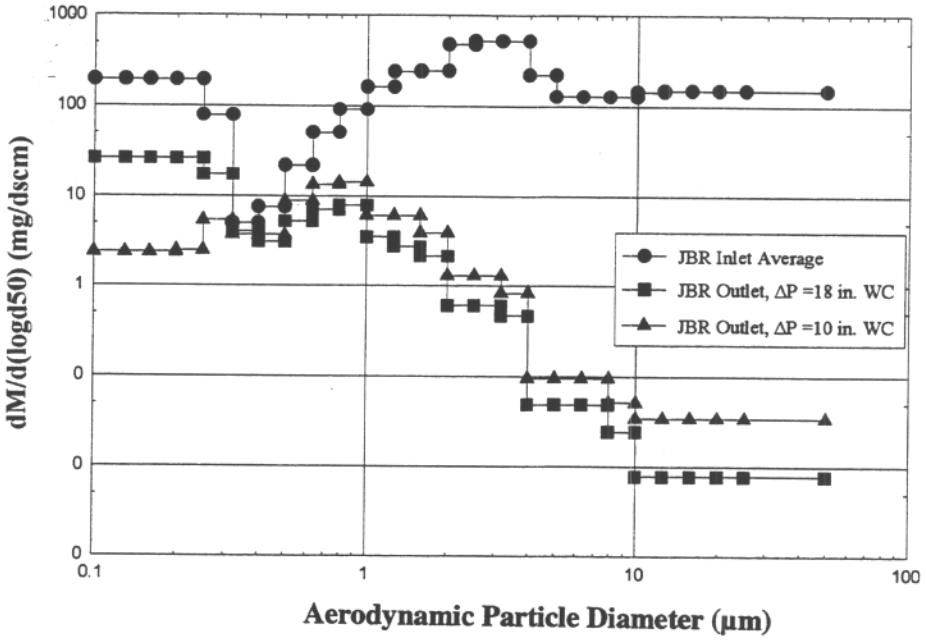

Figure 4-61. Moderate-Ash Differential Mass Distribution at 100 MWe

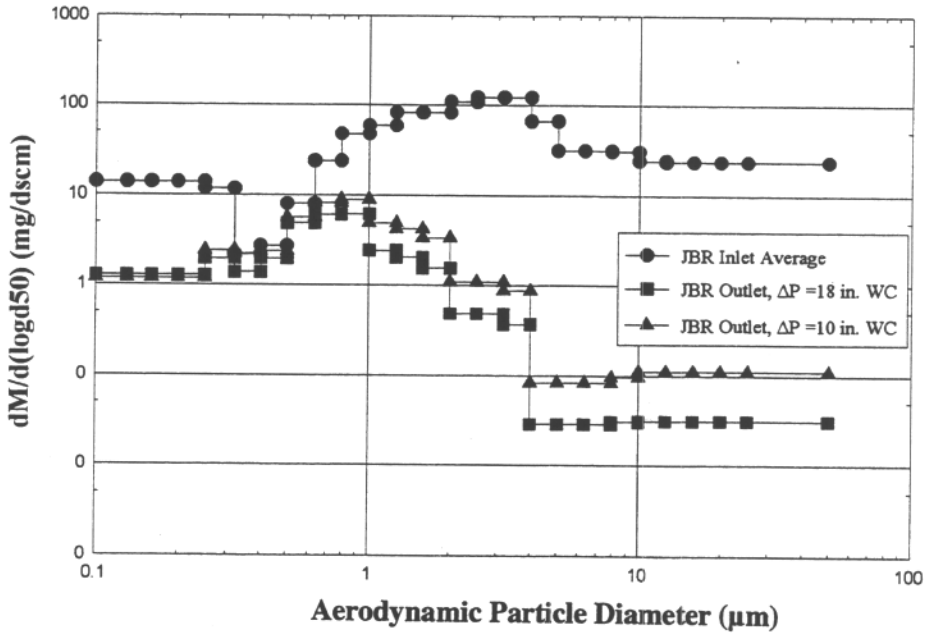

Figure 4-62. Moderate-Ash Differential Mass Distibution at 50 MWe

Average particle removal efficiency for each of the test conditions is presented in Figure 4-63. The dramatic change in removal efficiency for particles less than 1 µm in diameter is quite evident.

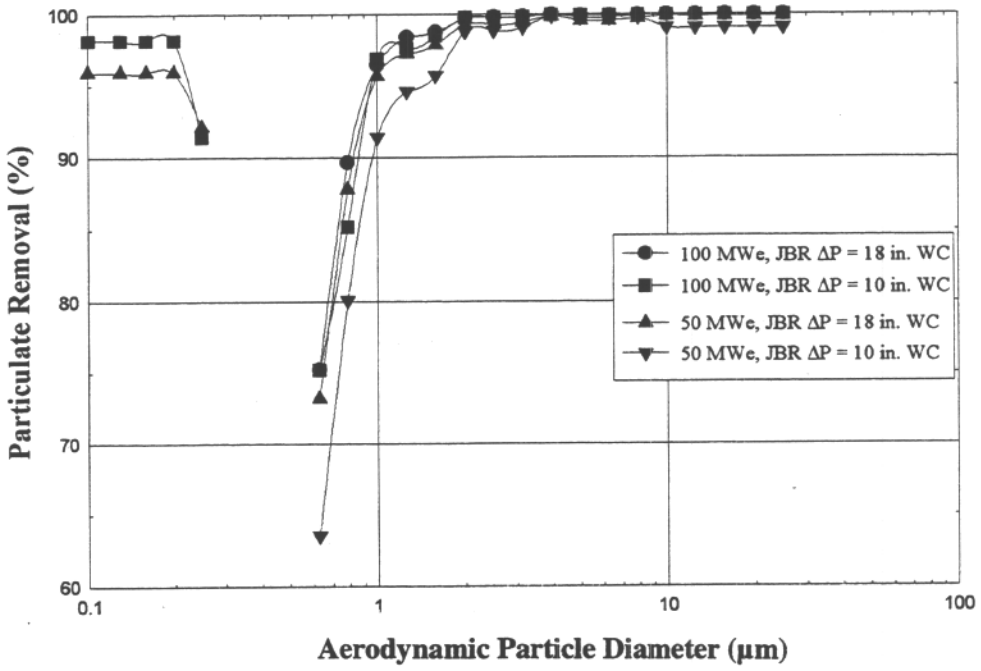

Figure 4-63. Moderate-Ash Scrubber Particulate Removal Efficiency

4.10 Air Toxics

Two toxic emissions test series were conducted. The first test series, sponsored by the U.S. Department of Energy (US DOE), was a comprehensive program which measured emissions from the scrubber stack, various internal streams, and all solid and liquid effluent streams. This program was conducted in June 1993 with the unit burning the project baseline high-sulfur coal, the ESP operating normally (i.e., 100% energized), JBR pressure drop at 14 inches WC, and the Unit 1 boiler at nominally 100 MWe. This test program was conducted as part of the Low-Particulate Parametric Test block.

The second air toxics program was performed in conjunction with the particulate loading measurement testing conducted under moderate-ash conditions using low-sulfur coal. The air toxics measurements during this second test focused exclusively at inorganic air emissions from the scrubber stack.

4.10.1 Low-Ash Air Toxics

The DOE-sponsored toxics characterization program was a comprehensive test series that included most of the internal and effluent process streams. The results of these tests are summarized in Tables F-1 through F-8 of Appendix F. The results presented in these tables represent the average of triplicate samples. Because the emphasis was on air toxics, the information presented in Table F-1, Gas Stream Data Summary, includes data on detailed aspects of the gaseous streams including:

- Vapor and particulate phase trace elements;
- Trace elements by particle size;
- Bioavailability of trace elements (three leaching procedures were used for particulate trace elements);
- Chromium VI;
- Mercury by the solid sorbent adsorption method;
- Reduced species (ammonia and cyanide);
- Anions (chloride, fluoride, and sulfate);
- Radionuclides;
- Volatile and semivolatile organics (only those compounds which were detected);
- Aldehydes; and
- Dioxins and furans.

The remainder of the data summary tables presented in Appendix F include toxics measurement information for the scrubber system, the coal streams, the boiler, the ESP hopper ash, FGD process solids, the aqueous ash sluice systems, and the aqueous streams associated with the FGD system.

Elemental results for the scrubber inlet and scrubber stack are presented in Table 4-29, along with the 95% confidence intervals (CI) and elemental removal efficiencies. The results for nickel indicate negative removal, however, the nickel data are considered biased as discussed below.

Emission factors from the scrubber stack for selected species from the low-ash test period are presented in Table 4-30 along with the 95% confidence intervals. The uncertainty associated with these types of measurements is generally high. In addition to the exceptions footnoted in Table 4-30, the value for nickel in this table is considered to be biased high, most likely due to sample contamination. The nickel data presented are derived from only two samples and further qualification of the data is not possible. However, the rationale for the high bias is evident in Figure 4-64. This figure presents the elemental mass flow rates for the ESP inlet, the JBR inlet and the stack. Nickel should be exclusively associated with the particulate and therefore be removed from the system proportionally to the particulate. Figure 4-64 shows an elemental reduction for all elements across the ESP and across the JBR with the exception of nickel. It is extremely unlikely that more nickel would be emitted from the JBR than is entering the JBR, which is the reason for the conclusion of a high bias.

4.10.2 Moderate-Ash Air Toxics

Air toxics testing performed during the High-Particulate Auxiliary Test block was done in conjunction with the evaluation and characterization of particulate loading (although the ESP was operated to produce moderate-ash loading, contrary to the title of the test block). In this section, data will be presented and compared to that obtained during the low-ash air toxics test period.

TABLE 4-29
LOW-PARTICULATE AIR TOXICS RESULTS SUMMARY

Analyte	Scrubber Inlet, $\mu g/Nm^3$		Scrubber Stack, $\mu g/Nm^3$		Removal Efficiency
	Average	95% CI	Average	95% CI	
Aluminum	12,200	NC	200	250	98%
Antimony	0.41	0.12	0.065	0.026	84%
Arsenic	17	6.6	1.2	0.24	93%
Barium	75	NC	2.9	10	96%
Beryllium	1.7	NC	0.099	0.29	94%
Boron	6,900	1,200	440	70	94%
Cadmium	1.3	NC	0.63	2.2	51%
Calcium	1,900	NC	290	830	85%
Chromium	23	NC	5.4	50	76%
Cobalt	5	NC	0.74	4	85%
Copper	17	1.9	2	1.8	88%
Iron	8,600	1,100	170	600	98%
Lead	19	NC	0.61	0.54	97%
Magnesium	670	NC	45	230	93%
Manganese	34	3.7	7.3	49	78%
Mercury	5.7	1.1	3.1	0.44	46%
Molybdenum	8.7	1.4	1.5	2.4	83%
Nickel	24	6.3	41	430	-71%
Phosphorus	110	NC	< 10	NC	91%
Potassium	2,200	NC	79	540	96%
Selenium	80	130	27	57	66%
Sodium	1,000	NC	65	130	93%
Strontium	45	NC	1.5	3.5	97%
Titanium	760	230	13	0.26	98%
Vanadium	55	10	2.2	1	96%
Total Particulate, (mg/Nm^3)	142	50	14.5	10	90%

NC = Not Calculated

TABLE 4-30
LOW-ASH AIR TOXICS EMISSION FACTORS FOR THE SCRUBBER STACK

Analyte	Emission Factor lb/10^{12} Btu	95% CI
Anions		
Chloride	740	650
Fluoride	120	67
Selected Elements[a]		
Antimony	0.06	0.01
Arsenic	1.2	0.2
Barium	2.8	9.9
Beryllium	0.1	0.1
Cadmium	0.6	2.1
Chromium	5.3	50
Cobalt	0.7	0.8
Copper	2	2.3
Lead	0.6	0.6
Manganese	7.2	48
Mercury	3	0.3
Molybdenum	1.5	2.6
Nickel	40	440
Selenium	27	58
Vanadium	2.1	0.5
Aldehydes		
Acetaldehyde	8.6	9.2
Formaldehyde	24	36
Volatile Organics[b,c]		
Benzene	1.3	0.3
Carbon Disulfide	2.2	1.2
Toluene	2	1

TABLE 4-30 (continued)

Analyte	Emission Factor lb/10^{12} Btu	95% CI
Semivolatile Organics [d]		
2-Methylphenol (o-cresol)	2.9	3.8
4-Methylphenol (p-cresol)	0.95	1.9
Acetophenone	3.2	0.7
Benzoic Acid	120	7
Benzyl Alcohol	2.8	12
Naphthalene	1.5	1
Phenol	9.2	8.8

[a] Run 1 particulate-phase data were invalidated for all elements included here except arsenic, selenium, and vanadium due to the filter background comprising 20% or greater of the measured concentration.

[b] Only those compounds with an average concentration above the detection limit are included.

[c] Methylene chloride, acetone, and other halogenated hydrocarbons are not included because their presence is strongly suspected to be the result of contamination.

[d] Phthalate esters are not included because their presence is suspected to be the results of contamination.

The trace element analysis for the low-sulfur coal is compared to that of the high-sulfur coal in Figure 4-65. The high-sulfur coal was burned during the Low-Particulate Auxiliary Test block, and the low-sulfur coal was burned during the High-Particulate Auxiliary Test block.

The two coals appear to be quite similar in trace element composition, with the exception of arsenic, molybdenum, and to a lesser extent, nickel and selenium. The coal analyses for all coals used in the process evaluation are provided in Appendix C.

The air toxics results from the moderate-ash testing are summarized in Table 4-31. The results are presented along with the 95% confidence interval and the elemental removal efficiency. The moderate-ash air toxics testing was performed with the unit operating at full load (100 MWe) and at a JBR ΔP of 10 and 18 inches water column.

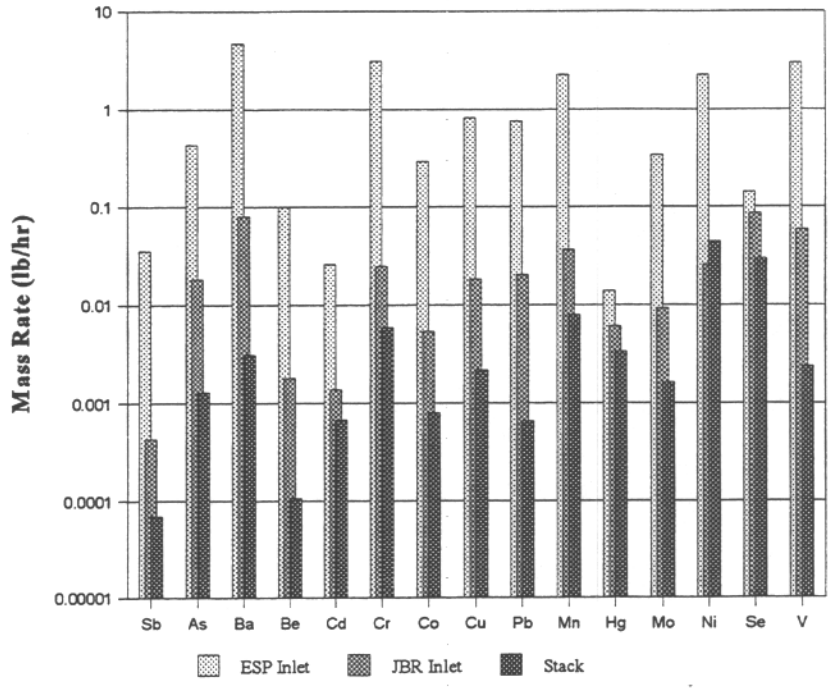

Figure 4-64. Low-Ash Elemental Mass Rates by Gas Stream

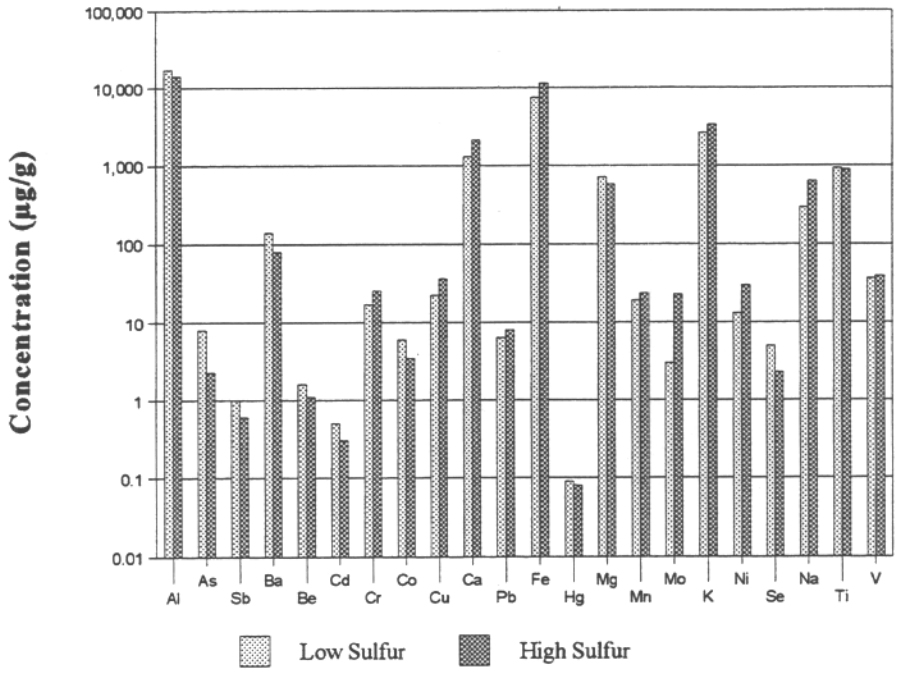

Figure 4-65. Trace Element Comparison for Low- and High-Sulfur Coal

TABLE 4-31
AIR TOXICS RESULTS SUMMARY

Analyte	JBR ΔP = 18 in. WC					JBR ΔP = 10 in. WC				
	Inlet ($\mu g/m^3$)		Outlet ($\mu g/m^3$)		Removal Efficiency	Inlet ($\mu g/m^3$)		Outlet ($\mu g/m^3$)		Removal Efficiency
	Average	95% CI	Average	95% CI		Average	95% CI	Average	95% CI	
Aluminum	144,000	77,000	550	190	99%	177,000	45,000	1,200	470	99%
Antimony	<41	--	<8.2	--	79%	<45	--	<8.8	--	81%
Arsenic	310	120	24	1.7	92%	360	97	32	7.4	91%
Barium	1,600	740	40	3.5	97%	2,000	620	54	9.9	97%
Beryllium	29	15	0.37	0.062	98%	35	8.7	0.6	0.13	98%
Cadmium	2	0.57	0.45	0.1	77%	2.7	0.97	0.54	0.25	79%
Calcium	13,000	7,700	260	62	98%	17,000	3,000	340	97	98%
Chromium	200	100	3.1	0.3	98%	260	100	4.6	1.3	98%
Cobalt	110	65	2.2	2.9	98%	150	52	2.6	2.3	98%
Copper	290	160	6.1	2	97%	380	140	13	2.7	96%
Iron	65,000	29,000	330	52	99%	75,000	17,000	590	180	99%
Lead	150	97	18	27	88%	200	72	8	10	95%
Magnesium	6,300	3,100	63	5.2	99%	7,700	2,100	98	31	98%
Manganese	200	87	7.7	13	96%	250	74	14	22	94%
Mercury	6.2	0.46	1.6	2.1	73%	6.4	0.18	2.4	0.07	62%
Molybdenum	28	11	7.4	0.74	73%	22	4.7	8.2	1.5	62%
Nickel	210	120	4.2	2.6	98%	280	100	5.7	4	97%
Potassium	24,700	12,000	200	7	99%	29,000	6,500	310	52	98%
Sodium	6,000	3,400	210	12	96%	6,100	3,100	180	92	97%
Selenium	40	23	24	5.7	40%	52	30	26	13	49%
Sulfur	3,600	2,000	540	460	84%	4,500	2,200	570	120	87%
Titanium	9,700	5,300	51	8.9	99%	12,000	2,500	97	29	99%
Vanadium	430	240	8.8	0.97	98%	540	110	13	1.7	97%
Total Particulate, mg/m^3	1300	520	28	50	97%	1500	520	9.4	4.8	99%

TABLE 4-32
MODERATE-ASH AIR TOXICS EMISSION FACTORS

Analyte	DP = 18 in. WC $1b/10^{12}$ Btu	DP = 10 in WC $lb/10^{12}$ Btu
Aluminum	550	1,200
Antimony	13	16
Arsenic	24	32
Barium	40	54
Beryllium	0.36	0.60
Cadmium	0.45	0.54
Calcium	260	330
Chromium	3.1	4.5
Cobalt	2.2	2.5
Copper	6.1	12
Iron	330	580
Lead	18	7.9
Magnesium	63	97
Manganese	7.7	14
Mercury	1.6	2.4
Molybdenum	7.4	8.1
Nickel	4.2	5.7
Potassium	200	310
Sodium	210	170
Selenium	24	26
Sulfur	540	560
Titanium	51	96
Vanadium	8.8	13

Emission factors for the two test conditions are presented in Table 4-32 and shown graphically in Figure 4-66. The elemental emissions are higher at the lower JBRΔP condition except for lead. The reasons for this are unknown, but, given the large confidence intervals around the analytical data, the apparent difference is statistically insignificant.

Notable differences are evident in the emission factors determined during the low-ash test period and those obtained during the moderate-ash tests. The emission factors for the low-ash tests are compared with those in the moderate-ash tests (two JBR ΔPs) and are shown in Figure 4-67. As expected, most of the emissions from the low-ash test period are

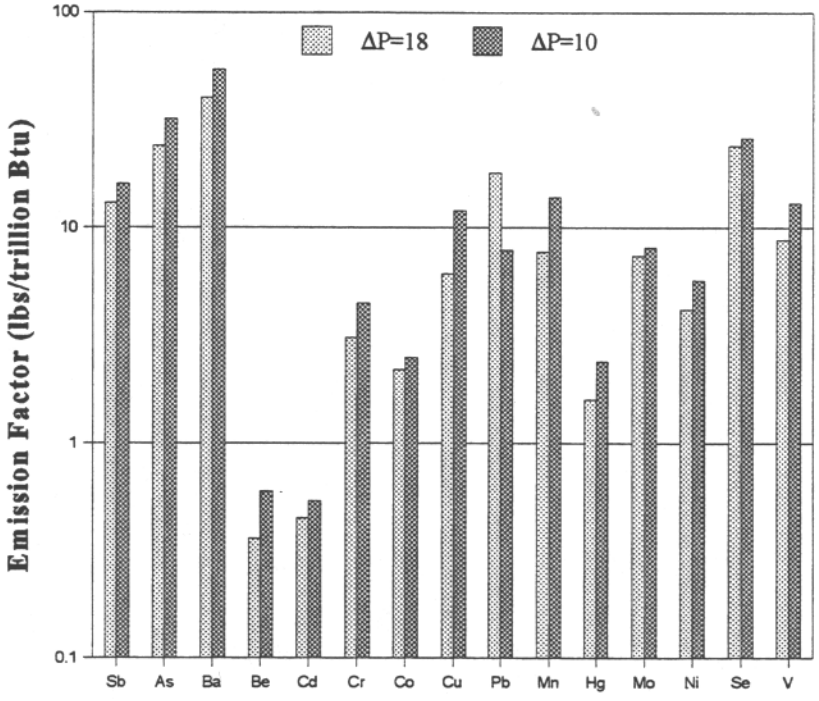

Figure 4-66. Moderate-Ash Emission Factors

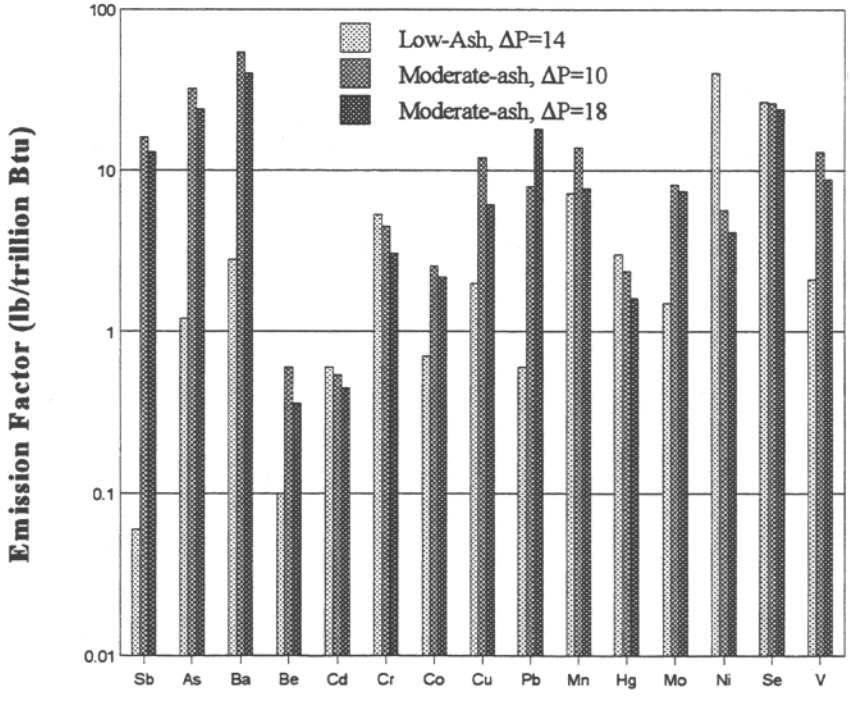

Figure 4-67. Low- and Moderate-Ash Emission Factors

significantly lower than those from the moderate-ash test conditions, since most of the elemental emissions are in the particulate phase. A notable exception for the low-ash emissions is for nickel, which is quite high. As discussed previously, the nickel data from the Low-Ash Test block is considered to be biased high, and includes a very large degree of uncertainty (40 ± 440).

4.11 Mist Eliminator Wash Testing

The frequency and duration of mist eliminator washing was evaluated throughout the high- and low-ash testing. The purpose of this testing was to determine the effects of washing on mist eliminator fouling and pressure drop (MEΔP). The mist eliminators comprise two horizontal-flow sections of chevron-type baffles. Gypsum recycle pond water is used to wash the front (section 1F) and rear (1R) of the first (upstream) stage. The front of the second (most downstream) stage (2F) is washed with plant make-up water, and the back of this stage (2R) has no wash capability. The wash system is made up of twelve wash headers per stage, with each header cycling sequentially at 130 gpm each time a wash is initiated. The wash frequencies listed in Table 3-21 (included in Section 3 of this report) are for full load (100 MWe). As load is decreased, the wash controller decreases the wash frequency to ensure that the JBR water balance does not become positive. At loads of 50 MWe and below, the wash frequency is one-half of that used during full load operations. Figure 2-4 (included in Section 2 of this report) shows a plan view of the mist eliminator stages.

As discussed in Section 3 of this report, the originally planned mist eliminator wash evaluation was altered during the first year of testing. Although the duration of each test phase, shown in Table 3-20 (included in Section 3 of this report), was lengthened to approximately 5 months, the data available for evaluation were often more limited. Because of operational constraints, inspections were not always conducted at the end of a mist eliminator wash test period, nor were the mist eliminators always manually washed at the beginning of each test period. Typically, 3 months of data were available for analysis for each test, with the exception of the final test. These data are presented in Table 4-33.

TABLE 4-33
MIST ELIMINATOR WASHING TEST RESULTS

Test Number Test Name	Test 1 Low Ash/ Low Wash Rate	Test 2 Low Ash/ High Wash Rate	Test 3 High Ash/ High Wash Rate	Test 4 High Ash/ Low Wash Rate
Duration [a] (months)	3	3	3	
Clean ME ΔP				
100 MW	0.45	0.65	0.45	0.60
75 MW	0.30	0.40	0.35	0.40
50 MW	0.20	0.25	0.20	0.20
Dirty ME ΔP				
100 MW	0.80	0.80	0.95	0.70
75 MW	0.50	0.50	0.65	0.50
50 MW	0.30	0.30	0.40	0.25
Change in ΔP				
100 MW	0.35	0.15	0.50	0.10
75 MW	0.20	0.10	0.30	0.10
50 MW	0.10	0.05	0.20	0.05

[a] Test duration is the actual duration of the data considered for analysis. Many tests were actually longer, but 3 months was the most common duration for which data was available.

[b] Only 1 month of data were available at these conditions due to operational constraints

Table 4-33 shows the ME ΔP at the beginning and end of each 3-month evaluation period, as well as the change in ME ΔP over each period. Note that the "clean" ME ΔP at the beginning of each test was not always the same because of differences in the effectiveness of the manual cleaning. The change in ME ΔP is also plotted versus boiler load in Figure 4-68. Boiler load determines the gas flow rate thorough the mist eliminators, which directly affects ME ΔP. The high-ash, low-wash rate test could only be conducted for 1 month due to the November 1994 boiler outage, during which time a full scrubber cleaning was planned.

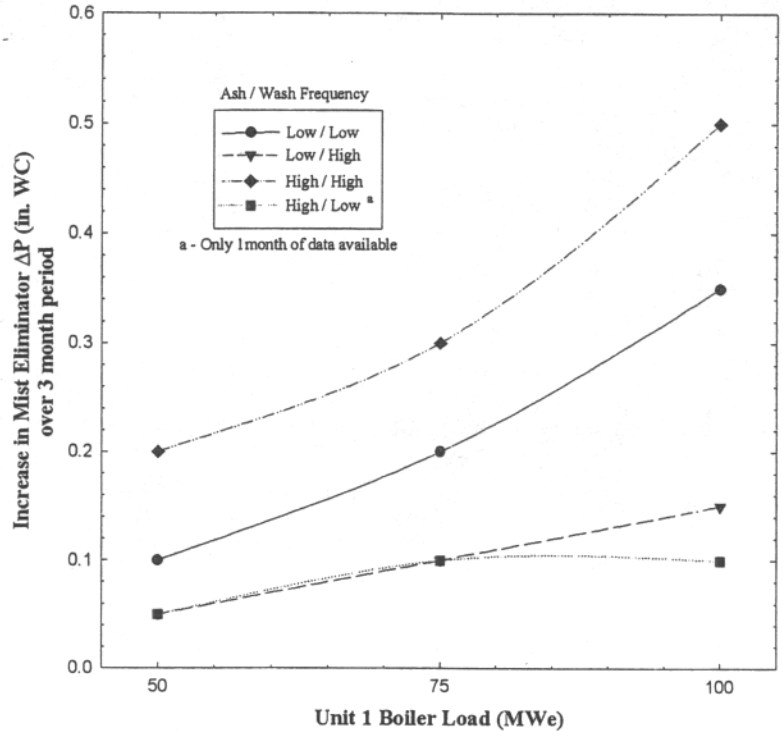

Figure 4-68. Effect of Load, Wash-Rate, and Ash-Loading on Mist Eliminator ΔP

As shown in Figure 4-68 the impact of high-ash loading in the scrubber is quite significant. The worst case scenario was the high-ash/high-wash rate, probably because the high-ash/low-wash rate test could not be performed for the full 3-month period. Additionally the high-ash/low-wash test was also performed at a moderate JBR outlet particulate loading (0.01 lb/MMBtu instead of 0.05 lb/MMBtu during the high-particulate test). The effects of high-ash loading to the scrubber, under a high ME wash rate are far worse that the impact of a low-wash rate with low scrubber particulate loading.

Figures 4-69 through 4-72 are photographs taken of the mist eliminator first stage (1F) at various times during the evaluation. In Figure 4-72, note that section 2F was remarkably clean, even though this photo was taken after the high-ash/high-wash rate period. After each test, it was noted that section 2F was always the cleanest, despite the fact that it was washed only once each 24 hours. Section 2R, shown in Figure 4-73 at the end of the high-ash

Figure 4-69. First Stage Mist Eliminator - Low-Ash, Low-Wash Rate Test (6 months)

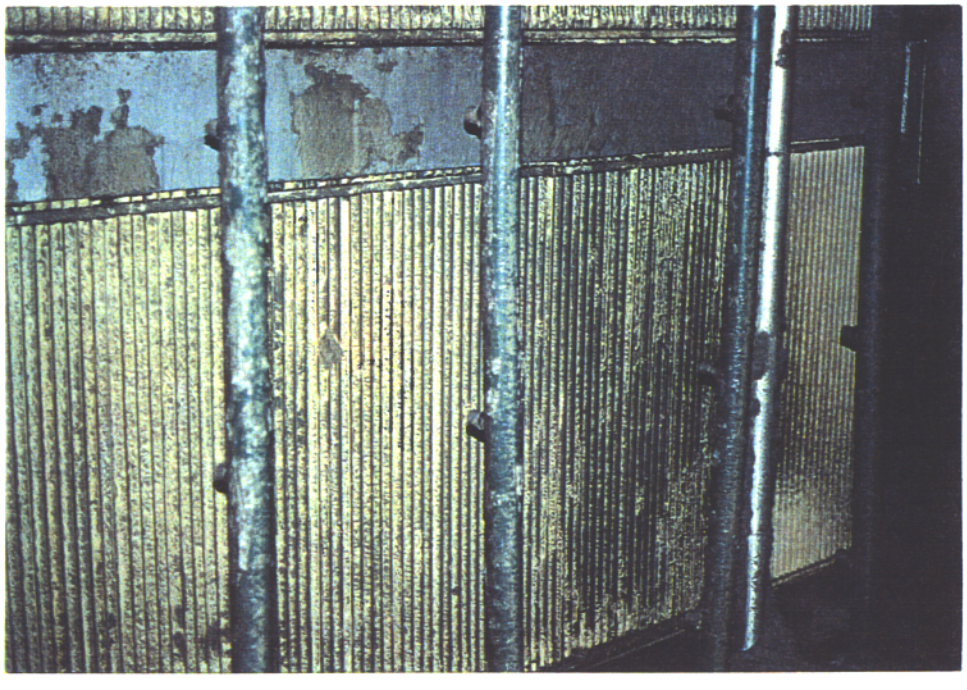

Figure 4-70. First Stage Mist Eliminator - Low-Ash, High-Wash Rate Test (3 months)

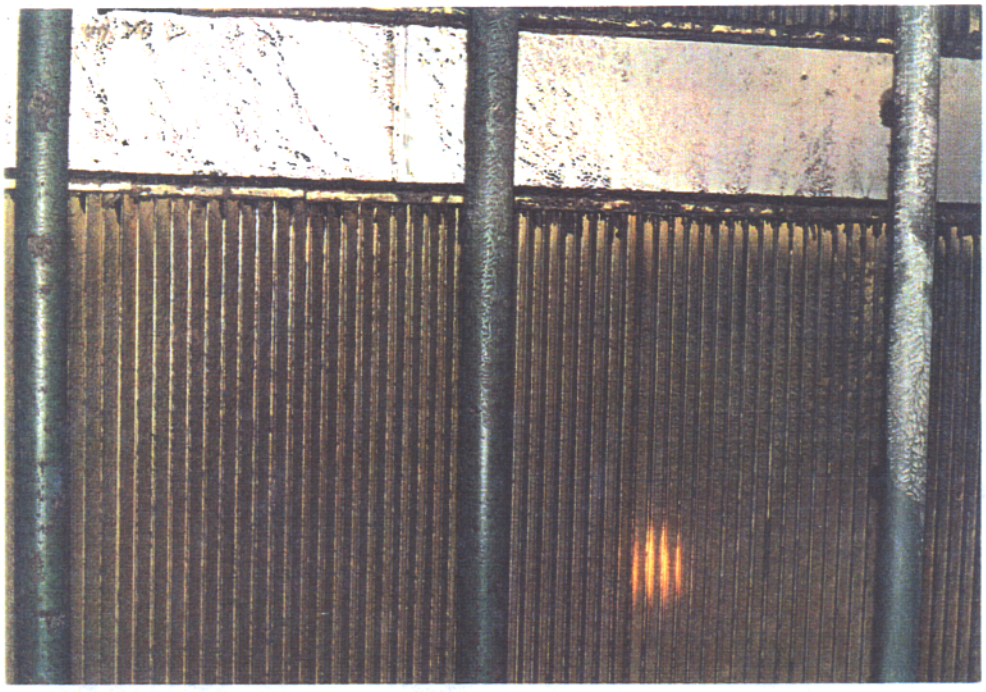

Figure 4-71. First Stage Mist Eliminator - High-Ash, High-Wash Rate Test (3 months)

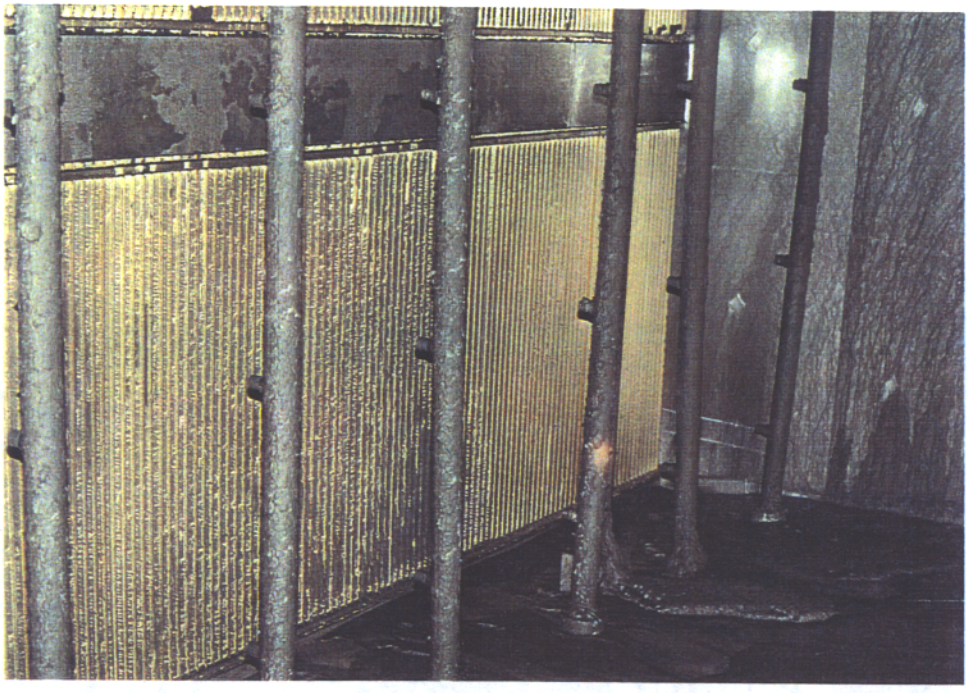

Figure 4-72. First Stage Mist Eliminator - Moderate-Ash, Low-Wash Rate Test (1 month)

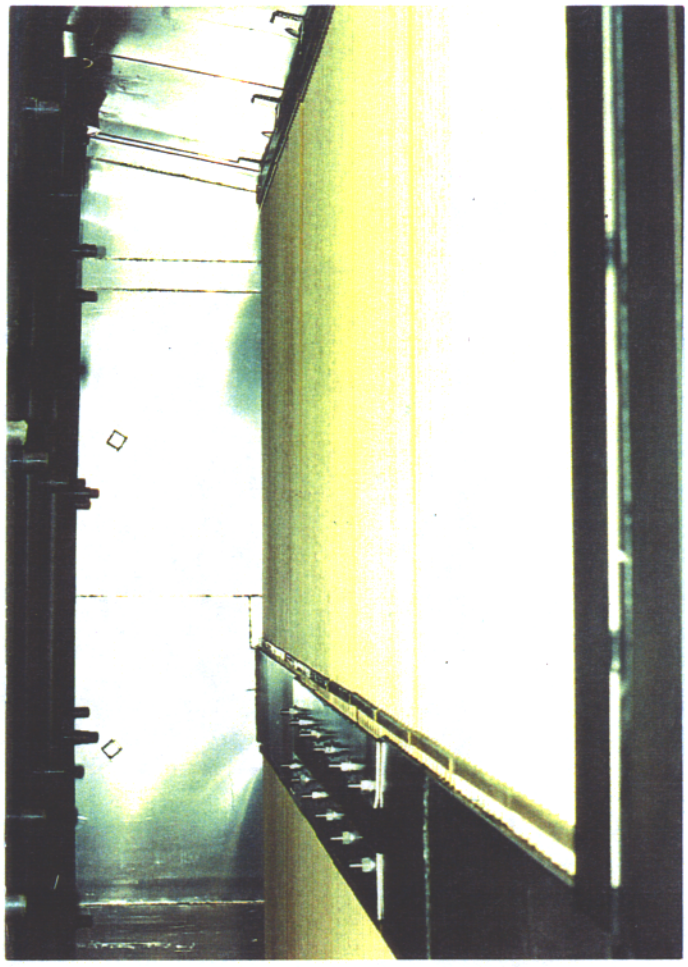

Figure 4-73. Second Stage (Front) Mist Eliminator - High-Ash, High-Wash Rate Test (3 months)

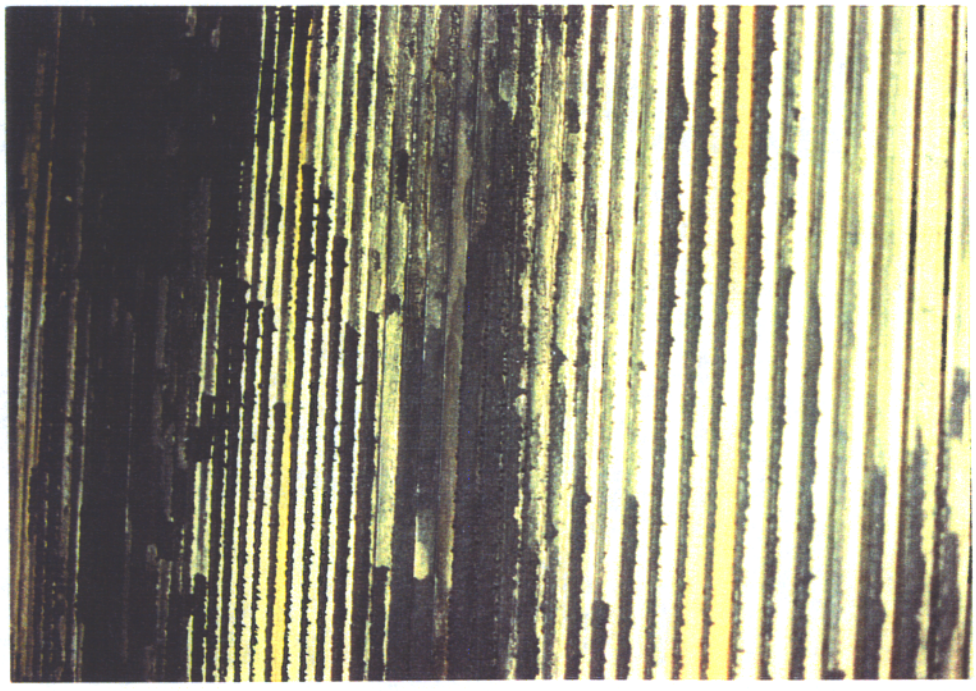

Figure 4-74. Second Stage (Rear) Mist Eliminator - High-Ash Test (3 months)

parametric testing, generally had some minor build-up, usually made up of ash clinging to the trailing edge of the mist eliminator blades. This build-up was found to be roughly proportional to the ash loading to the scrubber and likely remained because of the lack of wash headers at that stage.

Despite the observed increases in the ME ΔP over time, even with high-ash loading and low-wash rates, it should be noted that the pressure drop was still relatively small. The incentive for maintaining a low pressure drop is to keep fan power costs down. The worst-case increase in ME ΔP was only 0.5 in. WC after 3 months. It is highly unlikely that the scrubber will again be operated at conditions of high-ash loading, since the Unit 1 ESP is operational. Routine cleaning during planned outages should be adequate to ensure the pressure drop does not become costly.

4.11.1 Recommendations

Without modifications to the mist eliminator wash system, the best means of ensuring the minimum increase in ME ΔP over time is to utilize the high-wash rate settings in the controller, as given in Table 3-21 (shown in Section 3 of this report). This wash rate, coupled with the low- or moderate-ash loading planned for future compliance use of the scrubber, should ensure that once per year cleanings are adequate. This wash rate should be low enough to ensure that the water balance of the JBR remains negative (i.e., the desired JBR solids content can be maintained with the addition of make-up water).

4.12 Variable Operating Costs

An important result from this demonstration project is the relationship between operating conditions, SO_2 removal performance, and operating costs. This information can be used to choose lowest cost operating conditions for a desired SO_2 removal efficiency, and for comparison with other system designs such as open spray towers. This analysis will be limited to presenting the cost data and will not deal with comparisons to other CT-121 systems or to spray tower systems.

Variable costs are the focus for the purposes of this analysis. Parameters of interest that contribute to variable costs include: reagent (limestone), fan power, ball mill power, and miscellaneous auxiliary power. Miscellaneous power includes motor control center and switch gear feeder power, which are used to operate equipment such as the gas cooling pumps and the JBR agitator. The costs of operation throughout the demonstration project were evaluated on a dollars per ton of SO_2 basis. Fixed costs (i.e., costs independent of process operating parameters) such as operations and maintenance (O&M) and amortized capital expenditures are not included in this analysis. The basis for power consumption costs was $0.0174 per kilowatt-hour.

Typically, a scrubber retrofitted to a boiler will require a booster fan to overcome the additional pressure drop of the scrubber. Because of the planned high-ash period of testing, it was believed that the existing induced draft (I.D.) boiler fans would not be able to withstand the erosive forces of flue gas laden with fly ash. As a result, a larger, armor-plated I.D. fan was installed in lieu of the booster fan which would otherwise be used to supplement existing I.D. fans, and the existing I.D. fan rotors were removed. Fan power consumption data were credited with historical boiler I.D. fan power consumption rates to determine that portion of fan power consumption that was attributable to the scrubber. Detailed variable cost data are presented in Appendix D of this report.

4.12.1 Factors Affecting Variable Costs

Many of the "variable" costs are relatively invariant with respect to SO_2 pickup rate. Items such as gas cooling pumps, gypsum slurry transfer pumps, and limestone slurry pumps consume the same amount of power, regardless of SO_2 pickup rate. Others, such as limestone purchase costs, grinding power costs, and fan power costs are highly dependent on unit load and SO_2 pickup rates, which varied from test to test. The process parameter with the single largest impact on SO_2 removal efficiency was inlet SO_2 concentration. Because of the large variation in coal sulfur content during the tests, a large impact was observed in variable costs based on dollars per ton of SO_2 removed. For example, operating at 90% SO_2 removal

efficiency and 100% boiler load with 2.5% sulfur coal results in twice the tonnage of SO_2 removed than would the same conditions while burning 1.25% sulfur coal. In this case, the only difference in variable costs would be the contribution of limestone delivery and grinding costs, which are higher with a higher SO_2 pickup rate, assuming a constant purchase price. Hence, the cost to remove each ton of SO_2 would be higher for the lower sulfur coal, with all other conditions remaining constant. This point is illustrated in Table 4-34, which list the contribution to variable costs for each test block. A more detailed table of values is provided in Appendix D.

TABLE 4-34
YATES CT-121 VARIABLE OPERATING COSTS

Test I.D.	Coal Sulfur (%)	Limestone Cost ($/ton, delivered)	Costs ($/ton SO_2)			
			Fan Power	Auxiliary Power	Reagent	Total Variable
P-1	2.5-3.0	19.0	5.1	8.1	30.5	43.7
L-1	2.5	19.0	6.7	8.2	30.3	45.3
HR-1	2.5	19.0	7.8	8.0	30.7	46.5
AL-1	2.5	18.5	8.1	9.6	30.6	48.3
AC-1	4.3	18.5	4.8	8.0	30.7	43.5
P-2	2.5	18.5	6.7	10.1	31.4	48.2
L-2	2.5	18.5	8.4	11.3	30.3	49.8
HR-2	1.2	18.5	22.3	21.4	29.8	73.5
AL-2	1.2	13.5	15.6	23.8	22.2	61.6
AC-2	3.4	13.5	5.6	8.4	22.2	36.3

[a] Fan power costs are "credited" with historical average boiler I.D. fan power consumption values

[b] Auxiliary power costs are the sum of all power costs associated with the scrubber, except fan power costs Total variable costs are the sum of fan power, reagent, and auxiliary power costs

Similarly, extended operation at low boiler load would result in a higher cost per ton of SO_2 removed due to the lower pickup rate. Of course the difference in cost would be less than in the previous example because of the decrease in fan power costs associated with the lower load. This is exemplified by a comparison of the low- and high-ash long-term tests, labeled L-1 and L-2, respectively, in Table 4-34. During the high-ash long-term tests, the average

boiler load was only approximately 60 MWe, compared to that of the low-ash long-term test phase, when it was near 72 MWe. This decreased load contributed to the increase in variable costs from \$45.3/ton SO_2 removed to \$49.8/ton SO_2 removed. Note that the increase in variable costs from test P-1 to P-2 is largely due to excessive pluggage of the JBR and lower SO_2 removal efficiency during P-2 than to any other cause, as can be observed by the increase in fan and auxiliary power costs.

As is shown in Table 4-34, reagent costs make up 30-70% of the total variable costs, depending on the conditions. As a result, limestone utilization (the portion of the limestone added that is reacted), delivered cost, and purity have a significant impact on variable costs. This was one reason that limestone utilization was maintained as near to 100% as possible throughout the demonstration project. A more important reason for maintaining high limestone utilization is to prevent gypsum scaling from occurring. In Table 434, note that the low price of limestone resulted in decreased overall variable costs during the high-ash Alternate Limestone (AL-2) and Alternate Coal (AC-2) test periods. During test AL-2, the inexpensive limestone mitigated the cost increases resulting from burning low-sulfur coal, as can be demonstrated by comparing the total variable costs of tests HR-2 and AL-2. Without the higher cost (on a \$/ton SO_2 basis) associated with burning low-sulfur coal, and with the low limestone reagent costs, the cost to remove a ton of SO_2 in test AC-2 was the lowest of the entire demonstration project.

4.13 Analytical Results

Complete solid and liquid phase analyses of all scrubber process streams were performed at least weekly during the demonstration project, occurring with a higher frequency during periods of frequent process operating parameter changes. The results of these analyses are provided in Appendix B. These analyses serve several purposes including: monitoring the process liquor's approach to equilibrium, verifying proper oxidation and limestone utilization, confirming consistent limestone quality, and ensuring appropriate conditions exist for gypsum crystal formation. Proximate coal analyses were performed daily and ultimate analyses semi-annually to allow correlation of coal analyses with changes noted in process

chemistry or performance and to confirm the consistency of the coal source. On a monthly basis, samples were sent off-site for trace metal analysis, gypsum byproduct solids particle size distribution (PSD) measurement, and to obtain gypsum scanning electron micrographs (SEMs). These analyses were of critical importance in the evaluation of gypsum crystal size and morphology, and in the evaluation of changes in byproduct dewatering characteristics.

Two of the more critical analyses performed are the solid phase sulfite ($SO_3^=$) and carbonate ($CO_3^=$) titrations. Sulfite concentration provides information about the oxidation of sulfite to sulfate in the process. Complete oxidation is essential to the high SO_2 removal capability of the CT-121 process, particularly at the low pHs at which the process is operated, and for ensuring a high quality gypsum byproduct with acceptable dewatering properties. Carbonate analyses were important to confirm that limestone utilization was at an acceptable level.

4.13.1 Approach to Steady State

The gypsum recycle liquor pond can hold from 1 to 2 million gallons of process liquor. As such, the average process liquid phase residence time was over 200 days during the demonstration project. Because of the limited duration of the demonstration and several changes in coal and limestone reagent sources, the liquid phase species never truly reached their steady-state concentrations. The approach to steady-state of key components, such as chloride (Cl^-) was still monitored throughout the testing.

Chloride concentrations, documented in Appendix B, rose to values as high as 43,000 ppm in the gypsum pond and as high as 68,000 ppm in the JBR slurry (liquid phase). These values were tracked as part of the process chemistry monitoring plan and as part of the materials of construction evaluation. Elevated chloride concentrations can aggressively attack stainless steel, and even some of the more exotic alloys. Chloride stress corrosion, chloride pitting, and chloride cracking are some of the means by which typical alloys may fail. The resistance of the FRP construction materials to these highly elevated chloride concentrations was outstanding, as expected, and is discussed in more detail in the Materials and Maintenance volume of this report.

4.13.2 Limestone Utilization

Limestone utilization was measured throughout the demonstration project and is an important process chemistry consideration for two reasons:

1. Low limestone utilization results in wasting of reagent, one of the largest contributors to variable operating costs; and

2. Unreacted limestone in the JBR slurry that is sprayed into the lower deck and sparger tubes can react with the SO_2 in untreated flue gas to form gypsum scale, creating pluggage in the JBR.

During the low-particulate parametric test series, limestone utilization was measured across the full range of pH values tested, as well as at two different grind sizes: the baseline grind size of 90% smaller than a #200 mesh, and an alternate grind of 70% smaller than a #200 mesh. These data are shown graphically in Figure 4-75.

Limestone utilization was not affected significantly by pH up to pH 5.0. Calcium carbonate relative saturation increases with increasing pH, decreasing the driving force for limestone dissolution. However, there is a pH level where limestone utilization will fall off precipitously. Based on the results of these low-ash parametric tests, for this system chemistry and limestone the critical pH level is near pH 5.3. During the high-ash test phase, another factor -- aluminum fluoride blinding -- had an impact on limestone utilization. This is discussed in more detail in section 4.13.3 of this report.

The low-ash parametric tests were used to evaluate the effect of limestone grind on limestone utilization. Some tests were run with a limestone grind of 70% <#200 mesh instead of the baseline 90% <#200 mesh. At pH 4.0 and 4.5 little effect was seen; however, the very high utilization at these pHs makes it difficult to distinguish a change. At pH 5.0 and 5.6 the limestone utilizations were slightly lower (93% and 58%, respectively) than the 97% and 73% observed with the finer grind.

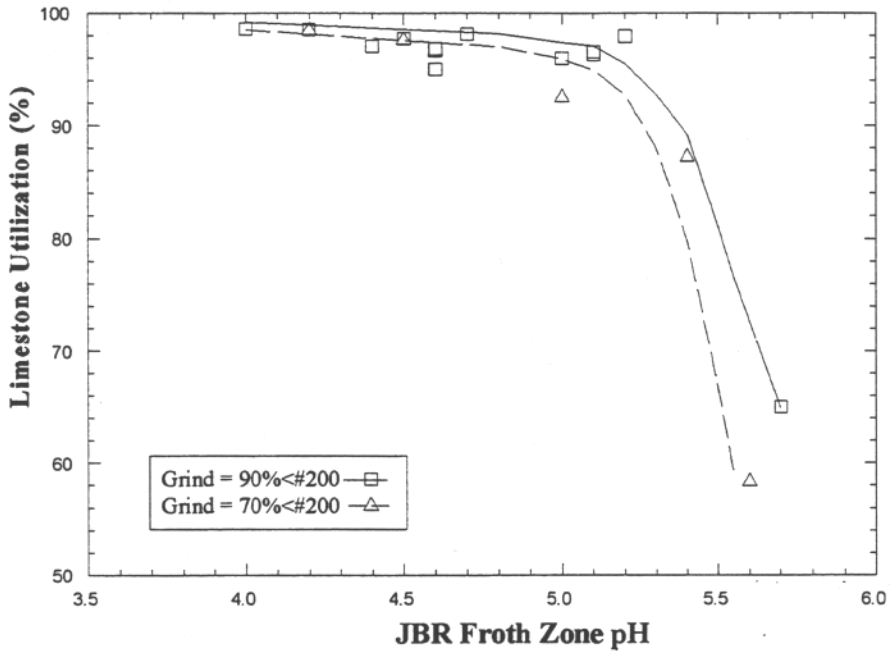

Figure 4-75. Effect of pH and Limestone Grind Size on Limestone Utilization

Normally, there is a trade-off between limestone grind and limestone utilization. The cost of increased limestone usage at coarser grinds must be weighed against grinding costs. However, for this project, two factors suggest that coarse grind should not be used:

1. Because the baseline limestone is easy to grind, the 90% <#200 mesh is about the coarsest material that can be made without ball mill modifications. Attempting to achieve a coarser grind with the existing equipment can lead to mill operations problems.

2. The milling power costs are so low (in part because of the ease of grinding) that significantly lowering grinding costs cannot be achieved by grinding the limestone more coarsely.

4.13.3 Aluminum Fluoride Blinding

Inhibited limestone dissolution due to the presence of elevated concentrations of dissolved aluminum and fluoride in the process liquor, also known as aluminum fluoride (Al-F) blinding, occurred at Yates during the high-ash phase of testing. Less than one day after high-ash testing began under the process conditions shown as P2-5 in Table 3-2, it became apparent that the process chemistry was affected by Al-F blinding. The bi-hourly solid phase carbonate analyses confirmed higher-than-normal levels of $CO_3^{=}$, symptomatic of an inhibited limestone dissolution (i.e., blinding) problem. Liquid phase samples were analyzed for sulfite, and correct operation of oxidation air blowers was confirmed to rule out loss of complete oxidation as a cause for the low limestone utilization. Based on the recent addition of ash to the process, the presence of Al-F blinding was suspected to be the cause of the inhibited limestone dissolution. Analyses of the scrubber liquor for Al and F confirmed that these species were present in sufficient concentrations and at a ratio of Al to F (2:1- 4: 1)[5] that has been observed to result in Al-F blinding.

Experience has shown that the limestone will completely dissolve, regardless of Al and F concentration, if the pH is low enough. Therefore, the process pH was lowered gradually over the next several days to determine the pH that would yield a reasonable limestone utilization. The results of this investigation indicated that, with the ESP fully deenergized, a pH of 4.0 or below would ensure nearly complete limestone dissolution.

Because of the Al-F effects on limestone utilization observed during the initial high-ash tests, the high-ash parametric test matrix was modified to reduce the range of tested pH from between 4.0 and 5.0 to between 3.5 and 4.0 during the remaining high-ash loading tests. This matrix is presented in Table 3-2 of this report. A review of the analytical results in Appendix B indicates that upon lowering the pH to 4.0, limestone utilization increased from 67% back to a more typical value of 97%. Some fluctuations in limestone utilization were still seen during the test block, particularly when pH was near or slightly above 4.0. This is indicative of operation under the influence of Al-F blinding. In fact, some minor blinding was probably

occurring during the tests conducted at a pH setpoint of 4.0, as evidenced by limestone utilization values below 97% (see Appendix B).

Aluminum fluoride blinding appeared to persist during the High-Ash Long-Term Test block, even though ash loading was decreased to more moderate levels. Therefore, the process pH was lowered to 4.0, a pH that was determined to yield a reasonable limestone utilization (i.e., >97%) in previous testing. The limestone utilization, which was only 81 % at pH 4.5, remained above 97% once operations at pH 4.0 began.

During the Alternate Limestone test series portion of the High-Particulate Auxiliary Test block, inhibited limestone dissolution was again experienced while the pH setpoint was maintained at 4.0. Previously conducted research has shown that many factors, including the dissolved concentration of other ionic species, can have an impact on the susceptibility of a process to Al-F blinding. In this case it was believed to have been triggered by the change in dissolved trace metals associated with the Florida Rock limestone. The blinding was successfully mitigated by reducing the operating pH setpoint to 3.75.

4.13.4 Gypsum Quality

Gypsum quality was measured on a periodic basis during the demonstration project. The quality of the gypsum byproduct can be determined through objective evaluations of purity (percent $CaSO_4 \cdot 2H_2O$), particle size distribution, dewatering properties (e.g., form filtration rate and settling rate tests), and color. It became apparent that one of the most significant factors affecting gypsum byproduct quality, particularly crystal size, was limestone selection. This has been discussed in detail in Section 4.8 of this report. Trace metal, particle size distribution, dewatering, and solid phase chemical analyses of the gypsum byproduct are all presented in Appendix B of this report. The JBR solids inert (acid insolubles) content increased sharply during the High-Ash Parametric Test block following the complete deenergization of the ESP. This effect was expected because of the increase in inlet particulate (fly ash) mass loading to the scrubber coupled with the high particulate removal efficiency of the CT-121 process. The scrubber byproduct composition was as high as 41 wt.% fly ash with as little as 55 wt.% gypsum. Because of the high ash content of the slurry

and the relatively small size of the ash particles compared to the gypsum crystals, the laboratory gypsum solids dewatering test results were often inconclusive during this test phase. The settling test was difficult to interpret because of unhindered settling. This occurs when gypsum particles are large enough to settle quickly but the fine ash remains suspended, obscuring the slurry-liquor interface and making it unreadable. Because of this effect, at some times, only final settled density measurements were available. Difficulties were also encountered in performing the filter leaf test. The fine ash particulate had a tendency to bind the filter media, preventing filter cake formation. Because stacking is used as the method of gypsum byproduct disposal at Yates, the final settled density data was found to be an adequate indicator of the potential for successful gypsum dewatering by stacking.

4.14 References

1. Hargrove, O.W. and G.E. Stevens, "Investigation of Gypsum Dewatering Properties at Georgia Power's Yates CT-121 FGD System", Radian Corporation Technical Note, December 15, 1993.

2. Garlinger, J.E. and T.S. Ingra, "Evaluation of Chiyoda Thoroughbred 121 FGD Process and Gypsum Stacking Volume 3: Testing the Feasibility of Stacking FGD Gypsum". CS-1579, Volume 3, EPRI Research Project 536-23. November, 1980. pp. 2-1 - 2-9.

3. 40 CFR 60, Appendix A. *Test Methods.* "Method 5B: Determination of Nonsulfuric Acid Particulate Matter from Stationary Sources."

4. ibid.

5. R.W. Farmer, et al., "Effects of Aluminum/Fluoride Chemistry on Wet Limestone Flue Gas Desulfurization," Presented at the 1987 Spring National AIChE Meeting, March 29 - April 2, 1987, Houston, Texas. p.18.

5.0 CONCLUSIONS

The two-year evaluation of the CT-121 flue gas desulfurization process at Georgia Power's Plant Yates provided insight into both the positive and negative aspects of operation under a wide variety of process conditions. Areas of evaluation included:

- Erosion and corrosion resistance of the fiberglass reinforced plastic (FRP) materials of construction;
- The ability of the process to simultaneously remove both SO_2 and particulate matter;
- Process reliability and availability under low-, high-, and moderate-ash loading conditions; and
- Process control systems unique to this CT-121 installation.

The process performed exceptionally during the evaluation. High SO_2 and particulate removal efficiencies were realized, while maintaining excellent limestone utilization and superior availability and reliability. Some operational difficulties were encountered, most related to some of the unique features of the Plant Yates-specific CT- 121 process design. With few exceptions, solutions have been developed during the course of the demonstration for each of these problems. Many of these solutions are presented in Section 6.0 of this report. Some were implemented during the process evaluation, others canbe retrofitted when an opportunity arises, and some will best be used in future CT-121 designs. In fact, many of the identified modifications have already been incorporated into the designs of new CT-121 processes, currently under construction.

5.1 Simultaneous SO_2 and Particulate Removal

SO_2 removal efficiency and particulate removal efficiency were evaluated throughout the demonstration project at conditions of varying boiler load, JBR ΔP, pH, coal sulfur content, and JBR inlet ash loading. The findings of this aspect of the evaluation include:

- SO_2 removal efficiency was generally excellent and greater than 90% efficiency was achieved during all test phases;
- Particulate removal efficiency was always above 97%, and usually in excess of 99%. Removal efficiency of particulate greater than 10 micrometers in size was typically greater than 99.9%;
- The particulate removal efficiency was generally a function of inlet particulate loading since outlet loading was relatively constant, regardless of the inlet loading or process conditions; and
- Approximately 20% of the outlet particulate under moderate ash loading conditions is sulfuric acid mist.

5.2 Process Flexibility

During the demonstration, process parameters were varied to allow a complete evaluation of scrubber performance as a viable SO_2 and particulate removal technology. This evaluation of the flexibility of the CT-121 process concluded that:

- The CT-121 process is adaptable to many new construction or retrofit scenarios, and excellent performance could be achieved with a wide variety of limestone and coal sources;
- Virtually any SO_2 removal efficiency can be selected within the design capability of the process by adjusting the JBR level (JBR ΔP); and
- The exact JBR ΔP required to achieve the required level of performance can be selected, and easily adjusted as changing boiler conditions warrant, thus optimizing the cost of compliance.

5.3 Robustness, Ease of Operation

The CT-121 process responded well to transients, process upsets, and operations outside of design parameters (e.g., coal sulfur content greater than 3.0%). Evidence of the robustness of this process included:

- Even with large amounts of sparger tube plugging (observed during the high-ash test period), high SO_2 removal efficiency was maintained by adjusting key process parameters (pH and JBR ΔP); and

- Despite the frequency of rotation of lead scrubber operators, even very inexperienced operators had little difficulty controlling the process, and operator errors were usually easily reversed and corrected with few adverse effects on the process.

As further evidence of the ease of operation of this process, continued operation of the scrubber following completion of the process evaluation phase of the demonstration project is occurring with a single operator responsible for controlling both the CT-121 scrubber and the Unit 1 boiler.

5.4 Limestone Utilization

One of the most attractive attributes of the CT-121 process is its ability to maintain very high limestone utilization while achieving high SO_2 removal efficiency. Some of the more significant findings with regard to limestone utilization include:

- The CT-121 process can operate at a lower pH than conventional spray tower wet limestone FGD processes (thus ensuring high limestone utilization) while still achieving very high SO_2 removal efficiency;

- Limestone utilization was typically 98% or greater during the low-ash periods of the process evaluation;

- Under low-ash loading conditions, limestone utilization remains above 98% at pH values up to 5.2;

- During high-ash testing, aluminum and fluoride concentrations in the scrubbing liquor resulted in inhibited limestone dissolution except when pH was restricted to 4.0 or lower; and

- Delivered limestone costs represent a significant portion (approximately *65%* while burning the project baseline high-sulfur coal) of the variable operating costs (on a \$/ton SO_2 basis).

The ability of the CT-121 process to maintain high utilization while still meeting performance goals for Phase I or Phase II compliance, and while maintaining high particulate removal efficiency, is a feature that sets it apart from many first generation scrubber technologies.

5.5 Availability and Reliability

Due to the simplicity and flexibility of the CT-121 process design, very high reliability and availability (both indices were 97%) were recorded during the entire process evaluation, with slightly better values during the low-ash test phase and lower values during the high-ash test phase. While these operating statistics are excellent, there is still some room for improvement. Reasons for the inherent reliability of the process include:

- With fewer pumps than a spray tower/reaction vessel design, there is less opportunity for failures that would render the process unable to achieve SO_2 removal efficiency targets;
- All key process instruments and critical pumps have installed spares; and
- The process is very forgiving of minor difficulties such as sparger tube plugging or clogged gas cooling nozzles. The scrubber is capable of operating at the desired level of performance despite these problems, which often can be resolved when the boiler is off-line for other reasons, without affecting availability.

5.6 Wet Chimney

The design of the FRP wet chimney is one of the most successful aspects of this demonstration. A scale model of the JBR outlet plenum, mist eliminator, and wet chimney was used to perform dynamic flow modeling that was designed to allow optimization of the wet chimney design, with the goal of eliminating rain-out. The final design included an internal gutter in the chimney to return condensing water vapor to the JBR, a set of internal baffles in the chimney elbow to prevent reentrainment of the condensate, and flow vanes m the JBR outlet plenum exit. As a result of these innovative design features:

- The need for reheat of the treated flue gas was eliminated and resulted in considerable capital and operating cost savings to the project; and

- Periodic observations were made during the over two years of testing and no rain-out was observed from the wet chimney, regardless of process conditions, boiler load, or meteorological factors.

5.7 FRP Erosion Resistance

The Yates CT-121 scrubber was the first of its kind to use FRP for all major process vessels, ductwork, and a significant portion of slurry piping. Considerable effort was expended to frequently evaluate the erosion and corrosion resistance of the FRP materials used in this CT-121 design. Significant findings include:

- With the exception of the JBR inlet plenum, the JBR vessel and all other process equipment and vessels constructed of FRP exhibited no signs of corrosion or erosion damage during the demonstration project;
- Erosion of the FRP materials in the gas cooling transition duct and JBR inlet plenum was one of the most difficult problems to resolve due to the proximity of the gas cooling nozzles to the JBR inlet plenum, the high superficial velocity of flue gas (approximately 60 ft/sec at full load), and high solids concentration (23 wt.%) of the gas cooling slurry;
- The erosion damage required patching during almost all but the earliest inspections of the JBR internals, but did not become severe enough to require a forced outage;
- Quantification of erosion damage was made easier by the FRP lay-up technique, in which FRP layers were of different colors to ease identification of the depth of erosion damage; and
- The high ionic strength slurry, which had measured chloride concentrations as high as 68,000 ppm, had no observed negative impact on the FRP.

In general, the wide use of FRP for this highly abrasive, high chloride, closed loop environment was successful. With some design modifications, the observed inlet plenum erosion could also be resolved in future applications of this technology. These modifications include moving the gas cooling section further from the JBR in future designs, replacing the FRP in the gas cooling section with stainless steel wallpaper, or applying erosion resistant coatings to the wear-prone surfaces. These recommendations are presented in moredetail in Section 6 of this report.

5.8 JBR Lower Deck Solids Build-Up

Because of the proximity of the gas cooling section to the JBR inlet plenum, another problem that resulted was a build-up of solids on the lower deck. There were several mechanisms for this build-up including:

- Because of the significant deposition of slurry on the JBR lower deck, the slurry solids would eventually "bridge" over and plug the sparger tubes. Increasing the number of lower deck drains and improving the efficiency of the wash system greatly decreased the amount of solids build-up observed on the lower deck during subsequent inspections; and
- During the high-ash test phase, fly ash that was moistened by the gas cooling section became very sticky and had a tendency to agglomerate inside of the tops of the sparger tubes which led to many sparger tubes being completely plugged. Because the sparger tube tops are raised several inches above the deck and the wash headers do not spray directly into the sparger tubes, the wash system was ineffective in removing the ash build-up.

5.9 Gas Cooling Nozzle Pluggage

The 40 silicon-carbide gas cooling nozzles, each with a 3/8" free-pass area, are prone to pluggage if there is any debris larger than 3/8" in the JBR where the gas cooling pump suctions are located. The debris found in the nozzles included: refuse left behind by work crews, pieces of rubber from rubber-lined piping that had failed, broken tests coupons (placed in the JBR to gauge erosion and corrosion), and scale and other byproduct solids that had been loosened during off-line cleaning efforts. Impacts of, and solutions to, this pluggage include:

- The nozzle pluggage can result in elevated temperatures in the JBR inlet plenum. On occasion, the temperatures rose to the alarm point, requiring a forced outage to remove the obstruction;
- Regardless of how carefully the JBR is cleaned, it takes only a few pieces of debris to clog the gas cooling nozzles sufficiently to require a forced outage due to temperature excursions; and

- Screens on the suction of the gas cooling pumps virtually eliminated the incidences of unwanted materials entering the suction of the gas cooling pumps.

5.10 JBR Level Control

The specified means to control JBR level in the original design consisted of 3 differential-pressure-type level instruments, spaced radially 120 degrees apart from each other in the JBR. Due to the high solids content of the scrubber slurry, these instruments were prone to plugging, which resulted in erroneous readings. The following attempted solutions were implemented during the demonstration:

- Wash water was supplied to the instruments to keep the reference and indicator legs free of solids. Although the wash water was effective in eliminating solids build up, it was difficult to balance the flows on the two instrument legs, resulting in continued erroneous readings; and

- The existing JBR gas-side differential pressure instrument was used as a surrogate for JBR level. This system worked well, and although no redundant instrumentation was available, no instrumentation problems were experienced. The only negative attribute to this type of JBR level control is that gas side differential pressure is not always proportional to JBR level, due to gradual fouling of the sparger tubes.

5.11 Effects of Limestone on Gypsum Quality

One of the most unexpected findings of the demonstration project was the impact of limestone selection on gypsum dewatering characteristics. Typically, limestone used in wet FGD systems is selected based on purity (% $CaCO_3$) and cost. Because the first limestone evaluated resulted in smaller than expected gypsum particle size and poor dewatering characteristics, a bench-scale limestone evaluation was conducted, followed by full scale evaluations of the most promising limestones. The following was learned from the limestone evaluation:

- The purity of the limestone (% $CaCO_3$) is not always the only true indicator of the quality of the resulting gypsum;

- High inert content and iron concentration in the limestone appeared to correlate well with the poor quality gypsum; and

- The results of the bench-scale evaluation of limestones correlated well with the full scale CT-121 evaluation results and would likely prove useful for any other wet-limestone FGD systems.

6.0 RECOMMENDATIONS

Several innovative design features, such as the widespread use of FRP, elimination of the prescrubber in a CT-121 design, and others, were first implemented in the Yates CT-121 demonstration project. Therefore, the effectiveness of many of these innovations was untested at the start of the demonstration. Not unexpectedly, some shortcomings in the design were identified, as well as areas of improvement for already satisfactory features. Some of these findings were discussed in the Results (Section 4) and Conclusions (Section 5) sections of this report. The following recommendations for improvements in future designs are detailed in this section, and include discussions of:

- Abrasion resistant material selection;
- Gas cooling system relocation;
- Cooling pump suction screens;
- Deck wash modifications;
- JBR level control;
- pH probe location and maintenance; and
- Process set point selection.

Note that some of these improvement recommendations have already been implemented in the Yates CT-121 process.

6.1 Abrasion Resistant Materials

To combat the problem of FRP erosion in the gas cooling duct, discussed in Section 5.7, several possible solutions were identified:

- The use of an alternate material of construction for the walls of the transition duct;
- The use of abrasion-resistant materials to coat the transition duct walls (downstream of the gas cooling nozzles) and other wear prone surfaces; and
- The addition of stainless steel alloy wall paper, such as Hastelloy™ C-22 or 317-LM on the walls of the transition duct.

Alternate transition duct materials or wall paper made of exotic alloys would certainly offer improved erosion resistance over FRP. However, it would do so at a higher cost and provide less corrosion resistance than FRP, particularly in a high chloride environment such as that observed in the Yates CT-121 process.

The solution involving the use of abrasion resistant coating was implemented at Plant Yates mid-way through the process evaluation. Several types of erosion resistant materials were applied to the surfaces most susceptible to erosion to determine which was the most suitable for this application. Eventually, a material (Duromix™) was selected that appeared to offer the highest level of erosion resistance, without sacrificing cost or corrosion resistance. The application of this Duromix™ is shown in Figures 4-9 through 4-11. With the exception of some minor adherence problems (a result of misapplication), the use of this material to improve erosion resistance was successful and should be considered for all future CT-121 applications that widely use FRP materials of construction. As shown in the photographs, this Duromix™ was also applied to the upstream face of the vertical structures in the JBR inlet plenum, although erosion in this area would best be remedied by the recommendations provided in Section 6.2 (i.e., moving the gas cooling section further upstream of the JBR).

6.2 Relocation of Gas Cooling System

The gas cooling system in the Yates CT-121 design was located only 18 feet upstream of the JBR inlet plenum which resulted in two primary difficulties:

- Erosion damage to the inlet plenum (as discussed in Section 5.7 of this report); and
- Lower deck solids build-up.

A single solution is proposed that should alleviate these two problems. Relocating the gas cooling section of the transition duct further upstream of the process would minimize these adverse effects in future designs by:

- Allowing the slurry to fall to the floor of the duct well upstream of the JBR, thus reducing the deposition of solids on the lower deck resulting in decreased lower deck wash requirements;
- Reducing erosion in the JBR inlet plenum since the flue gas would no longer be laden with slurry prior to impacting the vertical surfaces of the JBR; and
- Increasing the gas cooling residence time, allowing more opportunity for flue gas cooling and decreasing the likelihood that a few plugged gas cooling nozzles would result in high temperature excursions in the JBR inlet plenum.

6.3 Gas Cooling Pump Suction Screens

As discussed in Section 5.9, the gas cooling nozzles, with a 3/8-inch free pass area, can become easily plugged with loosened scale and other debris from the JBR reaction zone. Several solutions to this problem were considered, including:

- Installing strainers upstream of the gas cooling pumps;
- Installing strainers downstream of the gas cooling pumps;
- Replacement of existing nozzles with ones with a larger free pass area; and
- Installing screens surrounding the suctions of the gas cooling pumps in the JBR reaction zone.

The cost of construction and installation of various types of strainers was evaluated, and it was determined that strainers that were easy to clean on-line and constructed of materials that were adequate to withstand the high chloride content of the scrubbing slurry would be cost-prohibitive. Alternate nozzle designs were investigated, but could not be implemented without increasing the size of the gas cooling pumps at a considerable expense.

The solution that was ultimately selected and implemented utilized a single "hockey net" style screen in the JBR at the location of the suctions of the three gas cooling pumps. The suction screen was designed with the following features:

- The screen was large enough so that all three gas cooling pump suctions were within the same screen;
- The free pass area of the screen was selected at 3/8" so that any object small enough to pass though the screen would also be able to pass through the nozzles;
- The screen was constructed of FRP and PVC for corrosion and erosion resistance and to be consistent with the materials of construction of the JBR; and
- Because of the "hockey net" style and large surface area of the screen, there was little danger of fouling the gas cooling pump intake and starving the pumps, therefore, no cleaning mechanism was required, as would have been in an in-line strainer.

Figure 6-1 is a photograph of the partially assembled screens prior to installation, and Figure 6-2 shows the screens after installation. Also installed at this time were similar, but smaller, screens for the gypsum slurry draw-off pump suctions. These pumps had not experienced any plugging due to foreign materials, but some damage to the rubber volute liner and impeller had been noted in previous inspections.

It is recommended that all future CT-121 designs include such a suction screening device to prevent plugging of gas cooling nozzles. These types of screens are both erosion- and corrosion-resistant, result in no additional pressure drop penalty, are unlikely to plug, and keep the gas cooling nozzles free of debris that otherwise might plug them. The screens installed at Plant

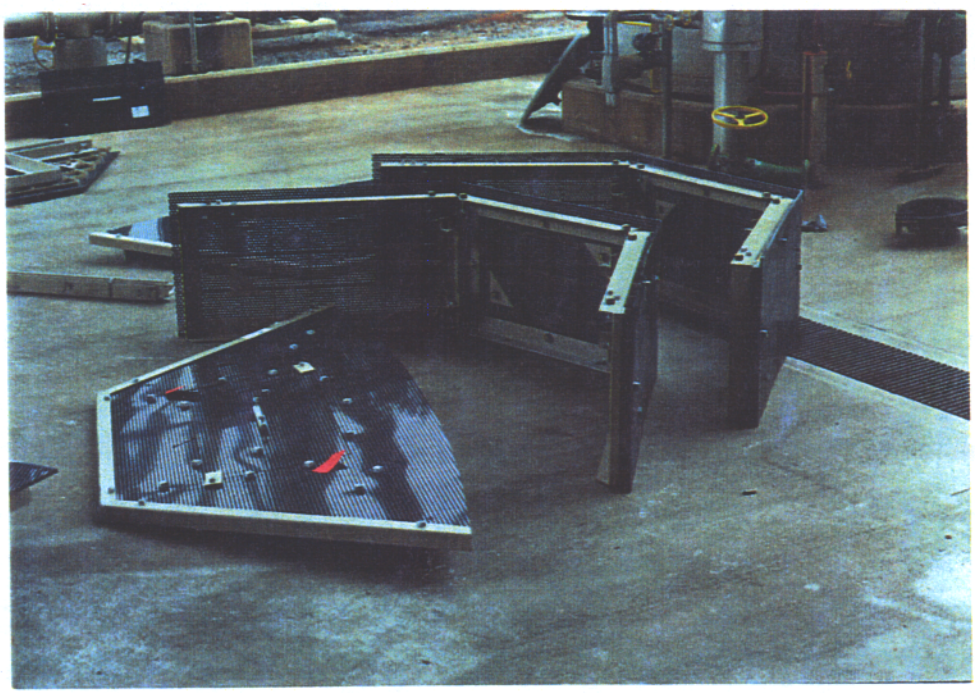

Figure 6-1. JBR Pump Suction Screens - Prior to Installation

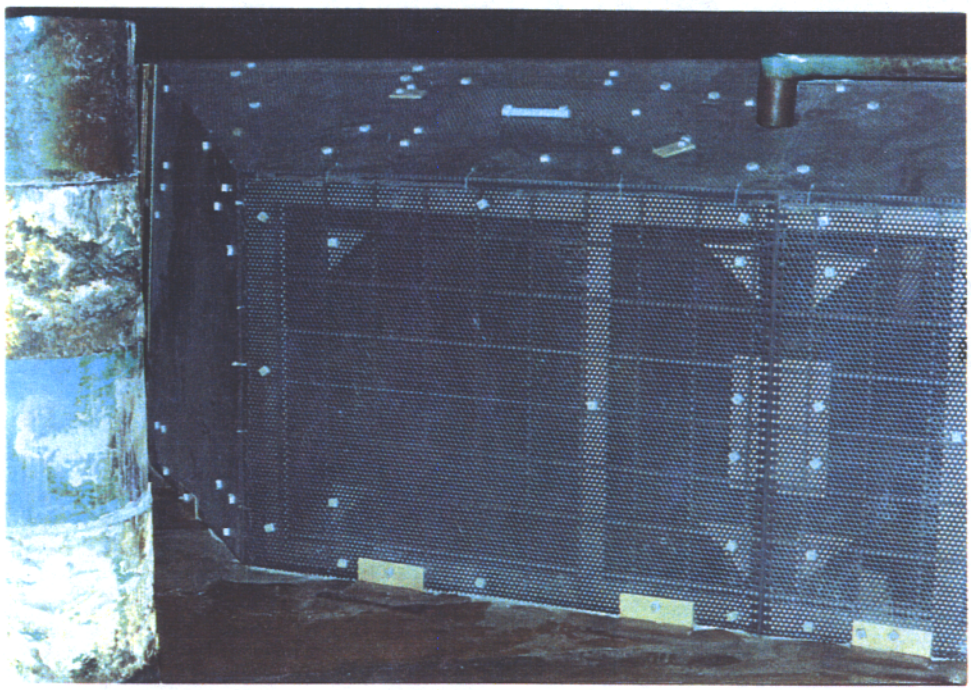

Figure 6-2. Installed Gas Cooling Pump Suction Screens

Yates proved successful in eliminating further JBR temperature excursions due to gas cooling nozzle pluggage.

6.4 JBR Deck Wash Modification

Keeping the JBR lower deck and sparger tubes free of solids is critical to ensuring consistent performance of the CT-121 process. As discussed in Section 5.8, lower deck solids build-up was effectively mitigated by increasing the number of deck drains and redesigning the deck wash system to ensure overlapping coverage was achieved. Unfortunately, this had little effect on abating the build-up of fly ash inside the sparger tubes during periods of elevated ash loading. This was a result of the design of the sparger tubes and mounting collars. The tops of the sparger tubes protrude approximately 4 inches above the deck, as shown in Figure 6-3. It would not be practicable to arrange the deck wash system so that the inside of each sparger tube was sprayed without adversely impacting the JBR water balance. To allow the sparger tubes to be washed, two solutions were devised:

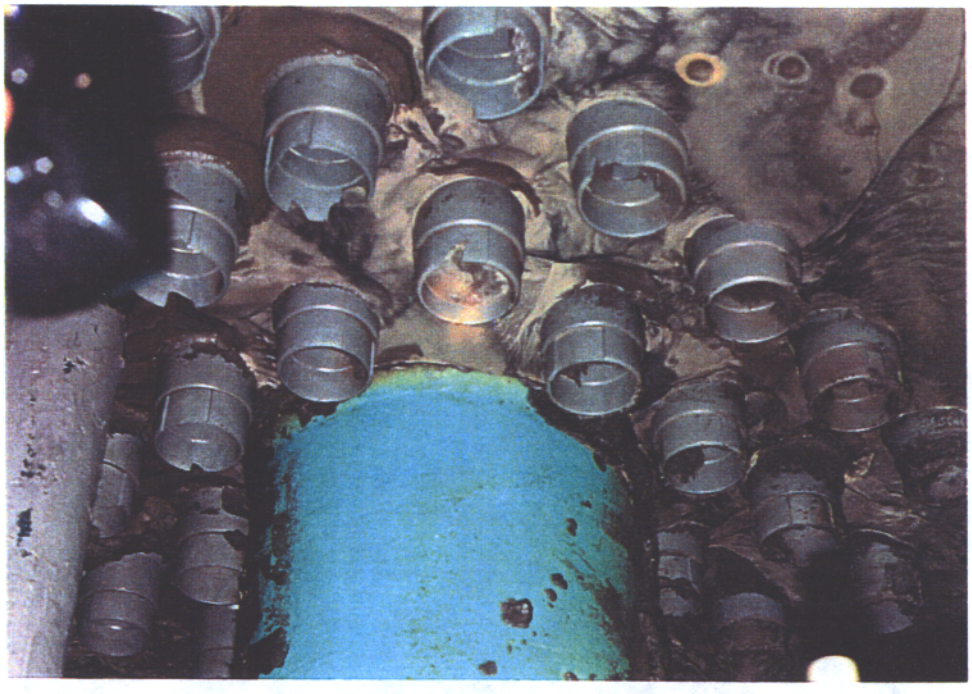

Figure 6-3. Sparger Tube Protrusion Above Lower Deck

- Install polystyrene-type foam on the lower deck, with cutouts for each of the sparger tube tops, effectively raising the lower deck surface and allowing each sparger tube to serve as a drain for the wash water; and
- Alter the design of the sparger tube mounting mechanism to allow the tops of the sparger tubes to remain flush with the lower deck, as shown in Figure 6-4.

The first proposed solution would be most practical for modifying the existing Yates CT-121 scrubber. Raising the deck flush with the sparger tube tops will allow the wash water to rinse the sparger tubes and keep them free of solids. It will also increase the effectiveness of the deck washing, since the solids that are resuspended by the wash water can more quickly drain to the JBR (before they settle on the deck again).

Redesigning the sparger tube mounting hardware will have the same effect as described for the retrofit recommendation: allowing the sparger tubes to serve as deck drains, effectively washing the sparger tube interior with the deck wash water.

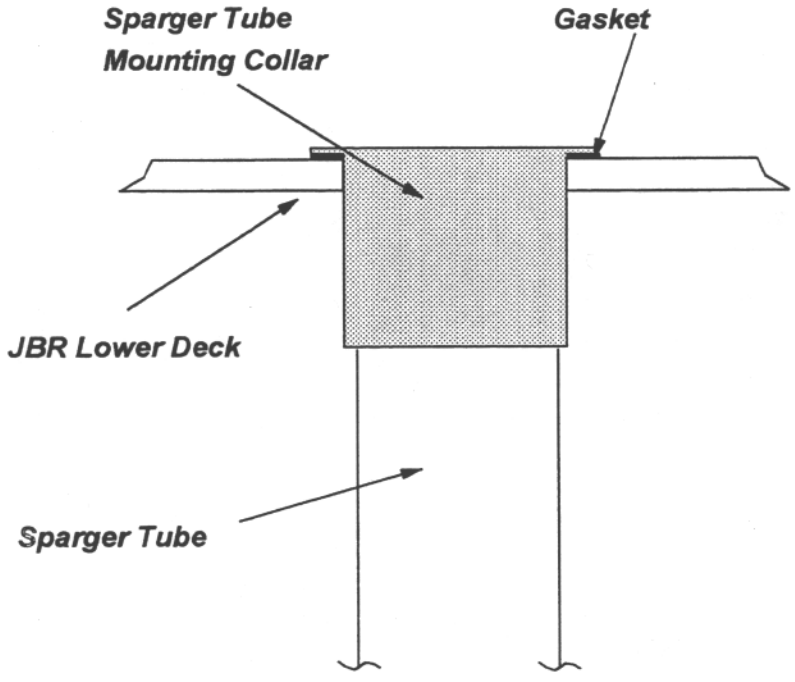

Figure 6-4. Sparger Tube Mounting - Recommended Design

6.5 JBR Level Control

One of the conclusions reached early in the process evaluation was the unsuitability of the differential-pressure type JBR level instruments selected for this application. This is discussed in detail in Section 5.10 of this report. Suggested methods for more reliable JBR level control include:

- Employing gas-side, differential pressure instruments as surrogates for level instrumentation (the benefits and shortcomings of this are discussed in Section 5.10); and
- Using alternate kinds of liquid level-based differential pressure instruments.

The gas-side differential pressure instrument was used at Yates because of the difficulty in retrofitting an alternate technology. Although only a single ΔP instrument was used previously, consideration should be given to adding a second and third instrument for redundancy and to aid in detection of malfunction in any instrument.

A recommendation for future CT-121 designs would be to use a level indication system less prone to plugging than the original system (which used small gauge tubing for the indication and reference legs). One option that will allow level measurement with a decreased likelihood of fouling of the instrument is a diaphragm-type pressure sensor. The sensor can be mounted as an integral part of the JBR reaction zone wall. Because there is no opportunity for pluggage of sensing lines, this approach has a higher inherent reliability. Of course on-line instrument replacement would be difficult, if not impossible, but that inconvenience can be overcome by the installation of several redundant instruments. Scaling is not expected to be a problem because of the flexible nature of these types of devices.

6.6 pH Probes

Two pH measurement units were evaluated during the demonstration:

- A Rosemount transmitter coupled to a Van London pH probe; and
- A TBI-Bailey transmitter and probe arrangement.

Only the Rosemount transmitter and a Van London probe proved durable enough to last the entire demonstration project. This was because of the simplicity of design of the Rosemount instrument (the TBI-Bailey instrument was too easily short-circuited by slurry sprayed during sampling) and the durability of the Van London probe.

Based on experiences at Yates, the "hot-tapping" (i.e., the ability to remove and insert pH probes while on-line) of pH probes is highly recommended in all future applications. The hot taps allowed the pH probes to be removed for cleaning, bench calibration, and replacement. Because of the high suspended and dissolved solids content of the slurry, frequent preventive maintenance is required to ensure that the pH probes operate properly. The suggested preventative maintenance practices include:

- In-situ calibration checks at least twice daily;
- Weekly cleaning (with a soft brush) of the reference junction;
- Bi-monthly replacement of the probe (to circumvent end-of-life degradation, which is difficult to diagnose in its early stages); and
- Programmed, control system comparison of at least two redundant pH probes.

Based on lessons learned regarding pH probe placement, the following are recommended:

- Redundant pH probes be used;

- pH probes should be placed immediately adjacent to one another to mitigate the effects of incomplete mixing in the froth zone, which can lead to radial stratification;

- The sample (calibration) port should also be placed in close proximity to the probes - preferably between them; and

- pH probes should be placed at least 12 inches below the bottom of the sparger tube openings to provide more stable pH readings with less fluctuation due to localized low-pH areas in the turbulent froth zone.

6.7 Smart Process Set-Point Recommendations

The application of the types of regression models discussed in Section 4.8 of this report to distributed control systems (DCS) is an excellent way to ensure that SO_2 removal efficiency objectives are met. Forms of the regression models developed from parametric performance results can be entered into the DCS and a "smart" system can be used to make recommendations to the process operator to allow the target SO_2 removal efficiency to be achieved. Based on operating experience, a pH can be selected that provides for high SO_2 removal efficiency while maintaining high limestone utilization. Once the pH has been selected, the smart system can recommend JBR ΔP set points to achieve the target level of performance.

It is not recommended, however, that a smart system be used to automatically adjust the operating parameters of the scrubber without operator action. Instrument errors, transients, or CEM calibration cycles could have a deleterious impact on the selected operating parameters, and human intervention is important to "filter" all recommended process parameter changes to confirm that they make sense and are necessary. For example, a known, short-duration load transient may not necessitate any process changes. An informed operator can decide whether or not to alter process parameters based on his knowledge of the brevity of such a transient.